

PhD. Thesis

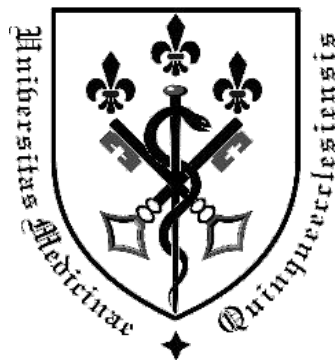
Lower Limb and Bone Age Assessment with the EOS System

Ian O'Sullivan BSc, M.D.

Department of Orthopaedics,
University of Pécs, Medical School,
University of Pécs,
Hungary

Topic supervisors:

Péter Than M.D., PhD.
Csaba Vermes, M.D., PhD.



University of Pécs,
Medical School,
Pécs
2020

TABLE OF CONTENTS

List of Abbreviations	5
I. INTRODUCTION	6
I. 1 The Lower Limb	6
I. 1.1 Introduction.....	6
I.1.2 Assessment of the Lower limb	7
I.1.3 An Important Parameter: Femoral Neck-shaft Angle.....	9
I.2. The EOS Scanner	11
I.2.1 What is the EOS Scanner?.....	11
I.2.2 Radiation and the Child	12
I.2.3 The EOS Scanner and Radiation	13
I.2.4 The EOS Scanner Reconstructions.....	13
I.2.5 Clinical Applications of the EOS	14
I.2.6 Limitations of the EOS	16
I.3. Bone age.....	17
I.3.1 The Skeleton and Ossification	17
I.3.2 History of Bone Age Assessment in Medicine.....	18
I.3.3 Role of Bone Age in Medicine	19
I.3.4 Methods for Bone Age Assessment.....	20
I.3.5 Bone Age Assessment Methods – A Brief Primer	22
I.3.6 Bone Age Assessment Method Usage by Speciality.....	22
PART 1 –Skeletal Maturation of the Lower Limb	23
II.1. Introduction.....	23
II.1.1 Aims of this study.....	23
II.2. Materials and Methods.....	24
II.2.1 Population.....	24
II.2.1.1 Lower Limb Evaluation.....	24
II.2.1.2 NSA Assessment Population.....	25
II.2.2.1 Parameters Evaluated	28
II.2.2.2 Neck-shaft Angle Investigation.....	30
II.2.2.3 Cervical Bone Age Assessment	31
II.2.3 Statistical Analysis	32
II.3. RESULTS	33
II.3.1 Reliability Results with Hassel-Farman Cervical Bone Age Method.....	33

II.3.2 Lower Limb Evaluation.....	33
II.3.3 Neck-shaft angle – A Closer Look.....	42
II.4. DISCUSSION.....	49
II.4.1 Lower Limb Biomechanical Parameters in the Developing Child.....	49
II.4.2 Longitudinal Parameters.....	49
II.4.3 Rotational / Torsional Parameters.....	50
II.4.4 Other features.....	51
II.4.5 Neck-shaft Angle development and Skeletal Maturity.....	51
II.4.6 Limitations.....	54
II.4.7 Summary.....	55
III. PART 2 – Alternative Bone Age Assessment Methods.....	56
III.1. Introduction.....	56
III.1.1 Introduction.....	56
III.1.2 Aims of this study.....	56
III.2. Materials and Methods.....	57
III.2.1 Bone Age Assessment Alternative Methods Population.....	57
III.2.1.1 Bone Age Methods Literature Review.....	57
III.2.1.2 Bone Age Methods Pilot Study – 6 methods.....	61
III.2.1.3 Bone Age Methods Main Study – 5 methods.....	62
III.2.2 Statistical Analysis.....	63
III.3. Results.....	64
III.3.1 Bone Age (Pilot Study).....	64
III.3.2 Bone Age (Main Study).....	64
III.4. Discussion.....	70
III.4.1 Bone Age and the EOS Scanner.....	70
III.4.2 Alternative Bone Age Methods.....	72
III.4.2.1 Calcaneus Method.....	72
III.4.2.2 Cervical Method.....	73
III.4.2.3 Risser ‘plus’ System.....	74
III.4.2.4 Knee Method.....	76
III.4.2.5 Oxford Hip Method.....	77
III.4.3 EOS & Bone Age Evaluation: Common Problems Encountered.....	79
III.4.3.1 Step Length.....	79
III.4.3.2 Resolution.....	79
III.4.3.3 Image size.....	80

III.4.3.4 Position.....	80
III.4.4 Limitations of this Study.....	81
III.4.5 Summary - EOS & Bone Age Evaluation.....	83
IV. SUMMARY OF THE THESIS	85
New Findings of This Thesis	86
References	88
Appendix (Supplementary Table 1)	100
Bibliography	117
- Journal Publications.....	117
- Presentations: International Conferences	117
- Presentations: National Conferences	118
- Posters: International Conferences	119
- Publications Not Connected to this Thesis	119
Acknowledgements.....	120

LIST OF ABBREVIATIONS

ALARA – ‘As Low As Reasonably Achievable’

AP - Anteroposterior

BA – Bone Age

CA – Chronological Age

CI – Confidence Interval

CT – Computed Tomography

FAA – Femoral Anatomical Axis

FHD – Femoral Head Diameter

FL-FS - Full-leg Full-spine

FM-FS - Femoral Mechanical Axis - Femoral Shaft [Angle]

FMA – Femoral Mechanical Axis

FNA – Femoral Neck Axis

FNL - Femur Neck Length

FO – Femoral Offset

FT – Femoral torsion/ Femoral Version

FTR – Femorotibial Rotation

ICC – Intraclass Correlation Coefficient

LMA – Lower Limb Mechanical Axis

MR – Magnetic Resonance

NS – Not Significant

NSA – Neck Shaft Angle

mTFA - Mechanical Tibiofemoral Angle

PCL – Posterior Condylar Line

PHV – Peak Height Velocity

ρ – ‘Rho’ the correlation coefficient estimated by the Spearman correlation test

RWT – Roche-Wainer-Thissen

SCFE – Slipped Capital Femoral Epiphysis

SD – Standard Deviation

TM – Transmalleolar Line

TMA – Tibial Mechanical Axis

TMA_n – Tibial Mechanical Angle

TT – Tibial Torsion

TW2 – Tanner-Whitehouse 2

TW3 – Tanner-Whitehouse 3

VIF – Variance Inflation Factor

WHO – World Health Organisation

2D – Two-dimensional

3D – Three-dimensional

I. INTRODUCTION

The growth of the skeletal system is a “volumetric revolution”¹. From the time of birth until adulthood the extremities and trunk change in body proportion, our height increases 350% and our body weight increases almost 20-fold¹.

The paediatrician and the orthopaedic physician avidly follow the changing skeletal parameters in the growing child and if there is deviation outside of the range of normal they must determine the cause and decide upon a course of action based on its origin. The causes of deviation however are manifold and may be endocrinological, genetic, neurological, congenital or idiopathic²⁻⁵.

The guidance of the developing skeleton has remained central to orthopaedics ever since Andry first coined the phrase ‘orthopédie’ in 1741⁶, exemplified by the persisting emblem of orthopaedic medicine, a splinted tree.

A clear understanding of what a ‘normal’ skeletal system is at any given age or stage of maturity is essential to this process. Furthermore, we must wrestle with concepts of how to effectively measure parameters of the skeleton and how we can estimate maturity in the most accurate manner, while minimising the risk of ionising radiation to the child.

I. 1 The Lower Limb

I. 1.1 Introduction

The lower limb is the primary actor in upright bipedal locomotion and plays a fundamental role in the maintenance of balance while erect. Its’ function is dependent upon the interaction of neural, muscular, bony and soft tissue elements and the “optimal alignment of bone structures and joints is critical for the efficient function of the musculoskeletal system”⁷. Damage to tissues may occur abruptly or accrue over time, and much of the damage the skeletal system endures can be understood as due to abnormal load on a normal joint, or normal load on an abnormal one⁸.

The assessment of biomechanical parameters in children may allow us to detect and correct a disorder in its' early pre-symptomatic stages, preventing a greater burden in later life⁹. Severe alterations in biomechanical parameters can cause significant hardship via pain, gait deviation¹⁰ and even joint luxation¹¹. Disorders such as limb length discrepancy and torsional deformities⁵ and others have been associated with later osteoarthritis¹², and femoral anteversion, leg length discrepancy and numerous other biomechanical parameters have been positively associated with increased risk of injury during sport and physical activity¹³.

I. 1.2 Assessment of the Lower limb

Evaluations of the biomechanics of the lower limb bones are performed by static or dynamic investigation.

Static investigation consists of imaging, allowing us to measure the features that play a role in limb function: the lengths, axes and angles that act as levers and fulcra in motion, stabilisation and stress transmission. Investigation modalities include:

- Conventional radiography: traditional X-rays are affordable and highly available, however the accuracy is questionable due to the magnification of the examined area that occurs, which increases depending on the distance from the source. Although patient position can easily affect the measurements¹⁴, this remains a modality in common clinical use for investigating deviations in the coronal and sagittal plane;
- Computed tomography (CT): CT is still regarded as the gold standard for quantitative three-dimensional measurement, however the ionising radiation burden associated means its use is somewhat limited in clinical practice and the patient must be supine during the examination, altering some of the biomechanical compensation mechanisms¹⁵. CT examinations can evaluate 'torsional' deformities in the axial plane, in addition to coronal and sagittal deformity;
- Magnetic resonance imaging (MRI): MRI can also generate three-dimensional measurements, however it's high cost, long acquisition time and supine position are clear disadvantages.

- EOS: the EOS scanner is a newer system, however it has clear advantages with regards to a lower radiation burden¹⁵⁻¹⁸, fast image acquisition time, images can be captured in the upright weight-bearing position and may be more accurate than CT scanning imaging¹⁶. Upright weight-bearing imaging is specifically advantageous for capture of compensatory processes, evidenced by Lazennec et al. who detected a limb length discrepancy with EOS in a patient with patellofemoral syndrome secondary to total hip replacement, that was not detectable by MRI or CT¹⁹. [Note: EOS is not an acronym!]

The current reference data in use for most static lower limb parameters consists of values determined by conventional radiology with subsequent attempts to compensate for magnification errors by applying correction formulae, as per Green et al in 1968²⁰ and Gindhart, in 1973²¹. Parameters of the lower limb include the femoral length²², femoral torsion^{23,24}, hip-knee-shaft angle²⁵ and the femoral ‘neck-shaft’ or collodiaphyseal angle²⁶ (see next section for more detail).

Dynamic investigations of lower limb parameters can be active or passive. Active dynamic investigations utilise video imaging to visualise the movements and changes in position, utilise sensors on the study subject or directly measure stress across tissues, yielding objective data about joint motion (kinematics), joint force and power (kinetics) and time-distance information (spatial-temporal data). While such active dynamic investigations can yield many important insights, they are not typically included as part of routine clinical management for practical reasons, and the vast amount of data generated can be difficult to interpret²⁷.

Passive investigations consist predominantly of clinical examinations of the passive range of motion of an individual with the aim of assessing the underlying bony anatomy. While these are cheap and easy to perform in a clinical setting, they do not assess the bony elements in isolation, but rather simultaneously assess tendonous, ligamentous, muscular and fascial tissues also.

I. 1.3 An important parameter: Femoral Neck-shaft Angle

The neck-shaft angle (NSA) of the femur - the angle formed between the femoral neck and shaft - is a fundamental parameter of the lower limb and plays a key role in the transfer of mechanical forces from the trunk to the lower extremity.

The modern understanding of hip biomechanics was established by Pauwels, wherein the magnitude and direction of forces is said to be determined by body weight, position of the centre of gravity, and the length of the abductor lever arm, as determined by the NSA and the neck length^{28,29}. Changes in the length of the lever arm alter the force that must be generated by the stabilizing muscles, as can be seen when the neck-shaft angle or femoral version changes. Alterations in loading from childhood can lead to later pathology, and the NSA has been found to be associated with a number of orthopaedic diseases including patellar subluxation and hip osteoarthritis^{5,12}.

The femoral neck and its' angle with the shaft are formed in utero while the femur is still a cartilage anlage³⁰. Throughout early development and childhood, it falls from what is originally a significantly valgus position (as high as even 160° in the neonate³¹) to reach that of normal adulthood by adolescence. The value of 'normal' however is still regarded by some medical school textbooks to be 135°³² whereas the true value is likely closer to 127°³³. While consensus exists that the NSA falls with increasing age, the exact values, the effect of geographic and climate influences^{33,34}, and whether there are gender differences at different age groups - or indeed if there are gender differences at all^{35,36} - are still the source of some debate.

Current disagreements about the measurement of the NSA have stemmed from clinicians and researchers a.) using a range of different indirect and direct modalities, from MRI and conventional radiography to anatomic specimens^{32,33}; b.) using different landmarks; and c.) using methods of varying reproducibility ranging from simple 'eye-balling' visual assessment, strict geometrical reference points to computer assistance^{14,24,33,37,38}.

Evaluations based on conventional anteroposterior (AP) radiographs for example give an

artificially elevated NSA due to the confounding effect of femoral anteversion^{14,39-41} (see Figure 1). This difference between the 'true' and the 'apparent' NSA has been proposed to explain the higher values reported by many teaching text books³² and raises questions about the accuracy of results gained using indirect methods, in spite of attempts to use patient positioning to compensate^{14,40}.

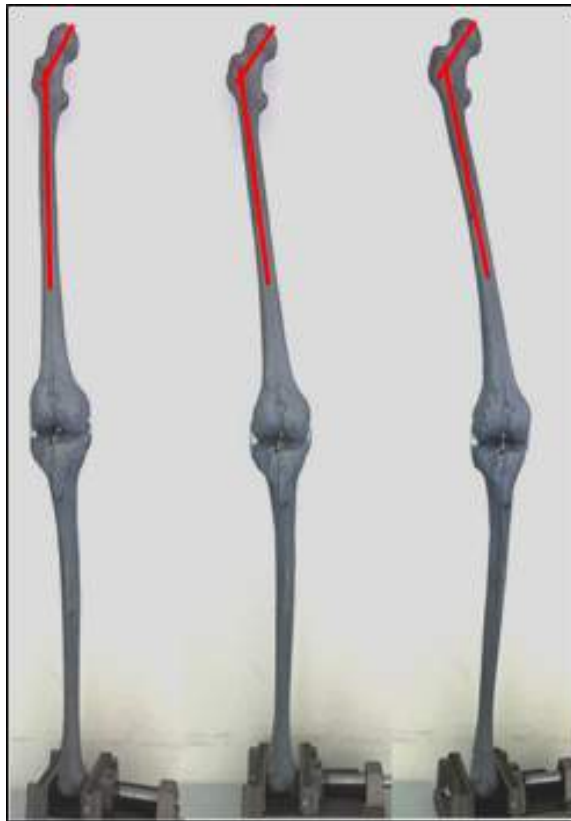


Figure 1. The effect of axial rotation on the appearance of the neck shaft angle (NSA). NSA of a cadaveric lower limb is seen to decrease from left to right, when positioned in external rotation, normal anteversion, and internal rotation, respectively. [Image reproduced from Hunt et al. 2006⁴¹].

While CT and MRI can eliminate anteversion-associated effects, they are associated with considerable radiation dose and expense. Some authors have reported use of the EOS 2D/3D scanner to assess proximal femoral morphology and avoid artefacts, and when Guenoun et al. compared NSA values measured on 2D EOS images and 3D reconstructions made from the same images, they found values to be 8.04 degrees higher in the 2D images which they attributed to artefacts caused by the femoral version⁴².

I. 2. The EOS Scanner

I. 2.1 What is the EOS Scanner?

The EOS scanner is a biplanar slot-scanning X-ray device capable of whole-body imaging (See Figure 2). The imaging device is unique in its ability to capture head-to-toe images with minimal image distortion and an extremely low radiation dose^{36,43}. This is achieved by three important features: 1. Slit collimators; 2. High-sensitivity detectors; 3. Internal adjustable gain.

- 1. Slit collimation at the source serves to narrow emitted radiation in the vertical dimension, creating a horizontal beam which can be scanned over the patient resulting in a near 1:1 image. In contrast, conventional radiography employs just a single fixed source, the shadow of which varies in magnification in each region in proportion to the distance from the source. Furthermore slit collimation blocks the scattered radiation that makes up a significant component of the dose received in traditional X-ray systems⁴⁴.
- 2. The detectors in the EOS system were developed based on George Charpak's multi-wire proportional chamber principle. Pressurised xenon gas in the detectors is used to amplify arriving photons into an electron cloud and then a subsequent 'avalanche' that serves to significantly boost the signal, thus reducing the number of photons that must pass through the patient.
- 3. Internal adjustable gaining within each detector further serves to adapt detection sensitivity to the incoming signal and results in high contrast images capable of almost 30,000 gray levels.

Combining these innovations with two fixed scanning-arms positioned at 90 degrees to each other, this low-radiation system can capture orthogonal image-pairs in the upright, weight-bearing position, from which 3D reconstructions can be generated by the bundled sterEOS software.



Figure 2. The EOS scanner is a biplanar imaging device with two X-ray sources and detectors. [Image reproduced with permission from eos-imaging.com, Paris, France].

I. 2.2 Radiation and the child

Imaging of the child is an essential component of diagnosis and management in the majority of orthopaedic disorders, and due to availability and low cost X-ray methodologies are most commonly employed⁴⁵. X-rays are high frequency magnetic waves that belong to the group of ‘ionizing radiations’, however they have known deleterious effects on cells. While early effects such as burns, nausea, cardiac problems are not typical at the doses applied in clinical settings, there is an increasing awareness of the risk of later neoplasm^{43,46-48}. Children are perhaps particularly susceptible to later neoplasm, due to the large number of growing mitotically active cells, the stochastic nature of late radiation effects and the one or more decades needed to develop⁴⁵.

The typical management of scoliosis patients involves serial X-rays at follow-up and McKenna et al. concluded in their 2012 review that there was a “clear association between increased risk of breast cancer mortality and diagnostic X-ray exposures for female

scoliosis⁴³. Ronckers et al. investigated 5,573 women in a study included in the aforementioned review, finding cancer mortality was 8% greater than expected in those with a history of scoliosis and repeated X-rays, predominantly due to a higher breast cancer mortality⁴⁸. In another smaller study of 159 women, endometrial cancer risk was also seen to be elevated in those with scoliosis when compared to the national average⁴⁹.

I. 2.3 The EOS Scanner and Radiation

In recent decades much work has been undertaken to improve the technology and practices of radiological interventions, such that harmful effects on the patient can be kept to a minimum while still achieving sufficient image quality for clinical decision making. These aims are described by the principle of ALARA ('As Low as Reasonably Achievable')⁵⁰.

The EOS scanner has been shown to expose the patient to 2-10x less radiation than conventional radiography⁴⁴. Such a radiation reduction gives us the possibility to make a full body image-pair with the potential for three dimensional reconstructions with just 1/3 the radiation of a typical chest X-ray⁵¹. Indeed, one study comparing modalities for limb measurements on a phantom limb, found that not only was radiation dose reduced from a mean 29.01 millirad (conventional radiography) and 3.74 millirad (CT scanogram) to just 0.86 millirad with the EOS scanner, but that the EOS gave significantly more accurate measurements than even CT differing on average just 0.8% vs 1.3% (CT) & 8.8% (conventional radiography)¹⁶.

I. 2.4 The EOS Scanner Reconstructions

Using its' proprietary 'sterEOS' software, the user can generate 3D reconstructions from EOS scanner image-pairs (see Figure 3). Reconstructions can be generated from the lower limb, pelvis and/or spine and are carried out in a user-guided three-step process. Firstly, the region of interest is selected and specific landmarks are tagged. Next, a computer-generated 'best-fit' template appears and must be adjusted by the user to match the contours of the bones. Finally, the software generates a three-dimensional reconstruction and automatically calculates biometric measurements based on the reconstruction.

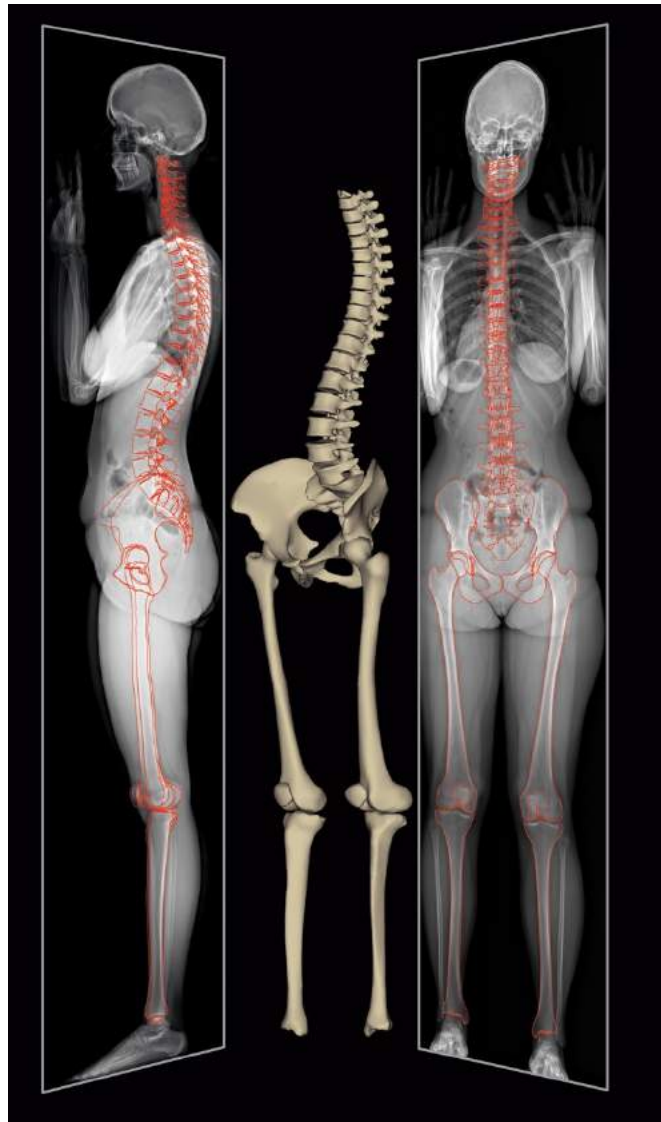


Figure 3. Three-dimensional reconstructions can be generated from image-pairs with the sterEOS software. ‘Best-fit’ templates are generated and adjusted by the user to fit the bones, before computer processing takes place. [Image reproduced with permission from eos-imaging.com, Paris, France].

I. 2.5 Clinical Applications of the EOS

The EOS scanner has seen increasing use in assessment of spinal disorders (such as scoliosis^{43,45}), lower limb disorders^{15,17,18,36,42,43,52,53} (such as limb length discrepancy) and in whole body imaging⁵⁴ since its introduction in 2008.

Spinal disorders such as scoliosis require regular follow-up, typically involving repeated imaging of children and adolescents over years, and patients can benefit greatly from the lower radiation burden associated with the EOS scanner. Idiopathic scoliosis is a three-dimensional deformity of the spine in which multiple segments of the vertebral column are displaced in three planes, most notably a displacement of more than 10° in the coronal plane⁵⁵, and it affects 1.5-3% of the population⁵⁶. Furthermore, in recent years attention has turned to the benefits of assessing pelvic parameters in idiopathic scoliosis patients^{18,57,58}. Measurements of the pelvic incidence, sagittal pelvic tilt and sacral slope, in addition to those of spinal curvature, can be assessed all with the same EOS scan⁵⁹ which is beneficial to both patient and health care service alike. Facet joint disease, arthritic degeneration and degenerative scoliosis of the spine can also be influenced by such pelvic parameters^{60,61}, indeed pelvic parameters and sagittal alignment may have the greatest impact on post-operative outcomes in adult spinal disorders^{61,62}.

Lower limb disorders that may be evaluated include limb length discrepancy⁶³, patellofemoral syndrome and pre-arthritic conditions like genu vara/valga and genu recurvatum/flexum. Osteoarthritis of the lower limb, especially for surgical planning and follow-up of total hip^{19,64,65} or knee replacements⁶⁶, has also been investigated in many institutes. The possibilities for assisting surgical planning in osteoarthritis alone indicate the considerable potential impact of the EOS. Osteoarthritis affects an estimated 9.6% of men and 18.0% of women over 60 years of age according to World Health Organisation (WHO) statistics⁶⁷, and of these 80% have limitations in movement, and 25% reported an impaired ability to perform some of their main daily activities. In the United States in 2005, 27 million people were estimated to be living with osteoarthritis⁶⁸. In 2004 alone, more than 1.07 million joint replacement surgeries were carried out in the US, mostly due to osteoarthritis⁵⁶. A 2014 study using the EOS found significant changes in some parameters in osteoarthritis patients - including acetabular angle, sacral slope, femoral mechanical angle, femoral head eccentricity, and femoral head diameter – and suggested longitudinal studies of such features could be a future possibility due to the low radiation dose from the EOS⁶⁹.

I. 2.6 Limitations of the EOS

The limitations of the EOS system should also be noted, specifically related to how 3D reconstructions are generated, body position within the device and the age of the patient.

As three-dimensional reconstructions are generated from two orthogonal 2D images, with reference to template reference structures they are not 'true' reconstructions. As a result they may not be appropriate for assessment of some complex three dimensional disorders such as tumours or fractures³⁶.

Patient positioning within the EOS system is optimised for spine, pelvis and lower limb assessment. In order to allow imaging of the spine, individuals assume the 'step-forward' position, with feet shoulder-width apart, left foot positioned approximately 10cm in front of the right and arms elevated in front, with elbows flexed back towards the shoulders or head (see Figure 2). In this position, however, much of the upper limb and hand are obscured making it impossible to perform reliable measurements or carry out hand-wrist based bone age evaluations.

While initial guidelines were not clear about the use in younger children, several studies have been performed successfully at younger ages^{15,45,53}. Below the age of 4, however, the growth plate position may prevent full spino-pelvic and lower limb reconstruction allowing measurement of just 6 of the potential 17 lower limb parameters (femur length, tibial length, total lower limb length, femoral head diameter, mechanical tibio-femoral angle and femoral shaft-mechanical axis angle)⁵³.

I. 3. Bone Age

Bone age is a metric that describes the state of maturity of an individual's skeletal system. By assessing the development of one or more bones, an estimation can be made that may serve as a useful indicator of biological age, and may be compared or contrasted to the chronological age, as described in years, months, weeks, days and hours.

In principal, bone age assessment can be performed by any investigation that aims to quantify maturity based on a feature of bone or the bony skeleton. This includes, but is not limited to, bone morphology as assessed directly or indirectly via an imaging modality, but may also be based on bone density⁷⁰ or even molecular composition (eg racemisation of aspartic acid in dentin⁷¹). Progression towards full maturity is described in relation to that region, however many methods relate a particular state of maturity to a 'typical' chronological age based upon comparison with a large population. While such comparisons are rife with error, they can be clinically helpful, if used carefully.

The assessment of bone age in the living is overwhelmingly performed by evaluation of bone morphology via imaging, predominantly X-ray investigation⁷², as described by the extent of ossification in the developing child.

I. 3.1 The Skeleton and Ossification

Osteogenesis is the process of bone formation, in which mesenchymal tissue is transformed into bone directly (intramembranous ossification) or via a cartilage intermediary stage (endochondral ossification). Intramembranous ossification occurs predominantly in the bones of the skull, whereas endochondral ossification occurs in the limbs, pelvis, vertebrae and most other bones⁷³.

Chondroblasts initially lay down a cartilage-type extracellular material and eventually transition to producing a denser matrix that is receptive to future calcium deposition. Osteoblasts lay down extracellular material and mineralised calcium hydroxyapatite onto the enlarging cartilage scaffold by the process of ossification, which begins in utero and continues deep into the 3rd decade or even later⁷³.

This osteoblast-led ossification process begins at specific foci in each bone. These are the so-called ‘primary ossification centres’. Arising mostly in prenatal life, a wave of ossification proceeds outwards from these centres. After birth, more foci develop, the ‘secondary ossification centres’, of which two types can be identified – *epiphyseal* and *apophyseal*⁷⁴.

- (i) *Epiphyseal secondary ossification centres* appear at the ends of long bones, contribute to the longitudinal growth of the bone, are covered in articular cartilage and typically do not have attachments for tendons or ligaments.
- (ii) *Apophyseal secondary ossification centres* can arise on all types of bone, and typically function as attachment sites for tendons or ligaments to improve stability and allow greater force production.

Ossification of tissue flows out from these starting points, and as radiopaque calcium hydroxyapatite-rich material is deposited we can follow this on the radiograph: bony protrusions and bumps correspond to sites of origins and insertions; while contours and curves correspond to articular surfaces, the edges of bone surfaces and of the growth plate.

While this is a continuous process, the presence or absence of ossification at certain landmarks or features can be clearly seen in a binary fashion. Such indicators may occur at highly variable or unique times; however, many occur at very typical, predictable times. Those predictable markers, which “tend to occur regularly, and in a definitive and irreversible order”⁷⁵ are termed ‘skeletal maturity indicators’. The description and identification of skeletal maturity indicators is the cornerstone of all bone age assessment methods based on morphology.

I. 3.2 History of Bone Age Assessment in Medicine

The use of bone age as a measure of maturity is an ancient concept, indeed, records have been found as far back as ancient Rome describing the use of the emergence of the second molar as an indicator for fitness of young males to enter military service⁷⁶.

Bone age analysis in modern medicine began with the advent of the X-ray and John Poland's 1898 publication of a '*Skiagraphic atlas showing the development of bones of the wrist and hand*'⁷⁷ - a book containing reprints of radiographs and descriptions from children aged 1 to 17 years old. Since then, a multitude of methods have been published, covering many regions of the body, and each reflects the particularities of the region: ranging from as early as intra-uterine life significant changes until late-adolescence; many describe long bones only, others only flat or irregular bones, while others still have many different bone types contained within their region of interest (see Appendix, Supplementary Table 1 for an exhaustive list of all methods accessible via pubmed.gov). Numerous modalities have also been used – from conventional radiography (the most commonly used) to ultrasound, computed tomography and magnetic resonance imaging.

I. 3.3 Role of Bone Age in Medicine

Bone age assessment is commonly used in combination with chronological age to assist with diagnosis, treatment indication and follow-up in paediatric orthopaedics, paediatric endocrinology, forensic medicine and orthodontic dentistry. Typically the bone age is used to assess where an individual lies on their progression towards full maturity, or where an individual lies with relation to the pubertal growth spurt, the time of peak height velocity (PHV). Forensic medicine however applies methods in reverse, using the bone age to make inferences about the possible chronological age of individual - living or deceased.

In orthopaedic medicine, bone age assessment is an essential component of the management of many disorders, most notably scoliosis and limb length discrepancy^{78,79}, and has shown a possible predictive role for contralateral slippage in slipped femoral capital epiphysis (SCFE)^{80,81}. However bone age is not typically a routine component of orthopedic lower limb assessment for most disorders as additional scanning is required.

Paediatric endocrinologists employ bone age investigations in conjunction with chronological age, hormone assays and height velocity when evaluating growth disorders such as constitutional growth delay, familial short stature, congenital adrenal hyperplasia, precocious puberty, or delayed puberty (for example as a result of hypothalamic-pituitary-adrenal axis disorders)⁸².

In dentistry, bone age assessment allows the orthodontist to plan the timing of intervention with respect to development of the face and the pubertal growth spurt⁸³.

Forensic applications typically use bone age in a ‘retrograde’ fashion with regards to the previous techniques, inferring the chronological age from the estimation. Complete or partial specimens are assessed in order to estimate ages for archaeological or criminal investigations. Chronological age estimation in the living is often requested in evaluation of undocumented individuals with regards to immigration status or applicability of penal system (juvenile vs. adult)⁸⁴, and for age confirmation in participation in age-category sport events⁸⁵⁻⁸⁷. It must be noted, however, that such estimates are fraught with error and are not generally regarded as accurate by experts despite the wishes of judiciary or governments⁸⁸.

I. 3.4 Methods for Bone Age Assessment

Two main approaches exist for the estimation of bone age from X-ray morphology – the *atlas method* and the *single region method* (Table 1).

- ***Atlas-based methods*** use images of a reference “normal” skeleton to which a patients’ radiograph may be compared. Such an approach involves matching of the examined bone(s) to the reference images and locating the chronological age that would be appropriate to such a level of skeletal maturity, and results are in the form of bone age ‘years’. These methods are popular as they are easy to learn and use - however they may mislead by implying that growth is a uniform process, and they may not be as accurate as the single-region method. Examples include Greulich-Pyle hand and wrist atlas⁷⁵.

- The ***single-region scoring approach*** describes the development of a region of interest, and results are given in the form of stages or percentages. Values describe the progression towards full maturity of that region only and reach the highest stadium or ‘100% maturity’, when that region of interest has fulfilled its growth potential, irrespective of other regions of the body. These methods are generally more accurate but often take longer to learn and are not as quickly understandable as the values are not reported as ‘years’, in a manner easily comparable with the chronological age. However, this fact means they are less prone to oversimplification or overgeneralisation to the whole body. Methods using this approach include Tanner-Whitehouse⁸⁹, Oxford hip method⁹⁰, Risser method⁹¹, Calcaneus method⁹², and the Hassel-Farman method⁹³.

	Atlas Methods		Single Region of Interest Method	
Hand-wrist	Greulich-Pyle	Greulich & Pyle, 1959 ⁷⁵	Björk	Björk 1967 ⁹⁴
			Fishman†	Fishman 1982 ⁹⁵
			Grave & Brown	Grave & Brown 1976 ⁹⁶
			Oxford Hand-Wrist	Acheson 1954 ⁹⁷
			Sanders	Sanders et al 2008 ⁶³
			Singer†	Singer 1980 ⁹⁸
			Tanner-Whitehouse	Tanner et al. 1972 ⁸⁹
Cervical vertebrae			Hassel-Farman	Hassel & Farman 1995 ⁹³
			Lamparski	Lamparski 1975 ⁹⁹
			Mito	Mito et al. 2002 ¹⁰⁰
			Roman	Roman et al. 2002 ¹⁰¹
Humerus			Walker & Lovejoy	Walker & Lovejoy 1985 ¹⁰²
Elbow			Sauvegrain	Sauvegrain 1962 ¹⁰³
Shoulder			Shaefer	Schaefer et al. 2015 ¹⁰⁴
Clavicle			Schmeling	Schmeling et al. 2004 ¹⁰⁵
First Rib			Michelson	Michelson et al. 1934 ¹⁰⁶
Hip – iliac crest			Risser	Risser 1958 ⁹¹
			Risser ‘plus’	Negrini et al. 2015 ¹⁰⁷
Pubic symphysis			McKern-Stewart	McKern-Stewart 1957 ¹⁰⁸
Hip			Oxford Hip	Acheson 1957 ⁹⁰
			Modified Oxford Hip	Stasikelis et al 1996 ⁸⁰
Femoral diaphysis			Stull	Stull et al 2014 ¹⁰⁹
Fibula			Tsai	Tsai et al. 2016 ¹¹⁰
Knee	Pyle & Hoerr	Pyle & Hoerr, 1969 ¹¹¹	McKern-Stewart	O’Connor et al. 2012 ¹¹²
			Oxford Knee	Acheson 1954 ⁹⁷
Ankle	Hoerr, Pyle & Francis	Hoerr et al. 1962		
Calcaneus			Nicholson	Nicholson ⁹²

Table 1. Popular manual methods of estimating bone age – Atlas methods and Single Region methods. †Methods more commonly used in the practice of orthodontics and dentistry. (See Supplementary Table in the Appendix for a comprehensive list of all methods available in the literature).

I. 3.5 Bone Age Assessment Methods – A Brief Primer

The most common region assessed is the left hand and wrist, using Greulich-Pyle⁷⁵ or Tanner-Whitehouse¹¹³ methods. In these methods an anteroposterior radiograph of the left forearm and carpals is taken using conventional X-ray and evaluation of the presence and shape of secondary ossification centres is performed manually or with digital assistance¹¹⁴. The left side was chosen by anthropologists during the 1900s as it is generally the non-dominant hand, and therefore less likely to be injured⁷⁵. Since then, imaging of the left hand has become routine.

In the management of scoliosis, orthopaedic surgeons often evaluate the excursion of the apophysis of the iliac crest as per the 6-stage Risser system as an alternative to hand-wrist imaging. The method is simple and memorable and the pelvic region is typically visible in the full-leg full-spine (FLFS) images commonly taken during scoliosis investigations, thus negating the need for additional radiographs. While the method is useful for predicting the end of the risk period for scoliosis curve progression^{115,116}, it is not useful for predicting peak height velocity (PHV) as its onset occurs before the first Risser stage has appeared⁷⁸.

I. 3.6 Bone Age Assessment Method Usage by Speciality

The bone age assessment method of choice is generally determined by the age of the patient and preference of the investigator.

Breen et al. surveyed members of the Society of Pediatric Radiology in the United States and found 97.6% respondents favoured the Greulich-Pyle hand-wrist method for over 3 year-olds⁷². Methods applied to the hemiskeleton saw use in the 0-3 year age category but the Greulich-Pyle method remained dominant at 69.8% in 0-1 year olds and 85.9% at 1-3 years old. Similarly, DeSanctis et al. reported 76% percent of European paediatricians¹¹⁷ preferred the Greulich-Pyle method.

Among orthopaedic surgeons, the Risser system is still often favoured, mostly due to its simplicity^{63,91}, or has been replaced by hand⁶³ or elbow¹¹⁸ methods that correlate better with the PHV.

II. PART 1 – SKELETAL MATURATION OF THE LOWER LIMB

II. 1. Introduction

The EOS scanner shows clear potential as a valuable tool for high accuracy, low radiation investigation of adult and paediatric spine and lower limb disorders, specifically in disorders such as idiopathic scoliosis and pre-arthritis conditions which affect significant portions of the population. A more accurate characterisation of the lower limb and its' changes throughout growth in relation to chronological age *and* skeletal maturity of children is essential to establishing what are 'normal' parameters and what are outside of the range of normal. Traditionally popular bone age methods cannot be applied to EOS images taken with the normal positioning protocol, however, as the raised upper limb position obscures the carpal region (shown in figure 2).

Cervical vertebrae bone age assessment is a possible alternative method that has been extensively investigated and seen use in orthodontistry. Several systems of staging based on the morphology of the vertebral body and its' upper and lower margins, have been described and correlation with chronological age and hand-wrist bone age assessed and validated¹¹⁹. The Hassel-Farman method is simple and one of the most commonly used. While few reports comparing the different methods can be found, Roman et al. showed the Hassel-Farman method to have a greater correlation with hand-wrist assessments than Mito's, Lamparski's methods, with a Spearman correlation of 0.995 similar to Roman's own, more complex, method (0.997)¹⁰¹.

II. 1.1. Aims of this Study

In this study we aimed to evaluate the relationship of cervical bone age, as per Hassel-Farman, and lower limb anatomical and biomechanical parameters in a population 2-24 years old. Furthermore, a specific focus was made to the neck-shaft angle, as a parameter of extra importance in orthopaedics.

II.2. MATERIALS AND METHODS

II. 2.1 Population

II. 2.1.1 Lower Limb Evaluation

The examined population was formed of EOS images collected in our department over the course of routine clinic practice from 2007-2012 (see Fig. 4), as reported in 2017⁵³. Patient records were reviewed, yielding a total of 7108 image-pairs, of which 3,473 were in the age group 2-24 years old, and individuals were excluded if they were found to show any biomechanical pathology of the lower limb, history of previous surgery of the lower extremity, previous disease affecting growth or any limb/ body asymmetry. Due to a higher number of older adolescent patients collected, image numbers were limited from the ages of 17-24 years old to 50 cases per year (25 males and 25 females) resulting in 400 cases. From the 2360 aged 2-16 years old, 727 remained after the aforementioned exclusion criteria were applied, for a total of 1127 individuals. sterEOS reconstruction failed in 105 and cervical evaluation was not possible in 17, resulting in 1005 cases.

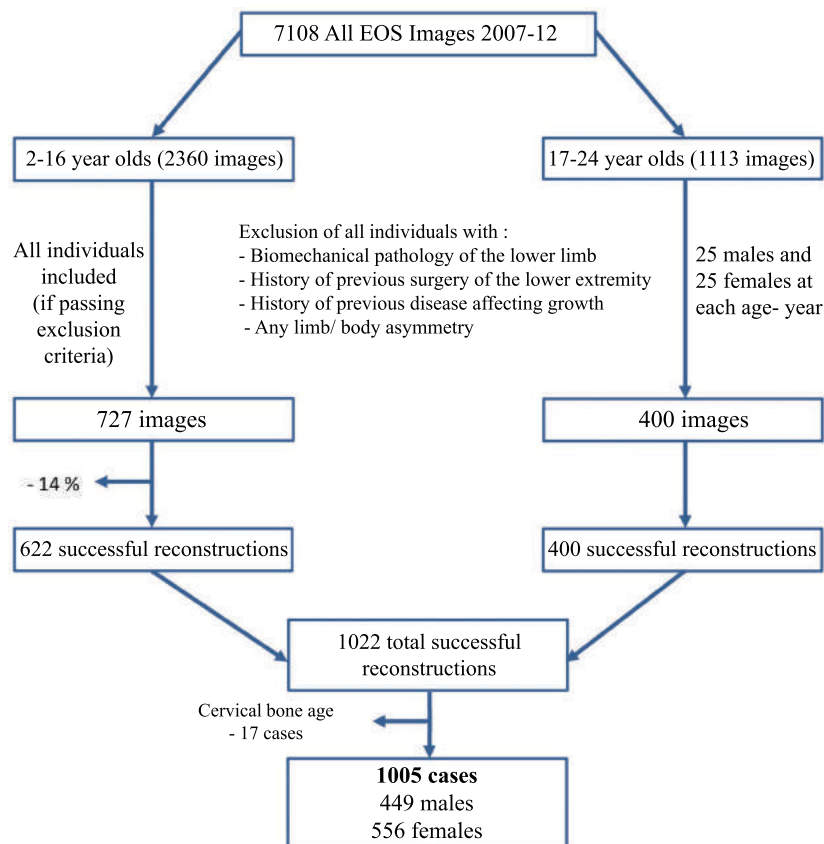


Figure 4. Schematic describing selection process for base population used for measurement of lower limb parameters vs. chronological and cervical bone age.

All images were taken with orthopaedic indications, but individuals were subsequently found to be disease-free, or found to have disorders that do not affect biomechanical parameters (see table 3 for list of indications). Although many subjects included in the study possessed some mild ‘spinal curvature deviation’ possessing a Cobb angle $<10^\circ$, a small study was performed to assess the possible significant differences in lower limb parameters in those children vs. patients lacking any disorder (those with a scan indication classified as “joint pain of unknown origin”). Ten subjects at each bone group and at chronological ages from 9-24 years old were compared with independent t-test.

II. 2.1.2 NSA Assessment population

After the original lower limb study, a closer look at the neck-shaft angle was later performed, however as the EOS software is not recommended for NSA measurement in individuals younger than four, individuals aged 2-3 were excluded from this study (12 individuals). 6 boys and 6 girls from aged 4-9 were randomly selected from our database from 2013 to return the total number to 1005 (449 male, 556 female), see Table 4.

Before the radiological examinations, written consent was obtained from the parents, including permission for the use of images for research purposes. All examinations and works were carried out according to the articles laid out in the Declaration of Helsinki.

	Duration (s)	Voltage (kV)	Power (mA)	DAP (mGy*cm ²)
AP	16.48±2.07	94.05±8.07	192.44±30.75	630.10±206.13
LAT	18.05±3.15	108.14±10.32	224.34±40.09	1067.00±200.34

Table 2. Technical parameters of the EOS system (AP= anteroposterior, LAT= lateral, DAP= dose area product). Values shown are mean ± standard deviation.

Part 1 – Skeletal Maturation of the Lower Limb

Calendar age (year)	Gender	n	Suspected Scoliosis (Cobb angle <10°)	Mild Functional kyphosis	Joint pain with un. orig.	Other
2	Male	4	3	0	0	1
	Female	3	3	0	0	0
3	Male	2	2	0	0	0
	Female	3	3	0	0	0
4	Male	7	4	0	0	3
	Female	13	12	0	1	0
5	Male	14	10	0	1	3
	Female	18	16	0	1	1
6	Male	13	10	0	1	2
	Female	14	13	0	0	1
7	Male	15	10	0	1	4
	Female	18	13	0	0	5
8	Male	16	10	0	1	5
	Female	20	15	0	2	3
9	Male	18	6	1	5	6
	Female	17	11	0	3	3
10	Male	21	12	0	7	2
	Female	20	16	0	2	2
11	Male	21	11	2	6	2
	Female	23	12	1	9	1
12	Male	21	12	2	5	2
	Female	40	32	1	4	3
13	Male	24	11	1	10	2
	Female	39	30	3	5	1
14	Male	25	10	1	12	2
	Female	40	32	2	4	2
15	Male	22	12	1	6	3
	Female	51	29	3	13	6
16	Male	26	19	0	5	2
	Female	37	21	2	13	1
17	Male	25	3	1	19	2
	Female	25	3	1	20	1
18	Male	25	5	1	19	0
	Female	25	5	0	14	6
19	Male	25	4	2	17	2
	Female	25	6	1	17	1
20	Male	25	4	0	20	1
	Female	25	7	1	16	1
21	Male	25	2	2	19	2
	Female	25	3	0	20	2
22	Male	25	1	0	23	1
	Female	25	1	1	21	2
23	Male	25	2	0	21	2
	Female	25	1	0	23	1
24	Male	25	2	0	21	2
	Female	25	1	0	21	3
SUM	Male	449	165	14	219	51
	Female	556	285	16	209	46

Table 3. Lower Limb Evaluation Population 2-24 years old. Indication of scans of population, divided by age and gender. ‘Other’ disorders consisted of mild degenerative signs, bone cysts of various types, juvenile aseptic bone changes, such as osteochondritis of the upper limb.

Calendar Age (Year)	Gender	n	Suspected Scoliosis (Cobb angle <10°)	Mild Functional Kyphosis	Joint Pain of Un. Orig.	Other
4	Male	8	5	0	0	3
	Female	14	13	0	1	0
5	Male	15	11	0	1	3
	Female	19	17	0	1	1
6	Male	14	11	0	1	2
	Female	15	14	0	0	1
7	Male	16	10	0	1	5
	Female	19	14	0	0	5
8	Male	17	10	0	2	5
	Female	21	15	0	3	3
9	Male	19	7	1	5	6
	Female	18	12	0	3	3
10	Male	21	12	0	7	2
	Female	20	16	0	2	2
11	Male	21	11	2	6	2
	Female	23	12	1	9	1
12	Male	21	12	2	5	2
	Female	40	32	1	4	3
13	Male	24	11	1	10	2
	Female	39	30	3	5	1
14	Male	25	10	1	12	2
	Female	40	32	2	4	2
15	Male	22	12	1	6	3
	Female	51	29	3	13	6
16	Male	26	19	0	5	2
	Female	37	21	2	13	1
17	Male	25	3	1	19	2
	Female	25	3	1	20	1
18	Male	25	5	1	19	0
	Female	25	5	0	14	6
19	Male	25	4	2	17	2
	Female	25	6	1	17	1
20	Male	25	4	0	20	1
	Female	25	7	1	16	1
21	Male	25	2	2	19	2
	Female	25	3	0	20	2
22	Male	25	1	0	23	1
	Female	25	1	1	21	2
23	Male	25	2	0	21	2
	Female	25	1	0	23	1
24	Male	25	2	0	21	2
	Female	25	1	0	21	3
SUM	Male	449	164	14	220	51
	Female	556	284	16	210	46

Table 4. NSA assessment population Indication of scans of 4-24 year old population investigated by neck-shaft angle, with respect to age and gender. ‘Other’ disorders consisted of mild degenerative signs, bone cysts of various types, juvenile aseptic bone changes, such as osteochondritis of the upper limb.

II. 2.2.1 Parameters Evaluated

Lower limb evaluations were performed using EOS 3D v1.4.4.5297 software (EOS Imaging, Paris, France). 3D-modelling of both lower limbs was performed, and 14 parameters of the lower limb measured (see Figure 5a-k):

1. Femur mechanical axis length/ 'Femur length' (Fig.5a);
2. Tibia mechanical axis length/ 'Tibia length' (Fig.5a);
3. Lower limb mechanical axis length/ 'lower limb length'(Fig.5a);
4. Femoral head diameter (Fig.5d);
5. Femoral neck length: the distance between the centre of the femoral head and the proximal diaphyseal axis, as measured along the axis of the femoral neck (Fig.5e);
6. Neck-shaft angle (NSA)/ collodiaphyseal angle (Fig.5f). This is the angle between the axes of the femoral neck and the proximal diaphysis;
7. Femoral offset (Fig.5g): the distance between the centre of the femoral head and the closest point along the axis of the femoral shaft;
8. Mechanical tibiofemoral angle (mTFA)/ 'hip-knee-ankle angle' (Fig.5b): the angle between the mechanical axes of the femur (passing from femoral head to the centre of the distal femur) and tibia (passing from the centre of the proximal tibia to the middle of the ankle) in the frontal plane of the knee. By convention values in the varus position are recorded as negative, and in valgus as positive;
9. Femoral mechanical axis-femoral shaft angle (FM-FS)/ hip-knee angle (Fig.5c): the angle between the mechanical and anatomical axes of the femur in the frontal plane of the knee;
10. Femoral mechanical angle (Fig.5k): angle between the femoral mechanical axis and the axis of the femoral condyles;
11. Tibial mechanical angle (Fig.5k): angle between the tibial mechanical axis and the tibial plateau;
12. Femoral version/ femoral torsion (Fig.5h): angle between the axis of the femoral neck and the posterior condylar line, projected on a plane perpendicular to the mechanical axis of the femur;
13. Tibial torsion (Fig.5j): angle between the transmalleolar and transcondylar axes, projected on a plane perpendicular to the mechanical axis of the tibia;

14. Femorotibial rotation (Fig.5i): angle between the tibia and the posterior femoral condylar line.

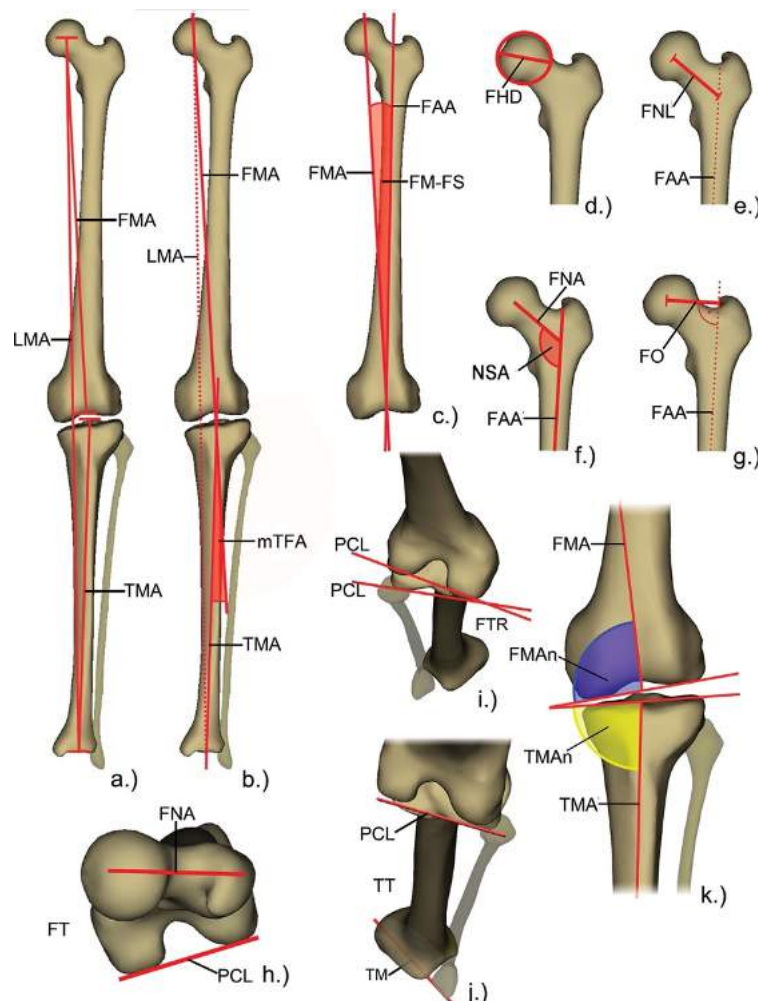


Figure 5. Lower limb parameters measured with the EOS software. NSA, Neck-shaft angle; FAA, Femur anatomical axis; FHD, Femoral head diameter; FMA, Femur mechanical axis; FMA_n, Femoral mechanical angle; FM-FS, Femoral mechanical axis-femoral shaft angle; FNA, Femoral neck axis; FNL, Femur neck length; FO, Femoral offset; FT, Femoral torsion/ femoral version; FTR, Femorotibial rotation; LMA, Lower limb's mechanical axis; mTFA, Mechanical tibiofemoral angle; PCL, posterior condylar line; TM, Transmalleolar line; TMA, Tibia mechanical axis; TMA_n, Tibial mechanical angle; TT, Tibial torsion. [Image reproduced with permission from Schlégl et al. 2013.]

In the 2-3-year-old age group, total 3D modelling was not possible due to the developing epiphyseal cartilages, thus in these cases, we used the “Lower Limb Alignment” mode of the software which assesses just six parameters:

1. Femur length;
2. Tibia length;
3. Limb length;
4. Femoral head diameter;
5. Mechanical tibiofemoral angle;
6. Femoral mechanical axis-femoral shaft angle.

Time taken for reconstruction was a mean of 15 minutes, though the time taken increased with decreasing age, from below the age of 10. Time taken rose to a mean of approximately 25 minutes in the 4-year-old population. The 3D-reconstruction took 2 minutes in “Lower Limb Alignment” mode.

Lower limb biomechanical values were recorded and their correlations with the calendar age and the cervical bone age were investigated using standard deviation (SD), Spearman correlation analysis and linear regression. Multicollinearity was examined with the Variance Inflation Factor (VIF) test. If VIF was greater than 1, then multicollinearity was said to be excluded, in $1 < \text{VIF} < 2$ mild multicollinearity was said to be present but does not significantly influence the results, or the value was over 2 then multicollinearity was deemed incongruent and we rejected the model.

II. 2.2.2 Neck-shaft Angle investigation

To further investigate the neck-shaft angle, the mean NSA value and SD at each chronological age and bone age were calculated and means were compared using independent t-test. The correlation between the NSA value and the chronological age, and the bone age, were each assessed using the Spearman correlation, as above, and linear regression analysis applied. The effect of the NSA on the chronological age and bone age, together and separately, was also assessed using Stepwise Multivariate Regression Analysis as described above.

Gender differences were also assessed using independent t-test and general linear modelling, with gender input as a dummy variable.

II. 2.2.3 Cervical Bone Age Assessment

Cervical bone age assessment based on the morphology of C2, C3 and C4 vertebrae was performed as per the six-stage Hassel-Farman method⁹³ (see Figure 6).

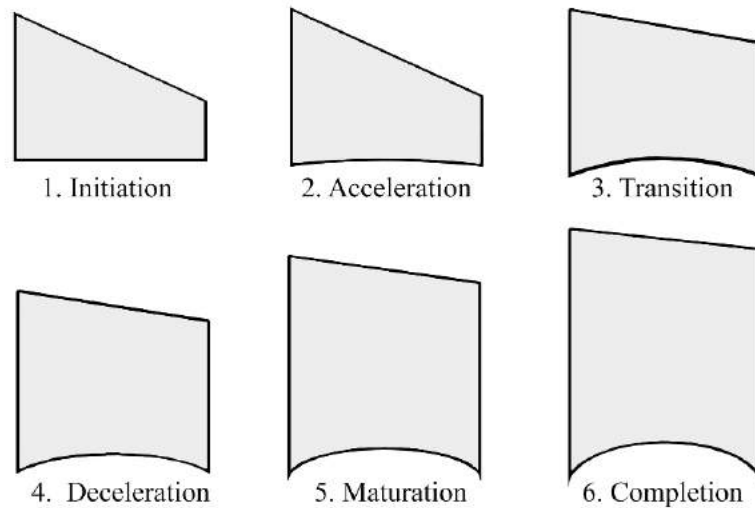


Figure 6. Cervical Vertebral Bone Age Assessment as per Hassel & Farman (1995) (Adapted from Schlégl et al. 2017).

1. **Initiation:** the inferior borders of C2, C3 and C4 are all flat. Upper borders taper from posterior to anterior giving the body a wedge shape;
2. **Acceleration:** C2 and C3 develop concavities in their inferior borders, while that of C4 remains flat. Bodies of C3 and C4 are almost rectangular in shape;
3. **Transition:** Concavities in C2 and C3 are now deeper and distinct with C4 beginning to develop a concave inferior border too. Bodies of C3 and C4 are rectangular in shape;
4. **Deceleration:** C2, C3 and C4 all have distinct concavities in their inferior borders, and the bodies of C3 and C4 are becoming more square in shape.
5. **Maturation:** Concavities of C2, C3 and C4 are more accentuated in the inferior borders, and C3, C4 bodies are almost square or square in shape;
6. **Completion:** Deep concavities are found in the inferior borders of C2, C3 and C4 and the bodies are square or column-like, with a vertical dimension greater than their horizontal dimension.

Reliability with the EOS images was first assessed, in which 55 cases were randomly selected and evaluated on 3 different days by three observers, after being taught the method

by one senior orthopaedic physician and one senior radiologist. Intraclass correlation coefficient (ICC) was estimated and reliability evaluated based on Winers criteria¹²⁰. Next, the method was applied to all 1022 EOS image-pairs, and was successful in all but 17 cases, leaving 1005 evaluations.

II. 2.3. Statistical Analysis

For randomization and selection, the RAND.BETWEEN formula of the Microsoft Excel v14.0.6112.5000 (Microsoft Corp., Redmond, WA) software was used. All statistical data was processed by the SPSS v22 (IBM Corp., Armonk, NY, USA) and by the Microsoft Office Professional Plus v14.0.6112.5000 (Microsoft Corp., Redmond, WA, USA) software packages. A p-value <0.05 was accepted as significant.

II.3. RESULTS

II. 3.1 Reliability Results with Hassel-Farman Cervical Bone Age Method

The ICC values for each observer were ‘excellent’ with intra-observer values of 0.959, 0.953 and 0.949. The inter-observer reliability was 0.976.

II. 3.2 Lower Limb Evaluation

Descriptive statistics of the measured lower limb parameters vs. chronological age and cervical bone age are shown in Figure 7 (a-m) and Table 6, see below for NSA values.

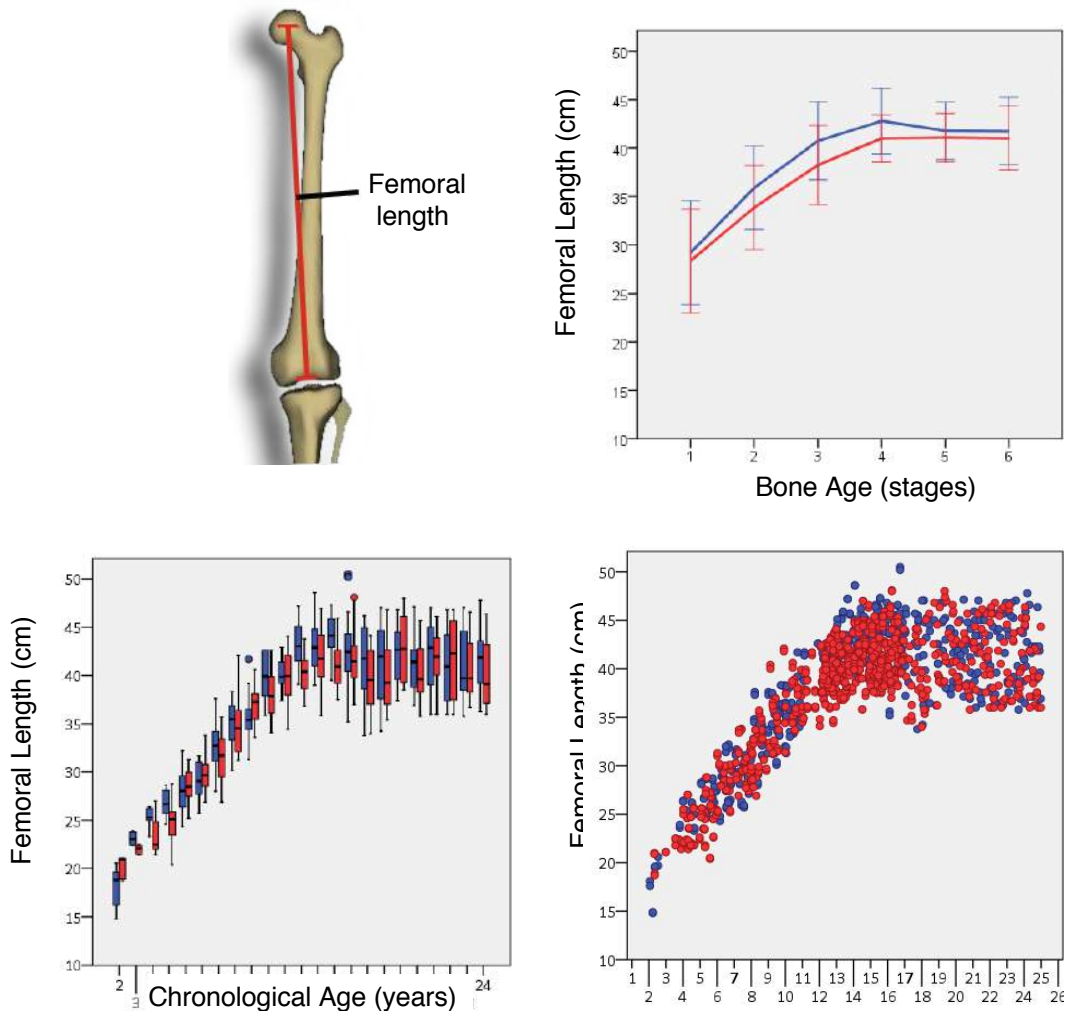


Figure 7. (a) . Femoral length vs. chronological age, cervical bone age. Error bars indicate \pm standard deviation. (Males = blue, females = red).

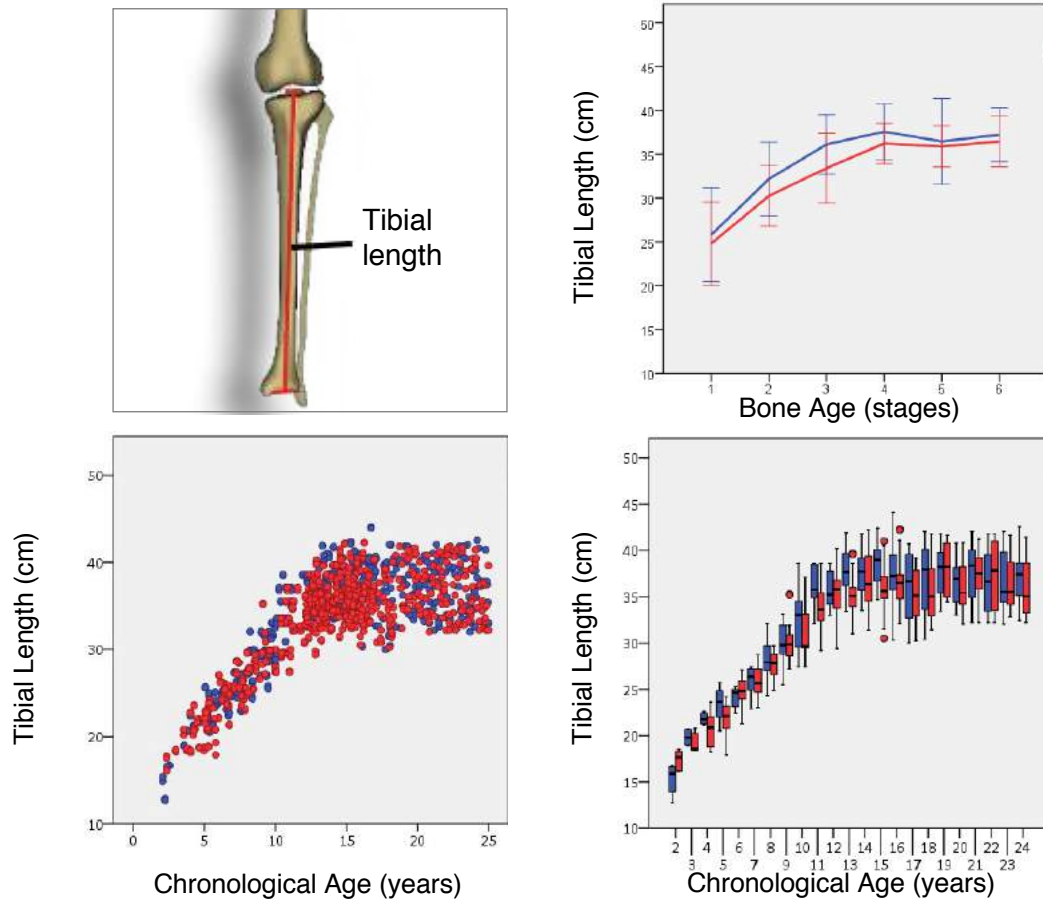


Figure 7. (b) . Tibial length vs. chronological age, cervical bone age.

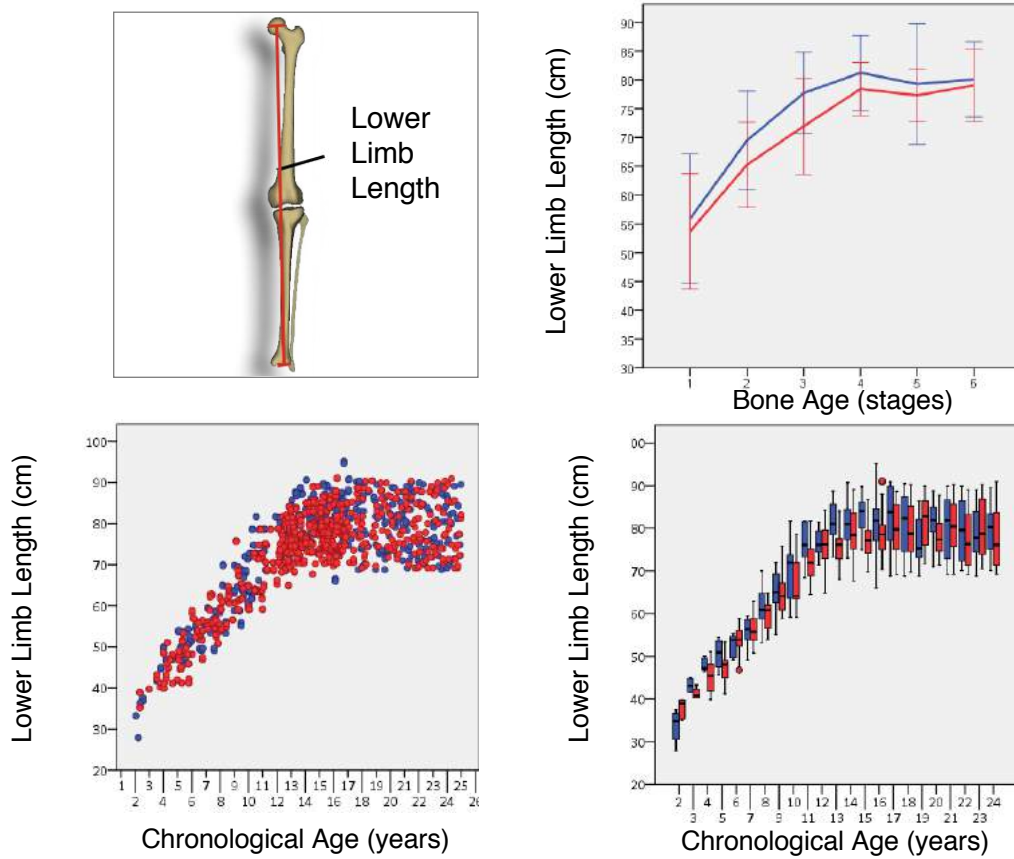


Figure 7. (c) . Lower limb length vs. chronological age, cervical bone age.

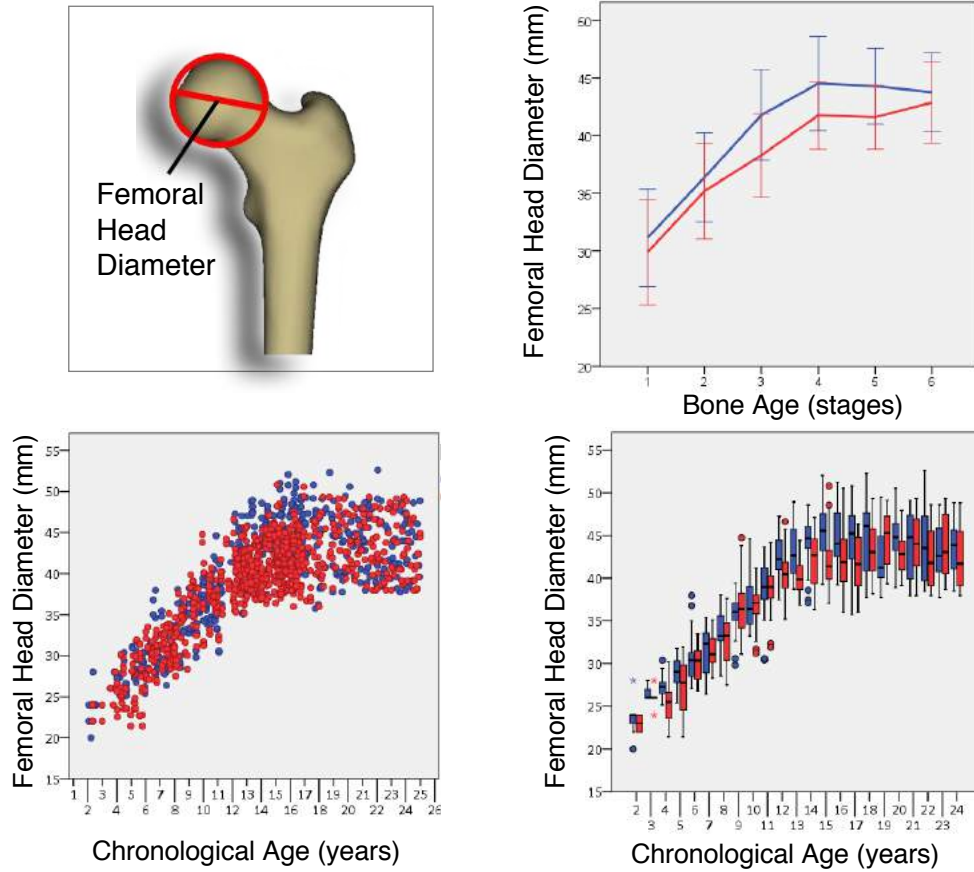


Figure 7. (d) . Femoral diameter vs. chronological age, cervical bone age.

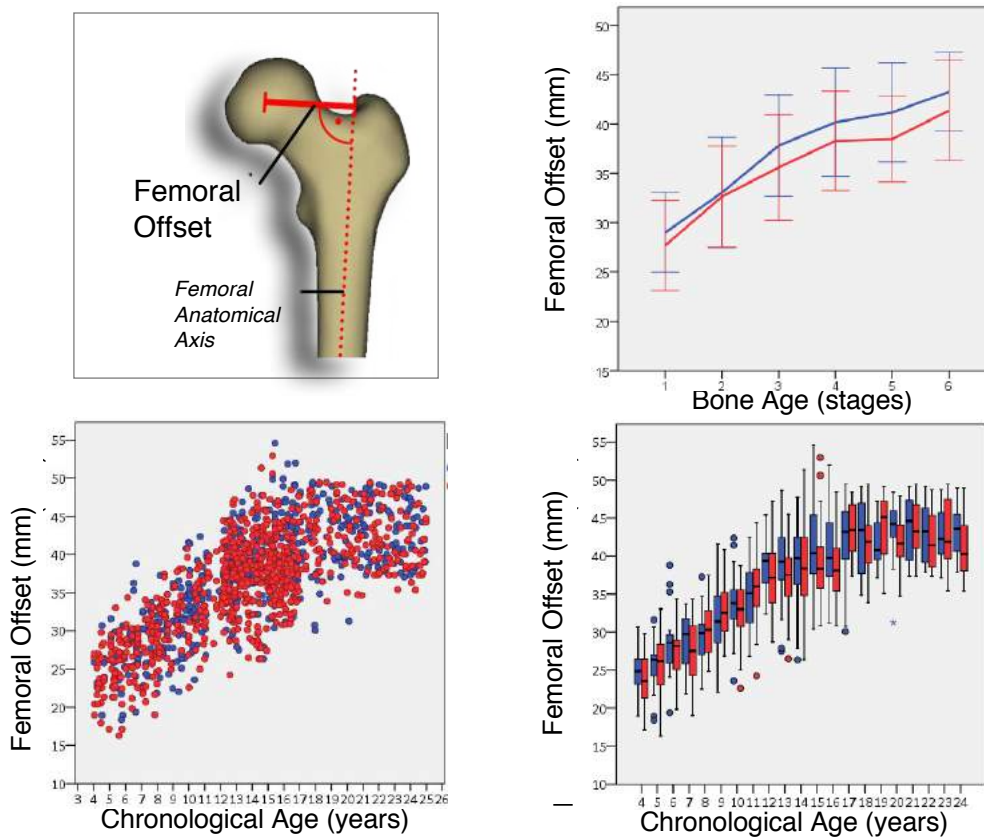


Figure 7. (e) . Femoral offset vs. chronological age, cervical bone age.

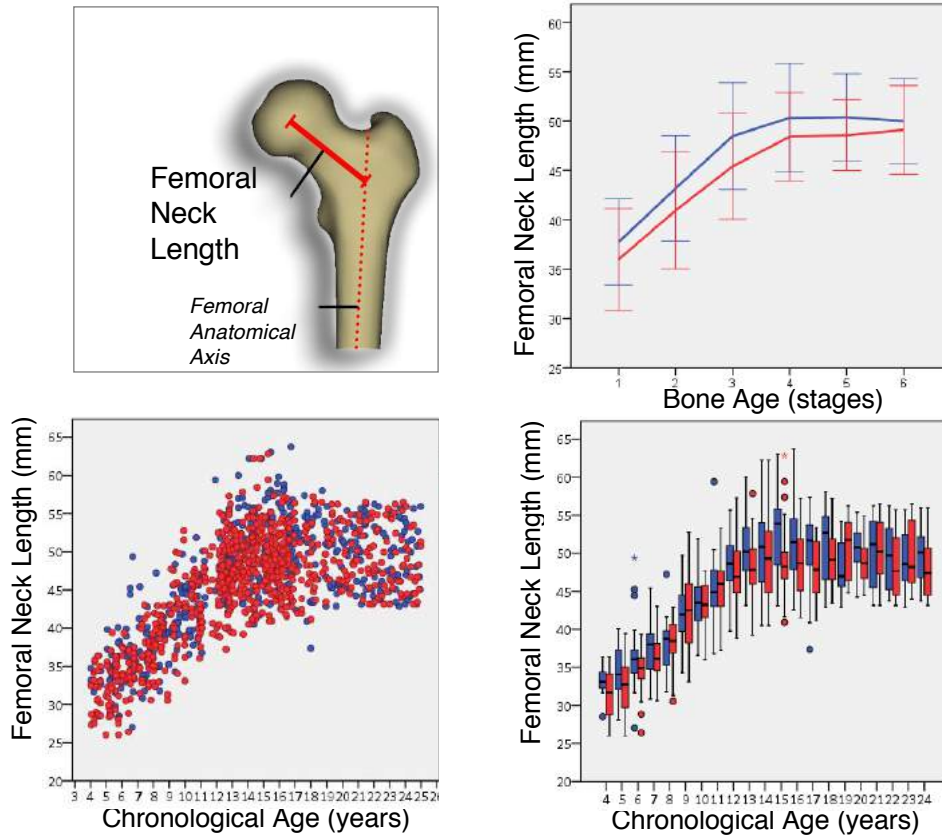


Figure 7. (f) . Femoral neck length vs. chronological age, cervical bone age.

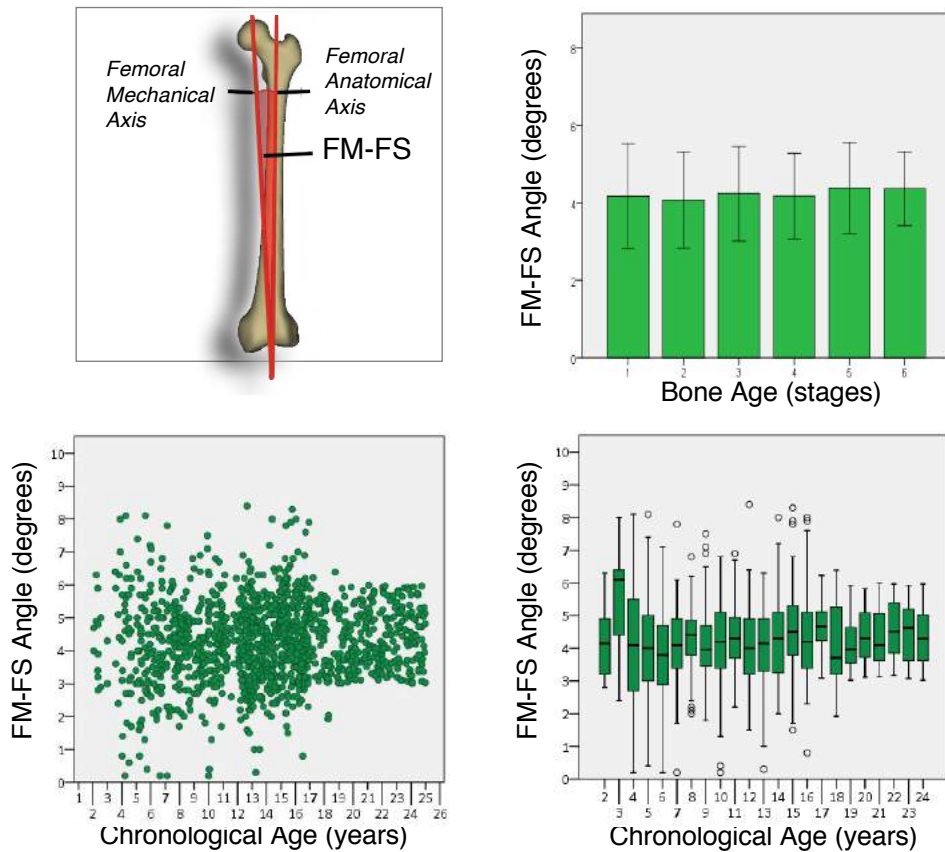


Figure 7. (g) . Femoral Mechanical – Femoral Shaft Angle. FM-FS vs. chronological age, cervical bone age.

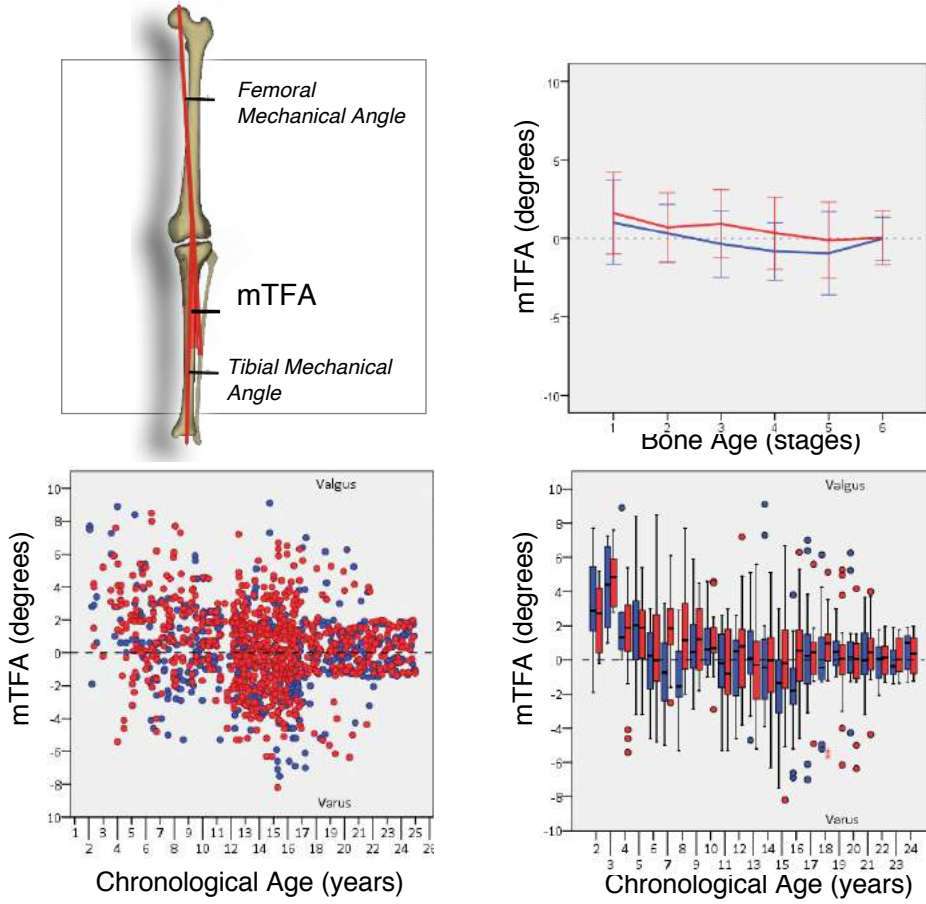


Figure 7. (h) . Mechanical tibio-femoral angle (mTFA) vs. chronological age cervical age, bone age.

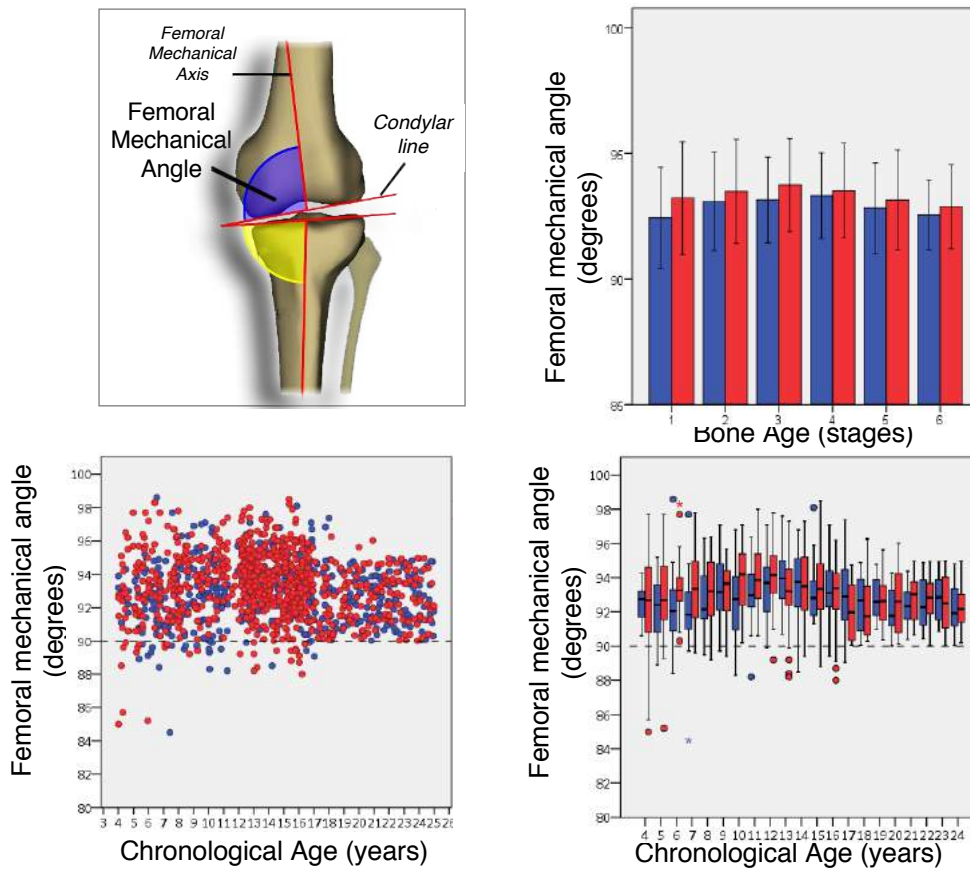


Figure 7. (i) . Femoral mechanical angle vs. chronological age, cervical bone age.

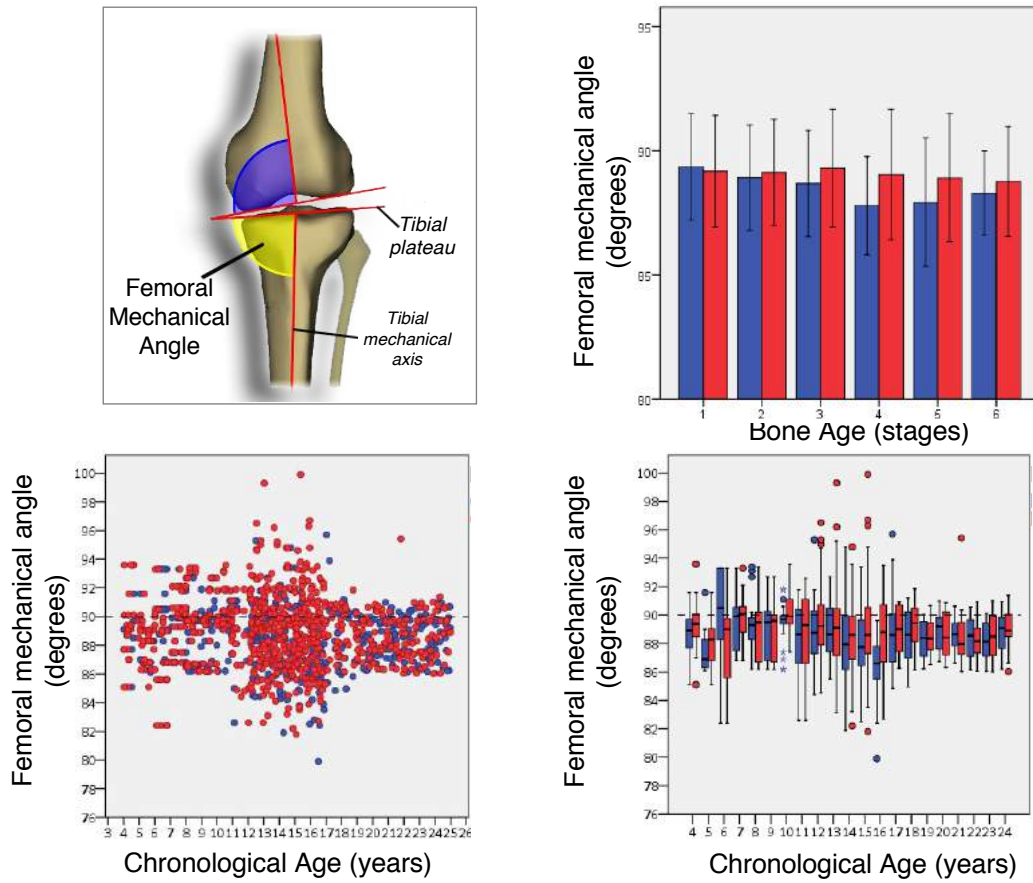


Figure 7. (j) . Tibial mechanical angle vs. chronological age, cervical bone age.

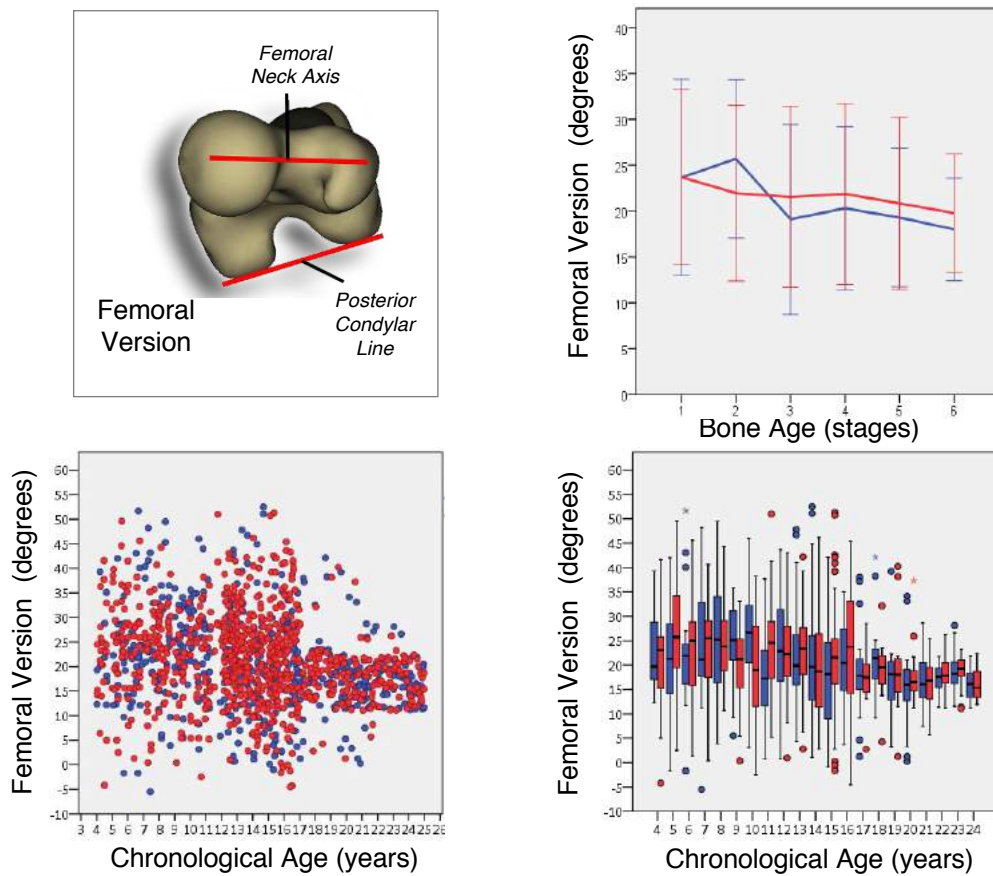


Figure 7. (k) . Femoral version vs. chronological age, cervical bone age.

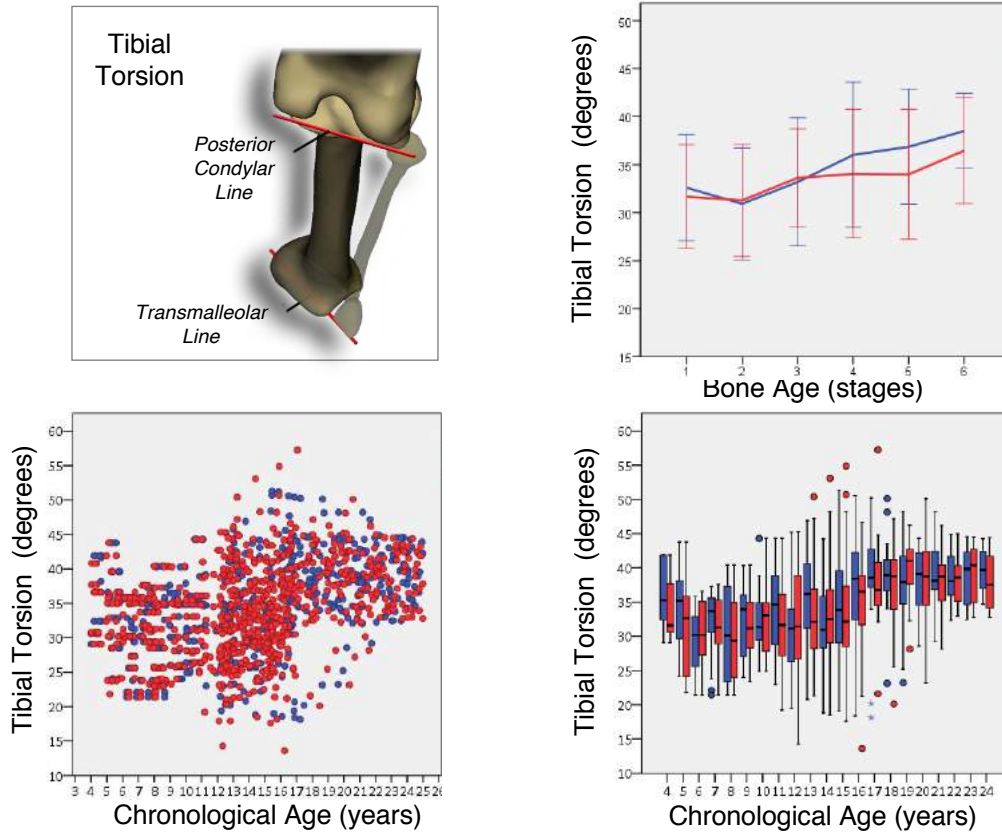


Figure 7. (l) . Tibial torsion vs. chronological age, cervical bone age.

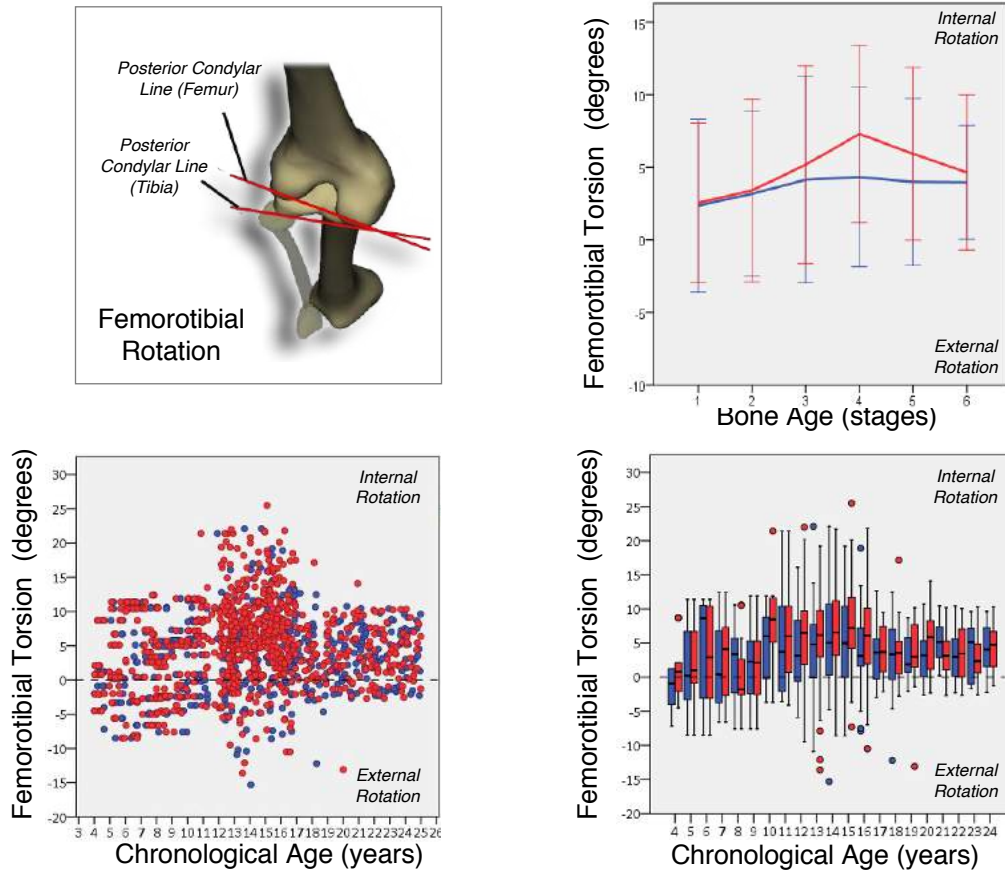


Figure 7. (m) . Femerotibial torsion vs. chronological age, cervical bone age.

Significant correlations were seen between lower limb parameters and chronological age in all metrics ($p < 0.05$) (Table 5). A positive correlation, with increasing values in association with increasing age, were seen in height, femur length, tibial length, limb length, femoral head diameter, femoral offset, neck length, tibial torsion, femorotibial rotations and FMFS angle while a negative correlation was seen at NSA, mechanical tibiofemoral angle, femoral mechanical angle, tibial mechanical angle and femoral torsion.

Analysis of lower limb correlation with cervical bone age also yielded significant results in all parameters. In five of the fourteen measured parameters, bone age showed a greater correlation than chronological age, which was small but significant ($p < 0.005$). These five parameters were the NSA (-0.164 vs. 0.13), femoral mechanical angle (-0.082 vs. -0.080), femoral torsion (-0.292 vs. -0.153), tibial torsion (0.240 vs. 0.146) and femorotibial torsion (0.345 vs. 0.187).

Parameter	Bone age		Chronological age	
	Correlation Coefficient	P	Correlation Coefficient	P
Bone age	-	-	-	-
Calendar age	0.852	<0.001	-	-
Height	0.772	<0.001	0.811	<0.001
Femur length	0.747	<0.001	0.781	<0.001
Tibia length	0.673	<0.001	0.766	<0.001
Lower limb length	0.582	<0.001	0.763	<0.001
Femoral head diameter	0.682	<0.001	0.738	<0.001
Femoral offset	0.664	<0.001	0.743	<0.001
Femur neck length	0.691	<0.001	0.703	<0.001
Neck-shaft angle	-0.164	<0.001	-0.130	<0.001
Mechanical tibiofemoral angle (mTFA)	-0.214	<0.001	-0.247	<0.001
Femoral mechanical angle	-0.082	0.027	-0.080	<0.001
Tibial mechanical angle	-0.117	<0.001	-0.119	<0.001
Femur mechanical axis – femoral shaft angle (FM-FS)	0.071	0.009	0.091	0.001
Femoral torsion	-0.292	<0.001	-0.153	<0.001
Tibial torsion	0.240	<0.001	0.146	<0.001
Femorotibial rotation	0.345	<0.001	0.187	0.001

Table 5. Correlations between the measured lower limb parameters and the cervical bone age and chronological age, assessed by Spearman correlation coefficient. [Reproduced from Schlégl et al. 2017.]

Part 1 – Skeletal Maturation of the Lower Limb

Bone Age	1		2		3		4		5		6	
	Male	Female	Male	Female	Male	Female	Male	Female	Male	Female	Male	Female
n	67 / 61*	82 / 76*	40	47	47	67	63	84	85	117	147	159
Femur Length (cm)	29.19 ± 5.36	28.36 ±5.36	35.90 ±4.30	33.87 ±4.31	40.74 ±4.02	38.24 ±4.09	42.79 ±3.39	41.01 ±2.45	41.78 ±2.94	41.08 ±2.49	41.73 ±3.48	41.01 ± 3.29
Tibia Length (cm)	25.81 ±5.33	24.82 ±4.74	32.17 ±4.22	30.24 ±3.43	36.11 ±3.37	33.40 ±3.99	37.56 ±3.17	36.22 ±2.28	36.45 ±4.88	35.87 ±2.34	37.21 ±3.05	36.46 ± 2.91
Lower Limb Length (cm)	55.89 ±11.22	53.68 ±10.03	69.46 ±8.56	65.25 ±7.38	77.69 ±7.07	71.95 ±8.34	81.23 ±6.48	78.40 ±4.63	79.28 ±10.48	77.31 ±4.54	80.08 ±6.53	79.04 ± 6.35
Femoral Head Diameter (mm)	31.13 ±4.22	29.88 ±4.55	36.37 ±3.85	35.18 ±4.16	41.78 ±3.92	38.29 ±3.62	43.93 ±6.63	41.75 ±2.92	44.28 ±3.28	41.59 ±2.75	43.76 ±3.42	42.86 ± 3.52
Femoral* Offset (mm)	29.00 ±4.04	27.69 ±4.57	33.05 ±5.58	32.64 ±5.09	37.80 ±5.14	35.59 ±5.35	40.13 ±5.53	38.28 ±5.03	41.17 ±5.03	38.45 ±4.35	43.24 ±4.00	41.36 ±5.08
Femoral Neck Length* (mm)	37.73 ±4.36	35.97 ±5.15	43.17 ±5.35	40.94 ±5.91	48.47 ±5.39	45.40 ±5.34	50.22 ±5.46	48.41 ±4.49	50.39 ±4.40	48.56 ±3.59	49.99 ±4.29	49.09 ±4.48
mTFA (°)	1.01 ±2.68	1.60 ±2.60	0.31 ±1.83	0.70 ±2.22	-0.36 ±2.12	0.93 ±2.18	-0.81 ±1.84	0.33 ±2.29	-0.94 ±2.65	-0.13 ±2.43	-0.03 ±1.38	0.03 ±1.73
Femur Mech. Angle* (°)	92.43 ±2.02	93.22 ±2.24	93.09 ±1.96	93.49 ±2.07	93.15 ±1.71	93.75 ±1.85	93.31 ±1.71	93.52 ±1.88	92.82 ±1.80	93.15 ±1.99	92.55 ±1.41	92.87 ±1.67
Tibial Mech. Angle* (°)	89.35 ±2.13	89.17 ±2.25	88.92 ±2.12	89.13 ±2.14	88.68 ±2.15	89.29 ±2.38	87.79 ±1.97	89.04 ±2.63	87.92 ±2.58	88.90 ±2.58	88.29 ±1.70	88.76 ±2.21
FM-FS (°)	4.06 ±1.37	4.26 ±1.34	4.07 ±1.44	4.08 ±0.98	4.26 ±1.33	4.22 ±1.12	4.26 ±1.15	4.13 ±1.08	4.36 ±1.28	4.39 ±1.13	4.39 ±0.86	4.35 ±1.01
Femoral Version* (°)	23.67 ±10.7	23.71 ±9.53	25.68 ±8.63	21.95 ±9.58	19.10 ±10.36	21.53 ±9.87	20.30 ±8.91	21.87 ±9.88	19.28 ±7.56	20.84 ±9.37	18.00 ±5.61	19.77 ±6.44
Tibial Torsion* (°)	32.60 ±5.56	31.65 ±5.43	30.92 ±5.83	31.27 ±5.83	33.20 ±6.66	33.62 ±5.13	33.52 ±8.14	32.06 ±7.04	32.16 ±7.13	32.89 ±6.87	28.34 ±5.01	29.83 ±5.85
Fem. tibial Rotation* (°)	2.36 ±5.95	2.55 ±5.50	3.17 ±5.68	3.40 ±6.29	4.15 ±7.12	5.18 ±6.82	4.34 ±6.19	7.30 ±6.12	3.99 ±5.76	5.93 ±5.95	3.96 ±3.92	4.65 ±5.35

Table 6. Changes in lower limb biomechanical parameters with respect to cervical bone age, as estimated by Hassel Farman method. Values shows are Mean ± Standard Deviation. (mTFA = mechanical tibiofemoral angle, FM-FS = Femur mechanical axis – femoral shaft angle) As only ‘Lower limb alignment mode’ could be applied for sterEOS reconstructions in 2 and 3 year olds, n values differ in 8 of the parameters (marked with an *). All of these individuals fell into Bone Age Stage 1.

Calculated linear model data are shown in table 7. Femoral mechanical angle, tibial mechanical angle and FMFS angles were best correlated with models based on the chronological age alone. The NSA, mTFA, femoral torsion, tibial torsion and femorotibial rotation however correlated best with mixed models combining both bone age and chronological age. Femoral, tibial and limb length, femoral head diameter, femoral offset and femoral neck length were better correlated with height than either chronological or cervical bone age.

Parameter	Calculated linear model	Beta coefficient	VIF
Femur length	Height	0.856	-
Tibia length	Height	0.811	-
Limb length	Height	0.912	-
Femoral head diameter	Height	0.912	-
Femoral offset	Height	0.834	-
Femur neck length	Height	0.857	-
Neck-shaft angle	Bone age - Calendar age	-0.322	0.875
Mechanical tibiofemoral angle (mTFA)	Calendar age - Bone age	-0.189	1.257
Femoral mechanical angle	Calendar age	-0.080	-
Tibial mechanical angle	Calendar age	-0.115	-
Femur mechanical axis - shaft angle (FM-FS)	Calendar age	0.093	-
Femoral torsion	Bone age - Calendar age	-0.240	0.741
Tibial torsion	Bone age - Calendar age	0.335	0.984
Femorotibial rotation	Bone age - Calendar age	0.237	1.356

Table 7. The calculated linear models based on stepwise regression analysis and variance inflation factor test (VIF). Beta-coefficient reflects the efficacy of the bone age, calendar age or height as a discriminating variable to separate discrete groups within the parameters. [Reproduced from Schlégl et al. 2017.]

II. 3.3 Neck-shaft angle – a closer look

A closer look at NSA values in relation to chronological and bone age are shown in tables 8 and 9, respectively. With respect to chronological age, the NSA started at average value $131.89^\circ \pm 6.07^\circ$ at 4 years old and fell thereafter to a mean value of $128.85^\circ \pm 4.46^\circ$ at 16, followed by a slower decrease until the age of 20, with mean value $127.81^\circ \pm 3.84^\circ$.

Chronological Age (Year)	N	Minimum	Maximum	Mean	Standard Deviation
4	22	121	140	131.89	6.072
5	34	121	140	129.91	5.627
6	29	123	137	130.50	4.076
7	35	117	143	130.46	6.265
8	38	118	141	129.81	5.171
9	37	121	143	131.52	6.070
10	41	122	145	131.40	6.434
11	44	117	138	129.82	4.956
12	61	121	142	129.85	5.167
13	63	121	143	130.68	5.195
14	65	120	143	130.58	6.146
15	73	120	140	129.25	4.704
16	63	119	135	128.85	4.464
17	50	123	132	128.43	3.485
18	50	121	133	128.40	3.273
19	50	123	135	127.96	3.454
20	50	120	135	127.81	3.842
21	50	121	133	127.70	3.472
22	50	118	134	127.88	3.822
23	50	122	136	127.75	3.910
24	50	124	132	127.31	3.179
Overall	1005				4.704

Table 8. Neck-shaft angle and chronological age - maximum, minimum and standard deviation values recorded (values in degrees). [Reproduced from O'Sullivan et al. 2020].

NSA values with respect to cervical bone age fell from a mean $130.91^{\circ} \pm 4.26^{\circ}$ at stage 1 to $128.07^{\circ} \pm 3.36^{\circ}$ by stage 6.

In addition to the small but stronger correlation seen between NSA and bone age (-0.164 vs. -0.130), previously reported, univariate linear regression found statistically significant models with bone age exhibiting a slightly higher R^2 value ($R^2= 0.101$ vs. 0.069 , beta-coefficient -0.286 vs. -0.264 , standard error of the estimate 4.001 vs. 4.176 , respectively).

Bone Age (Stage)	N	Minimum	Maximum	Mean	Standard Deviation
1	142	121	143	130.91	4.259
2	94	117	145	129.17	6.061
3	114	120	143	129.91	4.374
4	147	119	144	130.40	4.140
5	202	118	142	128.90	4.174
6	306	120	143	128.07	3.358
Total	1005				4.394

Table 9. Neck-shaft angle and bone age - maximum, minimum and standard deviation values recorded with respect to cervical bone age (values in degrees). [Reproduced from O’Sullivan et al. 2020].

When gender was added as a discriminating variable, investigation by t-test found a statistically significant difference in NSA values between males and females in chronological age-based assessment ($p=0.035$), however, with bone age-based analysis there was no significant difference ($p=0.265$). General linear modelling additionally found a small but statistically significant effect from gender compared to chronological age ($R^2=0.082$, $p<0.001$). No significant effect was found when gender was compared to bone age ($R^2=0.073$, $p=0.12$).

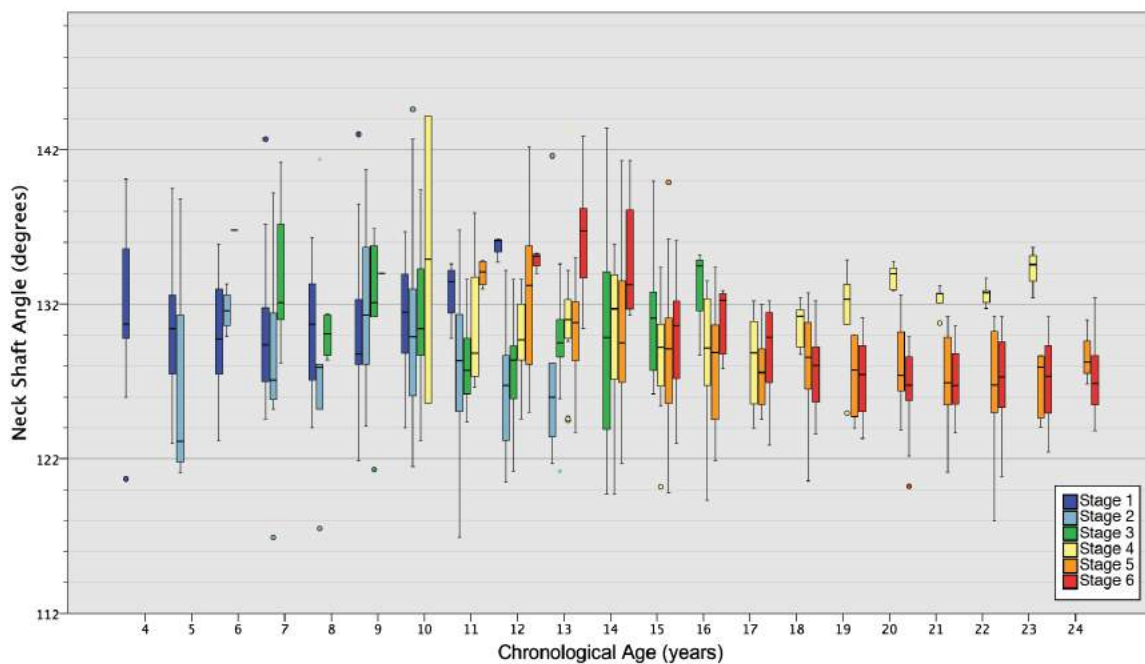


Figure 8. Boxplots representing the neck-shaft angle values vs. cervical bone age and chronological age of individuals from 4-24 years old. [Reproduced from O’Sullivan et al. 2020].

The boxplots in Figure 8 represent the bone age of individuals across all chronological ages. On further investigation, statistically significant differences were found between those children and adolescents with an elevated or delayed bone age compared to those of the same calendar age (see Figure 9). Individuals with a bone age of 2 or more stages above those at the same chronological age had a mean NSA 3.16° higher than their peers ($p < 0.001$), while those with a delayed bone age (2 or more stages below their peers) showed an average NSA that was 4.45° higher ($p < 0.001$). ‘Elevated’ and ‘delayed’ categories contained individuals with an age more than one standard deviation from the mean (outside of 68% of the population), with the exception of 65.5% of those aged 12, due to a particularly wide range of bone ages at this age-year. Overall, a mean 83.38% of individuals at each chronological age were found to lie at, or ≤ 1 stage from, the same bone age stage (the so-called ‘typical’ bone age stage).

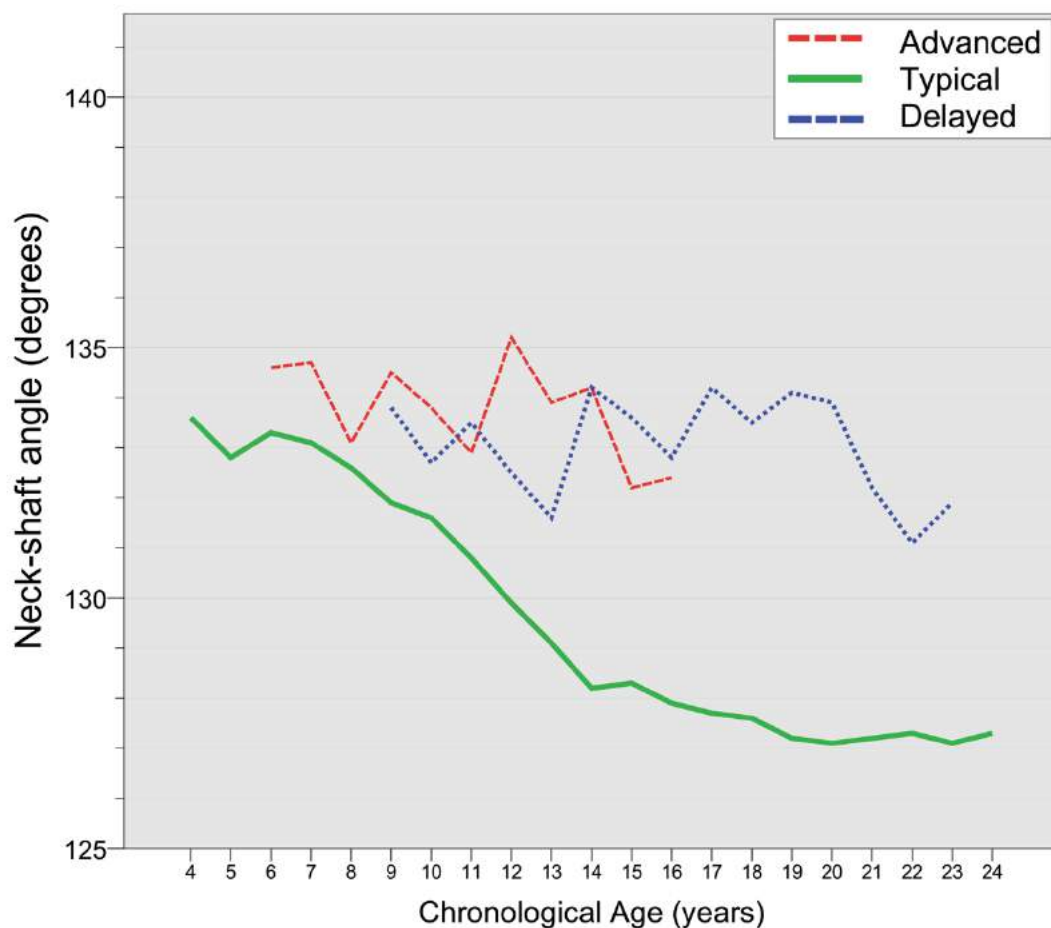
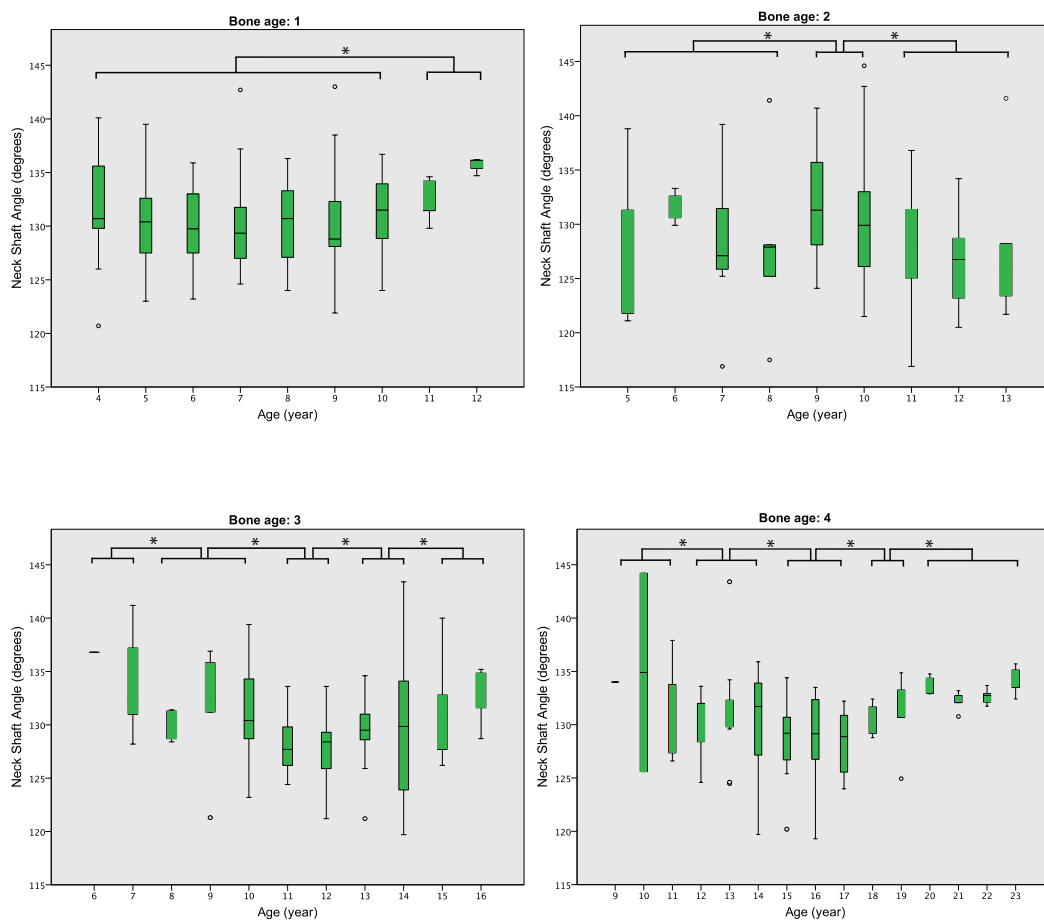


Figure 9. Neck-shaft angle vs. chronological age, sub-stratified by ‘delayed’ or ‘advanced’ cervical bone age. Individuals with a ‘delayed’ or ‘advanced’ bone age (≥ 2 bone age stages from the ‘typical’ stage seen by their peers) exhibited significantly elevated neck-shaft angles by a mean 4.45° and 3.16° , respectively ($p < 0.001$). [Reproduced from O’Sullivan et al. 2020].

Similarly, chronologically older and younger individuals at each bone age stage showed significantly higher neck-shaft angles compared to the others of the same stage (figure 10, or see Table 10 for population distribution). At stage 1, those aged eleven and twelve years old had significantly higher NSAs than the younger individuals of the same stage (133.1° , 134.8° vs. 130.9° , $p=0.002$, $p=0.032$). In stages 3 and 4 both younger and older individuals showed higher NSA angles with stage 3 values of 131.9° , 130.6° & 129.3° , 130.6° vs. 127.2° ($p=0.041$, <0.001 , 0.029 , 0.039) respectively, and in stage 4, 132.2° , 130.0° & 131.1° , 133.3° vs. 128.1° ($p=<0.001$, 0.022 , 0.004 , 0.011), respectively. At stages 5 and 6, NSA values were found to be higher if individuals were younger - 11 & 12 year-olds in stage 5 had values of 135° & 131.7° , respectively, while 13-23 year-olds showed mean 128° ($p<0.001$, <0.001). Younger individuals in stage 6 were found to have mean NSA 134.9° and 131° vs. 126° ($p<0.001$, <0.001). Although statistically significant difference between younger and older age groups was seen at bone age stage 2 a clear trend was not seen.



Part 1 – Skeletal Maturation of the Lower Limb

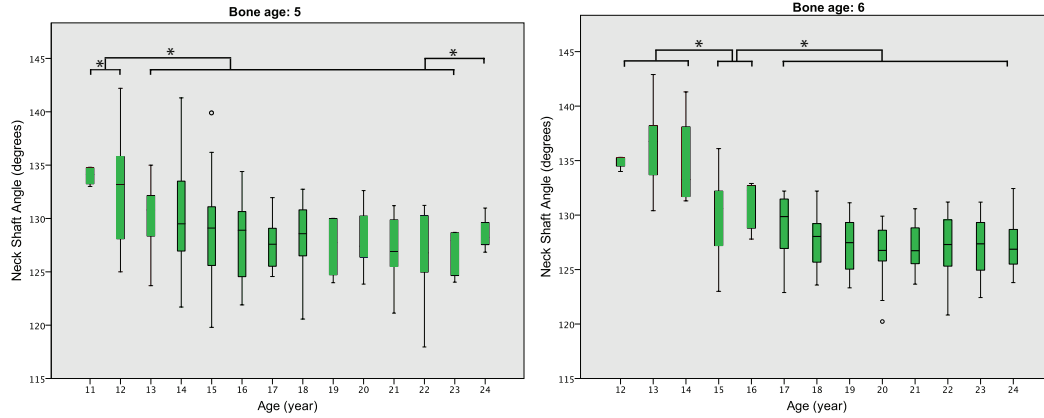


Figure 10. Neck-shaft angle at each cervical bone age stage, sub-stratified by chronological age. Individuals who were chronologically older or younger within one bone age stage, exhibit significantly higher neck-shaft angles at most bone age stages. [Reproduced from O’Sullivan et al. 2020].

Age (years)	Bone age stage						SUM	Age (years)	Bone age stage						SUM	
	1	2	3	4	5	6			1	2	3	4	5	6		
4	22						22	4	100.0%							2.2%
5	30	4					34	5	88.2%	11.8%						3.4%
6	22	5	2				29	6	75.9%	17.2%	6.9%					2.9%
7	17	12	6				35	7	48.6%	34.3%	17.1%					3.5%
8	19	12	7				38	8	50.0%	31.6%	18.4%					3.8%
9	10	19	7	1			37	9	27.0%	51.4%	18.9%	2.7%				3.7%
10	13	13	11	4			41	10	31.7%	31.7%	26.8%	9.8%				4.1%
11	6	10	15	7	6		44	11	13.6%	22.7%	34.1%	15.9%	13.6%			4.4%
12	3	13	19	8	12	6	61	12	4.9%	21.3%	31.1%	13.1%	19.7%	9.8%		6.1%
13		6	21	15	13	8	63	13		9.5%	33.3%	23.8%	20.6%	12.7%		6.3%
14			12	18	27	8	65	14			18.5%	27.7%	41.5%	12.3%		6.5%
15			11	17	33	12	73	15			15.1%	23.3%	45.2%	16.4%		7.3%
16			3	20	32	8	63	16			4.8%	31.7%	50.8%	12.7%		6.3%
17				14	13	23	50	17					28.0%	26.0%	46.0%	5.0%
18				8	18	24	50	18					16.0%	36.0%	48.0%	5.0%
19				8	5	37	50	19					16.0%	10.0%	74.0%	5.0%
20				7	11	32	50	20					14.0%	22.0%	64.0%	5.0%
21				7	12	31	50	21					14.0%	24.0%	62.0%	5.0%
22				7	8	35	50	22					14.0%	16.0%	70.0%	5.0%
23				6	7	37	50	23					12.0%	14.0%	74.0%	5.0%
24					5	45	50	24						10.0%	90.0%	5.0%
SUM	142	94	114	147	202	306	1005	SUM	14%	9%	11%	15%	20%	30%		

Table 10. Distribution of bone ages and chronological ages across the neck-shaft angle population (1005 children and adolescents, 4-24 years old). [Reproduced from O’Sullivan et al. 2020].

Analysis by multivariate linear regression found that changes in the NSA were predicted most accurately when a combined model utilizing both chronological and bone age was used ($R^2= 0.226$, beta-coefficient=-0.322, $p<0.001$, standard error of the estimates (SE)= 3.809, VIF=0.875; vs. univariate linear regression values $R^2=0.101$, 0.069).

After investigation by t-test, no significant difference was found in lower limb parameter values between individuals with mild spinal deviation and those with other indications ($p>0.05$).

II.4. DISCUSSION

II. 4.1 Lower Limb Biomechanical Parameters in the Developing Child

The lower limb plays a vital role in locomotion and balance. A combination of factors influence its function, and the actions needed for upright motion and balance require an interplay between the dynamic elements of the neuromuscular system and the fixed biomechanical parameters ie. the bony skeleton. The lower limb of the developing child and adolescent is constantly changing and if the bony biomechanical parameters exceed the range of normal it can be indicative of a developing disorder or pre-disease state^{5,12,52}

In this study, the results showed clear differences in how many lower limb parameters correlate with the chronological and bone age. Spearman correlation analysis with both the chronological and cervical bone age yielded significant results in all parameters, with bone age found to have a small but significant stronger correlation in five of the fourteen measured parameters ($p < 0.005$), specifically the NSA, femoral mechanical angle, femoral torsion, tibial torsion and femorotibial torsion.

While current lower limb standards have been typically assessed with reference to chronological age, our data may suggest that bone age should be included as a component of lower limb orthopaedic evaluation of the child. For a deeper look at the lower limb parameters assessed in this study, we can describe the parameter as being of one of two types: (i) Longitudinal, or; (ii) Rotational / Torsional.

II. 4.1.2 Longitudinal parameters

According to our findings, the longitudinal parameters of the lower limb showed a greater correlation with the calendar age than with the bone age (Table 5). Although bone age also correlated with these features, often exhibiting strong correlations, the chronological age was stronger – notable are femoral length (CA vs BA $\rho = 0.781$ vs 0.747), tibial length (0.766 vs 0.673), total lower limb length (0.763 vs 0.582) and femoral neck length (0.703 vs 0.691).

While bone age might have been expected to more closely correlate with the longitudinal parameters, indeed it used to assist in the management of leg limb discrepancy, it is perhaps an informative and important lesson regarding the unpredictability of growth. While Dimeglio recommends the use of more than one bone age method in addition to Tanner staging, he still insists that serial measurement must be performed on each child as bone age is still “the most impalpable and the most indiscernible parameter”¹.

Little et al. found in their study that bone and chronological age were no better than each other for predicting longitudinal growth in 120 patients⁷⁸. While some authors have since disagreed with Littles’ conclusions, our findings do not, although rotation features were not assessed in their study.

II. 4.3 Rotational / Torsional parameters

In contrast to longitudinal features, rotational parameters measure were found to have a stronger Spearman correlation to cervical bone age than the chronological age (Table 5). ‘Rotational’ parameters were femoral version (CA vs BA $\rho = -0.153$ vs. -0.292), tibial torsion (0.146 vs. 0.240), femorotibial rotation (0.187 vs. 0.345) and femoral mechanical angle (-0.080 vs. -0.082 , N.S.)

Although a Spearman correlation coefficient of 0.2-0.4 is regarded as weak, these ρ values were still significantly stronger than those with calendar age, so bone age could perhaps assist with such difficult-to-assess parameters.

Reasons for the closer correlation of rotational parameters to the bone age were not clear. However, as the developmental of rotational features is influenced by muscle contracture, it might not be surprising to see this stronger correlation. Indeed, as epiphyseal plates close during development, the force from the muscles is transmitted to a progressively more rigid bony structure, and hence one with a progressively decreasing capacity for flexibility within the bone, or even across the epiphyseal plate, such that more permanent remodelling takes place, manifesting as increased rotation. Van der Linden states that “normal torsion development is the result of muscle forces on the immature skeleton during normal gait”, and indeed the torsions and rotations of the lower limb are the result of a “complex

interaction between initial orientation of bony structures, muscle characteristics, and muscle forces during gait, and in frequently adapted positions, especially in the non-ambulatory phase¹²¹. Similarly this is seen in torsional abnormalities found in cerebral palsy patients who, in addition to gait abnormalities, have increased incidences of knee pain and patellofemoral discomfort, the severity of which was found to be often associated with external tibial torsion and increased femoral anteversion¹²².

When we went further and applied linear models using stepwise regression (Table 6), it was found that mixed models combining both bone age and chronological age showed the highest correlation coefficients for the rotational parameters of femoral torsion, tibial torsion and femorotibial rotation (and also the mTFA and NSA).

II. 4.4 Other features

The femoral offset parameter showed a good correlation with both bone age and chronological age, though that of chronological age was superior (0.743 vs 0.664), similar to the longitudinal-type parameters.

The neck-shaft angle showed a small but stronger correlation with the bone age (BA vs. CA: -0.164 vs. -0.13) and the strongest correlation with a mixed bone age-chronological age model (Beta coefficient -0.322, VIF =0.875). For an in-depth description of NSA results, see below.

II. 4.5 Neck-shaft Angle development and Skeletal Maturity

After the initial study of lower limb parameters was performed, the NSA was investigated more deeply (see Tables 8,9) and linear and multivariate modelling carried out in the 1005-individual population aged from 4-24 years old.

NSA in the studied population decreased from a mean of 131.89° at 4 years old and plateaued at 127° at 16-18 years old, similar to the values seen by Gilligan et al. in their study of 8,000 real femur specimens³³. These findings agree with the results of Guenon et al., supporting the theory that using the EOS and its' software can prevent the false

elevations of NSA caused by femoral anteversion that typically befall conventional radiographs⁴².

A small but superior relationship was found with the bone age vs. NSA compared to that of the chronological age: linear regression models presented an R^2 value of 0.101 vs. 0.069, mean standard deviation was lower (4.39° vs. 4.70°), in addition to the previously reported greater Spearman correlation ($\rho = -0.164$ vs. -0.130).

Next, multivariate linear regression analysis assessed a combination of bone and chronological age data and presented a model using both, and showed a stronger correlation than either alone ($R^2 = 0.226$ vs. 0.101, 0.069), and best reflected the changes of NSA during growth regardless of gender.

Looking closer at the data, several interesting patterns emerged when bone age stages were subdivided by chronological age (figures 8, 9 and 10).

The majority of children at a similar chronological age presented were found to have similar bone age stages. However, the range of values was quite wide (such that a 12 year-old could have nearly any bone age stage from 1 or 6), and within each age-year there was a sub-group of children who had a higher or lower bone age compared to their peers. We termed these as ‘slow-maturing’ and ‘fast-maturing’ groups, depending on whether the bone age stage of the cervical vertebrae of the child/ adolescent was below or elevated by 2 or more bone age stages compared to others of the same chronological age. Interestingly, the mean NSA of these individuals was significantly higher than their peers, irrespective of whether the child/ adolescent was slow-maturing or fast-maturing (see figure 9). On average the NSA in the fast-maturing group was 3.16° higher than their peers ($p < 0.001$), and in slow-maturing individuals 4.45° higher ($p < 0.001$). An elevated NSA in less mature individuals might be expected as the value is typically understood to fall with increasing development, however an elevated NSA in those with a higher bone age has not been previously reported.

Similarly, when the chronological age within each bone stage was investigated, the same relationship was seen again (see figure 10). At cervical bone age stage 1, children of older chronological age were found to have higher NSA values than the others. In stage 3, while

most children were of similar age, those children who were older or younger exhibited an elevated NSA. Stages 4 and 5 showed a similar pattern of older and younger individuals with higher NSA values. While in stages 5 and 6 the pattern in older individuals was less clear, this bone age stage encompassed a large age group from 17 to 24 years old.

According to our findings a typical 15-year-old exhibited an NSA of 128.3° , however if they were slow-maturing or fast-maturing compared to their peers they would be expected to show a higher values of 133.6 or 132.2° , respectively. Similar results associated with bone age were found throughout all age groups.

‘Force x Time’

Our findings led us to hypothesize that femoral neck development may possess a period of susceptibility during which biomechanical forces can act on the proximal femur to determine the angle of the femoral neck. According to this concept, neck angle morphology is an inverse product of ‘force x time’. A shortening of this susceptibility period, as may occur in ‘fast-maturers’, would result in a higher NSA as the cartilage ossifies earlier, before the neck has declined completely from the immature valgus configuration. It is not clear whether these fast-maturing individuals will later undergo a ‘catch-up’ decrease in NSA value or will remain with higher values. Without a longitudinal study, however, it is not possible for us to clarify.

Force. Proximal femoral geometry is known to be influenced by the biomechanical forces applied^{29,123}. Upright gait, and the stresses associated, acting on the femoral head and greater trochanter are responsible for the majority of childhood NSA and femoral version changes as demonstrated *in vivo* by the direct relationship between activity levels and proximal femoral parameters in children with cerebral palsy^{40,124}, and also by computer models and stress modeling^{125,126}.

Time. The timing of neck-shaft development has not been well studied, however. To support our hypothesis that a shortened period of susceptibility could lead to a higher NSA, it was considered that higher NSA values should then also be seen in individuals with earlier epiphyseal closure for some other reason or in those with an advanced bone age.

Precocious puberty, a condition of endocrinological origin, is associated with premature epiphyseal closure and short stature, however is not typically associated with changes in NSA. It could not be ruled out however, as reports on the NSA values were not found except in the case of co-existent fibrous osteotic dysplasia, (in this case as part of so-called McCune-Albright Syndrome) ^{127,128}.

Conversely, conditions leading to delayed bone age or a prolonged duration with open epiphyses would be expected to be associated with lower NSA values. Again, reports of proximal femur measurements in such conditions were very few and hard to come by, however. Although both thyroid disease ^{129,130} and growth hormone deficiency ^{131,132} are conditions known to delay epiphyseal development, no studies could be found describing NSA of patients that could give supporting or opposing evidence. The association between hypothyroidism and slipped capital femoral epiphysis (SCFE) has been reported many times ^{133,134}. SCFE has been linked to a decreased neck-shaft angle, however ¹³⁴. Furthermore, while numerous studies have found that age at menarche has decreased continuously over the last century, the NSA has not been reported to be falling. However, reports on the age of menarche from recent decades have not agreed upon whether this trend is ongoing, and the majority of NSA data are from this period ^{38,135–138}.

II.4.6 Limitations

This study contained several limitations. The grouping of children during growth, a notoriously individual and unpredictable process into ‘typical’ growth patterns is always an oversimplification. Groupings based on any arbitrary data point (even if related to distributions of a normal population) must always be regarded to be at risk of detecting events occurring simply due to chance. By examining a large sized population, 449 boys 556 girls, we believe we have minimized this chance.

II.4.7 Summary

We believe that our data indicates that the inclusion of cervical bone age assessment in a paediatric orthopaedic evaluation may be valuable, especially when the neck-shaft angle is in question. Bone age-based evaluation of NSA removed gender differences, and when combined with chronological age yielded the most accurate characterization of its angle during all stages of childhood and adolescence. Combined models using both bone age and chronological age can give the most accurate and individualized assessment of a child's NSA taking into account gender, nutrition, socioeconomic status, disease status, and could improve the definition of normal and diseased, and allow better indications for intervention.

III. PART 2 – Alternative Bone Age Assessment Methods

III. 1. Introduction

III.1.1 Introduction

In our previous results, a number of lower limb parameters including the NSA were found to show lower variation and gender differences with cervical bone age assessment, a method that can be included during evaluation of EOS image-pairs (see Part 1).

Cervical bone age assessments have been popular with orthodontists, however, they are not well known to most orthopaedic physicians. Furthermore, in settings where only the lower limb is to be investigated a full body image is not required and the cervical region is consequently not featured on the radiograph, so the cervical method of bone age assessment may not always be possible. A multitude of alternative bone age assessments have been described in the literature (see Table 1 or Appendix, Table 1) that may be closer to the region of interest, or faster to apply, however few have entered common use in modern orthopaedic medicine, and even fewer have been applied to EOS images. Some authors have described hand-wrist assessment using modified positioning during image capture, however such methods cannot be applied retrospectively to EOS images in a database¹³⁹.

III.1.2 Aims of this study

The aim of this study was to identify and assess alternative bone age methods for use with the EOS scanner, without the need for changes in position.

III.2. MATERIALS AND METHODS

III. 2.1 Bone Age Assessment Alternative Methods Population

The studied population was based on that described in the Materials & Methods section of Part 1 ‘NSA Assessment Population’. Due to the time differences and server transfers between parts of this study, 59 individuals’ scans were lost to the study. As a result, during bone age assessments of the 4-24 year-old population, the total population was 934 individuals.

III. 2.1.1 Bone Age Methods Literature Review

A literature review was conducted on March 30 2016 using the search terms “bone age”, “skeletal age” and “skeletal maturity” in Pubmed and 6075 publications using 185 different methods were described (See Appendix, Supplementary Table 1.). All methods requiring specialized positioning were excluded and after evaluation 9 promising methods, were selected:

1. Calcaneus (Nicholson 2015)⁹²;
2. Cervical vertebrae (Hassel & Farman 1995)⁹³;
3. Clavicle (Schmeling et al. 2004)¹⁰⁵;
4. Shoulder (Shaefer et al. 2015)¹⁴⁰;
5. Elbow (Sauvegrain et al. 1962)¹⁰³;
6. First rib (Michelson et al. 1934, Garamendi et al. 2011)^{106,141};
7. Hip (pelvis and proximal femur) (Acheson 1957)⁹⁰;
8. Iliac apophysis, Risser ‘plus’ method (Negrini et al. 2015)¹⁰⁷;
9. Knee (O’Connor et al. 2008)¹¹².

After discussion it was decided not to proceed with the clavicle, rib, and elbow methods due to insufficient resolution on conventional radiograph (clavicle) or the presence of severe shadowing preventing visualization of landmarks due to patient position in the EOS (first rib, elbow). This left six promising methods (see figure 11 a-e).

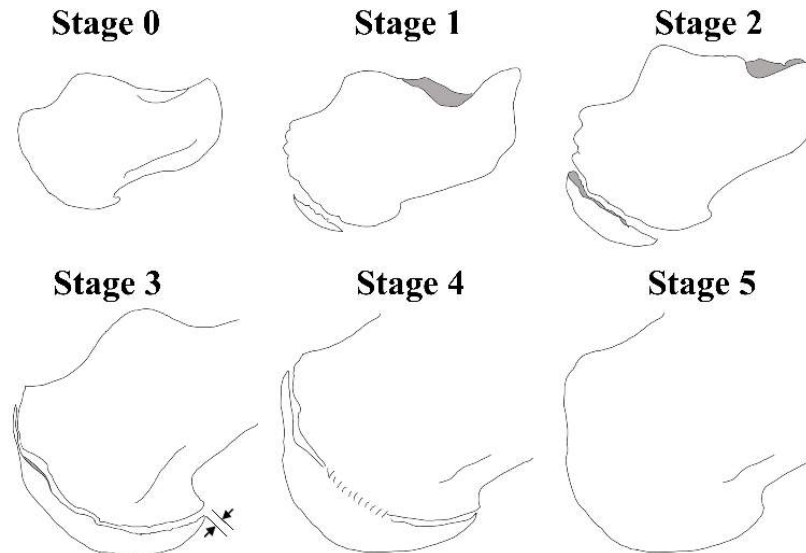


Figure 11.(a) Calcaneus. Adapted from Nicholson et al. 2015.

Stage 0: No ossification of the apophysis is evident;

Stage 1: The apophysis extends more quickly over the plantar than dorsal surface. The apophysis in this figure covers < 50% of the metaphysis;

Stage 2: The apophysis covers $\geq 50\%$ of the metaphysis but has not extended to the plantar edge. The radiolucent interval between the apophysis and metaphysis is wider near the areas of plantar and dorsal extension than in the central region;

Stage 3: Complete extension over the plantar surface is seen when the apophysis extends within 2 mm of the plantar edge of the calcaneal concavity, as shown by the black arrow. There is a narrow and relatively uniform radiolucent interval between the apophysis and metaphysis;

Stage 4: Fusion of the apophysis is occurring, but there are still visible intervals between the apophysis and metaphysis. Fusion begins in the central region of the interval between the apophysis and metaphysis;

Stage 5: Fusion of the apophysis is complete.

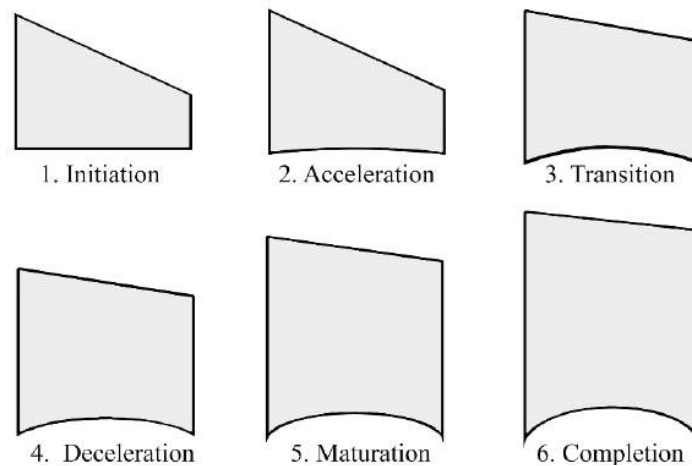


Figure 11 (b) Cervical Bone Assessment as per Hassel & Farman (1995) (Adapted from Schlégl et al. 2017). *1. Initiation:* the inferior borders of C2, C3 and C4 are all flat. Upper borders taper from posterior to anterior giving the body a wedge shape. *2. Acceleration:* C2 and C3 develop concavities in their inferior borders, while that of C4 remains flat. Bodies of C3 and C4 are almost rectangular in shape. *3. Transition:* Concavities in C2 and C3 are now deeper and distinct with C4 beginning to develop a concave inferior border too. Bodies of C3 and C4 are rectangular in shape. *4. Deceleration:* C2, C3 and C4 all have distinct concavities in their inferior borders, and the bodies of C3 and C4 are becoming more square in shape. *5. Maturation:* Concavities of C2, C3 and C4 are more accentuated in the inferior borders, and C3, C4 bodies are almost square or square in shape. *6. Completion:* Deep concavities are found in the inferior borders of C2, C3 and C4 and the bodies are square or column-like, with a vertical dimension greater than their horizontal dimension.

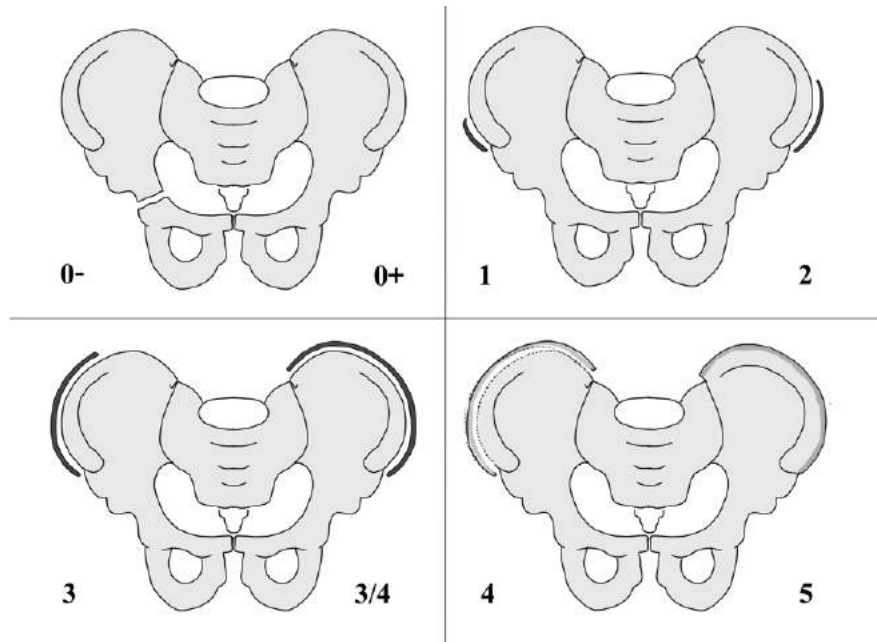


Figure 11 (c). Risser ‘Plus’ Method as per Negrini et al (2015). *Risser 0-*: Open triradiate cartilage; *Risser 0+*: Fused triradiate cartilage; *Risser 1*: 0-25% coverage of iliac crest; *Risser 2*: 25-50% coverage; *Risser 3*: 50-75% coverage; *Risser 3/4*: 75-100% coverage; *Risser 4*: Fusion started; *Risser 5*: Fusion completed.

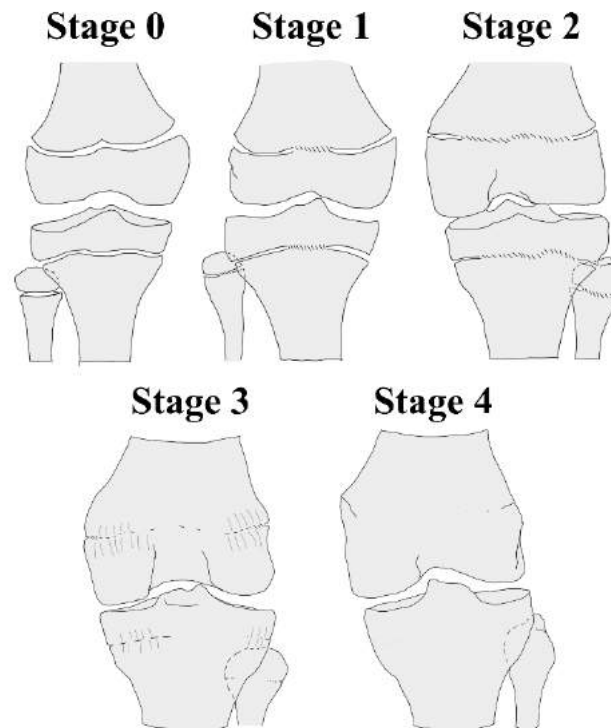


Figure 11 (d) Knee. Adapted from O’Connor et al. (2012)

Stage 0 – Non-Union: clear radiolucent strip between both sides of epiphyseal plate;

Stage 1 – Beginning Union: very narrow radiolucent strip, central hazy/ blurring as fusion starts (<50% of gap);

Stage 2 – Active Union: ‘Capping’ as epiphysis overlap the metaphysis. Fusion line/ area of greater density area where fusion is taking place. Some areas of radiolucency remain, but fusion area is >50% of gap.

Stage 3 – Recent Union: Fine line of fusion remains but epiphysis and metaphysis are united (so-called ‘complete capping’). May be small notches at margins of <2mm. Discontinuity of trabeculae between former epiphysis and diaphysis.

Stage 4 – Complete Union: mature bone, with no notches at margins, and continuous trabeculae. A thin terminal line or ‘epiphyseal scar’ may remain at the site of the epiphyseal plate.

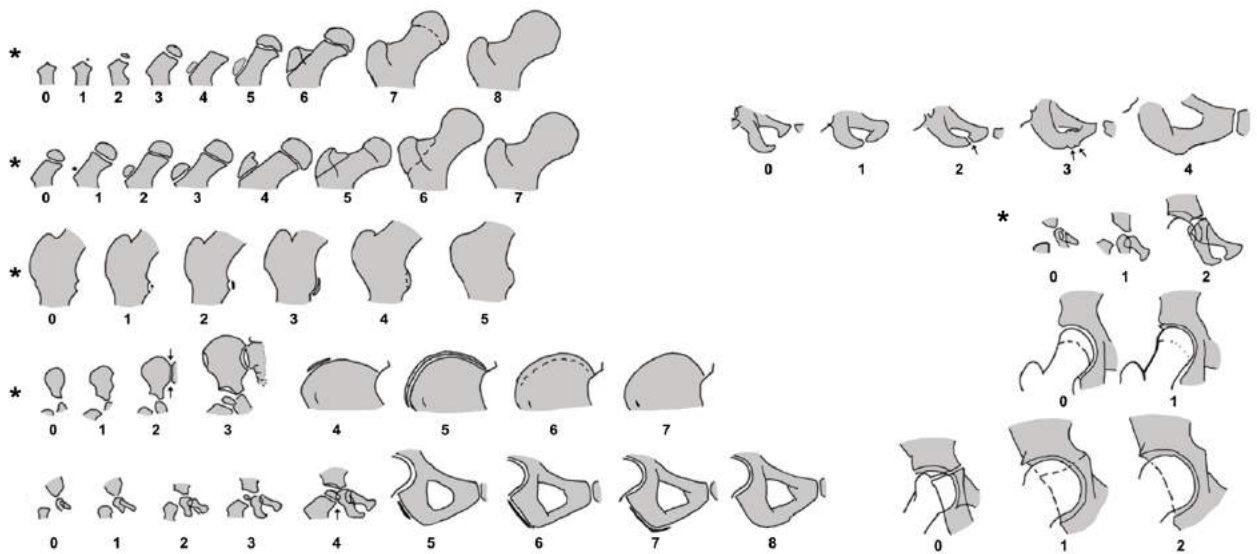


Figure 11. (e) Oxford Hip Method. Adapted from Acheson (1957) Nine regions are assessed as per pictorial below and values scores summed: femoral head, greater trochanter, lesser trochanter, iliac crest, ischium, ischio-pubic junction, pubic bone, acetabulum and tri-radiate cartilage. The five regions assessed in the abbreviated or ‘modified’ version of this method are marked with an asterisk (*) (Stasikelis et al. 1996).

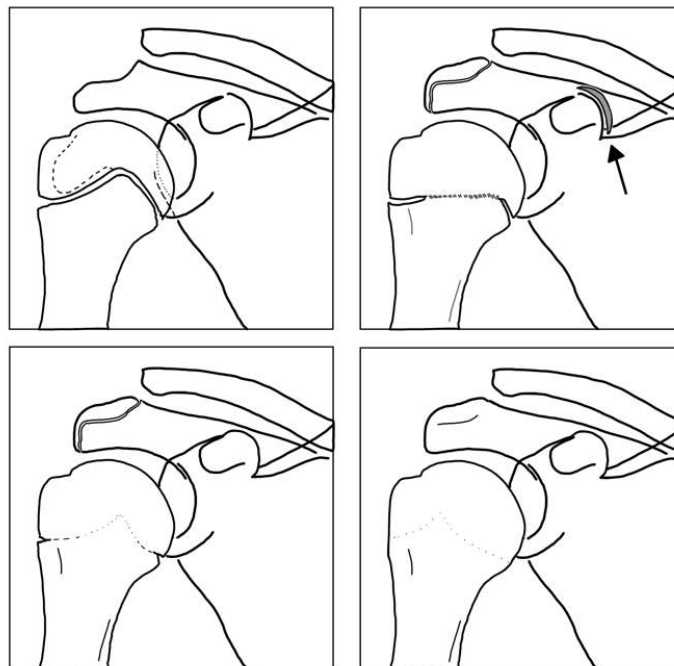


Figure 11 (f). Shoulder (as per Shaefer et al. 2015). Three landmarks are assessed and stages (called ‘phases’) are summed for a score ranging from 1-9.

1. Proximal Humerus:

- *Phase 1 Open union:* A continuous radiolucent line is observed along the contours of the entire epiphysis. The epiphysis itself may be slightly underdeveloped with some additional growth still required along its edges.
- *Phase 2 Fusing:* Epiphyseal union has begun or is just about to start. In early stages, this is indicated by a haziness that occurs centrally along the epiphysis. As union progresses, radiolucency becomes less apparent, however evidence of faint black lines remain.
- *Phase 3 Unfused notch:* Union is complete other than in a small area along the periphery of bone. This is typically evidenced by a blackened notch located under the greater tubercle.

Phase 4 Complete union: No areas of radiolucency are identified. The line of fusion may still be recognizable however as a ‘white’ radiopaque line.

2. *Acromion:*

- *Phase 0 Not present:* No apophysis is observed. The acromion is marked by a rounded and perhaps billowed surface.
- *Phase 1 Present; open or fusing:* The apophysis is present and a radiolucent line is clearly visible.
- *Phase 4 Complete union:* No line of radiolucency is evident.

3. *Angle/apex:*

- *Phase 1 Present; open or fusing:* The apophysis is clearly visible sitting on top of, or at the tip of, the coracoid process. A radiolucent line is clearly visible.

III. 2.1.2 Bone Age Methods Pilot Study – 6 methods

A pilot study was initiated to investigate the 6 possible methods. Three graders (one resident and two PhD candidate medical doctors) were trained in each of the methods by 1 senior orthopaedic specialist and 1 senior radiologist, and given text and pictorial descriptions of each method. 13 normal children aged 3-16 were randomly selected from the population database and their images were evaluated 3 times by 3 observers on separate days, with each of the methods. Bone assessment estimates and any difficulties or factors affecting the application of the methods were noted.

	After Literature Review	After Pilot Study	Main Study
1	Calcaneus ⁹²	Calcaneus	Calcaneus
2	Cervical vertebrae ⁹³	Cervical	Cervical
3	Oxford Hip ⁹⁰	Oxford Hip	Oxford Hip
4	Iliac apophysis, Risser ‘plus’ ¹⁰⁷	Risser ‘plus’	Risser ‘plus’
5	Knee ¹¹²	Knee	Knee
6	Shoulder ¹⁴⁰	Shoulder	
7	Clavicle ¹⁰⁵		
8	Elbow ¹⁰³		
9	First rib ^{106,141}		

Table 11. Schematic of potential bone age methods. After literature review 9 possible methods were identified, however after discussion three (the clavicle, elbow and first rib) were rejected. Six methods entered the pilot study, after which the shoulder method was then discontinued (see text for more).

III. 2.1.3 Bone Age Methods Main Study – 5 methods

After pilot study the shoulder method was excluded, and the calcaneus method was applied without assessment of first appearance of plantar sesamoid assessment (used to assist discrimination between certain stages), see results for more information. The five remaining methods were assessed based on:

1. Reliability: 30 images were randomly selected from the population and assessment performed 3 times by each of the 3 observers, on 3 separate occasions, separated by more than 24 hours. Intra- and interobserver reliability of each method was assessed by calculating intraclass correlation coefficient (ICC), with evaluation based on Winer's criteria¹²⁰.
2. Difficulty of Assessment: methods were assessed based on a four-point Likert scale:
 - '1' easy - the method was easy to apply;
 - '2' moderate - some minor exposure problems or minor obstruction were encountered, but evaluation could confidently be made;
 - '3' difficult - moderate obstruction encountered, such that an assumption must be made. Image was partially cut off eg 1/3 or less of a landmark obscured or cut off by radiograph edge;
 - '4' impossible – landmark of interest was not in the image or totally obstructed.

For the hip and knee methods, which use multiple landmarks, difficulties with individual landmarks were noted and if the sum of landmarks encountering difficulty exceeded 2 or 3, respectively, then the rating '3' ('difficult') was applied to the whole image. Note was made of the reasons for difficulties and grouped as: (i) technical reasons – difficulty caused by landmark(s) lying outside of the edge of an image; (ii) resolution issues – resolution insufficient to easily assess the image; (iii) positioning - a landmark that is not visible, or less clearly visible as a result of limb rotation or due to shadowing from other regions.

Reasoning: to find a method that can be used retrospectively on previously taken EOS images, and that can be performed without the need to modify the current EOS protocol.

3. Speed: Two observers used digital timers with each of the methods during the final 200 of the randomized images, to calculate mean evaluation time.

Reasoning: as time constraints are a real and practical factor in the clinic, time taken to carry-out any new grading system should be considered seriously.

Chronological age, step-length were also measured and descriptive statistics and Spearman correlations with difficulties performed.

Several authors have applied the Oxford Hip method in an abbreviated or ‘modified’ format in which just 5 landmarks are assessed: femoral head, greater trochanter, lesser trochanter, triradiate cartilage and the iliac crest^{80,81}. Due to its’ reported use in the assessment of slipped femoral capital epiphysis, assessment was also applied of this method based on the gradings made with the Oxford Hip method.

Cervical bone age assessment records from our previous report were re-evaluated and each scan assessed for difficulties as per the present study. 200 of these images were re-assessed for the purposes of timing only.

III.2.2 Statistical Analysis

For randomization and selection, the RAND.BETWEEN formula of the Microsoft Excel v14.0.6112.5000 (Microsoft Corp., Redmond, WA) software was used. All statistical data was processed by the SPSS v22 (IBM Corp., Armonk, NY, USA) and by the Microsoft Office Professional Plus v14.0.6112.5000 (Microsoft Corp., Redmond, WA, USA) software packages. A p-value <0.05 was accepted as significant.

III.3. RESULTS

III. 3.1 Bone Age (Pilot Study)

After discussion, due to the high level of inter-observer disagreement the decision was made not to proceed with the shoulder method. Observers found difficulties evaluating the region in 54-62% of the scans. Only one of the three required landmarks were found to be assessable in 23-38% of scans (3-5 of 13 scans), the apex/ angle of the coracoid process was not visible in 15-38% (2-5 of 13 scans) and observers reported low satisfaction using the method.

The calcaneal method includes the supplementary identification of plantar sesamoids however sesamoids could not be clearly identified in any of the 13 scans and in four of 13 scans (30.8%) were reported as ‘possibly present’. Reported difficulties were due to the use of AP images in the original description of the method by Nicholson et al., in addition to overlap from contralateral foot and a lower image quality often encountered at the inferior image edge.

Identification of sesamoids is secondary to the evaluation of the calcaneal apophysis in this method, however, so the calcaneus method was included in the main study without accessory evaluation of the presence of the plantar sesamoids.

All other methods could be applied satisfactorily.

III. 3.2 Bone Age (Main Study)

Figure 12 (a-e) shows the bone age and chronological age of individuals with each method. For clarity, scores from the Oxford hip method are shown grouped in 5-point intervals.

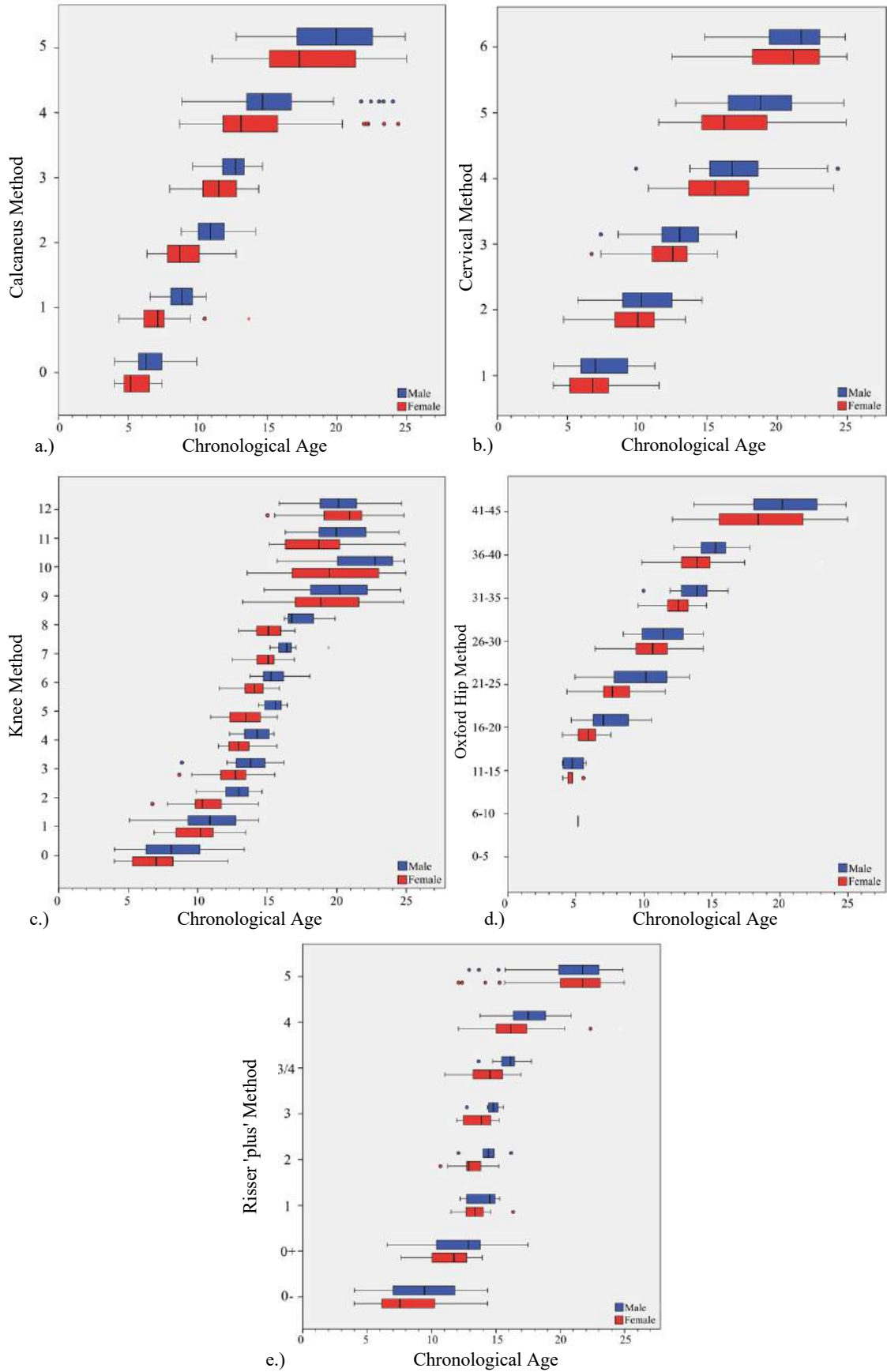


Figure 12 (a-e). Box plot representation of bone age values with respect to chronological age across the 934-individual population (4-24 years old), separated by gender.

1. Reliability

Intra- and interobserver reliability values are shown in Table 12. Excellent values, greater than >0.9 were found for the calcaneus, cervical, Oxford hip and Risser ‘plus’ methods. The knee method received a ‘good’ rating of 0.865 for interobserver reliability and intraobserver values ranged from good (0.841) to excellent (0.956).

	Calcaneus	Cervical	Knee	Oxford Hip	Risser Plus
Inter-observer reliability	0.945	0.976	0.865	0.902	0.94
Intra-observer reliability	0.953-0.999	0.949-0.959	0.841-0.956	0.949-0.993	0.982-0.969

Table 12. Intra- and interobserver reliability values as estimated by intraclass correlation coefficient. ‘Excellent’ reliability values are marked in bold - values were interpreted as per Winers’ criteria¹²⁰ where 0.9-1.0 is regarded as ‘excellent’, 0.7-0.89 as ‘good’, 0.50-0.69 ‘fair-to-moderate’, 0.25- 0.49 ‘low’, and 0-0.24 ‘absent-to-poor’. [Reproduced from O’Sullivan et al. 2018].

2. Difficulties with assessment

Reported difficulties in assessment and their causes are shown in Figure 13. a-e.

After assessment of all 934 scans, the Risser ‘plus’ method had the greatest number of ‘easy’ ratings (89.5%, 836/934), followed by the cervical (79.0%, 738/934), Oxford hip method (78.6%, 734/934), calcaneus (70.8%, 661/934) and the knee (68.2%, 667/934). The calcaneus method could not be applied at all in 6.2% of scans (58/934), followed by 4.2% with the cervical method (39/934), Risser ‘plus’ and both Oxford hip methods 0.2% of scans (2/934) and finally the knee 0.1% (1/934).

Images could be confidently evaluated, or with only mild difficulty, (rated 1 or 2) in the majority of scans: Risser ‘plus’ method, 98.7% of scans; modified Oxford hip 95.4%; Oxford hip 92.2%, knee 91.9%, cervical 90.1% and calcaneus 84.9%. However, 23.7% of images with the knee method were rated as ‘difficult (‘2’) (221 images) and 14.1% of calcaneal images (132 images).

Evaluation around the knee received the lowest number of ‘easy’ ratings – just 68.2% of scans (637/934) – and moderate difficulty was recorded for 23.7% of scans (221/934).

When problems with knee assessment are looked at closer, difficulties encountered were spread equally between each region: in 39.6% of cases to be due to the femur, 36.5% the tibia, and 23.9% at the fibula. The causes reported behind the 297 problematic images were predominantly: resolution (36.4%, 108/297), uncertainty (25.6%, 76/297), position (20.2%, 60/297) or other (16.8%, 50/297). When ‘uncertainty’ was reported (76 images) it was due to a lacking in precise differentiation between the stages in the original the original description, particularly between Stages 3 and 4.

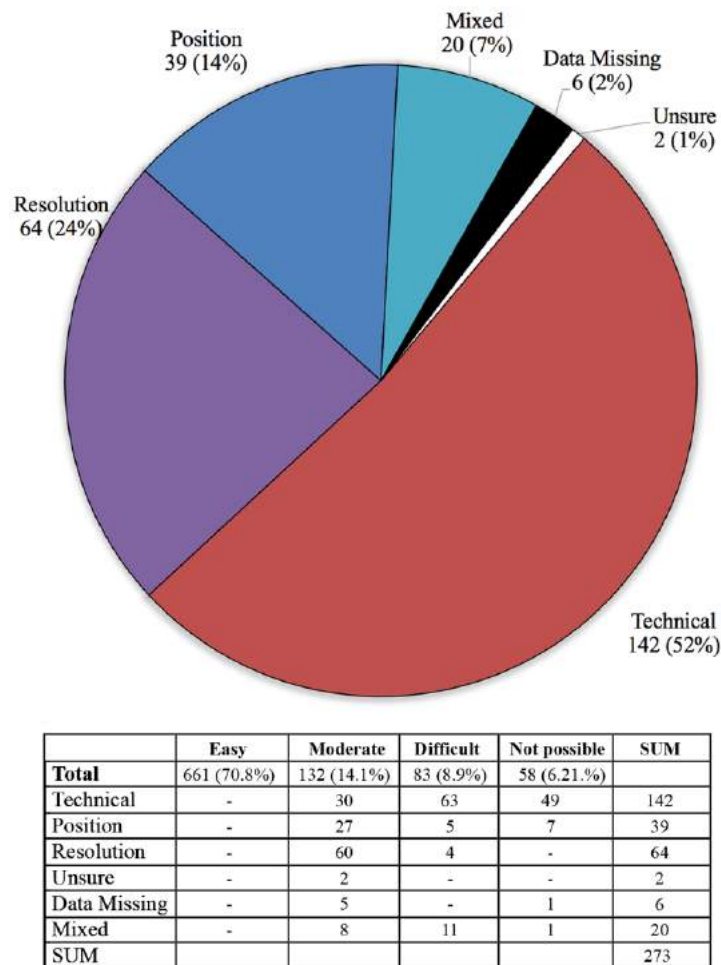


Fig 13 (a) Calcaneus

Figure 13 (a-e). Ratings and reported causes of difficulty for applying bone age assessment methods to EOS images. Reasons for difficulty were grouped as those due to (i) technical reasons – difficulty caused by landmark(s) lying outside of the edge of an image; (ii) resolution issues – resolution insufficient to easily assess the image; (iii) positioning - a landmark that is not visible, or less clearly visible as a result of limb rotation or due to shadowing from other regions. Furthermore general ‘unsure’ ratings were collected, related to original description of the method, and ‘mixed’ when more than one cause was present (eg the simultaneous presentation of a resolution and positioning problem).

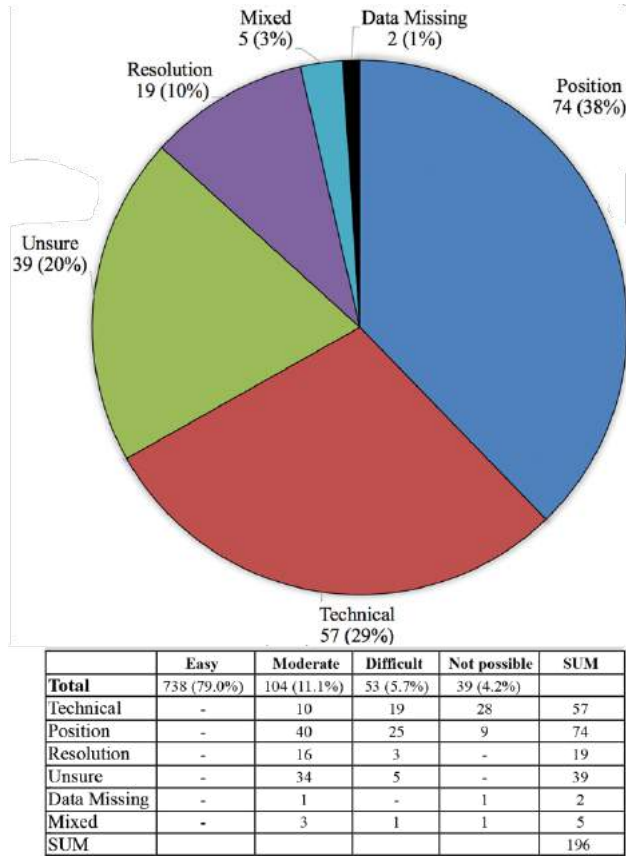


Fig 13 (b) Cervical

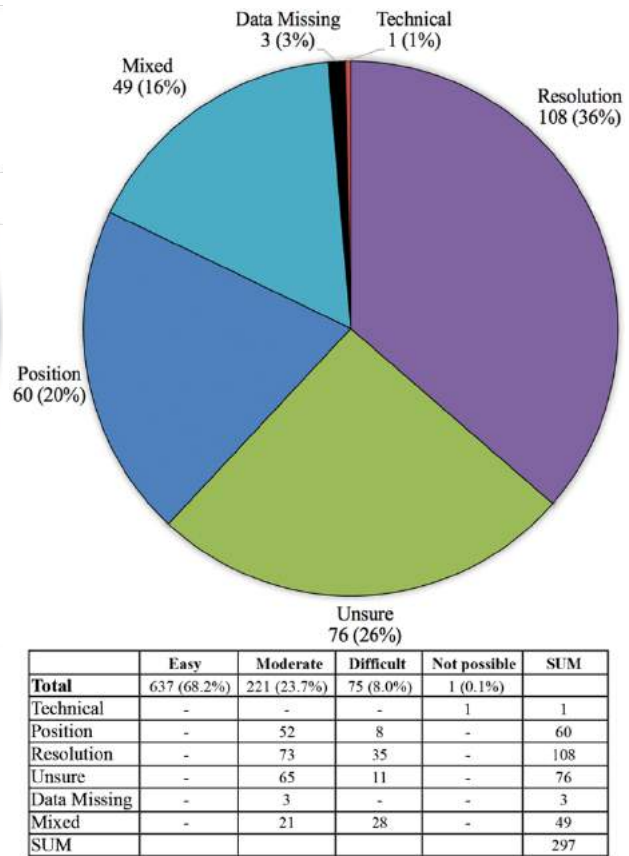


Fig 13 (c) Knee

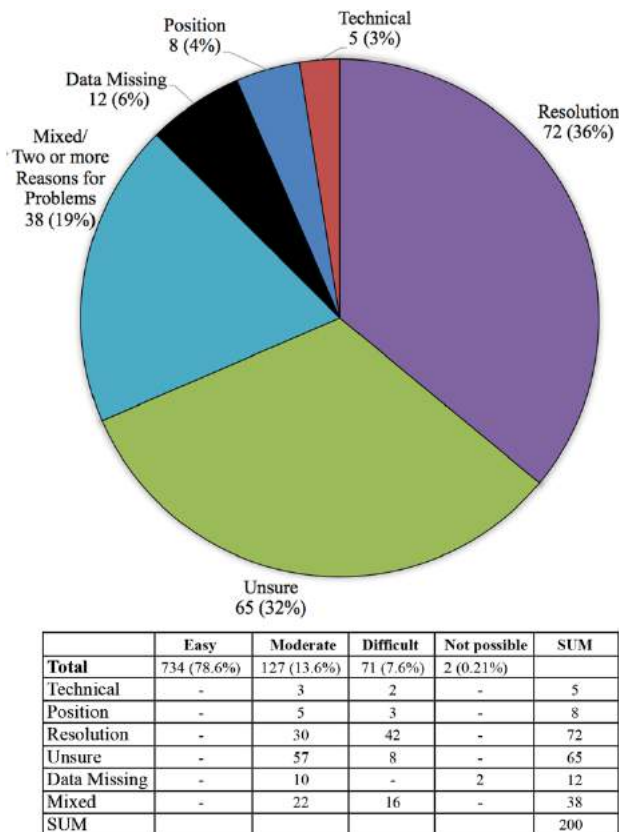


Fig 13 (d) Oxford Hip

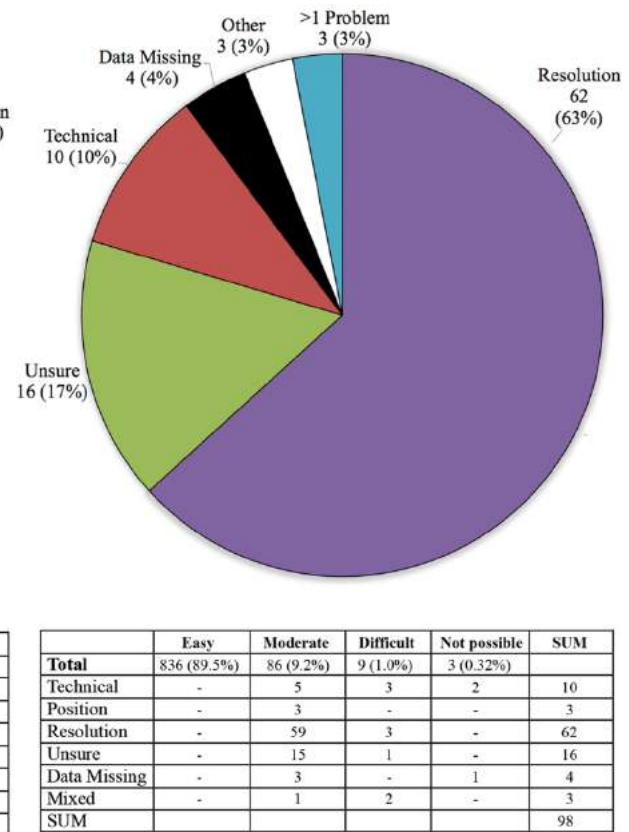


Fig 13 (e) Risser

3. Evaluation time

Values regarding time taken for evaluation are shown in Figure 14. Shorter evaluation times were seen in methods with fewer stages. With a mean 17.7 seconds, the six-stage calcaneus method was found to be fastest, significantly quicker than the second fastest, the cervical method, also a six-stage method, which was found to have a mean of 26.5s per scan (independent t-test, $p < 0.05$). The slowest evaluation time was seen with the Oxford hip method, at times taking more than four minutes – principally due to the nine regions of interest to be evaluated, for total of 45 stages, in addition to uncertainty caused by frequent lesser trochanter visibility problems (see discussion).

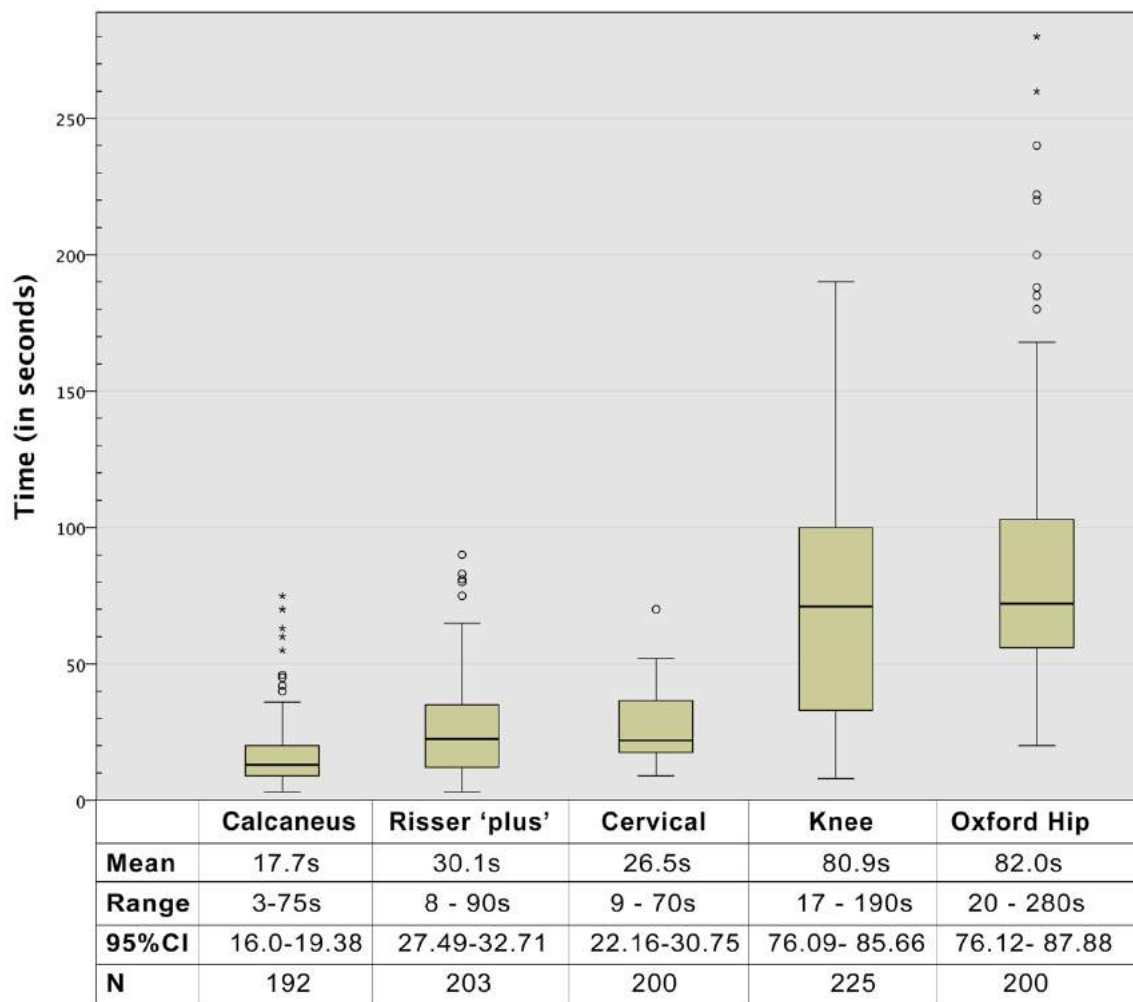


Figure 14. Box plots present the time taken per evaluation with the different bone age assessment methods. Timing data was collected using a digital timer over the last 200 evaluations by one observer (IOS).

III.4. DISCUSSION

III.4.1 Alternative Methods for Bone Age Assessment with the EOS Scanner

The biological age of a child is a related but distinct entity to chronological age. While the chronological age increases linearly with the passing of years, months and days, the biological age refers to the maturity of a particular tissue or system, and is influenced by genetics, hormones, diet and disease (eg. hypothyroidism, growth hormone insufficiency, dwarfism, celiac disease etc.), in addition to time. The bone age is an indicator of the biological age of the skeletal system.

Familiar stages are passed through by each child and adolescent as developing ossification centres of the apophyses and epiphyseal plates enlarge and carve out typical shapes at predictable intervals. Radiographs easily reveal these features and give us a snapshot of this process, a ‘still image’ of dynamic continuous events. While an increasing frequency of imaging allows us to follow the process more closely, the X-ray radiation burden similarly increases, and subsequent associated health risks^{43,46-48}.

After extensively reviewing the literature we identified 185 different methods (see Appendix, Supplementary Table 1). Methods dated as far back as 1931 and ranged from dental assessment, to hemiskeleton and whole-body investigations.

From the literature 9 methods appeared compatible with the EOS scanner, however after discussion 3 methods were rejected: the clavicle, as radiographs lacked sufficient clarity at the medial clavicle for the very fine landmarks requiring evaluation; the first rib, due to severe shadowing by the upper limb obscuring landmarks; and the elbow methods as the upper limb position means the elbow region is generally overshadowed by the contralateral limb, patients trunk or outside of the anterior limit of the scan.

Finally, the 6 methods were entered into a pilot study, in which difficulties were encountered with the calcaneus method and shoulder methods.

Observers reported problems in assessing one or more landmarks with the shoulder method in 54-62% of scans. Schaefer et al. themselves drew attention in their description of the method¹⁰⁴ to the difficulty of identifying the fine structure of the apex and angle of the coracoid, and indeed these were unidentifiable by some observers in up to 46% of scans. The shoulder method in its original description was based on multiple views of the shoulder, and most patients also had Y- and axillary views providing additional views when AP or lateral images were not sufficient. While the majority of landmarks were thought to be sufficiently visible for application to EOS images, it was clear that the absence of Y- and axillary views make it inappropriate and so this method was rejected.

The calcaneus method is primarily based on the assessment of the ossification centre of the calcaneal tuberosity, but also features additional evaluation of the plantar sesamoids around the hallux to define the entrance to stage 3. However, difficulty was reported in identifying the sesamoids on the EOS images, with none clearly identified on the scans, and a ‘possible’ presence reported in 4 of the scans (30.8%). In one case, in which an individual had received a conventional radiograph at the same visit as the EOS image, the EOS image reviewed was reported as negative, but a sesamoid was clearly visible on the conventional X-ray (see figure 15). The calcaneus method was included, but for this reason sesamoid evaluation was not included.

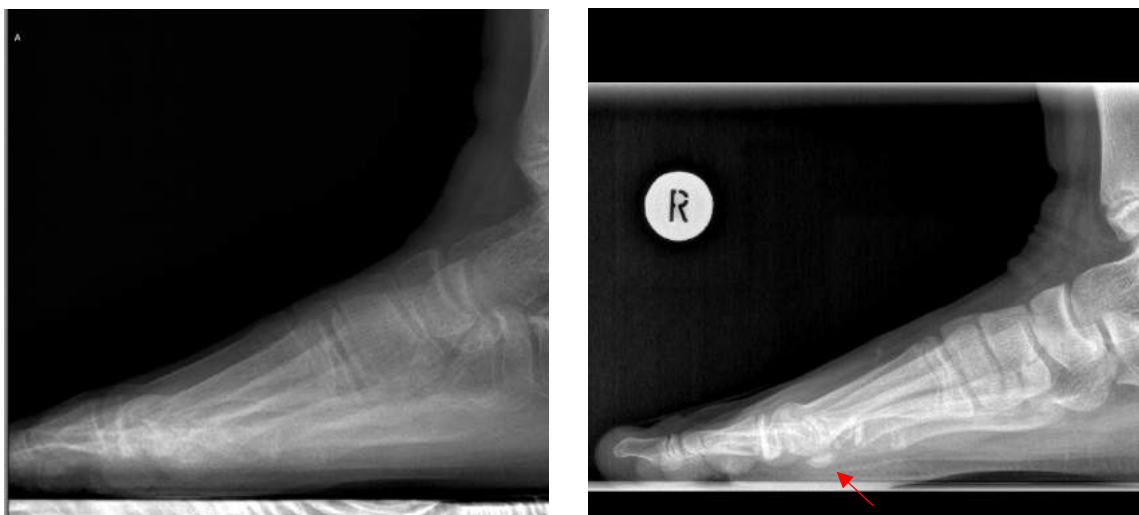


Figure 15. Lateral view of the foot in the same patient, taken with EOS (left) and conventional X-ray (right). While the plantar sesamoid was clearly visible on conventional X-ray (red arrow), due to overlap with the contralateral foot it was not clear on the EOS image. Images were taken within 24 hours of each other.

Five methods were then evaluated in our large population of children and adolescents. In assessing which of the methods could be ‘best’ or most valuable to the clinician using the EOS, we identified several important characteristics for each evaluation:

- (1) Reliability: reflecting how reliably different examiners assign the same stage to the EOS images (inter-observer) and how easily a method could be learned and reproduced by each examiner (intra-observer);
- (2) Assessability of scans: what proportion of standard EOS images taken previously can be assessed, and how easily. Furthermore if there is difficulty what are the causes of these difficulties?;
- (3) Speed: the time required for each method to be applied has clear influence on how appropriate a method may be for clinical vs. research use.

III.4.2 Alternative Bone Age Methods

III. 4.2.1 Calcaneus Method

The calcaneus method is the newest of the applied methods. First described in 2015 by Nicholson et al.⁹², it is based on observations in the historical ‘Brush’ population, a broad group of children investigated in Cleveland, Ohio and starting in 1926, the same population from which the Greulich and Pyle atlas was established^{75,142}.

Based on difficulties previously reported in the pilot study, the main population was evaluated for development of the calcaneal apophysis without accessory assessment of plantar sesamoids.

Images rated with the calcaneus method received an ‘easy’ rating in 70.8% (661/934) of scans and 58 of all scans could not be evaluated at all (6.2%). A total of 273 (29.2%) scans were reported to have some difficulty, however 52% (142) of these were specifically a result of the calcaneus lying partially or totally outside of the range of the scan. As the scans were not taken with the intention to investigate foot pathology, the inferior or

posterior margin of the scan was calibrated at the discretion of the radiographer or requesting physician in our clinic – as such, difficulties may arise when applying retrospective analysis of bone age with the calcaneus method, however prospective studies could easily employ it by ensuring sufficient image inferior margins (but without any necessary modifications to patient position). Foot positioning was the second most frequent cause of difficulty and was reported as the cause in 22.7% of ‘moderate difficulty’ ratings. Narrower step length was subjectively reported to lead to overlap of the contralateral heel and difficulty identifying the presence and extent of ossification or fusion, however a statistically significant difference was not seen ($p=0.202$).

As this method is based on the ‘Brush’ population from the early 20th century, some authors have recommended mild corrections for interpretation with modern children - Li et al. found that Stage 3 and 4 girls were delayed by 0.64 and 0.58 years, respectively, compared to this historical population¹⁴³. Our study showed similar delays, of 0.94 and 2.2 years in Stage 3 and 4 females, and even Stage 4 boys of 1.61 years, however as both our study and the investigation by Li et al. were retrospective, this may possibly be in part an artificial elevation of values compared to serial studies in which the earliest scan at each bone age stage can be identified.

III. 4.2.2 Cervical Method

Cervical bone age evaluation of the second to fourth vertebrae is popular with orthodontists as the upper vertebrae lie both within the range of a typical lateral cephalogram and above the shadow of a thyroid shield⁹³. The first such method was described by Lamparski in 1975⁹⁹ and though multiple alternate but similar systems have since been described, methods predominantly evaluate height-to-width ratio, inferior curve development and slope of the superior margin^{93,101,144–148}.

The Hassel-Farman method was selected as it is one of the most popular methods, and has been shown by Imanimoghadam et al. to have a higher correlation to Tanner-Whitehouse TW3 than other methods (such as Mito’s and Lamparski’s), with a spearman correlation coefficient of $\rho = 0.995$, similar to that of Roman (0.997)¹¹⁹. Furthermore, Uysal et al. also found a strong spearman correlation with hand-wrist evaluation ($\rho = 0.86$, $p < 0.001$), using

Bjork and Grave & Brown methods, in a large population of 503 Turkish children¹⁴⁴, as did Roman et al. in a population of 958 Spanish five to eighteen year-olds ($\rho = 0.79$ in males, $=0.85$ in females), with Grave & Brown hand-wrist method¹⁰¹.

In our study, the Hassel-Farman cervical method received the second highest number of ‘easy’ ratings 738/934 (79.0%), with just 39 scans unevaluable (4.2%). Overall, problems were most commonly caused by positioning (74 images or 38% of all problematic scans), most typically asymmetrical positioning of the neck and overshadowing of the upper cervical vertebrae by the hands during imaging and technical reasons (57 images, or 29% of all problematic scans) caused by the scan not extending superiorly enough to include the upper vertebrae.

Interobserver reliability values reported with the cervical method were excellent, indeed the highest of all methods (0.976), with equally excellent intra-observer reliabilities from 0.949-0.959. The cervical method was also the second fastest of all methods, at just 26.5 seconds (95% CI 22.16 – 30.75s).

III. 4.2.3 Risser ‘plus’ System

The Risser ‘plus’ system is a unified system made by combining the European and American Risser scales, along with triradiate cartilage assessment. The 2014 Consensus Report from the Society on Scoliosis Orthopedic and Rehabilitation Treatment (SOSORT), and Scoliosis Research Society – Non-Operative Management Committee recommended its’ use due to ongoing confusion in reporting of Risser system scores¹⁰⁷. European and American systems both consist of 6 stages from 0 to 5, but differ in their assessment of progression along the iliac crest. The European system starts with no ossification (0), and grades excursion of the iliac crest by thirds (1: less than one third ossified; 2: one to two thirds ossified; 3: more than 2/3 ossified), followed by the initiation (4) and completion of fusion (5). In contrast the American system starts with no ossification (0), and grades excursion by quadrants (1, 2, 3, 4), and stage 5 begins with the initiation of fusion (a process that may take up to 2 years)¹⁴⁹. The unified system adds an intermediate ‘Stage 3/4’ resulting in seven stages that are more clearly relatable to both.

Furthermore, the addition of triradiate cartilage evaluation results in the an 8-stage system that may confer more useful predictive information about curve progression and time to peak height velocity at younger ages, a consistent point of criticism for the traditional Risser system^{92,150,151}.

In our main study, images rated with the Risser ‘plus’ system saw the greatest number of ‘easy’ ratings (89.5%, 836/934 scans) in addition to excellent interobserver (0.94) and intraobserver reliability ratings (0.982 - 0.969). Mean evaluation time was relatively fast at 30.1s (95% CI 27.49-32.71s), likely related to most orthopaedics physician’s familiarity with the basics of the method and its’ simple well-described stages.

The effect of the inclusion of triradiate cartilage evaluation can be seen in Figure 16. The average age at Stage 0- was 8.69 years and Stage 0+ 11.70 years old in comparison with a mean 9.23 years of age in the traditional Stage 0. A clear difference in sensitivity can be seen by the addition of just one more stadium, as Stage 1 was not seen on average until 13.53 years of age. In line with previous reports, the biggest drawback of the Risser method is Stage 1 arrives after the onset of peak height velocity, greatly limiting its value, whereas triradiate inclusion increases it’s potential use^{143,151}.

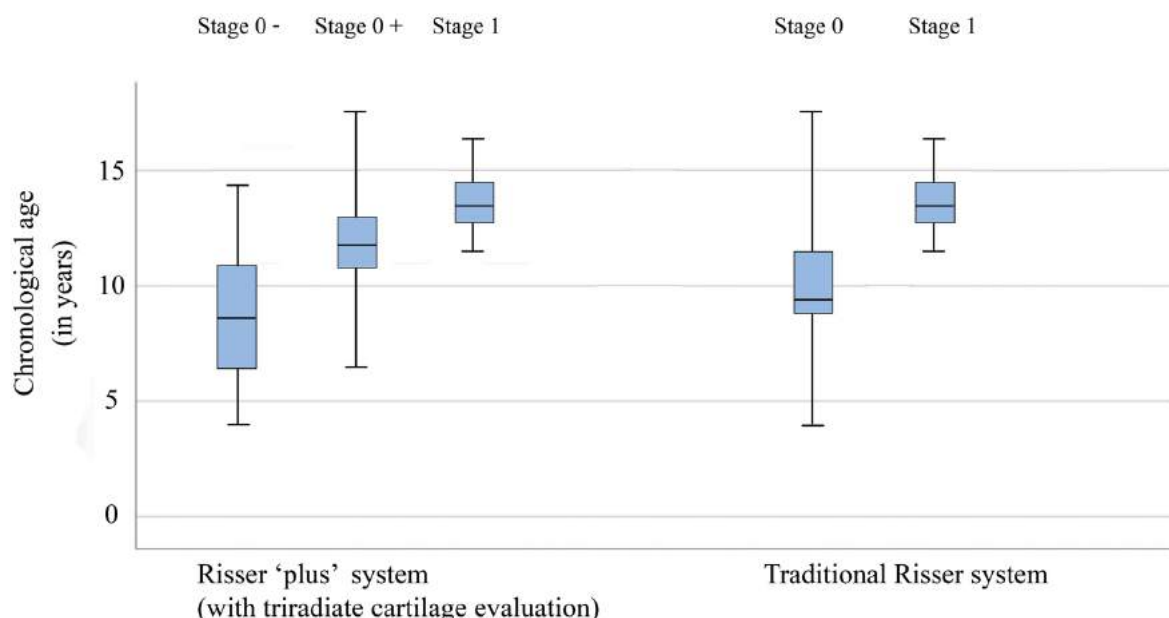


Figure 16. Boxplots presenting the Risser score of children with respect to chronological age of children when evaluated by the Risser ‘plus’ system and by the traditional Risser system (for clarity of comparison, only the lower Risser scores are shown, see figure 13e for Risser scores 2-5).

The most commonly reported problem with Risser ‘plus’ evaluation in the study was resolution, seen in 62 (6.6%) images leading to ‘moderate’ and ‘difficult’ ratings in 59 and 3 images, respectively. The most common cause was difficulty in the upper stages related to identification of the end of fusion of the iliac crest, and 40 of these images with resolution difficulties were in stages 4 or 5.

III. 4.2.4 Knee Method

As a frequent site of trauma, the knee is a commonly imaged but less commonly used region for bone age evaluation. In a 2016 survey of 410 American Society for Pediatric Radiology members, Pyle & Hoerr’s atlas method of knee evaluation was reported as the method of choice for use in infants (14.4% of respondents) and young children less than 3 years old (7.1% of respondents), but no respondents favoured it (0.0%) for use in those 4 years and over⁷².

Methods are based on systems developed in 1955 (Acheson⁹⁷, Pyle & Hoerr¹⁵²) or in 1975 (‘RWT’ / Roche-Wainer-Thissen method¹⁵³). In 2008, O’Connor et al. described an updated method of the RWT method with more stages, consisting of evaluation of the distal femur, proximal tibia and proximal fibular epiphyses, each on a 0-4 point scale, using lateral and anteroposterior images¹¹². As this was the greatest number of stages defined to date, this method was selected for the present study.

In the present study, the knee method received the lowest reported number of ‘easy’ ratings at 68.2% (637/934) of scans. While only 1 scan could not be evaluated, moderate difficulty was reported in 23.7% (221/934) of scans. Overall, problems were most often related to resolution difficulties in identifying the progression of fusion across the margin of the epiphysis and of distinguishing recent fusion with complete fusion (108 or 36% of all problematic scans). These factors also contributed to ‘unsure’ reports (76 or 26% of all problematic evaluations). Patient positioning associated with shadowing from the contralateral limb further contributed to difficulties (60 or 20% of all problematic scans) which was thought to be influenced by patient step length. Although subjective reports of lower step length causing problems, a Spearman correlation found only a weak inverse correlation (-0.100, $p < 0.05$) with ratings. However, step length was found to be

significantly lower in image-pairs in which the lateral image could not be evaluated, with a mean $58.31\text{cm} \pm 46.95$ vs. $78.45\text{cm} \pm 53.5$, ($p < 0.05$, independent t-test).

Interobserver reliabilities with the knee method were the lowest at 0.865 (albeit still a rating of ‘good’ by Winer’s criteria), intraobserver reliabilities were as low as 0.841 and as high as 0.956. The knee method was one of the slowest methods, at mean 80.9s (95% CI 76.09s – 85.66s). Interestingly, similar mean evaluation times were found to the Oxford hip method (82.0s, 95%CI 76.12 – 87.88s), despite a significantly lower number of evaluated regions, the fine differences between each knee stage combined with the need to evaluate each region from two directions before selecting the lower likely contribute to this elevated assessment time.

III. 4.2.5 Oxford Hip Method

The Oxford hip method was first described by Dr. Roy Acheson in 1957⁹⁰, and though of English origin is similarly predominantly based on the Brush population from Ohio. Assessment consists of the evaluation of nine different regions around the pelvis and proximal femur, for a total of 45 stages.

While just 7.6% (71/934) had ‘difficult’ ratings and only 0.20% (2/934) of EOS image pairs could not be assessed using the Oxford hip method, this was influenced by the larger number of landmarks to evaluate. As described in the Materials & Methods, difficulty with just one landmark was not recorded as ‘difficulty’, but rather only if 2 landmarks had some level of difficulty then ‘moderate’ rating was awarded, and if 3 or more, then ‘difficult’ rating assigned. However if scans are counted that had any difficulty reported from even one landmark, an additional 334 scans would be included – predominantly due to difficulties assessing the lesser trochanter, which were encountered in 40.9% of all scans (382/934), accounting for 248 (74.3%) of single landmark difficulty scans, but also the ischium (30/334, 8.9%), femur head (15/334, 4.5%) and greater trochanter (15/334, 4.5%).

Omission of the lesser trochanter has been previously suggested by other authors⁸⁰ as the apophysis is a small delicate structure that can be easily overshadowed, and often totally

hidden depending on rotation of the femur. Our results reporting difficulty in 40.9% of EOS scans would support its omission from evaluation methods. With this modification, the Oxford method may be quite suitable, if time can be invested to familiarise oneself with the technique.

Excellent reliability values were returned particularly for the intra-observer values (ICC = 0.949-0.993), although inter-observer reliability value was slightly lower at 0.902, further pointing towards the importance of adequate teaching and familiarisation of the method.

While the relatively high number of stages is advantageous - conferring a finer gradation of maturity and potentially lowering its sensitivity to observer error – multiple landmarks with unique evaluations make the method cumbersome, steepening the learning curve and increasing time required per scan. As a result, the Oxford method was the slowest of assessment systems evaluated, with mean time taken per scan of 82.0s (95% CI 76.12 – 87.88s) ranging from as low as 20 seconds, especially in easy evaluations such as the very young, but going up as high 280 seconds. However, this mean time required by an experienced observer was still significantly swifter than the two most popular hand-wrist methods: the Tanner-Whitehouse TW2 method has a reported mean 7.8 minutes assessment time¹¹⁷, while Greulich-Pyle's faster atlas method still is estimated at 1.4 minutes per image¹⁵⁴.

Several authors have described a 'modified Oxford hip method'^{80,81,155}, an abbreviated system consisting of evaluation just 5 landmarks: femoral head, greater trochanter, lesser trochanter, the iliac crest and the ischium. When our measurements for the full Oxford hip method were abbreviated to just these five landmarks, the number of 'easy' ratings rose from 78.6% (734/934) to 83.9% (784/934). The lesser trochanter is still included in this method, however, so many images still had difficult landmark evaluations. As the modified Oxford hip method was not assessed separately, no separate timing data was collected, however the omission of 4 landmarks should clearly result in shorter evaluation time.

III. 4.3 EOS & Bone Age Evaluation: Common Problems Encountered

The retrospective application of any evaluation method to images not specifically taken for such purposes, will almost inevitably encounter problems. Several types of difficulty were commonly reported and will be discussed in turn, most notably: (i) step length, (ii) resolution, (iii) image size and (iv) patient position.

III. 4.3.1 Step Length

A lower step length was reported by observers to cause problems when using calcaneus and knee methods. However when evaluated by Spearman correlation, only a minor correlation was found between ratings of the knee and step length (-0.100 , $p < 0.05$) and no significant correlation found in the case of calcaneal evaluation ($p = 0.202$).

When investigated further, however, a significantly lower step length was found in cases which had a lateral knee image that was reported as unevaluable, due to the presence of the overlapping contralateral knee $58.31\text{cm} \pm 46.95$ vs. $78.45\text{cm} \pm 53.5$, ($p < 0.05$, independent t-test).

III. 4.3.2 Resolution

EOS image resolution has been shown to be satisfactory for morphological and structural evaluations⁴⁵ however some bone age assessment methods require staging of very fine features, some of which yielded difficulty. Specific reports of difficulties related to evaluating continuity of trabeculae in the knee, and defining the end of fusion of the calcaneal apophysis (Stage 4 vs. 5), knee (Stage 3 vs. 4) and the femoral head (Stage 6 vs. 7).

The extreme inferior edge appeared to have reduced resolution causing some of these problems with the calcaneal method, resulting in a doubled or multi-layered shadow on the inferior cortex giving an 'onion-skin' appearance (reported in 25 of stage 4 and 5 calcanei, or 7.1% and 3.3% of stage 4 and 5 images).

III. 4.3.3 Image size

Although EOS scans are so-called ‘full body’ images, a number of the image-pairs in our database did not encompass the full extent of the patient from head to sole. In our clinic, physician or radiographer preference resulted on occasion in an altered superior or inferior image margin such that part or all of a region lay outside of the radiograph. Examples of excluded regions included:

- Lower superior image margin resulting in upper cervical vertebrae lying partly (20 cases) or completely outside of the image (26 cases);
- Higher inferior margin leading to the calcaneus partly (95 cases) or totally lying outside of the image;
- Posterior margin lying more anterior / or posterior foot lying posteriorly, leading to the posterior calcaneal pole lying outside of the image (16 cases).

While such problems cannot be solved retrospectively, it is easily achievable to avoid in future scans without modifying any protocols.

III. 4.3.4 Position

Cervical vertebral assessment was affected by variations in head and hand position during imaging in 77 scans. The most common causes were: lateral head tilt (seen in 37 images) leading to moderate (24), difficult (11) or impossible evaluations (2); patients hand and/or finger placement partially covering the upper cervical vertebrae in 30 images (patients standing with an open hand often extended their thumb posteriorly, resulting in a shadow covering C2 and even C3 vertebrae) – this led to moderate (13), difficult (11) or impossible evaluations (6); head rotation in the transverse plane (6 cases); posterior head tilt (2 cases) and hands positioned on either side of the head (2 cases).

III. 4.4 Limitations of this Study

This study has a number of limitations, particularly (i) subjectivity associated with rating systems; (ii) lack of direct comparison with a ‘gold standard’; (iii) multi-landmark methods were perhaps favoured.

- (i) Any rating-based system that aims to describe what method is ‘better’ or ‘more suitable’ such as that used as part of this study, relies on the subjective judgements of observers in both the establishing of the rating system and in its’ application. Every effort was made, however, to ensure consistency and include experiences with the methods – both good and bad – to be of maximum benefit to the reader.

- (ii) Bone age assessment is traditionally performed on conventional radiographic films or their digital representations. While a comparison with the ‘gold standard’ would be of clear use, due to the ethical implications of exposing large numbers of children and adolescents to unnecessary ionising radiation, however, we were unable to perform a direct comparison. Furthermore, our population was retrospectively selected such that not one, but *two* new images would required for such a prospective study. During the initial steps of this investigation, medical records were investigated to locate any individuals who may have had conventional radiographs taken of one or more regions at the same or similar date to their EOS image, however only very few cases were found such that no useful evaluation could be performed (total 31 cases, of which 9 foot radiographs, 19 hip or lower back images such as the oblique spinal Dittmar view, in which all hip parameters could not be evaluated, 2 cervical and 1 knee radiograph).

- (iii) As discussed earlier, the rating system used may also have favoured methods that use more than one landmark. An ‘impossible’ rating was less likely to occur with such systems, however it was felt that if just one landmark led to a ‘moderate’ or ‘difficult’ rating it was not representative of the observers experience. Efforts were made to describe all associated difficulties and causes to supplement the ratings and give the reader a better insight into each method.

Note must be made of a recent study by Jackson et al., who reported on the use of hand-wrist evaluation methods with the EOS scanner by modification of the upper limb position¹³⁹. However in their study the effect of upper limb position changes on spinal

position were neither controlled nor directly measured, indeed they noted that position “may alter the spinal alignment and affect sagittal balance or shoulder height”. We find that to be a grave omission as in our department attempts to alter upper extremity position were trialled but quickly abandoned due to clear alterations in thoracic and cervical spine position (unpublished data).

III. 4.5 Summary - EOS & Bone Age Evaluation

The results of this study support the use of the Risser system with EOS scans but with the inclusion of tri-radiate cartilage assessment as recommended by the guidelines of the Scoliosis Research Society. While the Oxford hip method had the highest mean time per evaluation, its' large number of stages and broad age range coverage suggests it is an appropriate choice for research settings – however omission of the lesser trochanter may be considered, as recommended by other authors⁸⁰. The calcaneus method may not be appropriate for retrospective evaluation, as in our clinic not all images included the full extent of the foot. However, if efforts are made to image the foot and calcaneus during image capture, it may prove a very useful tool – especially in a clinical setting - due to its speed, ease of use and clear description.

	Calcaneus	Cervical	Knee	Oxford Hip	Risser Plus
Reliability	· Excellent (0.945)	· Excellent (0.976)	· Good (0.865)	· Excellent (0.902)	· Excellent (0.940)
Readability	70.8% of scans easily assessed, 6.2% of scans unassessable · Image length affected readability: Image must cover entire length of lower limb or not possible · Resolution: can be difficulty distinguishing the timing of end of fusion (stage 4 vs. 5).	79.0% of scans easily assessable · Image length affected readability: EOS image must cover entire length of cervical spine or not possible · Positioning: (i) Head tilt can lead to mild difficulties. (ii) Hand position can obscure vertebrae making evaluation difficult or position (strict EOS protocol must be applied!)	68.2% of scans easily assessable · Step length: can influence readability of lateral radiographs. · Resolution: harder to assess features important in more mature stages (trabecular continuity, end of fusion)	78.6% of scans easily assessable · Complicated: large number of regions must be evaluated. · Modified Oxford: simplified 5-region method may be superior for the clinician – note: omission of lesser trochanter may be required.	· 89.5% of scans easily assessed (highest rated)
Speed	· Fastest method (17.1s)	· Fast (26.5s)	· Slower (80.9s)	· Slowest method (82s)	· Fast (30.1s)
Age Range	· Broad age range: (4.32 - 11.03y)	· Broad age range (4.73 - 13.57y)	· Broad age range (5.07 - 15.02y)	· Broadest age range (4.0 - 15.08 y)	· Stages start later than other methods (6.55 - 15.27y)
Other	· Simple & Easy to learn · High rater satisfaction	· High rater satisfaction	· Low rater satisfaction	· High rater satisfaction though time consuming.	· High rater satisfaction · Familiar to orthopaedists

Table 13. Summary of main features of each bone age assessment method based on results of evaluation in 934 individuals 4-24 years old.

We hope that the findings presented reveal that rather than a limited range of options, the orthopaedist and paediatric radiologist have a broad palette from which to choose for maturity assessment. Bone age assessment method selection can be based not just on tradition but upon consideration of:

- Setting/ time constraint: clinical (Risser ‘plus’/calcaneus) vs. experimental (Oxford hip);
- Region of Interest: Upper (cervical), Trunk/ Proximal Lower Limb (Risser +‘plus’), Lower body (calcaneus);
- Retrospective vs. prospective: Risser ‘plus’ vs calcaneus.

IV. SUMMARY OF THE THESIS

Bone age is a metric describing the progression of a child towards skeletal maturity, and reflects the state of epiphyseal and/or apophyseal development rather than merely the passing of years and months. The biomechanical parameters of the developing lower limb play an important role in normal function and their alteration may be a component or cause of disease or pre-disease states, such as limb length discrepancy, gait deviation and torsion, however reference values are typically compared to chronological age alone. The EOS scanner has shown an increasing role in paediatric orthopaedics over the past decade due to its' capability for high accuracy, full-body imaging with a low radiation dose burden, however bone age assessment of the hand-wrist cannot be performed without modification of body position, which likely affects spinal posture.

In this study, we aimed to retrospectively assess the lower limb parameters of 1005 children aged 2-24 years old and evaluate the correlations with cervical bone age in addition to chronological age, using a large EOS database. Additionally, our goal was to identify and assess alternative bone age methods that can be applied to EOS images, without the need for modification to the positioning protocol.

Summary of Results:

1. The EOS scanner was demonstrated to show great potential for lower limb assessment with low radiation and accurate assessment.
2. While the majority of lower limb parameters showed greater correlation with chronological age, significantly stronger correlation was found with bone age and rotational parameters (femoral version, tibial torsion, femorotibial rotation) and the neck-shaft angle.
3. Combined models showed even higher correlations for NSA and the rotational parameters, suggesting bone age assessment may be of value to include during lower limb assessment.

4. Neck-shaft angle decreases with increasing maturity, which we first measured at $131.89^\circ \pm 6.07^\circ$ at 4 years old, falling to mean $127.81^\circ \pm 3.84^\circ$ at the age of 20, in contrast to that still reported in some Anatomy textbooks.
5. A higher NSA angle seen in children/adolescents may be normal in those who have an advanced or delayed cervical bone age compared to their peers.
6. Four alternative bone age assessment methods were identified which can be applied to EOS images: the best results were seen in three - the cervical, Oxford hip, and Risser 'plus' methods.
7. The calcaneus method also showed promise as a quick and convenient tool, although analysis of images in our database was not possible in many EOS images as due to physician preference the radiograph did not include the full foot. While this problem is easily solved in future scans, it may be problematic when applied for retrospective purposes.
8. Bone age evaluations can be performed on EOS scans without the need for further scans, reducing radiation dose and administrative & financial burden on the health system and family.

NEW FINDINGS OF THIS THESIS

1. The lower limb parameters and cervical bone age were assessed in a population of 1005 individuals aged 2-24, the largest reported population to be found in the literature.
2. The Hassel-Farman cervical bone age method was applied for the first time in EOS images. This method was found to be effective and showed excellent inter- and intra-observer reliability values.
3. Some biomechanical parameters were found to be associated with the cervical bone age more than the chronological age – the femoral version, tibial torsion, femorotibial rotation, and neck-shaft angle.
4. Combining cervical bone age and chronological age assessments during neck-shaft angle assessment revealed that those with bone ages >1 stage higher or lower than those of similar chronological age, showed significantly higher neck-shaft angles (3.16° and 4.45° higher, respectively), a novelty in the literature.
5. Furthermore, combined cervical bone age and chronological age assessments of neck-shaft angle assessment were found to correlate greater with neck-shaft values and remove gender difference.
6. The bone age was measured with multiple methods in a large population of 941 individuals aged 2-24 years old.
7. Five methods were found to be applicable to EOS images– cervical, Risser ‘plus’, Oxford hip, calcaneus and knee methods. Best results were seen with cervical, Risser ‘plus’ and Oxford hip methods, while the calcaneus method is effective if the foot is visible on the image.

REFERENCES

1. Dimeglio A. Growth in Pediatric Orthopaedics. 2001:549-555.
2. Martin DD, Wit JM, Hochberg Z, et al. The use of bone age in clinical practice – Part 1. *Horm Res Paediatr*. 2011;76(1):1-9.
3. Martin DD, Wit JM, Hochberg Z, et al. The use of bone age in clinical practice - Part 2. *Horm Res Paediatr*. 2011;76(1):10-16.
4. Sanders JO. Maturity indicators in spinal deformity. *J Bone Jt Surg*. 2008;89-A(Supplement 1):14-20.
5. Joseph B, Nayagam S, Loder RT, Torode I. *Paediatric Orthopaedics : A System of Decision-Making*. Hodder Arnold; 2009.
6. Andry N, Le Thieullier L-J. *L'Orthopédie Ou l'art de Prévenir et de Corriger Dans Les Enfants, Les Difformités Du Corps. Le Tout Par Des Moyens à La Portée Des Peres & Des Meres, & de Toutes Les Personnes Qu Ont Des Enfants à Élever. Par M. Andry... Avec Figures*. éditeur non identifié; 1741.
7. Schwab F, Patel A, Ungar B, Farcy J-P, Lafage V. Adult spinal deformity—postoperative standing imbalance: how much can you tolerate? An overview of key parameters in assessing alignment and planning corrective surgery. *Spine (Phila Pa 1976)*. 2010;35(25):2224-2231.
8. Gunderman RB. Essential radiology. Clinical presentation, pathophysiology, imaging. 2. 2006.
9. Sass P, Hassan G. Lower extremity abnormalities in children. *Am Fam Physician*. 2003;68(3):461-468.
10. Bruderer-Hofstetter M, Fenner V, Payne E, Zdenek K, Klima H, Wegener R. Gait deviations and compensations in pediatric patients with increased femoral torsion. *J Orthop Res*. 2015;33(2):155-162.
11. McCarthy JJ, Noonan KJ, Nemke B, Markel M. Guided Growth of the Proximal Femur. *J Pediatr Orthop*. 2010;30(7):690-694.
12. Mills HJ, Horne JG, Purdie GL. The relationship between proximal femoral anatomy and osteoarthritis of the hip. *Clin Orthop Relat Res*. 1993;(288):205-208.
13. Neely FG. Biomechanical risk factors for exercise-related lower limb injuries. *Sport Med*. 1998;26(6):395-413.
14. Kay RM, Jaki KA, Skaggs DL. The effect of femoral rotation on the projected femoral

- neck-shaft angle. *J Pediatr Orthop*. 2000;20(6):736-739.
15. Gaumétou E, Quijano S, Ilharreborde B, et al. EOS analysis of lower extremity segmental torsion in children and young adults. *Orthop Traumatol Surg Res*. 2014;100(1):147-151.
 16. Escott BG, Ravi B, Weathermon AC, et al. EOS low-dose radiography: a reliable and accurate upright assessment of lower-limb lengths. *JBJS*. 2013;95(23):e183.
 17. Schlégl ÁT, Szuper K, Somoskeöy S, Than P. Evaluation of the usefulness of the EOS 2D/3D system for the measurement of lower limbs anatomical and biomechanical parameters in children. *Orv Hetil*. 2014;155(43):1701-1712.
 18. Márkus I, Schlégl ÁT, Burkus M, et al. The effect of coronal decompensation on the biomechanical parameters in lower limbs in adolescent idiopathic scoliosis. *Orthop Traumatol Surg Res*. 2018;104(5):609-616.
 19. Lazennec JY, Brusson A, Dominique F, Rousseau M-A, Pour AE. Offset and anteversion reconstruction after cemented and uncemented total hip arthroplasty: an evaluation with the low-dose EOS system comparing two-and three-dimensional imaging. *Int Orthop*. 2015;39(7):1259-1267.
 20. Green WT, Wyatt CGM, Anderson M. Orthoroentgenography as a method of measuring the bones of the lower extremities. *Clin Orthop Relat Res*. 1968;61:10-15.
 21. Gindhart PS. Growth standards for the tibia and radius in children aged one month through eighteen years. *Am J Phys Anthropol*. 1973;39(1):41-48.
 22. Ruff C. Body size prediction from juvenile skeletal remains. *Am J Phys Anthropol*. 2007;133(1):698-716.
 23. Kingsley P, Olmsted K. A study to determine the angle of anteversion of the neck of the femur. *J Bone Jt Surg*. 1948;30(3):745-751.
 24. Yoshioka Y, Siu D, Cooke TD. The anatomy and functional axes of the femur. *J Bone Joint Surg Am*. 1987;69(6):873-880.
 25. Sabharwal S, Zhao C. The hip-knee-ankle angle in children: reference values based on a full-length standing radiograph. *JBJS*. 2009;91(10):2461-2468.
 26. Birkenmaier C, Jorysz G, Jansson V, Heimkes B. Normal development of the hip: A geometrical analysis based on planimetric radiography. *J Pediatr Orthop Part B*. 2010;19(1):1-8.
 27. Cimolin V, Galli M. Summary measures for clinical gait analysis: a literature review. *Gait Posture*. 2014;39(4):1005-1010.
 28. Pauwels F. Über die Verteilung der Spongiosadichte im coxalen Femurende und ihre

- Bedeutung für die Lehre vom funktionellen Bau des Knochens. In: *Gesammelte Abhandlungen Zur Funktionellen Anatomie Des Bewegungsapparates*. Berlin, Heidelberg: Springer Berlin Heidelberg; 1965:386-399.
29. Pauwels F. *Biomechanics of the Normal and Diseased Hip*. Berlin, Heidelberg: Springer Berlin Heidelberg; 1976.
 30. Ogden J. Hip development and vascularity: the relationship to chondro-osseous trauma in the growing child. *Hip, Proc Ninth Open Sci Meet Hip Soc*. 1981;(St. Louis: CV Mosby.):139-187.
 31. Daldrop-Link H, Gooding C. *Essentials of Pediatric Radiology: A Multimodality Approach*. 1st ed. New York: Cambridge University Press; 2010.
 32. Standring S, Borley NR, Henry G. *Gray's Anatomy: The Anatomical Basis of Clinical Practice*. 40th ed. Edinburgh: Churchill Livingstone/ Elsevier; 2008.
 33. Gilligan I, Chandraphak S, Mahakkanukrauh P. Femoral neck-shaft angle in humans: Variation relating to climate, clothing, lifestyle, sex, age and side. *J Anat*. 2013;223(2):133-151.
 34. Child SL, Cowgill LW. Femoral neck-shaft angle and climate-induced body proportions. *Am J Phys Anthropol*. 2017;164(4):720-735.
 35. Pujol A, Rissech C, Ventura J, Turbón D. Ontogeny of the male femur : geometric morphometric analysis applied to a contemporary Spanish population. *Am J Phys Anthropol*. 2016;159(1):146-163.
 36. Szuper K, Schlégl ÁT, Leidecker E. Three-dimensional quantitative analysis of the proximal femur and the pelvis in children and adolescents using an upright biplanar slot-scanning X-ray system. *Paediatr Radiol*. 2015;45:411-421.
 37. Kim JS, Park TS, Park SB, Kim JS, Kim IY, Kim SI. Measurement of femoral neck anteversion in 3D. Part 1: 3D imaging method. *Med Biol Eng Comput*. 2000;38(6):603-609.
 38. Boese CK, Dargel J, Oppermann J, et al. The femoral neck-shaft angle on plain radiographs: a systematic review. *Skeletal Radiol*. 2016;45(1):19-28.
 39. Boese CK, Frink M, Jostmeier J, et al. The modified femoral neck-shaft angle: Age- and sex-dependent reference values and reliability analysis. *Biomed Res Int*. 2016;2016.
 40. Robin J, Graham HK, Selber P, Dobson F, Smith K, Baker R. Proximal femoral geometry in cerebral palsy: A Population-Based Cross-Sectional Study. *J Bone Jt Surg - Br Vol*. 2008;90-B(10):1372-1379.

41. Hunt MA, Fowler PJ, Birmingham TB, Jenkyn TR, Giffin JR. Foot rotational effects on radiographic measures of lower limb alignment. *Can J Surg*. 2006;49(6):401.
42. Guenoun B, Zadegan F, Aim F, Hannouche D, Nizard R. Reliability of a new method for lower-extremity measurements based on stereoradiographic three-dimensional reconstruction. *Orthop Traumatol Surg Res*. 2012;98(5):506-513.
43. Mckenna C, Wade R, Faria R, et al. EOS 2D / 3D X-ray imaging system : a systematic review and economic evaluation. 2012;16(14).
44. Deschênes S, Charron G, Beaudoin G, et al. Diagnostic imaging of spinal deformities: reducing patients radiation dose with a new slot-scanning X-ray imager. *Spine (Phila Pa 1976)*. 2010;35(9):989-994.
45. Pedersen PH, Petersen AG, Østgaard SE, Tvedebrink T, Eiskjær SP. EOS Micro-dose Protocol: First Full-spine Radiation Dose Measurements in Anthropomorphic Phantoms and Comparisons with EOS Standard-dose and Conventional Digital Radiology. *Spine (Phila Pa 1976)*. 2018;43(22):E1313-E1321.
46. Pace N, Ricci L, Negrini S. A comparison approach to explain risks related to X-ray imaging for scoliosis, 2012 SOSORT award winner. *Scoliosis*. 2013;8(1):11.
47. Ronckers CM, Doody MM, Lonstein JE, Stovall M, Land CE. Multiple diagnostic X-rays for spine deformities and risk of breast cancer. *Cancer Epidemiol Prev Biomarkers*. 2008;17(3):605-613.
48. Ronckers CM, Land CE, Miller JS, Stovall M, Lonstein JE, Doody MM. Cancer mortality among women frequently exposed to radiographic examinations for spinal disorders. *Radiat Res*. 2010;174(1):83-90.
49. Simony A, Christensen SB, Jensen KE, Carreon LY, Andersen MO. Incidence of cancer and infertility, in patients treated for adolescent idiopathic scoliosis 25 years prior. *Eur Spine J*. 2015;24(S6):S740.
50. Protection R. ICRP publication 103. *Ann ICRP*. 2007;37(2.4):2.
51. Hull NC, Binkovitz LA, Schueler BA, Kolbe AB, Larson AN. Upright biplanar slot scanning in pediatric orthopedics: Applications, advantages, and artifacts. *Am J Roentgenol*. 2015;205(1):W124-W132.
52. Schlégl ÁT, Szuper K, Somoskeöy S, Than P. Three dimensional radiological imaging of normal lower-limb alignment in children. *Int Orthop*. 2015;39(10):2073-2080.
53. Schlégl ÁT, O'Sullivan I, Varga P, Than P, Vermes C. Determination and correlation of lower limb anatomical parameters and bone age during skeletal growth (based on 1005 cases). *J Orthop Res*. 2017;35(7):1431-1441.

54. Khung S, Budzik JF, Amzallag-Bellenger E, et al. Skeletal involvement in Langerhans cell histiocytosis. *Insights Imaging*. 2013;4(5):569-579.
55. Canale ST, Beaty JH, Campbell WC. *Campbell's Operative Orthopaedics*. Elsevier/Mosby; 2013.
56. Idiopathic Scoliosis in Children and Adolescents. American Academy of Orthopedic Surgeons. <https://www.aaof.org/afp/2014/0201/p193.html>. Accessed September 9 2014.
57. Mac-Thiong J-M, Berthonnaud É, Dimar JR, Betz RR, Labelle H. Sagittal alignment of the spine and pelvis during growth. *Spine (Phila Pa 1976)*. 2004;29(15):1642-1647.
58. Burkus M, Schlégl ÁT, O'Sullivan I, Márkus I, Vermes C, Tunyogi-Csapó M. Sagittal plane assessment of spino-pelvic complex in a Central European population with adolescent idiopathic scoliosis: a case control study. *Scoliosis spinal Disord*. 2018;13(1):10.
59. Dubousset J, Ilharreborde B, Le Huec J-C. Use of EOS imaging for the assessment of scoliosis deformities: application to postoperative 3D quantitative analysis of the trunk. *Eur Spine J*. 2014;23(4):397-405.
60. Jentzsch T, Geiger J, Bouaicha S, Slankamenac K, Nguyen-Kim TDL, Werner CML. Increased pelvic incidence may lead to arthritis and sagittal orientation of the facet joints at the lower lumbar spine. *BMC Med Imaging*. 2013;13(1):1-10.
61. Roussouly P, Nnadi C. Sagittal plane deformity: an overview of interpretation and management. *Eur spine J*. 2010;19(11):1824-1836.
62. Burkus M, Márkus I, Niklai B, Tunyogi-Csapó M. Assessment of sacroiliacal joint mobility in patients with low back pain. *Orv Hetil*. 2017;158(52):2079-2085.
63. Sanders JO, Khoury JG, Kishan S, et al. Predicting scoliosis progression from skeletal maturity: a simplified classification during adolescence. *JBJS*. 2008;90(3):540-553.
64. Knafo Y, Houfani F, Zaharia B, Egrise F, Clerc-Urmès I, Mainard D. Value of 3D Preoperative planning for primary total hip arthroplasty based on biplanar weightbearing radiographs. *Biomed Res Int*. 2019;2019.
65. Mainard D, Barbier O, Knafo Y, Belleville R, Mainard-Simard L, Gross J-B. Accuracy and reproducibility of preoperative three-dimensional planning for total hip arthroplasty using biplanar low-dose radiographs: a pilot study. *Orthop Traumatol Surg Res*. 2017;103(4):531-536.
66. Zheng G, Hommel H, Akcoltekin A, Thelen B, Stifter J, Peersman G. A novel technology for 3D knee prosthesis planning and treatment evaluation using 2D X-ray

- radiographs: a clinical evaluation. *Int J Comput Assist Radiol Surg*. 2018;13(8):1151-1158.
67. Chronic diseases and health promotion: Chronic rheumatic conditions. World Health Organisation. <http://www.who.int/chp/topics/rheumatic/en/>. Accessed September 9 2014.
 68. Hootman JM, Helmick CG. Projections of US prevalence of arthritis and associated activity limitations. *Arthritis Rheum Off J Am Coll Rheumatol*. 2006;54(1):226-229.
 69. Bendaya S, Lazennec J-Y, Anglin C, et al. Healthy vs. osteoarthritic hips: a comparison of hip, pelvis and femoral parameters and relationships using the EOS® system. *Clin Biomech*. 2015;30(2):195-204.
 70. Soejima U, Motegi E, Sasaki M, et al. Broadband ultrasonic attenuation of children and young adults in Japan. *Bull Tokyo Dent Coll*. 2002;43(1):1-5.
 71. Schmidt S, Mühler M, Schmeling A, Reisinger W, Schulz R. Magnetic resonance imaging of the clavicular ossification. *Int J Legal Med*. 2007;121(4):321-324.
 72. Breen MA, Tsai A, Stamm A, Kleinman PK. Bone age assessment practices in infants and older children among Society for Pediatric Radiology members. *Pediatr Radiol*. 2016;46(9):1269-1274.
 73. Gilbert SF. *Osteogenesis: The Development of Bones (Developmental Biology)*. Sunderland, MA Sinauer Assoc. 2000.
 74. Maclean C, Bartley D, Carey T, Cashin M, Kishta W. The role of secondary ossification centers in the management of epiphyseal and apophyseal fractures. *J Orthop Trauma Surg Relat Res*. 2017;12(2):32-39.
 75. Greulich WW, Pyle SI. Radiographic Atlas Of Skeletal Development Of The Hand And Wrist. *Am J Med Sci*. 1959;238(3):393.
 76. Schmeling A, Reisinger W, Geserick G, Olze A. Forensic age estimation of live adolescents and young adults. In: *Forensic Pathology Reviews*. Springer; 2009:269-288.
 77. Poland J. *Skiagraphic Atlas Showing the Development of the Bones of the Wrist and Hand*. London: Smith, Elder & Co.; 1898.
 78. Little DG, Song KM, Katz D, Herring JA. Relationship of peak height velocity to other maturity indicators in idiopathic scoliosis in girls. *JBJS*. 2000;82(5):685-693.
 79. Kelly PM, Diméglio A. Lower-limb growth: how predictable are predictions? *J Child Orthop*. 2008;2(6):407-415.
 80. Stasikelis PJ, Sullivan CM, Phillips WA, Polard AJ. Slipped capital femoral epiphysis:

- prediction of contralateral involvement. *JBSJ*. 1996;78(8):1149-1155.
81. Nicholson AD, Huez CM, Sanders JO, Liu RW, Cooperman DR. Calcaneal scoring as an adjunct to modified Oxford hip scores. *J Pediatr Orthop*. 2016;36(2):132-138.
 82. Spadoni GL, Cianfarani S. Usefulness of bone age in paediatric endocrinology.
 83. Flores-Mir C, Nebbe B, Major PW. Use of skeletal maturation based on hand-wrist radiographic analysis as a predictor of facial growth: a systematic review. *Angle Orthod*. 2004;74(1):118-124.
 84. Kreitner K-F, Schweden FJ, Riepert T, Nafe B, Thelen M. Bone age determination based on the study of the medial extremity of the clavicle. *Eur Radiol*. 1998;8(7):1116-1122.
 85. Cole TJ. The evidential value of developmental age imaging for assessing age of majority. *Ann Hum Biol*. 2015;42(4):379-388.
 86. Dvorak J, George J, Junge A, Hodler J. Age determination by magnetic resonance imaging of the wrist in adolescent male football players. *Br J Sports Med*. 2007;41(1):45-52.
 87. Engebretsen L, Steffen K, Bahr R, et al. The international olympic committee consensus statement on age determination in high-level young athletes. *Br J Sports Med*. 2010;44(7):476-484.
 88. Ording Müller LS, Offiah A, Adamsbaum C, et al. Bone age for chronological age determination — statement of the European Society of Paediatric Radiology musculoskeletal task force group. *Pediatr Radiol*. 2019:4-7.
 89. Tanner JM, Whitehouse RH, Healy MJR, Goldstein H. A revised system for estimating skeletal maturity from hand and wrist radiographs with separate standards for carpals and other bones (TW II system). *Stand Skelet Age*. 1972.
 90. Acheson RM. The Oxford method of assessing skeletal maturity. *Clin Orthop Relat Res*. 1957;10:19-39.
 91. Risser JC. The Iliac apophysis; an invaluable sign in the management of scoliosis. *Clin Orthop*. 1958;11:111-119.
 92. Nicholson AD, Liu RW, Sanders JO, Cooperman DR. Relationship of calcaneal and iliac apophyseal ossification to peak height velocity timing in children. *J Bone Jt Surg*. 2015;97(2):147-154.
 93. Hassel B, Farman AG. Skeletal maturation evaluation using cervical vertebrae. *Am J Orthod Dentofacial Orthop*. 1995;107(1):58-66.
 94. Björk A, Helm S. Prediction of the age of maximum pubertal growth in body height.

- Angle Orthod.* 1967;37(2):134-143.
95. Fishman LS. Radiographic evaluation of skeletal maturation: a clinically oriented method based on hand-wrist films. *Angle Orthod.* 1982;52(2):88-112.
 96. Grave KC, Brown T. Skeletal ossification and the adolescent growth spurt. *Am J Orthod.* 1976;69(6):311-619.
 97. Acheson RM. A method of assessing skeletal maturity from radiographs; a report from the Oxford child health survey. *J Anat.* 1954;88(4):498-508.
 98. Singer J. Physiologic Timing of Orthodontic Treatment. *Angle Orthod.* 1980;50(4):322-333.
 99. Lamparski DG. Skeletal age assessment utilizing cervical vertebrae. 1975;67(4):458-459.
 100. Mito T, Sato K, Mitani H. Cervical vertebral bone age in girls. *Am J Orthod Dentofac Orthop.* 2002;122(4):380-385.
 101. Román PS, Palma JC, Oteo MD, Nevado E. Skeletal maturation determined by cervical vertebrae development. *Eur J Orthod.* 2002;24(3):303-311.
 102. Walker RA, Lovejoy CO. Radiographic changes in the clavicle and proximal femur and their use in the determination of skeletal age at death. *Am J Phys Anthropol.* 1985;68(1):67-78.
 103. Sauvegrain J, Nahum H, Bronstein H. Study of bone maturation of the elbow. In: *Annales de Radiologie.* Vol 5. ; 1962:542.
 104. Schaefer M, Aben G, Vogelsberg C. A demonstration of appearance and union times of three shoulder ossification centers in adolescent and post-adolescent children. *J Forensic Radiol Imaging.* 2015;3(1):49-56.
 105. Schmeling A, Reisinger W, Loreck D, Vendura K, Markus W, Geserick G. Effects of ethnicity on skeletal maturation: consequences for forensic age estimations. *Int J Legal Med.* 2000;113(5):253-258.
 106. Michelson N. The calcification of the first costal cartilage among whites and negroes. *Hum Biol.* 1934;6(3):543.
 107. Negrini S, Hresko TM, O'Brien JP, et al. Recommendations for research studies on treatment of idiopathic scoliosis: Consensus 2014 between SOSORT and SRS non-operative management committee. *Scoliosis.* 2015;10(1):1-12.
 108. McKern TW, Stewart TD. *Skeletal Age Changes in Young American Males Analysed from the Standpoint of Age Identification.* Quartermaster Research And Engineering Command Natick MA; 1957.

109. Stull KE, L'Abbé EN, Ousley SD. Using multivariate adaptive regression splines to estimate subadult age from diaphyseal dimensions. *Am J Phys Anthropol*. 2014;154(3):376-386.
110. Tsai A, Stamoulis C, Bixby SD, Breen MA, Connolly SA, Kleinman PK. Infant bone age estimation based on fibular shaft length : model development and clinical validation. 2015.
111. Pyle SI, Hoerr NL. *A Radiographic Standard of References for the Growing Knee (Revised)*. Springfield, IL: Charles C Thomas; 1969.
112. O'Connor JE, Bogue C, Spence LD, Last J. A method to establish the relationship between chronological age and stage of union from radiographic assessment of epiphyseal fusion at the knee: an Irish population study. *J Anat*. 2008;212(2):198-209.
113. Tanner JM. *Scholar.*; 1983.
114. Thodberg HH, Kreiborg S, Juul A, Pedersen KD. The BoneXpert method for automated determination of skeletal maturity. *IEEE Trans Med Imaging*. 2009;28(1):52-66.
115. Karol LA, Johnston 2nd CE, Browne RH, Madison M. Progression of the curve in boys who have idiopathic scoliosis. *JBJS*. 1993;75(12):1804-1810.
116. Urbaniak JR, Schaefer WW. Iliac apophyses. Prognostic value in idiopathic schliosis. *Clin Orthop Relat Res*. 1976;(116):80-85.
117. De Sanctis V, Maio S, Soliman A, Raiola G, Elalaily R, Millimaggi G. Hand X-ray in pediatric endocrinology: Skeletal age assessment and beyond. *Indian J Endocrinol Metab*. 2014;18(7):63.
118. Charles YP, Diméglio A, Canavese F, Daures J-P. Skeletal age assessment from the olecranon for idiopathic scoliosis at Risser grade 0. *J Bone Jt Surg*. 2007;89(12):2737-2744.
119. Imanimoghadam M, Heravi F, Khalaji M, Esmaily H. Evaluation of the correlation of different methods in determining skeletal maturation utilizing cervical vertebrae in lateral cephalogram. *J Mashhad Dent Sch*. 2008;32(2):95-102.
120. Winer BJ. *Statistical Principles in Experimental Design*. 1st ed. McGraw-Hill; 1962.
121. van der Linden ML, Hazlewood ME, Hillman SJ, Robb JE. Passive and dynamic rotation of the lower limbs in children with diplegic cerebral palsy. *Dev Med Child Neurol*. 2006;48(3):176-180.
122. Rethlefsen SA, Nguyen DT, Wren TAL, Milewski MD, Kay RM. Knee pain and patellofemoral symptoms in patients with cerebral palsy. *J Pediatr Orthop*.

- 2015;35(5):519-522.
123. Maquet PGJ. Biomechanics of the Hip. In: *Biomechanics of the Hip*. Berlin, Heidelberg: Springer Berlin Heidelberg; 1985:1-45.
 124. Lee MC, Ebersson CP. Growth and Development of the Child ' s Hip. *Orthop Clin North Am*. 2006;37:119-132.
 125. Giorgi M, Carriero A, Shefelbine SJ, Nowlan NC. Effects of normal and abnormal loading conditions on morphogenesis of the prenatal hip joint: Application to hip dysplasia. *J Biomech*. 2015;48(12):3390-3397.
 126. Shefelbine SJ, Carter DR. Mechanobiological predictions of growth front morphology in developmental hip dysplasia. *J Orthop Res*. 2004;22(2):346-352.
 127. Leet AI, Wientroub S, Kushner H, et al. The correlation of specific orthopaedic features of polyostotic fibrous dysplasia with functional outcome scores in children. *J Bone Jt Surg - Ser A*. 2006;88(4):818-823.
 128. Nelson MD. The radiological approach to precocious puberty: Pictorial review. *Br J Radiol*. 2000;73(May 2014):560-567.
 129. Salerno M, Micillo M, Di Maio S, et al. Longitudinal growth, sexual maturation and final height in patients with congenital hypothyroidism detected by neonatal screening. *Eur J Endocrinol*. 2001;145(4):377-383.
 130. Williams GR, Bassett JHD. Thyroid diseases and bone health. *J Endocrinol Invest*. 2017;41(1):99-109.
 131. Cantu G, Buschang PH, Gonzalez JL. Differential growth and maturation in idiopathic growth-hormone-deficient children. *Eur J Orthod*. 1997;19(2):131-139.
 132. Mary L Ee Vance , M.D., and N Elly Mauras MD. G Rowth H Ormone T Herapy in a Dults and C Hildren. *N Engl J Med*. 1999:879-884.
 133. Nissen N, Hauge EM, Abrahamsen B, Jensen JEB, Mosekilde L, Brixen K. Geometry of the Proximal Femur in Relation to Age and Sex: a Cross-Sectional Study in Healthy Adult Danes. *Acta radiol*. 2005;46(5):514-518.
 134. Azar FM, Canale ST, Beaty JH, Preceded by: Campbell WC (Willis C. *Campbell's Operative Orthopaedics*. 12th ed. Oxford: Mosby - Elsevier; 2013.
 135. Onland-Moret NC, Peeters PHM, Van Gils CH, et al. Age at menarche in relation to adult height: The EPIC study. *Am J Epidemiol*. 2005;162(7):623-632.
 136. Wang Q, Chen D, Cheng SM e., Nicholson P, Alen M, Cheng S. Growth and aging of proximal femoral bone: a study with women spanning three generations. *J Bone Miner Res*. 2015;30(3):528-534.

137. Pearce MS, Birrell FN, Francis RM, Rawlings DJ, Tuck SP, Parker L. Lifecourse study of bone health at age 49-51 years: The Newcastle thousand families cohort study. *J Epidemiol Community Health*. 2005;59(6):475-480.
138. Freedman DS, Khan LK, Serdula MK, Dietz WH, Srinivasan SR, Berenson GS. Relation of Age at Menarche to Race , Time Period , and Anthropometric Dimensions : The Bogalusa Heart Study. 2002;110(4).
139. Jackson TJ, Miller D, Nelson S, Cahill PJ, Flynn JM. Two for One: A Change in Hand Positioning During Low-Dose Spinal Stereoradiography Allows for Concurrent, Reliable Sanders Skeletal Maturity Staging. *Spine Deform*. 2018;6(4):391-396.
140. Schaefer M, Aben G, Vogelsberg C. A demonstration of appearance and union times of three shoulder ossification centers in adolescent and post-adolescent children. *J Forensic Radiol Imaging*. 2015;3(1):49-56.
141. Garamendi PM, Landa MI, Botella MC, Alemán I. Forensic age estimation on digital X-ray images: medial epiphyses of the clavicle and first rib ossification in relation to chronological age. *J Forensic Sci*. 2011;56:S3-S12.
142. Nelson S, Hans MG, Broadbent BH, Dean D. The brush inquiry: An opportunity to investigate health outcomes in a well-characterized cohort. *Am J Hum Biol*. 2000;12(1):1-9.
143. Li SQ, Nicholson AD, Cooperman DR, Liu RW. Applicability of the calcaneal apophysis ossification staging system to the modern pediatric population. *J Pediatr Orthop*. 2019;39(1):46-50.
144. Uysal T, Ramoglu SI, Basciftci FA, Sari Z. Chronologic age and skeletal maturation of the cervical vertebrae and hand-wrist: Is there a relationship? *Am J Orthod Dentofac Orthop*. 2006;130(5):622-628.
145. Baccetti T, Franchi L, McNamara JA. The Cervical Vertebral Maturation (CVM) method for the assessment of optimal treatment timing in dentofacial orthopedics. *Semin Orthod*. 2005;11(3):119-129.
146. Caldas M de P, Ambrosano GMB, Haiter Neto F. New formula to objectively evaluate skeletal maturation using lateral cephalometric radiographs. *Braz Oral Res*. 2007;21(4):330-335.
147. Chen L-L, Xu T-M, Jiang J-H, Zhang X-Z, Lin J-X. Quantitative cervical vertebral maturation assessment in adolescents with normal occlusion: a mixed longitudinal study. *Am J Orthod Dentofac Orthop*. 2008;134(6):720-e1.
148. Yang Y, Lee J, Kim Y, Cho B, Park S. Axial cervical vertebrae-based multivariate

- regression model for the estimation of skeletal-maturation status. *Orthod Craniofac Res.* 2014;17(3):187-196.
149. Bitan FD, Veliskakis KP, Campbell BC. Differences in the Risser grading systems in the United States and France. *Clin Orthop Relat Res.* 2005;(436):190-195.
150. Sanders JO, Browne RH, McConnell SJ, Margraf SA, Cooney TE, Finegold DN. Maturity assessment and curve progression in girls with idiopathic scoliosis. *J Bone Jt Surg - Ser A.* 2007;89(1):64-73.
151. Little DG, Sussman MD. The Risser sign: a critical analysis. *J Pediatr Orthop.* 1994;14(5):569-575.
152. Pyle SI, Hoerr NL. *A Radiographic Standard of Reference for the Growing Knee.* CC Thomas; 1955.
153. Roche AF, Wainer H, Thissen D. *Skeletal Maturity: The Knee Joint as a Biological Indicator.* Plenum Medical Book Company; 1975.
154. Van Rijn RR, Thodberg HH. Bone age assessment: Automated techniques coming of age? *Acta radiol.* 2013;54(9):1024-1029.
155. Murray DW, Fitzpatrick R, Rogers K, et al. The use of the Oxford hip and knee scores. *J Bone Joint Surg Br.* 2007;89(8):1010-1014.

APPENDIX

Supplementary Table 1. Table shows all bone age and dental age assessment methods found during our literature review. Literature review was performed via the website pubmed.gov [accessed 2016.03.30]. A search performed using keywords "bone age", "skeletal age" and "skeletal maturation" with no language or date restrictions yielded 4758 publications, after removal of 433 duplicates. All abstracts were investigated and articles accessed if promising, or information not available in the abstract. Types of assessment methods can be described as atlas type ('Atlas') or scoring types ('Scoring') methods, Scoring methods are described in this table by the format of scoring i.e. number of stages, linear equation, continuous scale, counting appearance of ossification centres etc. The number of citations of each paper (as per scholar.google.com) were collected time of preparation of the present table (2019.10.09). *'Article not found'*: describing article could not be located, despite our best efforts; *'Foreign Language [language]'*: some lesser known methods were described in languages other than English, and the original article could not be located. Three methods included were described after the original search date (marked *), however they have been included due to potential future interest. One method was included that was found indirectly during the review, it has been included for the sake of completeness and marked with a cross (†) symbol. (AP: Anteroposterior, CT: Computed tomography, GP: Greulich-Pyle Atlas, HF: Hassel-Farman method, mo: months, MR: Magnetic resonance, y: years)

Region	Author	Year of Pub.	Type	Citations	Modality	Image type	No. of Stages	Summary of Method	Reference
Ankle & Foot	Hoerr, Pyle, Francis	1962	Atlas	5	X-ray	Lateral & AP Foot	31 ages	Atlas method of ankle and foot.	Hoerr NL, Pyle SI, Francis CC. Radiological Atlas of the Foot and Ankle. Charles C Thomas, Springfield., 1962.
Calcaneus	Nicholson	2015	Scoring	20	X-ray	Lateral foot	6 stages	Calcaneal apophysis is scored based on presence, extent and state of fusion.	Nicholson AD, Liu RW, Sanders JO, Cooperman DR. Relationship of Calcaneal and Iliac Apophyseal Ossification to Peak Height Velocity Timing in Children. J Bone Jt Surg. 2015;97(2):147-154.
	Sherif	2003	Scoring	3	Ultrasound	Ultrasound	Linear scale	Normal range of calcaneal volume values in a 0-6 year old Egyptian population have been presented, as measured by ultrasound.	Sherif H, Noureldin M, Bakr AF, Mahfouz AE. Sonographic Measurement of Calcaneal Volume for Determination of Skeletal Age in Children. J Clin Ultrasound. 2003;31(9):457-460.
Cervical	Alhadlag & Al-shayea	2013	Scoring	6	X-ray	Lateral cephalogram	5 stages	Angular based method: user traces C2-C3-C4 and calculates the angles between a line running along the base, and the highest point of the inferior concavity. 5 stages were identified correlating to Baccetti's method. Only males.	Alhadlaq AM, Al-shayea EI. New method for evaluation of cervical vertebral maturation based on angular measurements. Saudi Med J. 2013;33(4):388-394.
	Baccetti: 6-stage	2002	Scoring	655	X-ray	Lateral cephalogram	6 stages	Second to fourth cervical vertebrae are assessed by morphology: height, inferior curvature and shape. "CS" or "cervical stage" method.	Baccetti T, Franchi L, McNamara Jr JA. An improved version of the cervical vertebral maturation (CVM) method for the assessment of mandibular growth. Angle Orthod. 2002;72(4):316-323.
	Baccetti modified: Semi-automated	2012	Scoring	11	X-ray	Lateral cephalogram	6 stages	User selects 13 landmarks on C2-C4 indicating anterior inferior, posterior inferior, anterior superior (C3 & C4 only) and posterior superior points (C3 & C4 only), and the highest point of the inferior concave. Stages as per Baccetti are then applied using computer software.	Baptista RS, Quaglio CL, Mourad LMEH, et al. A semi-automated method for bone age assessment using cervical vertebral maturation. Angle Orthod. 2012;82(4):658-662.
	Baccetti modified: CT	2015	Scoring	29	CT	Cone-beam CT	6 stages	Lateral cephalogram generate from CBCT and evaluated.	Angelieri F, Franchi L, Cevidanes LHS, McNamara Jr JA. Diagnostic performance of skeletal maturity for the assessment of midpalatal suture maturation. Am J Orthod Dentofac Orthop. 2015;148(6):1010-1016.
	Baccetti modified: 5 stage	2006	Scoring	23	X-ray	Lateral cephalogram	5 stages	Sixth stage is not included.	Santos ECA, Bertoz FA, Arantes FDM, Reis PMP, Bertoz APDM. Skeletal maturation analysis by morphological evaluation of the cervical vertebrae. J Clin Pediatr Dent. 2006;30(3):265-270.
	Caldas	2007	Scoring	42	X-ray	Lateral cephalogram	Linear regression equation	Based on a formula, reader traces and then measures height, width, angle etc.	Caldas M de P, Ambrosano GMB, Haiter Neto F. New formula to objectively evaluate skeletal maturation using lateral cephalometric radiographs. Braz Oral Res. 2007;21(4):330-335.
	Caldas modified: Semi-automated	2010	Scoring	25	X-ray	Lateral cephalogram	Linear regression equation	Based on a formula, selects landmarks indicating anterior/posterior and superior/inferior poles, and software calculates bone age based on Caldas' equation.	Caldas M de P, Bovi Ambrosano GM, Neto FH. Computer-assisted analysis of cervical vertebral bone age using cephalometric radiographs in Brazilian subjects. Braz Oral Res. 2010;24(1):120-126.
	Chen	2008	Scoring	64	X-ray	Lateral cephalogram	4 stages	So-called "Quantitative cervical morphology" or QVCM. Tracings of C3, C4: ant height, posterior height, middle height and superior/midline/inferior anteroposterior length. Formula made based on these can calculate SMI (as used in Fishman maturity)	Chen L-L, Xu T-M, Jiang J-H, Zhang X-Z, Lin J-X. Quantitative cervical vertebral maturation assessment in adolescents with normal occlusion: a mixed longitudinal study. Am J Orthod Dentofac Orthop. 2008;134(6):720-e1.

Franchi	2000	Atlas	420	X-ray	Lateral cephalogram	6 stages	Cervical vertebral morphology are assessed at C2-C6. Baccetti et al. method is based on a abbreviated system.	Franchi L, Baccetti T, McNamara JA. Mandibular growth as related to cervical vertebral maturation and body height. Am J Orthod Dentofac Orthop. 2000;118(3):335-340.
Harfin	2008	-	3	X-ray	Lateral cephalogram	-	Not found - foreign language [Polish]	Harfin, J.F., Kahn de Gruner, S.E., Porta, G. and Kaplan, A., 2008. Nowy sposób określania wieku szkieletowego oparty na wtórnych ośrodkach kostnienia kręgów szyjnych. In Forum Ortod (Vol. 4, No. 2, pp. 33-43).
Hassel-Farman	1995	Scoring	713	X-ray	Lateral cephalogram	6 stages	C2-C4 morphology based on shape, inferior curve depth, and height.	Hassel B, Farman AG. Skeletal maturation evaluation using cervical vertebrae. Am J Orthod Dentofac Orthop. 1995;107(1):58-66..
Hassel-Farman modification: C3 only	2005	Scoring	26	X-ray	Lateral cephalogram	6 stages	HF method, only assessing C3.	Seedat AK, Forsberg CD. An evaluation of the third cervical vertebra (C3) as a growth indicator in Black subjects. SADJ. 2005 May;60(4):156,158-60
Hassel-Farman modification: Semi-automated	2015	Scoring	3	X-ray	Lateral cephalogram	6 stages	Software assisted. Physician traces the vertebrae, and it helps estimate.	Dzemidzic, V., Sokic, E., Tiro, A. and Nakas, E., 2015. Computer based assessment of cervical vertebral maturation stages using digital lateral cephalograms. Acta Informatica Medica, 23(6), p.364.
Hassel-Farman modification: 3D-CT	2016	Scoring	6	CT	Lateral image 3D CT	6 stages	HF method, using lateral aspect as generated from 3D CT images.	Bonfim MAE, Costa ALF, Fuziy A, Ximenez MEL, Cotrim-Ferreira FA, Ferreira-Santos RI. Cervical vertebrae maturation index estimates on cone beam CT: 3D reconstructions vs sagittal sections. Dentomaxillofac Radiol. 2016;45(1):20150162.
Lamparski	1972	Scoring	17	X-ray	Lateral cephalogram	6 stages	First cervical morphology method described.	Lamparski DG. Skeletal age assessment utilizing cervical vertebrae. 1975;67(4):458-459.
Mito	2002	Scoring	180	X-ray	Lateral cephalogram	Linear regression equation	C3 & C4 tracings made and measurements of anterior height, posterior height, midpoint height and anteroposterior length. Equation made based on these.	Mito T, Sato K, Mitani H. Cervical vertebral bone age in girls. Am J Orthod Dentofac Orthop. 2002;122(4):380-385.
Rhee	2015	Scoring	2	CT	Cone-beam CT	Linear regression equation	C2-C4: 8 points per vertebra, 6 points on odontoid process. Linear regression generated equations	Rhee CH, Shin SM, Choi YS, et al. Application of statistical shape analysis for the estimation of bone and forensic age using the shapes of the 2nd, 3rd, and 4th cervical vertebrae in a young Japanese population. Forensic Sci Int. 2015;257:513.e1-513.e9.
San Roman	2002	Scoring	254	X-ray	Lateral cephalogram	Linear regression equation	C3 & C4: equation based on stages of 3 features: inferior concavity (6 stages), vertebral shape (6 stages) and height vs. width (6 stages).	Román PS, Palma JC, Oteo MD, Nevado E. Skeletal maturation determined by cervical vertebrae development. Eur J Orthod. 2002;24(3):303-311.
Santiago	2014	Scoring	5	X-ray	Lateral cephalogram	4 stages	User selects 13 landmarks on C2-C4 indicating anterior inferior, posterior inferior, anterior superior (C3 & C4 only) and posterior superior points (C3 & C4 only), and the highest point of the inferior concave. Stages as per Baccetti are then applied using computer software. Stages correlated to Fishman SMI 1:1-3, 2: 4-7, 3: 8-9, 4:10-11.	Santiago RC, Cunha AR, Júnior GC, et al. New software for cervical vertebral geometry assessment and its relationship to skeletal maturation-a pilot study. Dentomaxillofac Radiol. 2014;43(2).
Su	2006	Scoring	0	-	-	Linear regression equation	Description in Chinese: Abstract - equation based on vertebral anterior height, height, anteroposterior length of C3 and C4.	Su L, Lü Y, Wang HM. Cervical vertebral bone age during puberty. Zhonghua kou qiang yi xue za zhi= Zhonghua kouqiang yixue zazhi= Chinese J Stomatol. 2006;41(12):728-729.
Varshosaz	2012	Scoring	9	X-ray	Lateral cephalogram	Linear regression equation	Anterior height of C4 measured and used as part of equation. 91 Iranian individuals aged 8-18 years	Varshosaz M, Ehsani S, Nouri M, Tavakoli MA. Bone age estimation by cervical vertebral dimensions in lateral cephalometry. Prog Orthod. 2012;13(2):126-131.
Yang	2014	Scoring	8	CT	Cone-beam CT	Linear regression equation	C1-C4: Axial images generated and 23 points selected across the vertebrae, (most anterior point,	Yang Y, Lee J, Kim Y, Cho B, Park S. Axial cervical vertebrae-based multivariate regression model for the estimation of skeletal-maturation status. Orthod Craniofac Res. 2014;17(3):187-196.

								posterior point etc). Linear regression derived equations could then be applied to establish bone age. Equations not shown in paper, though they find several regions alone were correlated well with maturation.	
Clavicle	Kreitner	1998	Scoring	249	CT	Multi-slice CT	3 stages	Appearance, partial fusion and complete fusion of medial epiphyseal ossification center.	Kreitner K-F, Schweden FJ, Riepert T, Nafe B, Thelen M. Bone age determination based on the study of the medial extremity of the clavicle. Eur Radiol. 1998;8(7):1116-1122.
	Schmeling: 5 stage	2004	Scoring	296	X-ray	Chest X-ray	5 stages	Initial 4 stages based on common schema: non-fused, fusing, almost fused, fused, in addition to a further fifth stage when no scar can be seen.	Schmeling A, Schulz R, Reisinger W, Mühler M, Wernecke K-D, Geserick G. Studies on the time frame for ossification of the medial clavicular epiphyseal cartilage in conventional radiography. Int J Legal Med. 2004;118(1):5-8.
	Schmeling modified: 4 stage	2015	Scoring	18	CT	Multi-slice CT	4 stages	Initial 4 stages based on common schema: non-fused, fusing, almost fused, fused (independent of presence or absence of scar) some studies such as Zhang et al. have used this 4 stage method.	Zhang K, Chen X, Zhao H, Dong X, Deng Z. Forensic Age Estimation Using Thin-Slice Multidetector CT of the Clavicular Epiphyses Among Adolescent Western Chinese. J Forensic Sci. 2015;60(3):675-678.
	Schmeling modified: MR	2010	Scoring	87	MR	MR	5 stages	Initial 4 stages based on common schema: non-fused, fusing, almost fused, fused, in addition to a further stage 5 when no scar can be seen.	Hillewig E, De Tobel J, Cuche O, Vandemaële P, Piette M, Verstraete K. Magnetic resonance imaging of the medial extremity of the clavicle in forensic bone age determination: A new four-minute approach. Eur Radiol. 2011;21(4):757-767.
	Schmeling modified: 4 stage	2010	Scoring	179	CT	Thin slice CT	9 stages	Second and third stages are expanded with 3 substages each.	Kellinghaus M, Schulz R, Vieth V, Schmidt S, Pfeiffer H, Schmeling A. Enhanced possibilities to make statements on the ossification status of the medial clavicular epiphysis using an amplified staging scheme in evaluating thin-slice CT scans. Int J Legal Med. 2010;124(4):321-325.
	Schmidt	2007	Scoring	133	MR	MR	4 stages	Presence of ossification at the secondary center, extent and completion are assessed at the medial clavicle.	Schmidt S, Mühler M, Schmeling A, Reisinger W, Schulz R. Magnetic resonance imaging of the clavicular ossification. Int J Legal Med. 2007;121(4):321-324.
	Schulz	2008	Scoring	99	Ultrasound	Ultrasound	4 stages	Appearance and fusion of medial clavicle ossification centre are assessed, in addition to epiphyseal plate shape and state of ossification.	Schulz R, Zwiesigk P, Schiborr M, Schmidt S, Schmeling A. Ultrasound studies on the time course of clavicular ossification. Int J Legal Med. 2008;122(2):163-167.
Cranial	Lottering	2015	Scoring	22	CT	Multi-slice Head CT	6 stages	6 stages based on Spheno-Occipital Synchronosis ossification.	Lottering N, MacGregor DM, Alston CL, Gregory LS. Ontogeny of the spheno-occipital synchronosis in a modern Queensland, Australian population using computed tomography. Am J Phys Anthropol. 2015;157(1):42-57.
	Lottering	2016	Scoring	9	CT	Cranial/ cervical multi-slice CT	24 stages, different region: (total 19).	6 fontanelles & osteosynchronosis regions are assessed. The time of closure of each region is described by as few as 2 or as many as 4 stages.	Lottering N, Macgregor DM, Alston CL, Watson D, Gregory LS. Introducing Computed Tomography Standards for Age Estimation of Modern Australian Subadults Using Postnatal Ossification Timings of Select Cranial and Cervical Sites. J Forensic Sci. 2016;61(3):39-52.
	Bassed	2010	Scoring	74	CT	Multi-slice CT	5 stages	Ossification extent from superior to inferior of the spheno-occipital chondrosis. (Staging modified from Powell and Brodie, 1963 - forensic study with X-ray).	Bassed RB, Briggs C, Drummer OH. Analysis of time of closure of the spheno-occipital synchronosis using computed tomography. Forensic Sci Int. 2010;200(1-3):161-164.
	Shirley & Jantz	2011	Scoring	78	CT	Cone-beam head CT	3 stages	The open/fusing/fused state is assessed at the spheno-occipital osteochondrosis.	Shirley NR, Jantz RL. Spheno-occipital synchronosis fusion in modern Americans. J Forensic Sci. 2011;56(3):580-585.
	Franklin & Flavel	2014	Scoring	34	CT	Multi-detector CT	4 stages	Spheno-occipital osteochondrosis is evaluated for open/fusing/fused with scar/ fused with no scar.	Franklin D, Flavel A. Brief Communication: Timing of spheno-occipital closure in modern Western Australians. Am J Phys Anthropol. 2014;153(1):132-138.

	Ertürk	1968	Scoring	5	X-ray	Lateral cephalogram	No stages	Frontal sinus maximum dimension height and width measured and can be compared against standards.	Ertürk, N., 1968. Teleroentgen studies on the development of the frontal sinus. Fortschritte der Kieferorthopadie, 29(2), pp.245-248.
Dental	Cameriere	2006	Scoring	247	X-ray	Panoramic X-ray	Linear regression equation	Open root apices of the teeth are measured, and summed. Data can be entered into linear regression equation.	Cameriere R, Ferrante L, Cingolani M. Age estimation in children by measurement of open apices in teeth. Int J Legal Med. 2006;120(1):49-52.
	Demirjian	1973	Scoring	2031	X-ray	Panoramic X-ray	63 stages	Seven left mandibular permanent teeth are rated in the order of the second molar, first molar, second premolar, first premolar, canine, lateral incisors and central incisor into eight stages [A-H] of tooth mineralization, stage 0 marks absence/ non-appearance of a tooth. All ratings are compared against a table to give a maturity score per tooth, which are summed, and then overall maturity score can be compared against a developmental percentile chart for each gender.	Demirjian A, Goldstein H, Tanner JM. Demirjian, A., A New System of Dental Age Assessment, Human Biology, 45:2 (1973:May) p.211. Hum Biol. 1973;45(2):211-227.
	Demirjian modified: Chaillet	2005	Scoring	158	X-ray	Panoramic X-ray	63 stages	"Multi-ethnic weighted score" chart, that allows use independent of knowledge of ethnicity.	Chaillet N, Nyström M, Demirjian A. Comparison of Dental Maturity in Children of Different Ethnic Origins: International Maturity Curves for Clinicians. J Forensic Sci. 2005;50(5):1-11.
	Demirjian modified: Third Molar only	1993	Scoring	500	X-ray	Panoramic X-ray	8 stages	Third molar only. All 4 evaluated and averaged.	Mincer HH, Harris EF, Berryman HE. The A.B.F.O. Study of Third Molar Development and Its Use as an Estimator of Chronological Age. J Forensic Sci. 1993;38(2):13418J. doi:10.1520/jfs13418j
	Demirjian modified: Willems	2001	Scoring	417	X-ray	Panoramic X-ray	63 stages	Updated chart for Belgian children to avoid overestimation of bone age.	Willems G, Van Olmen A, Spiessens B, Carels C. Dental age estimation in Belgian children: Demirjian's technique revisited. J Forensic Sci. 2001;46(4):893-895.
	Demirjian modified: Four Tooth Modification	1989	Scoring	70	X-ray	Panoramic X-ray	36 stages	Using just 4 teeth. Based on Finnish standards.	Kataja M, Nyström M, Aine L. Dental maturity standards in southern Finland. Proc Finn Dent Soc. 1989;85(3):187-197.
	Gat	1972	Scoring	2	X-ray	Panoramic X-ray	84 stages	Fourteen permanent teeth on mandible and maxilla are scored from 1-5, excluding the third molar, and the sum of the values is the 'dental age'.	Gat H. An evaluation of dental ages of Norwegian children from the Bergen area. Univ Bergen, Bergen. 1972.
	Gleiser & Hunt	1995	Scoring	442	X-ray	Lateral mandibular	15 stages	First right mandibular permanent molar evaluated.	Gleiser I, Hunt Jr EE. The Permanent Mandibular First Molar: Its Calcification, Eruption and Decay. Am J Phys Anthropol. 1995;(13):253-283.
	Gleiser & Hunt modification: Kullman	1992	Scoring	251	X-ray	Panoramic X-ray	7 stages	Third molar root development is evaluated.	Kullman L, Johanson G, Akesson L. Root development of the lower third molar and its relation to chronological age. Swed Dent J. 1992;16(4):161-167.
	Gleiser & Hunt modification: Liversidge	2008	Scoring	157	X-ray	Panoramic X-ray/ Supplementary apical in some cases	15 stages	Third molar evaluated based on progressive stages described by changes in the crypt, cusp, crown, cleft, root and apex: applicable on from 16 years and above.	Liversidge HM. Timing of human mandibular third molar formation. Ann Hum Biol. 2008;35(3):294-321.
	Gustafson & Koch	1974	Scoring	432	X-ray	Panoramic X-ray	90 stages	Emergence and 3 maturation stages for right lower and left upper teeth are shown in their diagrams. Values are compared against a reference	Gustafson G, Koch G. Age estimation up to 16 years of age based on dental development. Odontol Revy. 1974;25(3):297-306.

								chart which gives weighting, and corresponding dental age.	
	Haavikko	1974	Scoring	203	X-ray	Panoramic X-ray	6 stages	Upper and lower first molar, canine, 1st incisor and lower 2nd molar, 1st premolar and 2nd incisor are scored, and averaged. This can then allow division into 6 groups.	Haavikko K. Tooth formation age estimated on a few selected teeth. Proc Finn Dent Soc. 1974;70:15-19.
	Leinonen	1972	Scoring	10	X-ray	Panoramic X-ray	8 stages	Staging applied 0-7 of each mandibular tooth, the two sides were averaged.	Leinonen A, Wasz-Höckert B, Vuorinen P. Usefulness of the dental age obtained by orthopantomography as an indicator of the physical age. Proc Finn Dent Soc. 1972;68(5):235-242.
	Liljeqvist & Lundberg	1971	Scoring	172	X-ray	Full oral series	8 stages per tooth	8 weighted stages applied based on dental morphology of crown, root etc, all teeth evaluated excepting upper pre-molar and molars.	Liljeqvist B, Lundberg M. Skeletal and tooth development: a methodologic investigation. Acta Radiol Diagnosis. 1971;11(2):97-112.
	Moorrees	1963	Scoring	2148	X-ray	Lateral & intraoral radiographs (two population samples combined therefore differing radiograph types)	14 stages	Mandibular teeth evaluated based on progressive stages described by changes in the crypt, cusp, crown, cleft, root and apex.	Moorrees CFA, Fanning EA, Hunt EE. Age Variation of Formation Stages for Ten Permanent Teeth. J Dent Res. 1963;42(6):1490-1502.
	Moorrees modification: Anderson	1976	Scoring	332	X-ray	Panoramic X-ray	14 stages	Mandibular and maxillary teeth assessed, applied to as many teeth as possible and the score averaged. They provided alternative tables that some authors prefer.	Anderson DL, Thompson GW, Popovich F. Age of attainment of mineralization stages of the permanent dentition. J Forensic Sci. 1976;21(1):191-200.
	Moorrees modification: London Atlas	2010	Atlas	577	X-ray	Panoramic X-ray	Atlas	"London Atlas" combining emergence data and the Moorrees method, applicable from the first prenatal trimester to 23 years old.	AlQahtani SJ, Hector MP, Liversidge HM. Brief communication: The London atlas of human tooth development and eruption. Am J Phys Anthropol. 2010;142(3):481-490.
	Nicodemo	1974	Atlas	73	X-ray	Panoramic X-ray	Foreign Language [Chinese]	Foreign Language [Chinese]	Nicodemo RA, Moraes LC, Médici Filho E. Tabela cronológica da mineralização dos dentes permanentes entre brasileiros. Rev Fac Odontol São José dos Campos. 1974;3(1):55-56.
	Nolla	1960	Scoring	1129	X-ray	Full oral series	70 stages	Each permanent tooth the left mandible is rated as per calcification stage (1-10) and values summed.	Nolla CM. The development of permanent teeth. 1952.
	Schour & Massler	1941	Atlas	340	X-ray	Panoramic X-ray	21 chronologica ages	21 stages identified: 2 prenatal followed by 0 months, 6mo , 9mo, 1 year, 16mo, 2y, 3y, 4y, 5y, 6y, 7y, 8y, 9y, 10y, 11y, 12y, 15y, 21y, 35y.	Massler M, Schour I, Poncher HG. Developmental pattern of the child as reflected in the calcification pattern of the teeth. Am J Dis Child. 1941;62(1):33-67.
Elbow	Sauvegrain	1962	Scoring	53	X-ray	Elbow: AP and Lateral	27 points	Lateral condyle, trochlea, olecranon apophysis and proximal radial epiphysis evaluated.	Sauvegrain J, Nahum H, Bronstein H. Study of bone maturation of the elbow. In: Annales de Radiologie. Vol 5. ; 1962:542.
	Sauvegrain modified: Dimeglio	2005	Scoring	117	X-ray	Elbow: AP and Lateral	30 point	Intermediate scores added between 3 points, for a total of 30 points.	Accuracy of the Sauvegrain Method in Determining Skeletal Age During Puberty. 2005:1689-1696.
	Sauvegrain modified: Dimeglio (Simplified)	2001	Scoring	76	X-ray	Elbow: Lateral only	8 points	Simplified method in which only olecranon apophysis assessed.	Diméglio A. Growth in pediatrics orthopaedics. In: Lovell, Winter, eds. Vol. I chapter II, 5th ed. Lippincott; 2001 (in press).
Face	Braga	2007	Scoring	58	CT	CT	Linear Equation	8 foramina identified, computer applies a cage/ mesh made and the shape is related to maturity via linear regression equation.	Braga J, Treil J. Estimation of pediatric skeletal age using geometric morphometrics and three-dimensional cranial size changes. Int J Legal Med. 2007;121(6):439-443.

Femur	Castriota-Scanderbe & De Micheli	1995	Scoring	32	Ultrasound	Hip Ultrasound	Continuous Scale	Femoral head cartilage thickness measured, decreases with increasing age and can be compared to table.	Castriota-Scanderbeg A, De Micheli V. Ultrasound of femoral head cartilage: a new method of assessing bone age. <i>Skeletal Radiol.</i> 1995;24(3):197-200.
	Stull	2014	Scoring	32	X-ray	Femur: AP	Linear Equation	Based on femoral measurements, diaphyseal length can be correlated reliably with age until 6 years old, or with multivariate models entailing predominantly diaphyseal width for older individuals.	Lodox Statscan, invented in South Africa for mining industry . Similar to EOS.
Foot	Whitaker	2002	Scoring	27	X-ray	Foot AP & Lateral	10 stages	Calcaneus primary and secondary ossification centers are rated 0-4, and on their fusion state from 0-4. All three scores are summed.	Whitaker JM, Rousseau L, Williams T, Rowan RA, Hartwig WC. Scoring system for estimating age in the foot skeleton. <i>Am J Phys Anthropol Off Publ Am Assoc Phys Anthropol.</i> 2002;118(4):385-392.
	Whitaker	2002	Scoring	27	X-ray	Foot AP & Lateral	10 stages	All distal phalangeal and proximal phalangeal primary and secondary ossification centers are rated 1-4, and on their fusion state from 1-4. All three scores are summed and converted to a 10 point scale. Uniquely, images were marked with a special score if ossification was not visible or obscured due to image quality or obstruction.	Whitaker JM, Rousseau L, Williams T, Rowan RA, Hartwig WC. Scoring system for estimating age in the foot skeleton. <i>Am J Phys Anthropol Off Publ Am Assoc Phys Anthropol.</i> 2002;118(4):385-392.
Hand-wrist	Björk & Helm	1967	Scoring	563	X-ray	Right Hand	8 stages	Key events are recorded at the second finger, third finger, thumb sesamoid and radius are evaluated.	Björk A, Helm S. Prediction of the age of maximum puberal growth in body height. <i>Angle Orthod.</i> 1967;37(2):134-143.
	Cameriere	2006	Scoring	76	X-ray	Left Hand	Linear Equation	The ratio of the area occupied by the carpal bones versus the total area of the radial and ulnar epiphysis and carpals is calculated and compared against a reference line.	Cameriere R, Ferrante L, Mirtella D, Cingolani M. Carpals and epiphyses of radius and ulna as age indicators. <i>Int J Legal Med.</i> 2006;120(3):143-146.
	Cameriere modification: De Luca	2016	Scoring	4	X-ray	Left Hand	Linear Equation	Updated formula for greater accuracy.	De Luca S, Mangiulli T, Merelli V, et al. A new formula for assessing skeletal age in growing infants and children by measuring carpals and epiphyses of radio and ulna. <i>J Forensic Leg Med.</i> 2016;39(January):109-116. doi:10.1016/j.jflm.2016.01.030
	Chang et al.	1990	Scoring	4	X-ray	Hand (side not found)	9 stages	"National Taiwan University Hospital Skeletal Maturity Index". Five locations on the thumb, index finger, middle finger and radius are evaluated.	Chang HF, Wu K-M, Chen KC. A cross-sectional study on the skeletal development of the hand and wrist from preadolescence to early adulthood among Chinese in Taiwan. <i>Zhonghua ya yi xue hui za zhi.</i> 1990;9(1):1-11.
	Chinese National Sports Committee	1992	Foreign Language [Chinese]	3	X-ray	Foreign Language [Chinese]	Foreign Language [Chinese]	So-called 'Chinese Standard' method. Metacarpal, phalanges and carpal bone developmental stages are assessed.	Committee NS. Assessment of development of metacarpals, phalanges and carpals of Chinese people: national standard of People's Republic of China. <i>Beijing Natl Sport Comm.</i> 1992.
	Choi et al.	2018	Scoring	5	X-ray	Left or Right	Continuous	Area of the capitate and hamate is measured and summed. Value can be input to regression equation.	Choi JA, Kim YC, Min SJ, Khil EK. A simple method for bone age assessment: The capitohamate planimetry. <i>Eur Radiol.</i> 2018;28(6):2299-2307.
	DeRoo & Schroder	1976	Atlas	34	X-ray	Hand (side not found)	Atlas	Similarities to Greulich-Pyle atlas, though initiated in Dutch European children.	de Roo T, Schröder HJ. <i>Pocket Atlas of Skeletal Age.</i> Springer Science & Business Media; 2012.
	Luk	2014	Scoring	22	X-ray	Distal Radius-Ulna	11 & 9 stages	"DRU" (distal radius ulna) method, in which the radius epiphysis is scored from 1-11 stages and the ulna from 1-9 stages, each can be	Luk KDK, Saw LB, Grozman S, Cheung KMC, Samartzis D. Assessment of skeletal maturity in scoliosis patients to determine clinical management: a new classification scheme using distal radius and ulna radiographs. <i>Spine J.</i> 2014;14(2):315-325.

							individually compared to chronological age.	
Ebri	1993	Scoring	1	X-ray	Left Hand	Linear Equation	Maximum dimensions of carpal and phalangeal epiphyseal are measured and evaluated compared to a linear regression equation.	Ebri BT. New method for evaluating ossification of the carpal bone. From a study with 5225 Spanish children. <i>Pediatric</i> . 1993;48(11):813-817.
Eklöf & Ringertz	1967	Scoring	94	X-ray	Left Hand	Linear Equation	Distances are measured that correspond to the width and length of the hand and wrist bones, in ten ossification centers.	Eklöf O, Ringertz H. A method for assessment of skeletal maturity. In: <i>Annales de Radiologie</i> . Vol 10. ; 1967:330-336.
Eklöf & Ringertz modification: 3 bone method	2009	Scoring	1	X-ray	Left Hand	Linear Equation	Abbreviated version for only 3 ossification centers.	Olivete CJ, Rodrigues ELL. ER5 and ER3: bone age assessment by simplifications of the Eklof and Ringertz method = Maturidade óssea: estimação por simplificações do método de Eklof e Ringertz. <i>Rev Odontol Ciênc</i> . 2009;24(4):361-366.
Eklöf & Ringertz modification: 5 bone method	2009	Scoring	1	X-ray	Left Hand	Linear Equation	Abbreviated version for only 5 ossification centers.	Olivete CJ, Rodrigues ELL. ER5 and ER3: bone age assessment by simplifications of the Eklof and Ringertz method = Maturidade óssea: estimação por simplificações do método de Eklof e Ringertz. <i>Rev Odontol Ciênc</i> . 2009;24(4):361-366.
Engström	1983	Scoring	189	X-ray	Left Hand	5 stages	Only 4 key events at specific regions are noted: epiphysis of the 2nd proximal phalanx is wide as the diaphysis; the epiphysis of the 3rd middle phalanx caps its diaphysis; complete epiphyseal fusion of the distal phalanx of 3rd finger; complete union of the distal epiphysis of the radius.	Engström C, Engström H, Sagne S. Lower Third Molar Development in relation to Skeletal Maturity and Chronological Age. <i>Angle Orthod</i> . 1983;53(2):97-106.
Fishman	1982	Scoring	664	X-ray	Left Hand	11 stages	Key events are recorded at the third finger, fifth finger, radius and thumb sesamoid appearance. Fishman described these as 'skeletal maturity indicators' for correlation with mandibular and maxillary development, therefore favoured by orthodontists.	Fishman LS. Radiographic evaluation of skeletal maturation: a clinically oriented method based on hand-wrist films. <i>Angle Orthod</i> . 1982;52(2):88-112.
Flory	1936	Atlas	155	X-ray	Right Hand	Atlas: newborn 19 years old	Phalangeal and carpal atlas.	Flory CD. Osseous development in the hand as an index of skeletal development. <i>Monogr Soc Res Child Dev</i> . 1936;1(3):i-141.
Gilsanz & Ratib	2005	Atlas	216	X-ray	Left Hand	Atlas	A digital hand atlas for assessment of phalanges, metacarpals and carpals.	Gilsanz V, Ratib O. <i>Hand Bone Age: A Digital Atlas of Skeletal Maturity</i> . Springer Science & Business Media; 2005.
Grave & Brown	1976	Scoring	382	X-ray	Hand (side not found/listed)	14 stages	Fourteen ossification events are assessed first, second and third fingers in addition to the pisiform, hamate and distal radial epiphysis. Events are also correlated with peak growth velocity.	Grave KC, Brown T. Skeletal ossification and the a adolescent growth spurt. <i>Am J Orthod</i> . 1976;69(6):311-619.
Gretych	2007	Atlas	117	X-ray	Left Hand	Atlas	Second, third and fourth phalanges in addition to the carpals are evaluated with computer assistance in with reference to Caucasian, African-America, Asian and Hispanic children.	Gertych A, Zhang A, Sayre J, Pospiech-Kurkowska S, Huang HK. Bone Age Assessment of Children using a Digital Hand Atlas. <i>Comput Med Imaging Graph</i> . 2007;31(4-5):322-331.
Greulich & Pyle	1950/1959	Atlas	7699	X-ray	Left Hand	Atlas	The most well-known phalangeal and carpal atlas, first published in 1950, updated and expanded in 1959.	Greulich WW, Pyle SI. <i>Radiographic Atlas Of Skeletal Development Of The Hand And Wrist</i> . <i>Am J Med Sci</i> . 1959;238(3):393.

Greulich & Pyle modification: Individual Scoring	1971	Atlas	53	X-ray	Left Hand	Atlas	All bones are scored individually and then average bone age calculated.	Roche AF, Eyman SL, Davila GH. Skeletal age prediction. <i>J Pediatr.</i> 1971;78(6):997-1003. doi:10.1016/S0022-3476(71)80430-4.
Greulich & Pyle modification: Weighted Modification	1972	Atlas	23	X-ray	Right or Left Hand	Atlas	All bones are scored individually and summed by region (carpals, phalanges-metacarpals or forearm), and weighting is performed based on each region.	Kimura K. Skeletal maturation of children in Okinawa. <i>Ann Hum Biol.</i> 1976;3(2):149-155.
Greulich & Pyle modification: Weighted Modification	1986	Atlas	4	X-ray	Left Hand	Atlas	Regions are scored individually and summed according to a weighted formula.	Aicardi G, Di Battista E, Naselli A, Vignolo M, De Scrolli A. Affidabilità dei più comuni metodi di previsione della statura adulta in un campione di adolescenti italiani. <i>Acta Med Auxol.</i> 1986;18:55-65.
Greulich & Pyle modification: Weighted Modification	1971	Atlas	10	X-ray	Left Hand	Atlas	Higher weighting to metacarpals and phalanges II to V.	Peritz E, Sproul A. Some aspects of the analysis of hand-wrist bone-age readings. <i>Am J Phys Anthropol.</i> 1971;35(3):441-447.
Greulich & Pyle modification: Line Drawings	1950	Atlas	90	X-ray	Left Hand	Atlas	Greulich-Pyle Atlas converted to line drawings for easier use.	Buckler JMH, Buckler JMH. A Reference Manual of Growth and Development. Blackwell Science London; 1997.
Greulich & Pyle modification: Shorthand Bone Age	2013	Atlas	30	X-ray	Left Hand	Atlas	Abbreviated version of Greulich-Pyle atlas in which 10 specific events at the first and second digit, hamate, and radial epiphysis are assessed.	Heyworth BE, Osei DA, Fabricant PD, et al. The shorthand bone age assessment: a simpler alternative to current methods. <i>J Pediatr Orthop.</i> 2013;33(5):569-574.
Greulich & Pyle modification: Ultrasound	2003	Atlas	56	Ultrasound	Left Hand	Atlas	Tracings are made from ultrasound evaluations to represent the full hand and wrist, which can then be evaluated as per the GP atlas.	Bilgili Y, Hizel S, Kara SA, Sanli C, Erdal HH, Altinok D. Accuracy of skeletal age assessment in children from birth to 6 years of age with the ultrasonographic version of the Greulich-Pyle atlas. <i>J Ultrasound Med.</i> 2003;22(7):683-690.
Greulich & Pyle modification: 'Segmented'	2001	Atlas	51	X-ray	Left Hand	Atlas	Seven regions are scored as groups - the carpals, metacarpals, proximal, medial and distal phalanges, radius, and ulna - and the sum divided by seven.	Mul D, Oostdijk W, Waelkens JJJ, Schulpen TWJ, Drop SLS. Gonadotrophin releasing hormone agonist treatment with or without recombinant human GH in adopted children with early puberty. <i>Clin Endocrinol (Oxf).</i> 2001;55(1):121-129.
Greulich & Pyle modification: Thumb Sesamoid only	2008	Scoring	4	X-ray	Left Hand	2 stages	Binary staging of presence or absence of ulnar sesamoid of the first digit. Not recommended by the authors for use alone.	Chaumoitre K, Adalian P, Colavolpe N, et al. Value of the sesamoid bone of the thumb in the determination of bone age. <i>J Radiol.</i> 2008;89(12):1921-1924.
Gu's method	-	-	-	-	-	-	Foreign Language [Chinese]	Zhang Z, Li K, Yu RJ, Zhang Q. Preliminary study on the applying value of two measurements for bone age in the cases of minors. <i>Fa Yi Xue Za Zhi.</i> 2004;20(4):212-214.
Haavikko	1974	-	7	-	-	-	Original article could not be obtained.	Haavikko K. Skeletal age estimated in a few selected ossification centres of the hand wrist. A simple method for clinical use. <i>Proc Finn Dent Soc.</i> 1974;70(1):7-14.
Hägg & Taranger	1980	Scoring	325	X-ray	Right Hand	10 stages	First and third finger are assessed in addition to the radial distal epiphysis. First finger ulnar sesamoid (presence/absence), 3rd finger distal phalangeal fusion/non-fusion, 3rd finger middle phalangeal	Hägg U, Taranger J. Skeletal stages of the hand and wrist as indicators of the pubertal growth spurt. <i>Acta Odontol Scand.</i> 1980;38(3):187-200.

								fusion progression; distal radial epiphyseal fusion progression.	
Hägg & Taranger modification: MP3 method	1982	Scoring	536	X-ray	Right Hand	5 stages		"MP3" Method: Third middle phalanx only evaluated, based on distal epiphyseal plate morphology.	Hägg U, Taranger J. Maturation indicators and the pubertal growth spurt. Am J Orthod. 1982;82(4):299-309.
Hägg & Taranger modification: Modified MP3 Method	2002	Scoring	76	X-ray	Right Hand	6 stage		"Modified MP3" Method: Third middle phalanx only evaluated, with 1 additional intermediate stage.	Rajagopal R, Kansal S. A comparison of modified MP3 stages and the cervical vertebrae as growth indicators. J Clin Orthod JCO. 2002;36(7):398.
Helm	1971	Scoring	154	X-ray	Right Hand	7 stages		Only 7 key events at specific regions are noted. Sesamoid presence in the thumb, 2nd finger proximal phalanx, and distal, middle and proximal phalanges of the third finger are evaluated.	Helm S, Siersbaek-Nielsen S, Skieller V, Björk A. Skeletal maturation of the hand in relation to maximum puberal growth in body height. Tandlaegebladet. 1971;75(12):1223-1234.
Kopczyńska-Sikorska	1969	Atlas	22	X-ray	Left Hand	Atlas		Atlas of Polish children.	Kopczyńska-Sikorska J. Atlas Radiologiczny Rozwoju Kośćca Dłoni i Nadgarstka. Państwowy Zakład Wydawnictw Lekarskich; 1969.
Li Guozhen	-	-	-	-	-	-		Li Guozhens' "Percent Numeration" No description found, only references in Chinese language journals.	Zhang Z, Li K, Yu RJ, Zhang Q. Preliminary study on the applying value of two measurements for bone age in the cases of minors. Fa Yi Xue Za Zhi. 2004;20(4):212-214.
Liaokawa	-	-	-	-	-	-		No description found, only references in abstract of Chinese language journals.	
Mackay	1952	Scoring	105	X-ray	Left & Right Hand	21 stages		Appearance of ossification centres of each carpal & phalanx in East Africans	Mackay DH, Service CM, Development C, Acts W. Skeletal maturation in the hand: a study of development in East Africa children. 1952.
Marti-Henneberg	1974	Scoring	4	X-ray	-	-		Original article could not be obtained.	Marti-Henneberg C, Patois E, Niiranen A, Roy MP, Masse NP. Bone maturation velocity. Compte Rendu la XIIe Reun des Équipes Charg des Études sur la Croissance le Développement l'Enfant Norm Paris, Cent Int l'Enfance, Paris. 1974:107-112.
Martins & Sakima	1977	Scoring	46	X-ray	Left Hand	18 stages		Carpal ossification evaluated which can be compared to pubertal growth spurt.	Martins JCR, Sakima T. Considerações sobre a previsão do surto de crescimento puberal. Ortodontia. 1977;10(3):164-170.
Mentzel	2005	Scoring	93	Ultrasound	Right or Left Hand	Atlas-like result (score correlated to GP bone age)		BonAge' ultrasound device allows evaluation of the change in speed of waves across the distal radial and ulnar epiphyses which returns a skeletal age value correlated to the G-P atlas.	Mentzel H-J, Vilser C, Eulenstein M, et al. Assessment of skeletal age at the wrist in children with a new ultrasound device. Pediatr Radiol. 2005;35(4):429-433.
Modi	1957/ 1969	Atlas	58	X-ray	-	-		Original article could not be obtained.	Modi JP. Modi's Textbook of Medical Jurisprudence and Toxicology. NM Tripathi; 1969.
Rachmiel	2013	Scoring	3	Ultrasound	Ultrasound	Linear		The distance across and speed of soundwave travel across the third phalanx, carpal region and wrist are measured. A linear equation gives output correlated to the GP atlas.	Rachmiel M, Naugolani L, Mazor-Aronovitch K, Levin A, Koren-Morag N, Bistrizter T. Bone age assessment by a novel quantitative ultrasound based device (SonicBone), is comparable to the conventional Greulich and Pyle method. Horm Res Pediatr. 2013;80(Suppl 1):35.
Roche	1988	Scoring	379	X-ray	Left Hand	Continuous Scale		Ninety-eight 'maturity indicators' across the radius, ulna, carpals, metacarpals and phalanges are recognised or measured, with different indicators assessed at different ages. Computer software returns a skeletal age with standard error and confidence limits.	Roche AF, Thissen D, Chumlea W. Assessing the Skeletal Maturity of the Hand-Wrist: Fels Method. Thomas; 1988.

Sempé & Pavia	1979	Scoring	697	X-ray	Left Hand	1000 point scale	Assessment is converted to a 'Skeletal Maturity Level' corresponding to 0 at birth to 999 at full maturity.	Sempé M, Pédrón G, Roy-Pernot M-P. Auxologie: Méthode et Séquences.; 1979.
Sempé & Pavia modification: Maturós 4.0	2001	Atlas	10	X-ray	Left Hand	Atlas	Semi-automated method in which twenty-two maturity indicators are considered and the user selects between one of 3 software-suggested ratings for each region, depending on chronological age.	Bouchard M, Sempé M. "MATUROS 4.0" CD: un nouvel outil d'évaluation de la maturation squelettique. Biométrie Hum Anthropol. 2001;19(1-2):9-12.
Sato et al.	1999	Scoring	11	X-ray	Hand (side not found/listed)	Linear	Computer aided skeletal maturity system (CASMAS). Third phalanx is extracted automatically and epiphyseal, metaphyseal widths measured, in addition to the width of the overlapping regions, and a multiple regression equation reports the bone age.	Sato K, Ashizawa K, Anzo M, et al. Setting up an automated system for evaluation of bone age. Endocr J. 1999;46(Suppl):S97-S100.
Singer	1980	Scoring	65	X-ray	Hand (side not found)	6 stages	All hand bones, with specific attention in the early stages to several events in the pisiform, hamate, ulna, second proximal phalanx, third middle and third distal phalanges.	Singer J. Physiologic Timing of Orthodontic Treatment. Angle Orthod. 1980;50(4):322-333.
Speyer	1950	Atlas	-	X-ray	Hand (side not found)	Atlas	Original article could not be obtained.	Speyer. Betekenis En Bepaling van de Skeletleeftijd. Leiden: Sijthoff; 1950.
Stuart	1962	Scoring	68	X-ray	Hand (side not found)	Ossification center appearance	Appearance and ossification of 29 centers in the hand wrist are evaluated.	Stuart HC, Pyle SI, Cornoni J, Reed RB. Onsets, completions and spans of ossification in the 29 bone-growth centers of the hand and wrist. Pediatrics. 1962;29(2):237-249.
Sugiura	1961	Scoring	5	X-ray	Hand (side not found)	-	Original article could not be obtained.	Sugiura Y, Nakazawa O, Kunishima Y, Aoki M, Ito H. A method of assessing skeletal age (2nd report). J Japanese Orthop Assoc. 1961;35:429-439.
Sugiura & Nakazawa	1968	Scoring	4	X-ray	Hand (side not found)	-	Scoring of hand and wrist centers, based on Japanese population.	Sugiura Y, Nakazawa O. Bone Age. Roentgen Diagnosis of Skeletal Development. Tokyo: Chugai-Igaku; 1968.
Tanner & Whitehouse: TW1	1959	Scoring	363	X-ray	Left Hand	Continuous Scale	Carpal, metacarpal and phalangeal assessment.	Tanner JM. A new system for estimating skeletal maturity from the hand and wrist, with standards derived from a study of 2600 healthy British children. Part II Scoring Syst. 1959.
Tanner & Whitehouse: TW1 - B5 Modification	2003	Scoring	6	X-ray	Left Hand	Continuous Scale	Radius, ulna, capitate, trapezium and the proximal epiphysis of the first phalanx of the fifth finger are evaluated individually as per TW1 and summed.	Guimarey L, Morcillo AM, Orazi V, Lemos-Marini SH V. Validity of the use of a few hand-wrist bones for assessing bone age. J Pediatr Endocrinol Metab. 2003;16(4):541-544.
Tanner & Whitehouse: TW2	1972	Scoring	2786 (1975)	X-ray	Left Hand	Continuous Scale	Carpal, metacarpal and phalangeal assessment. Alternative methods included carpals only or radius-ulna-short (RUS) bone modifications.	Tanner JM, Whitehouse RH, Healy MJR, Goldstein H. A revised system for estimating skeletal maturity from hand and wrist radiographs with separate standards for carpals and other bones (TW II system). Stand Skelet Age. 1972.
Tanner & Whitehouse: TW2 MR: RUS	2013	Scoring	47	MR	Left Hand: Open Compact MR	Continuous Scale	TW2 radius-ulna-short bones method applied to MR images from an open compact MR.	Terada Y, Kono S, Tamada D, et al. Skeletal age assessment in children using an open compact MRI system. Magn Reson Med. 2013;69(6):1697-1702.
Tanner & Whitehouse: TW2 MR: Fully automated	2014	Scoring	19	MR	Left Hand MR	Continuous Scale	Fully automated method in which 3D MR images are assessed by computer using the TW2 method.	Stern D, Ebner T, Bischof H, Grassegger S, Ehammer T, Urschler M. Fully automatic bone age estimation from left hand MR images. In: International Conference on Medical Image Computing and Computer-Assisted Intervention. Springer; 2014:220-227.

	Tanner & Whitehouse: TW2 MR: RUS*	2016	Scoring	14	MR	Left Hand MR	Continuous Scale	T1 weighted 3D VIBE sequence used and hand-wrist evaluated as per TW2 - RUS.	Urschler M, Krauskopf A, Widek T, et al. Applicability of Greulich-Pyle and Tanner-Whitehouse grading methods to MRI when assessing hand bone age in forensic age estimation: A pilot study. <i>Forensic Sci Int.</i> 2016;266:281-288.
	Tanner & Whitehouse: TW2 CASAS	1994	Scoring	69	X-ray	Left Hand MR	Continuous Scale	Computer Assisted Skeletal Assessment System (CASAS). User must position the radiograph under a camera, the computer then creates a digital representation which is scored automatically and can be output as per British or other populations. The process must be repeated individually for each bone.	Tanner JM, Gibbons RD. A computerized image analysis system for estimating Tanner-Whitehouse 2 bone age. <i>Horm Res Paediatr.</i> 1994;42(6):282-287.
	Tanner & Whitehouse: TW3	2001	Scoring	-	X-ray	Left Hand	Continuous Scale	Carpal, metacarpal and phalangeal assessment. Alternative methods included carpals only or radius-ulna-short bone modifications.	Tanner J, Healy M, Goldstein H, Cameron N. <i>Assessment of Skeletal Maturity and Prediction of Adult Height (TW3 Method)</i> . 3rd ed. London: WB Saunders, Harcourt Publishers Ltd; 2001.
	Tanner & Whitehouse: Sanders modification	2008	Scoring	54	X-ray	Left Hand	8 stages	TW3 - RUS system scoring is applied to the second to fifth phalanges and metacarpals, in addition to the distal radius epiphysis. Stages were made with specific emphasis on their correlation with event in scoliosis curve progression.	Sanders JO. Maturity indicators in spinal deformity. <i>J Bone Jt Surg - Ser A.</i> 2008;89(SUPPL. 1):14-20.
	Thiemann & Nitz	1986	Atlas	93 (2006 edition)	X-ray	Hand (side not found)	Atlas	Atlas of German children.	Thiemann H, Nitz I. <i>Roentgenatlas Der Normalen Hand Im Kindesalter</i> . Leipzig: Thieme; 1986.
	Thodberg	2009	Atlas/Scoring	232	X-ray	Left Hand	Atlas/Scoring	Automated method in which fifteen bones are identified by software and each is scored individually - first to fifth metacarpals, phalanges of the first, third and fifth digits, and the distal radial and ulnar epiphyses. Bone age can then be output as per Tanner-Whitehouse or GP Atlas values.	Thodberg HH, Kreiborg S, Juul A, Pedersen KD. The BoneXpert method for automated determination of skeletal maturity. <i>IEEE Trans Med Imaging.</i> 2009;28(1):52-66.
	Todd	1937	Atlas	335	X-ray	Left Hand	Atlas	Atlas method.	Todd TW. <i>Atlas of skeletal maturation</i> . 1937.
	Tomei	2014	Scoring	10	MR	Hand MR	85 points	Radius, ulna, capitate, hamate, pisiform and first and third proximal phalanges and metacarpals are evaluated and scored.	Tomei E, Semelka RC, Nissman D. <i>Text-Atlas of Skeletal Age Determination: MRI of the Hand and Wrist in Children</i> . Wiley Online Library; 2014.
	Wilkins	1950	-	34	-	-	Original article could not be obtained.	Method is not separated by genders.	Wilkins L. The diagnosis and treatment of endocrine disorders in childhood and adolescence. Charles C. Thomas, Springfield. 1950;2.
Hip	Acheson	1957	Scoring	245	X-ray	Pelvic	45 stages	"Oxford method": 9 regions of the hip are evaluated - iliac, triradiate cartilage, ischiopubic junction, pubis, ischium, acetabulum, femoral head, greater trochanter and lesser trochanter.	Acheson RM. The Oxford Method of Assessing Skeletal Maturity. <i>Clin Orthop Relat Res.</i> 1957;10:19-39.
	Acheson modified: Modified Oxford	1996	Scoring	97	X-ray	Pelvic	30 stages	Modified Oxford: only head of femur, greater trochanter, lesser trochanter, iliac crest and triradiate cartilage are evaluated.	Stasikelis PJ, Sullivan CM, Phillips WA, Polard AJ. Slipped capital femoral epiphysis: prediction of contralateral involvement. <i>JBJS.</i> 1996;78(8):1149-1155.

	Triradiate cartilage	-	Scoring	-	X-ray	Pelvic	2 stages	Open or closed stages	No original publication could be found. For a useful reference however see, Dimeglio A. Growth in Pediatric Orthopaedics. 2001:549-555.
Humerus	Li*	2018	Scoring	4	X-ray	Left Shoulder	5 stages	Proximal humeral epiphyseal closure assessed from open plate until fusion. Peak height velocity correlation possible.	Li DT, Cui JJ, Devries S, et al. Humeral Head Ossification Predicts Peak Height Velocity Timing and Percentage of Growth Remaining in Children. J Pediatr Orthop. 2018;38(9):e546-e550.
	Ogden	1978	Atlas	47	X-ray	Shoulder X-Ray	Atlas	Forensic specimen derived method, the proximal humerus ossification centers appearance, fusion with each other and the developing epiphysis are assessed.	Ogden JA, Conlogue GJ, Jensen P. Radiology of Postnatal Skeletal development: The proximal humerus. Skeletal Radiol. 1978;2(3):153-160.
	Walker & Lovejoy	1985	Scoring	137	X-ray	Proximal humerus	8 stages	Proximal humerus are evaluated by relative lucency.	Walker RA, Lovejoy CO. Radiographic changes in the clavicle and proximal femur and their use in the determination of skeletal age at death. Am J Phys Anthropol. 1985;68(1):67-78.
Iliac	Risser	1958	Scoring	529	X-ray	Pelvic	No stages	Full excursion of the iliac crest apophysis is correlated with the ending of spinal growth (no stages described at this time).	Risser JC. The Iliac apophysis; an invaluable sign in the management of scoliosis. Clin Orthop. 1958; 11: 111-119.
	Risser: US system	-	Scoring	-	X-ray	Pelvic	6 stages	Presence, extent of excursion divided into quarters and initiation of fusion of the iliac crest apophysis are evaluated.	First reference could not be found, as also noted by Bitan et al. For description of this method see: Bitan FD, Veliskakis KP, Campbell BC. Differences in the Risser grading systems in the United States and France. Clin Orthop Relat Res. 2005;(436):190-195.
	Risser: EU system	-	Scoring	-	X-ray	Pelvic	6 stages	Presence, extent of excursion divided into thirds, initiation and completion of fusion of the iliac crest apophysis are evaluated.	First reference could not be found, as also noted by Bitan et al. For description of this method see: Bitan FD, Veliskakis KP, Campbell BC. Differences in the Risser grading systems in the United States and France. Clin Orthop Relat Res. 2005;(436):190-195.
	Risser: Combined	1985	Scoring	146	X-ray	Pelvic	7 stages	Combined method in which stages 2-4 are altered and one intermediate stage "3/4" is added.	Stagnara P. Les Déformations Du Rachis: Scolioses, Cyphoses, Lordoses. Masson; 1985.
	Risser modified: Triradiate evaluation	2010	Scoring	55	X-ray	Pelvic	7 stages	Triradiate cartilage evaluation is included as an additional "-1" stage.	Nault M-L, Parent S, Phan P, Roy-Beaudry M, Labelle H, Rivard M. A modified Risser grading system predicts the curve acceleration phase of female adolescent idiopathic scoliosis. JBJS. 2010;92(5):1073-1081.
	Risser modified: Risser 'plus'	2015	Scoring	47	X-ray	Pelvic	8 stages	Triradiate cartilage is evaluated in addition to the iliac crest in a method combining EU and US systems. Recommended by SOSORT guidelines, 2015.	Negrini S, Hresko TM, O'Brien JP, et al. Recommendations for research studies on treatment of idiopathic scoliosis: Consensus 2014 between SOSORT and SRS non-operative management committee. Scoliosis. 2015;10(1):1-12.
	Risser modified: Ultrasound	1995	Scoring	41	Ultrasound	Ultrasound	6 stages	US Risser method applied by comparing presence of apophysis to the extent of iliac crest as palpated by clinician.	Wagner UA, Diedrich V, Schmitt O. Determination of skeletal maturity by ultrasound: a preliminary report. Skeletal Radiol. 1995;24(6):417-420.
	Risser modified: Four stage method	1985	Scoring	412	X-ray	Pelvic	4 stages	The extent of excursion is not scored, such that stages describe the absence of the apophysis, it's presence, ongoing fusion, or completed fusion. First described in forensic reports.	Webb PAO, Suchey JM. Epiphyseal union of the anterior iliac crest and medial clavicle in a modern multiracial sample of American males and females. Am J Phys Anthropol. 1985;68(4):457-466.
	Schmidt	2011	Scoring	57	Ultrasound	Ultrasound Left Iliac Crest	4 stages	The absence, presence, ongoing fusion and complete fusion of the left iliac crest apophysis are evaluated.	Schmidt S, Schmeling A, Zwiesigk P, Pfeiffer H, Schulz R. Sonographic evaluation of apophyseal ossification of the iliac crest in forensic age diagnostics in living individuals. Int J Legal Med. 2011;125(2):271-276.
	Wittschieber	2012	Scoring	35	X-ray	Pelvic	8 stages	Alternative method described in forensic evaluation, evaluating iliac crest apophyseal presence/absence,	Wittschieber D, Vieth V, Domnick C, Pfeiffer H, Schmeling A. The iliac crest in forensic age diagnostics: Evaluation of the apophyseal ossification in conventional radiography. Int J Legal Med. 2013;127(2):473-479.

Knee	Acheson	1954	Scoring	215	X-ray	Knee AP	12 points	extent of excursion, extent of fusion, and completion of fusion. Femur and tibia are scored from 0-5 based on epiphyseal morphology (though not on the presence of fusion), patella and fibular epiphyses presence is scored 0 or 1.	Acheson RM. A method of assessing skeletal maturity from radiographs; a report from the Oxford child health survey. <i>J Anat.</i> 1954;88(4):498-508.
	Dedouit	2012	Scoring	91	MR	Knee MR	5 stages at 2 regions	Femur and tibial epiphyses are scored separately I-V and can be compared against age charts.	Dedouit, F., Auriol, J., Rousseau, H., Rougé, D., Crubézy, E. and Telmon, N., 2012. Age assessment by magnetic resonance imaging of the knee: a preliminary study. <i>Forensic science international</i> , 217(1-3), pp.232-e1.
	Nakase	2012	Scoring	24	Ultrasound	Ultrasound Left Iliac Crest	3 stages	Developing tibial tuberosity is described by 3 events adapted from Ehrenberg's radiographic description (1962) :increased cartilage, the presence of ossifying island, or connection by bone bridge to the tibial epiphyses.	Nakase J, Aiba T, Goshima K, et al. Relationship between the skeletal maturation of the distal attachment of the patellar tendon and physical features in preadolescent male football players. <i>Knee Surgery, Sport Traumatol Arthrosc.</i> 2014;22(1):195-199.
	O'Connor	2008	Scoring	70	X-ray	Knee AP & Lateral	15 stages	Epiphyses of the long bones around the knee are scored 0-4 and summed. Modified from McKern Stewart 1957 report from a forensic sample.	O'Connor JE, Bogue C, Spence LD, Last J. A method to establish the relationship between chronological age and stage of union from radiographic assessment of epiphyseal fusion at the knee: an Irish population study. <i>J Anat.</i> 2008;212(2):198-209.
	Pennock*	2018	Atlas	7	MR	Knee MR	Atlas	Cross-sectional atlas using sagittal and coronal slices used to evaluate femur, tibia, fibula and patella based on ossification, shape and specific features of the regions such as tibial spine development and subchondral epiphyseal cartilage.	Pennock AT, Bomar JD, Manning JD, Diego S, Diego S. The creation and validation of a knee bone age atlas utilizing MRI. <i>JBJS.</i> 2018;100(4):e20.
	Pyle & Hoerr	1955	Atlas	140	X-ray	Knee AP & Lateral	Atlas	Femur, tibia, fibula and patellar are assessed by atlas method.	Pyle SI, Hoerr NL. A Radiographic Standard of Reference for the Growing Knee. CC Thomas; 1955.
	Roche-Wainer-Thissen	1975	Scoring	117	X-ray	Knee AP	34 stages	Thirty four maturity indicators at the knee are evaluated.	Roche AF, Wainer H, Thissen D. <i>Skeletal Maturity: The Knee Joint as a Biological Indicator.</i> Plenum Medical Book Company; 1975.
	Wang	2010	Scoring	3	X-ray	Knee AP & Lateral	-	Foreign Language [Chinese]	Wang YH, Zhu GY, Ying CL, Fan LH, Wan L. The trend of epiphyseal development of knee and ankle joints in teenagers and age estimation. <i>Fa Yi Xue Za Zhi.</i> 2010;26(2):91-96.
Lower limb	von Harnack	1974	-	-	-	-	-	Foreign Language [German]	von Harnack, G. A. "Determination of skeletal maturation in childhood (author's transl)." <i>Zeitschrift fur Geburtshilfe und Perinatologie</i> 178, no. 4 (1974): 237.
Mandible	Singer	1987	Scoring	77	X-ray	Lateral cephalogram	2 stages	Antegonial notch depth is measured and rated whether "deep" (>3mm depth) or not.	Singer CP, Mamandras AH, Hunter WS. The depth of the mandibular antegonial notch as an indicator of mandibular growth potential. <i>Am J Orthod Dentofac Orthop.</i> 1987;91(2):117-124.
Metacarpal	Faruch-Bilfeld	2008	Scoring	4	X-ray	Hand X-ray	Linear	Second metacarpal is measured to establish the ratio between epiphysial diameter and metaphysial diameter. This value can be correlated to chronological age.	Faruch-Bilfeld M, Dedouit F, Soumah M, et al. Value of radiographic evaluation of the second metacarpal in the determination of bone age. <i>J Radiol.</i> 2008;89(12):1930-1934.
	Garn	1972	Scoring	227	X-ray	Left Hand	Linear	The longitudinal length of nineteen tubular bones of the hand are measured and compared against age standards. Prospective standard based on FELS population.	Garn SM, Hertzog KP, Poznanski AK, Nagy JM. Metacarpophalangeal length in the evaluation of skeletal malformation. <i>Radiology.</i> 1972;105(2):375-381.
Pubic symphysis	Omel'chenko & Sukhomlinova	1976	-	1	X-ray	Pelvic	-	Ischiopubic synchondrosis is evaluated. Foreign Language [Russian]	Omel'chenko RM, Sukhomlinova OP. Duration of synostosis of the ischiopubic synchondrosis. <i>Arkh Anat Gistol Embriol.</i> 1976;70(4):91-95.

Radius	Dvorak	2007	Scoring	137	MR	Coronal Left Hand MR	6 stages	Distal radial growth plate is evaluated and initiation, extent or completion of fusion is graded I-VI.	Dvorak J, George J, Junge A, Hodler J. Age determination by magnetic resonance imaging of the wrist in adolescent male football players. <i>Br J Sports Med.</i> 2007;41(1):45-52.
	Karami	2014	Scoring	2	Ultrasound	Ultrasound	Linear	The width of the hypochoic growth plate is measured along the long radius' axis and compared to tables. Only cut-off points for the majority 16, 17 and 18 years old were investigated.	Karami M, Moshirfatemi A, Daneshvar P. Age determination using ultrasonography in young football players. <i>Adv Biomed Res.</i> 2014;3(1):174.
	Schmidt	2013	Scoring	38	Ultrasound	Ultrasound	4 stages	Distal radius evaluated for absence/presence of secondary center, the initiation of fusion, and the completion of fusion. (based on 4 stage ossification template as per Schulz et al, similar to many methods)	Schmidt S, Schiborr M, Pfeiffer H, Schmeling A, Schulz R. Age dependence of epiphyseal ossification of the distal radius in ultrasound diagnostics. <i>Int J Legal Med.</i> 2013;127(4):831-838.
Rib	Moskovitch	2010	Scoring	25	CT	Multi-slice CT	5 stages	Sternal end of the right first rib is imaged and virtual reconstructions created, and assessed based on Kunos et al. macroscopic ratings, which yielded 5 stages around 15-30 years old, based on shape, surface topography and form of the margin, and on the presence of osseous bridges in the sternocostal cartilage.	Moskovitch G, Dedout F, Braga J, Rougé D, Rousseau H, Telmon N. Multislice computed tomography of the first rib: A useful technique for bone age Assessment. <i>J Forensic Sci.</i> 2010;55(4):865-870.
	Michelson	1934	Scoring	43	X-ray	X-ray	4 stages	Medial side of first rib is evaluated as first described in German by Ernst (1920), based on presence, extent and completion of epiphyseal ossification.	Michelson N. The calcification of the first costal cartilage among whites and negroes. <i>Hum Biol.</i> 1934;6(3):543.
Shoulder	Schaefer	2015	Scoring	3	X-ray	Shoulder X-Ray: AP, Axillary & Y-view.	3 scores: 4 point and 2 point	Proximal humerus , coracoid process and acromion are evaluated separately (on 4-, 3- and 2-point scales respectively).	Schaefer M, Aben G, Vogelsberg C. A demonstration of appearance and union times of three shoulder ossification centers in adolescent and post-adolescent children. <i>J Forensic Radiol Imaging.</i> 2015;3(1):49-56.
Sternum	Gemeler*	2019	Scoring	3	CT	Chest MDCT	5 stages	Vertical fusion between three or four ossification centers of the sternal body and manubrium are assessed, and fusions proceeds superiorly with increasing maturity. (Measured in individuals up to 30 years old)	Gumeler E, Akpinar E, Ariyurek OM. MDCT evaluation of sternal development. <i>Surg Radiol Anat.</i> 2019;41(3):281-286.
	Riach †	1967	Scoring	23	X-ray	Chest X-ray	Continuous	Tracings made of ossification center numbers and area calculated. Fusion is completed by 6-7 years old. (Method only described in forensic studies of excised sterna)	Riach IC. Ossification in the sternum as a means of assessing skeletal age. <i>J Clin Pathol.</i> 1967;20(4):589-590.
Wrist	Wang	2014	Scoring	0	X-ray	Left Hand	5 stages	Five 'developmental stages' were applied for the radius and the ulna. No more information available - foreign Language [Chinese]	Wang YH, Wang ZS, Wei H, Wan L, Ying CL, Zhu GY. Automated assessment of developmental levels of epiphysis by support vector machine. <i>Fa Yi Xue Za Zhi.</i> 2014;30(6):422-426.
	Kangne	1999	Scoring	12	X-ray	Hand (side not found/listed)	4 stages	Distal radius epiphyseal fusion is evaluated from no fusion, partial fusion, near total fusion leaving only a thin line to complete fusion.	Kangne RN, Sami SA, Deshpande VL. Age estimation of adolescent girls by radiography. <i>J Forensic Med Toxicol.</i> 1999;16(1):20-26.

	Kangne modification: Two-stage	1999	Scoring	12	X-ray	Hand (side not found/listed)	2 stages	The first and second stages are combined, as are the third and fourth, resulting in 2 stages: 'not fused' and 'fused'.	Kangne RN, Sami SA, Deshpande VL. Age estimation of adolescent girls by radiography. J Forensic Med Toxicol. 1999;16(1):20-26.
Multi-region	Francis	1940	Scoring	47	X-ray	Many	Ossification center appearance	Ossification center appearances of 17 regions from humerus to iliac crest, sesamoids etc presented from 6-15 years old	Francis CC. The appearance of centers of ossification from 6 to 15 years. Am J Phys Anthropol. 1940;27(1):127-138.
	Girdany & Golden	1952	Scoring	-	X-ray	Many	-	Based on the appearance of ossification centers, the wrist, elbow, shoulder, spine, hip, knee, ankle can be evaluated depending on age.	Girdany BR, Golden R. Centers of ossification of the skeleton. Am J Roentgenol Radium Ther Nucl Med. 1952;68(6):922-924.
	Gök	1985	Atlas	7	X-ray	Many	Atlas	Turkish atlas of boys aged 11-22 based on the epiphyses of the shoulder, elbow, hand-wrist, and pelvic bones.	Gök Ş, Erölçer N, Özen C. Age Determination in Forensic Medicine. 2nd ed. Council of Forensic Medicine Press; 1985.
	Graham	1972	-	74	-	-	-	Original article could not be obtained.	Graham CB. Assessment of bone maturation-methods and pitfalls. Radiol Clin North Am. 1972;10(2):185-202.
	Schinz	1939	-	-	X-ray	Many	-	Hand, wrist, elbow, skull, hip, iliac crest, spine and knee are assessed. No further description found. Foreign Language [German]	Schinz H., Baensch WE, Friedl E, Uehlinger E. Lehrbuch der Röntgendiagnostik. In: Stuttgart: Thieme; 1950:761-776.
	Spencer	1981	Scoring	9	Bone Scan	Full body scan with γ -camera.	Ossification center appearance	The appearance times of 71 ossification centers from 0-26 years old with ^{99m}Tc -MDP or related compound uptake bone scans are listed.	Spencer RP, Sami S, Karimedini M, Sziklas JJ, Rosenberg R. Role of bone scans in assessment of skeletal age. Int J Nucl Med Biol. 1981;8(1):33-38.
	Zhu	2008	Scoring	2	X-ray	Many	not found foreign language	Seven regions are assessed and compared to so-called 'Grading Standards' :sternal end of clavical and left shoulder, elbow, carpal, hip, knee and ankle joints. No further description found in English (original article in Chinese).	Zhu GY, Fan LH, Zhang GZ, et al. Staging methods of skeletal growth by X-ray in teenagers. Fa Yi Xue Za Zhi. 2008;24(1):18-24.
	Zhu: Knee-Ankle only	2008	Scoring	3	X-ray	Many	not found foreign language	Only knee and ankle assessed. No further description found in English (original article in Chinese).	Wang YH, Zhu GY, Ying CL, Fan LH, Wan L. The trend of epiphyseal development of knee and ankle joints in teenagers and age estimation. Fa Yi Xue Za Zhi. 2010;26(2):91-96.
	Elgenmark: <5 years old	1946	Scoring	110	X-ray	Hemiskelton	24 age groups	Hand-wrist, knee, foot, prox femur, elbow, shoulder, applicable until 5 years old. In this 'numerical' method, the number of ossification centers is summed and this value is compared to chronological age.	Elgenmark O. The Normal Development of the Ossific Centres During Infancy and Childhood: A Clinical, Roentgenologic, and Statistical Study. Almqvist & Wiksell; 1946.
	Ruckenstein	1931	-	47	X-ray	-	Foreign Language [German]	Does not divide based on gender.	Ruckenstein E. Die Normale Entwicklung Des Knochensystems Im Röntgenbild. Vol 15. Leipzig: Thieme; 1931.
	Lurie	1943	Scoring	18	X-ray	Many	20 stages	Hand-wrist, elbow, pelvis and foot on the right side. Age at appearance and fusion times are described, with specific landmarks highlighted as indicators of age such as the greater trochanter.	Lurie LA, Levy S, Lurie ML. Determination of bone age in children. J Pediatr. 1943;23(6):131-140.
	Caffey	1945	Atlas	1628	X-ray	Many	-	A method made from several regions including hand-wrist as per Vickers & Vogt, it is not usable for	Caffey J, Silverman FN. Pediatric X-Ray Diagnosis. Chicago: Year Book Medical Publishers; 1945.

Vogt & Vickers	1938	Atlas	52	X-ray	Many	Atlas	children older than 14 years old. Original article could not be located. Hand, wrist and feet from birth to 6 1/2 years old, ossification center appearance of the bones of the upper and lower extremities can be evaluated. Prospective atlas.	Vogt EC, Vickers VS. Osseous growth and development. Radiology. 1938;31(4):441-444.
----------------	------	-------	----	-------	------	-------	---	---

BIBLIOGRAPHY

Publications related directly to the thesis:

Journal Publications

O'Sullivan IR, Schégl ÁT, Varga P, Than P, Vermes C. Femoral neck-shaft angle and bone age in 4-to 24-year-olds based on 1005 EOS three-dimensional reconstructions. *Journal of Pediatric Orthopedics. Part B*. 2020 Jul 17 (online ahead of print). **IF: 0.832, SJR: 0.41 (Q2)**.

O'Sullivan I, Schlégl ÁT, Varga P, Kerekes K, Vermes C, Than P. Csontkor–a csontrendszeri érettség mérésének lehetősége EOS készülékkel. *Orvosi Hetilap*. 2019 Apr;160(16):619-28. **IF:0.497, SJR: 0.18 (Q3)**.

Schlégl ÁT, **O'Sullivan I**, Varga P, Than P, Vermes C. Determination and correlation of lower limb anatomical parameters and bone age during skeletal growth (based on 1005 cases). *Journal of Orthopedic Research*. 2017;35(7):1431-1441. **IF: 3.414, SJR: 1.181 (Q1)**.

O'Sullivan IR, Schégl ÁT, Varga P, Than P, Vermes C. Alternative Methods for Skeletal Maturity Estimation with the EOS Scanner – Experience from 934 Patients; Submitted for Publication.

Presentations – International

O'Sullivan I, Varga P, Schlégl ÁT, Than P, Vermes C. Bone Age Evaluation With The EOS Scanner – An Assessment Of Five Methods. 19th EFORT Congress, Barcelona, May 30- June 1, 2018. <https://www.efort.org/barcelona2018/scientific-content/advanced-scientific-programme/details/?id={4B9FA67E-BDC2-4EF6-BC8B-1E139E86F6B9}>

O'Sullivan I, Schlégl ÁT, Varga P, Than P, Vermes C. The Correlation Between Collodiaphyseal Angle And Bone Age Based On 1005 EOS 3D-Reconstructions. 18th EFORT Congress, Vienna, May 30- June 1, 2017. Programme p 131.

Schlégl ÁT, **O'Sullivan I**, Varga P, Than P, Vermes C. Bone Age - A Potential Indicator Of Lower Limb's Anatomical And Biomechanical Parameters. 17th EFORT Congress, Geneva, 01-03 June, 2016. Programme p 162.

Presentations – National

Schlégl ÁT, **O'Sullivan I**, Varga P, Kerekes K, József, K, Burkus M, Tunyogi-Csapó M, Vermes C. Csontkor mérési lehetőségek vizsgálata FL-FS és EOS felvételeken. Magyar Ortopéd Társaság Congress, Jun 29 – Jul 01, 2017.

O'Sullivan I. The torsional and rotational parameters of the lower limb in childhood as related to bone age- VII. International XIII. National Interdisciplinary Grastyán Conference, Pécs, 2015.

Varga P, **O'Sullivan I**, Schlégl ÁT. Examination of the lower limb's torsional parameters in point of bone age VII. International XIII. National Interdisciplinary Grastyán Conference, Pécs, 2015.

Schlégl ÁT, Varga P, **O'Sullivan I**, Vermes C. Az alsó végtag biomechanikai paramétereinek vizsgálata a csontkor függvényében. Magyar Ortopéd Társaság Congress, Szombathely-Sárvár, Jun 11-13, 2015

Schlégl ÁT, **O'Sullivan I**, Varga P, Than P, Vermes Cs. A Hassel–Farman módszer alkalmazása a csontkor meghatározására, valamint ennek összefüggése az alsó végtag biomechanikai paramétereivel.: Magyar Traumatológia Ortopédia Kézsebészet Plasztikai Sebészet. 2015;58(4):105-121.

Posters – International Conferences

Schlégl ÁT, Varga P, Maróti P, **O’Sullivan I**, Vermes C, Than P. Patient specific 3D printed hip models for easier teaching and better understanding the total hip arthroplasty in developmental dysplasia of the hip – AMEE 2016, Barcelona, 27-31. August 2016. Abstract Book pp. 587.

Schlégl ÁT, **O’Sullivan I**, Varga P, Than P, Vermes C. Bone Age - A potential indicator of lower limb’s anatomical and biomechanical parameters – 17th EFORT Congress, Geneva, 1- 3. June 2016.

Publications Not Connected to this Thesis

József K, Burkus M, Márkus I, **O’Sullivan I**, Schlégl ÁT, Than P, Tunyogi-Csapó M. Maximal axial vertebral rotation in adolescent idiopathic scoliosis - is the apical vertebra the most rotated? *Global Spine Journal*. [accepted April 2020].

Burkus M, Schlégl ÁT, József K, **O’Sullivan I**, Márkus I, Tunyogi-Csapó M. Analysis of Proximal Femoral Parameters in Adolescent Idiopathic Scoliosis. *Advances in orthopedics*. 2019 Apr 1;2019.

Burkus M, Schlégl ÁT, **O’Sullivan I**, Márkus I, Vermes C, Tunyogi-Csapó M. Sagittal plane assessment of spino-pelvic complex in a Central European population with adolescent idiopathic scoliosis: a case control study. *Scoliosis and spinal disorders*. 2018 Dec 1;13(1):10.

Acknowledgements

I warmly thank my supervisors Prof. Péter Than and Dr. Csaba Vermes for their guidance, support, leadership, patience and advice. For not keeping the leash too tight, but giving me the opportunity to carry out this work. I am truly grateful.

I wish to thank Dr. Ádám Schlégl for his indescribable energy, talent, professionalism and work ethic. Without his initial work and ideas this project could never have started and without his advice, support and patience this would never have had a hope of coming to life and I owe him much.

I am thankful for Dr. Péter Varga for his work on this project, in planning, concepts and performing measurements which contributed greatly to the study.

Furthermore, Dr. Kamilla Kerekes for her helping bring my research into the Hungarian language and Prof. László Poto for his assistance with statistical matters.

I would like to thank the entire staff of the Department of Orthopaedics and the PhD. Office, for welcoming me, assisting me and making it a warm and friendly environment, even for a külföldi, like myself.

I am very grateful to my family for their support, my sister Aisling for her wisdom with numbers and big data, and my dear partner Annamaria for her charisma, uniqueness, nerve and talent.

Kis-Gadóné Wenczler Mária, Németh Tamásné Tímea, and Tamaskóné Sóstai Erika of the Phd Office, without whom I would have been lost at sea! Nagyon köszönöm!

This work was supported by European Grant no. EFOP 3.6.1.-16-2016-00004 for which I am very grateful.

And to Seán – the true engine behind it all, your tireless strength has given me strength. ‘To the victor go the spoils’.

Femoral neck-shaft angle and bone age in 4- to 24-year-olds based on 1005 EOS three-dimensional reconstructions

Ian R. O'Sullivan, **Ádám T. Schégl**, Péter Varga, Péter Than and Csaba Vermes

The aim of the study was to assess the correlation between femoral neck-shaft angles (NSAs) and skeletal maturity in EOS reconstructions from a large population of children. Full-body three-dimensional (3D) reconstructions were generated from 1005 children and young adults (4–24 years old; 449 male, 556 female) using the EOS three-dimensional/3D scanner, with images taken during routine clinical practice. The true NSAs were measured and assessed for correlation with individuals' chronological age and bone age, based on cervical vertebral morphology. Statistical analysis was performed using Spearman correlation, independent *t*-test and multiple linear regression. NSAs of older and younger individuals within each bone age group and chronological age were further assessed by *t*-test. NSA values fell from mean $131.89^\circ \pm 6.07^\circ$ at 4 years old to $128.85^\circ \pm 4.46^\circ$ at the age of 16, with only minor decreases thereafter. Significantly higher NSAs (3.16° and 4.45° , respectively) were found in those with a bone age advanced or delayed by more two or more stages compared to their peers of the same

chronological age ($P < 0.001$; $P < 0.001$). Similarly, within most bone age stages, individuals of advanced or delayed chronological age exhibited elevated values (mean difference ranged from 2.9° to 8.9° , $P < 0.05$). Incorporation of bone age assessment into proximal femoral evaluation allowed identification of 'fast maturing' and 'slow maturing' sub-categories in developing children, with different expected NSAs. The earlier ossification seen in faster-maturing individuals may lead to the NSA becoming fixed in a more immature valgus conformation. *J Pediatr Orthop B* XXX: 000–000 Copyright © 2020 Wolters Kluwer Health, Inc. All rights reserved.

AQ1

AQ2

AQ3

Journal of Pediatric Orthopaedics B 2020, XXX:000–000

Keywords: bone age, EOS, lower limb development, neck-shaft angle

Department of Orthopaedics, Medical School, University of Pécs, Pécs, Hungary

Correspondence to Ian O'Sullivan, MD, Akác str. 1, Pécs 7632, Hungary
Tel: +36 30 536 800; fax: +36 72 536 840; e-mail: iosullivan@gmail.com

AQ4

Received 2 August 2019 Accepted 6 June 2020

Introduction

The neck-shaft angle (NSA) of the femur is a key actor in the transfer of mechanical forces from the trunk to the lower extremity. Altered loading from childhood can lead to later pathology, and the NSA has been shown to be associated with a number of orthopaedic diseases such as patellar subluxation and hip osteoarthritis [1,2].

The NSA is still regarded by some medical school textbooks to be 135° [3]; however, the true value is likely closer to 127° [4]. Evaluations based on conventional anteroposterior radiographs for example give an artificially elevated NSA due to the confounding effect of femoral anteversion [5,6], in contrast to cadaveric or computed tomography/MR-based 'true' NSA measurements. While the consensus is that the NSA falls with increasing age, there is still debate about the exact values, and about sex, geographic, climate influences [4,7].

The comparison of any skeletal changes to the age alone may be conceptually flawed, however. Orthopaedic surgeons DiMeglio and Canavase wrote that 'age is a difficult notion to define', and recommend the use of chronological age, bone age estimates and Tanner signs together in

planning treatment for skeletal growth disorders such as scoliosis [8].

The present study aimed to evaluate the changes in the NSA and the relationships with both chronological age and bone age in a population of 1005 4- to 24-year-olds, using an EOS scanner. The EOS is a biplanar ultra-low dose X-ray scanner capable of generating 3D reconstructions which can be used for the measurement of bony structures, independent of vertical distortion and the effect of femoral version, to generate a 'true' measurement of the NSA [9–12].

Materials and methods

Images were reviewed from our database of 7108 EOS image-pairs collected during routine clinic work between 2007 and 2012. The population was narrowed to include only those 4–24 years old, resulting in 3473 image-pairs, and patients were excluded if they had any biomechanical pathology of the lower limb, history of previous lower limb surgery, previous disease influencing growth or any limb or body asymmetry. Due to the higher number of older patients collected, a limit of 50 cases per year in the ages from 17–24 years old was placed. Data on this population were previously reported in another study of individuals aged 2–24 years old [13]. Twelve individuals aged 2 and 3 (six boys and six girls) were replaced in this

Supplemental Digital Content is available for this article. Direct URL citations appear in the printed text and are provided in the HTML and PDF versions of this article on the journal's website, www.jpo-b.com.

study as the EOS software is not recommended for NSA measurements in individuals younger than four. Six boys and six girls from ages 4–9 were randomly selected from our database from 2013 to return the total number to 1005 (449 male and 556 female). The diagnoses of those involved are shown in Table 1.

T1

All imaging was performed with orthopaedic indication, in the ‘step-forward’ position, in which the subject stands upright with left foot approximately 10cm forward. Due to the nature of this positioning, the Hassel–Farman method of bone age estimation was selected, which describes six different stages of skeletal maturity based upon the cervical vertebral morphology [14] (Fig. 1). This method has been found to be reliable and compatible with EOS images, as reported in Schlégl *et al.* [13]. Bone age estimation was performed by three independent observers (two PhD candidate medical doctors and a PhD-MD orthopaedic resident) after special training

F1

with two senior orthopaedic surgeons and a specialist radiologist).

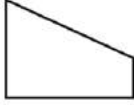





The NSA was measured using the sterEOS three-dimensional (2D)/3D software package (V1.4.4.5297, EOS Imaging, Paris, France) in which a model of the femur is first automatically generated from an image-pair, and then verified by a technician (in this case, a medical resident under guidance from a senior orthopedic surgeon) who must check that 16 different landmarks are aligned on the femur, to ensure accuracy of the model. Landmarks for proximal femoral alignment consisted of: centre of femoral head, diameter of femoral head, middle of femoral diaphysis, intercondylar fossa, intercondylar line, and femoral neck (at the narrowest point) in addition to points on the femoral shaft, as per EOS protocol. NSA was then automatically calculated as the angle between the femoral neck axis and the axis of the proximal diaphysis using the bundled sterEOS software.

Table 1 Data on the studied population

Calendar age (years)	Sex	<i>n</i>	Suspected scoliosis (Cobb angle <10°)	Mild functional Kyphosis	Joint pain of Un. Orig.	Other
4	Male	8	5	0	0	3
	Female	14	13	0	1	0
5	Male	15	11	0	1	3
	Female	19	17	0	1	1
6	Male	14	11	0	1	2
	Female	15	14	0	0	1
7	Male	16	10	0	1	5
	Female	19	14	0	0	5
8	Male	17	10	0	2	5
	Female	21	15	0	3	3
9	Male	19	7	1	5	6
	Female	18	12	0	3	3
10	Male	21	12	0	7	2
	Female	20	16	0	2	2
11	Male	21	11	2	6	2
	Female	23	12	1	9	1
12	Male	21	12	2	5	2
	Female	40	32	1	4	3
	Male	24	11	1	10	2
13	Female	39	30	3	5	1
	Male	25	10	1	12	2
14	Female	40	32	2	4	2
	Male	22	12	1	6	3
15	Female	51	29	3	13	6
	Male	26	19	0	5	2
16	Female	37	21	2	13	1
	Male	25	3	1	19	2
17	Female	25	3	1	20	1
	Male	25	5	1	19	0
18	Female	25	5	0	14	6
	Male	25	4	2	17	2
19	Female	25	6	1	17	1
	Male	25	4	0	20	1
20	Female	25	7	1	16	1
	Male	25	2	2	19	2
21	Female	25	3	0	20	2
	Male	25	1	0	23	1
22	Female	25	1	1	21	2
	Male	25	2	0	21	2
23	Female	25	1	0	23	1
	Male	25	2	0	21	2
24	Female	25	1	0	21	3
	Male	449	164	14	220	51
SUM	Female	556	284	16	210	46

After imaging, all cases of suspected scoliosis had a normal or <10° Cobb angle. (Other disorders: mild degenerative signs, bone cysts of various types, juvenile aseptic bone changes such as osteochondritis of the upper limb).

Fig. 1

No.	Name of the Stage	Line Sketch of the C3 Vertebra's Shape	Description of the Stage
1	Initiation		The inferior borders of C2, C3, and C4 are all flat, and upper borders taper from posterior to anterior, giving the body a wedge shape.
2	Acceleration		C2 and C3 develop concavities in their inferior borders, while that of C4 remains flat, and bodies of C3 and C4 are almost rectangular in shape.
3	Transition		Concavities in C2 and C3 are now deeper and distinct, with C4 beginning to develop a concave inferior border too, bodies of C3 and C4 are rectangular in shape.
4	Deceleration		C2, C3, and C4 all have distinct concavities in their inferior borders, and the bodies of C3 and C4 are becoming more square in shape.
5	Maturation		Concavities of C2, C3, and C4 are more accentuated in the inferior borders, and C3, C4 bodies are almost square or square in shape.
6	Completion		Deep concavities are found in the inferior borders of C2, C3, and C4 and the bodies were square or were column like, with a vertical dimension greater than their horizontal dimension.

Cervical Bone Age Assessment, as described by Hassel and Farman (1995). Second, third and fourth cervical vertebrae are assessed by morphology, based on shape, superior border and inferior border together [reproduced from Schlégl *et al.* (2017) [13]].

For a more detailed description of the EOS protocol, see Supplementary Figure 1, supplement digital content 1, <http://links.lww.com/JPOB/A39>. Fifty-five cases were randomly selected and evaluated on three different days by the three observers and intraclass correlation coefficient calculated to assess intraobserver and interobserver reliability of the reconstructions due to the user verification step and for the bone age estimation method.

Although many subjects included in the study possessed some mild spinal curvature deviation (Cobb angle $<10^\circ$), a study of 10 subjects at each bone group and at chronological ages 9–24 was performed to investigate the presence of any significant differences in their lower limbs compared to the others.

The mean NSA value and SDs at each chronological age and bone age were subsequently calculated and means were compared using the independent *t*-test. The correlation between change in NSA and chronological age and bone age was assessed using the Spearman correlation and linear regression. The influence on the NSA of

chronological age and bone age, together and separately, was also assessed using Stepwise Multivariate Regression Analysis. Multicollinearity was examined with the Variance Inflation Factor (VIF) test. When $VIF < 1$ multicollinearity was said to be excluded, in $1 < VIF < 2$ mild multicollinearity was believed to be present but does not influence significantly the results, over 2 the multicollinearity was deemed incongruent and the model rejected. Sex differences were also assessed using independent *t*-test and general linear modelling, with sex input as a dummy variable.

All statistical evaluations were performed with IBM SPSS (IBM Corp., Armonk, New York, USA), version 22. For randomized selection the RAND.BETWEEN formula of the Microsoft Excel v14.0.6112.5000 (Microsoft Corp., Redmond, Washington, USA) software was used. *P*-value < 0.05 was accepted as significant. At the time of initial radiological evaluation, written consent was collected for future retrospective studies. This study was approved by our Institutional Review Board.

Results

T2 NSA values compared to bone and chronological age are shown in Tables 2 and 3. Bone age stage 1 exhibited an average value of $130.91^\circ \pm 4.26^\circ$ falling to $128.07^\circ \pm 3.36^\circ$ by stage 6. Compared to chronological age NSA fell from $131.89^\circ \pm 6.07^\circ$ at 4 years old, to an average of $128.85^\circ \pm 4.46^\circ$ at 16, and exhibited a slowing decline until 20 years old, (mean: $127.81^\circ \pm 3.84^\circ$). Univariate linear regression found statistically significant models between NSA and both bone age and chronological age, with bone age exhibiting a slightly higher R^2 value ($R^2=0.101$ vs. 0.069 , beta-coefficient -0.286 vs. -0.264 , standard error of the estimate 4.001 vs. 4.176 , respectively). The spearman test also found the correlation between NSA and bone age to be stronger than that with chronological age but was small in magnitude (bone age -0.164 vs. chronological age -0.130). Distribution of subjects across bone and chronological ages is shown in Table 4.

T4 Gender-based NSA differences were found by *t*-test when included in chronological age comparisons ($P=0.035$), but no statistically significant difference was found with bone age-based analysis ($P=0.265$). Similarly, when general linear modelling was performed the effect of gender was small but statistically significant compared to chronological age ($R^2=0.082$, $P<0.001$) but NS when compared to bone age ($R^2=0.073$, $P=0.12$).

F2 NSA values of all individuals and the bone age across all chronological ages as shown in boxplot in Fig. 2.

F3 Significant differences were seen between those individuals with an elevated or delayed bone age compared to those of the same age – the NSA values of those with bone ages 2 or more stages above their peers were on average elevated 3.16° , ($P<0.001$), while those with a delayed bone age (2 or more stages below their peers) showed an average elevation of 4.45° ($P<0.001$), see Fig. 3. ‘Elevated’ and ‘delayed’ categories corresponded to those outside of at least one SD or 68% of the population, with the exception of 65.5% at age 12, due to the wide range of bone ages at this age-year. On average 83.38% of individuals at each chronological age-year were found at or ≤ 1 stage from the ‘typical’ bone age.

F4 At most bone age stages, the older and younger individuals also showed significantly elevated NSAs compared to the others in that stage (Fig. 4a–f). In stage 1, 11 and 12-year olds had significantly higher NSAs than the younger individuals in that stage (133.1° , 134.8° vs. 130.9° , $P=0.002$, $P=0.032$). In stages 3 and 4, both younger and older individuals showed higher NSA angles with stage 3 values of 131.9° , 130.6° and 129.3° , 130.6° vs. 127.2° ($P=0.041$, <0.001 , 0.029 , 0.039), respectively, and in stage 4, 132.2° , 130.0° and 131.1° , 133.3° vs. 128.1°

Table 2 Maximum, minimum and SD values recorded with respect to bone age (values in degrees)

Bone age (stage)	N	Minimum	Maximum	Mean	SD
1	142	121	143	130.91	4.259
2	94	117	145	129.17	6.061
3	114	120	143	129.91	4.374
4	147	119	144	130.40	4.140
5	202	118	142	128.90	4.174
6	306	120	143	128.07	3.358
Overall	1005				4.394

Table 3 Maximum, minimum and SD values recorded with respect to chronological age (values in degrees)

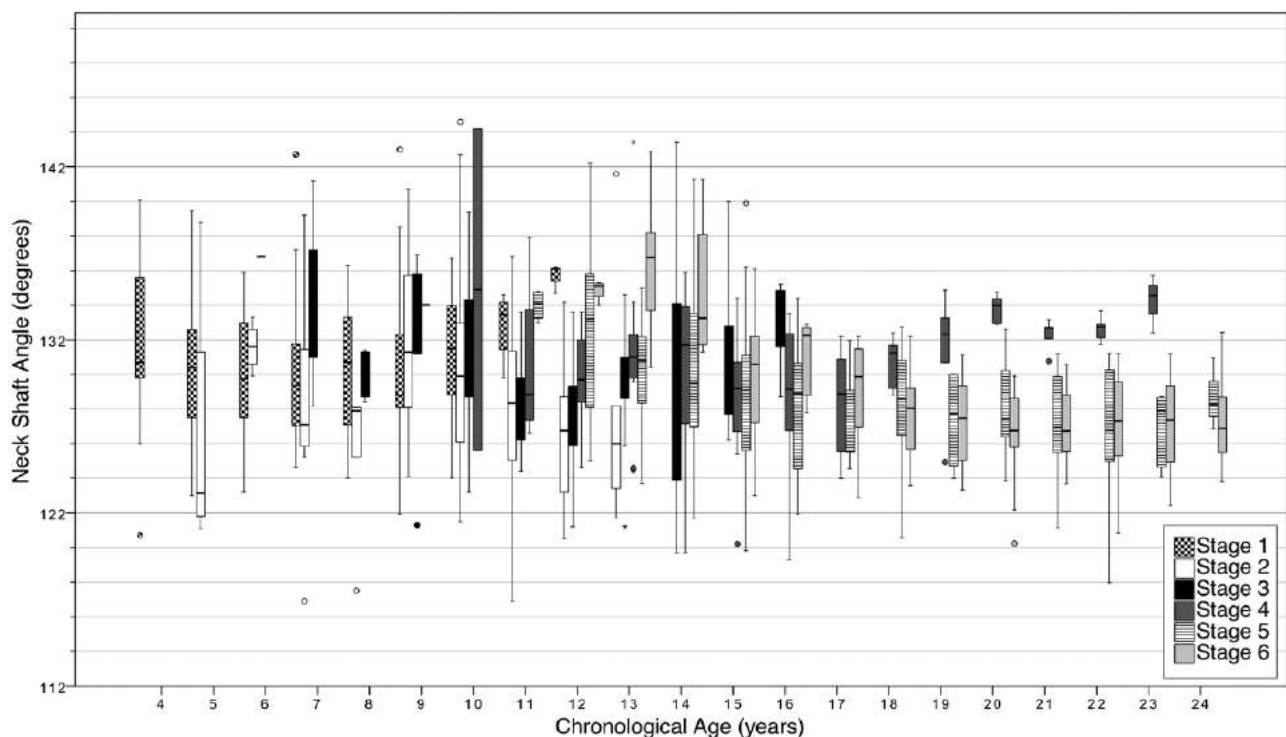
Calendar age (years)	N	Minimum	Maximum	Mean	SD
4	22	121	140	131.89	6.072
5	34	121	140	129.91	5.627
6	29	123	137	130.50	4.076
7	35	117	143	130.46	6.265
8	38	118	141	129.81	5.171
9	37	121	143	131.52	6.070
10	41	122	145	131.40	6.434
11	44	117	138	129.82	4.956
12	61	121	142	129.85	5.167
13	63	121	143	130.68	5.195
14	65	120	143	130.58	6.146
15	73	120	140	129.25	4.704
16	63	119	135	128.85	4.464
17	50	123	132	128.43	3.485
18	50	121	133	128.40	3.273
19	50	123	135	127.96	3.454
20	50	120	135	127.81	3.842
21	50	121	133	127.70	3.472
22	50	118	134	127.88	3.822
23	50	122	136	127.75	3.910
24	50	124	132	127.31	3.179
Overall	1005				4.704

Table 4 Distribution of the calendar age within the bone age stages

Age (years)	Bone age stage						Sum	Age (years)	Bone age stage						Sum	
	1	2	3	4	5	6			1	2	3	4	5	6		
4	22						22	4	100.0%							2.2%
5	30	4					34	5	88.2%	11.8%						3.4%
6	22	5	2				29	6	75.9%	17.2%	6.9%					2.9%
7	17	12	6				35	7	48.6%	34.3%	17.1%					3.5%
8	19	12	7				38	8	50.0%	31.6%	18.4%					3.8%
9	10	19	7	1			37	9	27.0%	51.4%	18.9%	2.7%				3.7%
10	13	13	11	4			41	10	31.7%	31.7%	26.8%	9.8%				4.1%
11	6	10	15	7	6		44	11	13.6%	22.7%	34.1%	15.9%	13.6%			4.4%
12	3	13	19	8	12	6	61	12	4.9%	21.3%	31.1%	13.1%	19.7%	9.8%		6.1%
13		6	21	15	13	8	63	13		9.5%	33.3%	23.8%	20.6%	12.7%		6.3%
14			12	18	27	8	65	14			18.5%	27.7%	41.5%	12.3%		6.5%
15			11	17	33	12	73	15			15.1%	23.3%	45.2%	16.4%		7.3%
16			3	20	32	8	63	16			4.8%	31.7%	50.8%	12.7%		6.3%
17				14	13	23	50	17				28.0%	26.0%	46.0%		5.0%
18				8	18	24	50	18				16.0%	36.0%	48.0%		5.0%
19				8	5	37	50	19				16.0%	10.0%	74.0%		5.0%
20				7	11	32	50	20				14.0%	22.0%	64.0%		5.0%
21				7	12	31	50	21				14.0%	24.0%	62.0%		5.0%
22				7	8	35	50	22				14.0%	16.0%	70.0%		5.0%
23				6	7	37	50	23				12.0%	14.0%	74.0%		5.0%
24					5	45	50	24					10.0%	90.0%		5.0%
SUM	142	94	114	147	202	306	1005	SUM	14%	9%	11%	15%	20%	30%		

Absolute values are shown on the left and the incidence (in percent) within each age group, on the right.

Fig. 2

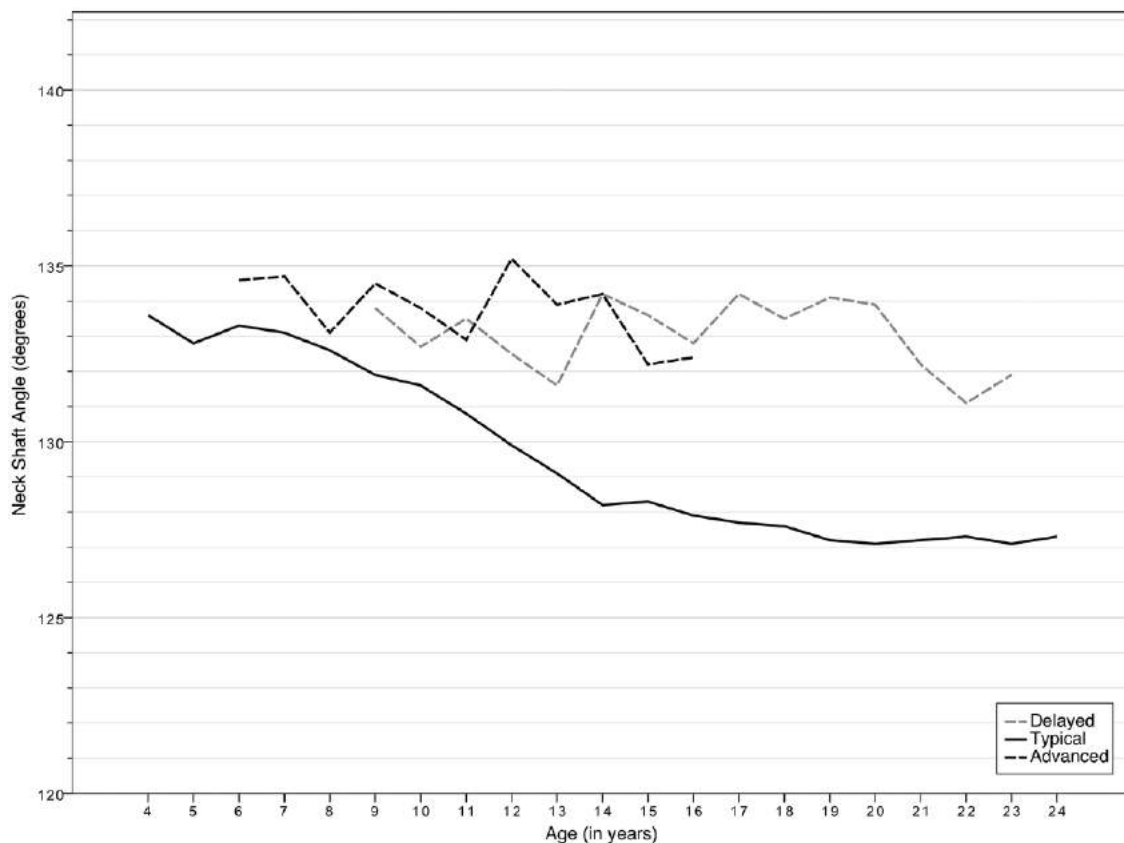


NSA and bone age within each chronological age. When the NSA and bone age of all individuals are shown, younger and less mature individuals were seen to have higher NSA values; however, elevated values can also be seen in those exhibiting higher bone ages at a younger age. The earliest individuals in stages 3 (in green), 5 (orange) and 6 (red), for example, show elevated NSA values compared do their peers of the same chronological age. NSA, neck-shaft angle.

($P < 0.001$, 0.022, 0.004, 0.011), respectively. In stages 5 and 6, NSA was elevated if individuals were younger, with stage 5 individuals 11 and 12 years old vs. those aged

13–23 exhibiting values of 135° , 131.7° vs. 128° ($P < 0.001$, < 0.001), and in stage 6, younger individuals showing 134.9° , 131° vs. 126° ($P < 0.001$, < 0.001). Stage 2 values

Fig. 3



NSA vs. chronological age. Sub-stratification by bone age. Statistically significant differences were found in those with advanced ('fast-maturing') or delayed ('slow-maturing') bone age, relative to the average NSA within that stage. 'Advanced' or 'delayed' bone age was defined if individuals differed from the average bone age within the group by ≥ 2 bone age stages (NSA). * indicates statistical significance, $P < 0.05$. NSA, neck-shaft angle.

had statistical significance between younger and older age groups but did not show a clear trend.

Multivariate linear regression models generated indicated that NSA changes are predicted most accurately when both chronological and bone age are used together ($R^2 = 0.226$, beta-coefficient = -0.322 , $P < 0.001$, standard error of the estimates = 3.809 , VIF = 0.875 ; vs. univariate linear regression values $R^2 = 0.101$, 0.069).

No significant difference in proximal femur values was found between those with and without mild orthopaedic disorders in our population, based on calendar age or bone age ($P > 0.005$). Interobserver and intraobserver reliabilities were all excellent, ICC > 0.9 (see Supplementary Table 1), supplement digital content 2, <http://links.lww.com/JPOB/A40>.

Discussion

Chronological age reflects the passing of years, months and weeks. Bone age on the other hand is influenced by sex, race, nutrition, genetics, sickness or health and socioeconomic status, and so may possess a better relationship

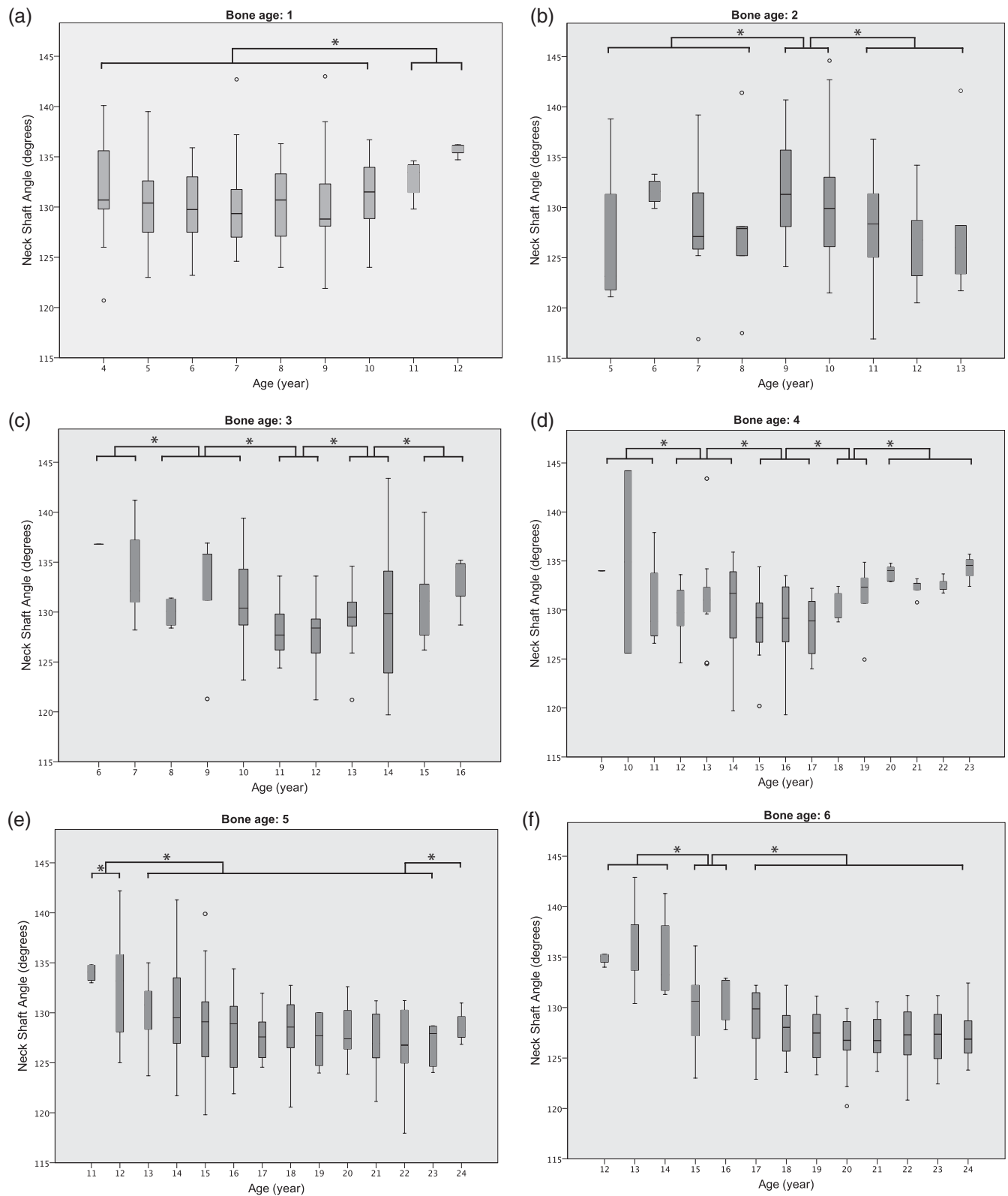
with the physiological state, and hence provide a better yardstick for development. We considered that comparisons between a child's proximal femur morphology and their bone age may yield interesting results and give a more reliable basis for comparing growth between groups of children.

Our results found that bone age demonstrated a small but superior relationship with the NSA compared to that of the chronological age – linear regression models showed an R^2 value of 0.101 vs. 0.069 , SD was lower (4.39° vs. 4.70°) and Spearman correlation was higher (-0.164 vs. -0.130). However, our multivariate linear regression analysis found that a model using both bone age and chronological age was the most accurate ($R^2 = 0.226$ vs. 0.101 , 0.069) and best reflected the changes of NSA in boys or girls, throughout growth and development.

When bone age stages were subdivided by chronological age, several interesting patterns emerged.

While the majority of children at a similar chronological age had similar bone age scores, at each age there was

Fig. 4



(a-f). NSA and chronological age at each bone age stage. NSA values were significantly higher in older individuals in stages 1, 3, 4 and 5 and also in those of lower age in stages 3, 4, 5 and 6 ($*P < 0.05$). NSA, neck-shaft angle.

a subset of children who showed a delayed or advanced bone score compared to the group, which we termed 'slow-maturing' and 'fast-maturing' groups. A child or adolescent was considered 'slow-maturing' or 'fast-maturing' if the cervical vertebrae differed by two or more bone age stages from others of the same chronological age (see Fig. 3). In these cases, irrespective of whether the individual was slow-maturing or fast-maturing, their NSA was significantly higher than that of their peers. On average, the value seen in the fast-maturing was elevated by 3.16° , ($P < 0.001$), and in slow-maturing individuals by 4.45° ($P < 0.001$). While this might be expected in the case of a lower bone age stage, the presence of younger children with higher bone scores exhibiting a higher NSA than their less-developed peers has not been reported before.

Conversely, when the age distribution was examined within each individual bone age group, a similar relationship was seen again (Fig. 4a–f). Within bone age stage 1, those children who were of older age had a higher NSA than the others. In stage 3, the majority of children were of similar age; however, if they were older or younger than the 'typical' stage 3 children their NSA was elevated. A similar pattern was also seen in stages 4 and 5 individuals. In stages 5 and 6, the pattern was less clear in older individuals; however, this is likely as the range of ages within the group was much broader, encompassing 17- to 24-year-olds.

These findings meant that while a typical 15-year-old was found to have an NSA of 128.3° , those who were slow-maturing or fast-maturing had higher values (133.6° and 132.2° , respectively, see Fig. 3), and similar results were present throughout all age groups. Our results suggested to us that femoral neck development undergoes a period of susceptibility during which biomechanical forces may act on the proximal femur to determine the NSA – such that proximal morphology is determined by 'force \times time'. If this period is shortened, as it is in 'fast-maturers', then the NSA remains elevated as the cartilage ossifies earlier before the neck has fallen completely from the immature valgus configuration. It is not clear whether these fast-maturing individuals finally undergo a 'catch-up' decrease in NSA or remain with elevated values; however, without a longitudinal study, it is not possible for us to clarify.

Biomechanical forces have long been regarded as the drivers of proximal femoral geometry [15]; however, the effect of timing on the geometry has not been well studied. To support our hypothesis, we considered that patients with advanced bone age or a shortened duration with open epiphyseal plates for other reasons would likely have higher NSA values also. Precocious puberty results in premature epiphyseal closure and short stature; however, it is not typically associated with changes in NSA, though it has not been explicitly described by reports on the disease except in the case of co-existent

fibrous osteolytic dysplasia, as part of McCune–Albright syndrome [16,17].

Similarly, we considered that patients with delayed bone age or a prolonged duration with open epiphyseal plates for other reasons should have lower NSA values. However, reports of proximal femur measurements in conditions in which bone age is delayed are few. Despite the known delay of epiphyseal development associated with such conditions as thyroid disease [18,19] and growth hormone deficiency [20,21], we could find no studies describing NSA of patients that could give supporting or contradicting evidence although the association between hypothyroidism and slipped capital femoral epiphysis has been described many times [22,23]. However, the pathogenesis of slipped capital femoral epiphysis has been linked to a decreased NSA [23]. While studies have found that the age at menarche fell continuously since the 19th century, the NSA has not been reported to be on the decrease. The majority of menarche data from recent decades; however, has not been in agreement about the continuation of this trend and the majority of NSA values are from this time [24–28].

The strengths of our study lie in its large population size, one of the largest living cohorts studied for proximal femur assessment, and the use of the EOS 2D/3D scanner to eliminate anteversion associated artifacts. There were several limitations to our study. Our study was a cross-sectional study, rather than prospective; however, the unnecessary exposure of children to radiation raises difficult ethical questions. It must also be noted that our study population was not completely free of minor skeletal deformities; however, the results of our small control study previously performed and reported, found no difference in the lower limbs of those included with mild orthopaedic disorders and those without, so we feel satisfied all values can be taken as normal [13]. The most commonly used bone age estimation methods assess the hand and wrist; however, due to patient positioning in the EOS images, the cervical method was chosen. Although this also prevented us from comparing the results with the hand-wrist and the cervical method, numerous studies have previously validated the Hassel–Farman method in comparison to hand-wrist [14,29,30]. Furthermore, the grouping of growing children into 'typical' growth patterns or otherwise based on a somewhat arbitrary data point (in this case, slow-maturer or fast-maturer categories were based on those exhibiting bone age stage difference of 2 or more than those at the same chronological age) and so must always be regarded as at risk of detecting events that occurred simply due to chance; however, due to the size of our population, we feel this is less likely.

In conclusion, while NSA development is known to be the result of biomechanical forces acting across the proximal femur, it may be possible to define a period of susceptibility in which the neck-shaft undergoes these changes. Combined models using both bone age and chronological

age can give a more accurate and individualized assessment of a child's NSA development, taking into account gender, nutrition, socioeconomic status, disease status, and could improve diagnosis and better define indications and goals of intervention in the treatment of NSA disorders such as coxa vara and in developmental dysplasia of the hip with coxa valga.

Acknowledgements

Centre of Excellence Program, Government of Hungary (20765-3/2018/FEKUTSTRAT).

Conflicts of interest

AQ5

There are no conflicts of interest.

References

- Mills HJ, Horne JG, Purdie GL. The relationship between proximal femoral anatomy and osteoarthritis of the hip. *Clin Orthop Relat Res* 1993; **205**–208.
- Joseph B, Nayagam S, Loder RT, Torode I. *Paediatric orthopaedics: a system of decision-making*. Hodder Arnold; 2009.
- Standing S, Borley NR, Henry G. *Gray's anatomy: the anatomical basis of clinical practice*. 40th ed. Edinburgh: Churchill Livingstone/Elsevier; 2008.
- Gilligan I, Chandraphak S, Mahakkanukrauh P. Femoral neck-shaft angle in humans: variation relating to climate, clothing, lifestyle, sex, age and side. *J Anat* 2013; **223**:133–151.
- Boese CK, Frink M, Jostmeier J, Haneder S, Dargel J, Eysel P, et al. The modified femoral neck-shaft angle: age- and sex-dependent reference values and reliability analysis. *Biomed Res Int* 2016; **2016**:8645027.
- Kay RM, Jaki KA, Skaggs DL. The effect of femoral rotation on the projected femoral neck-shaft angle. *J Pediatr Orthop* 2000; **20**:736–739.
- Child SL, Cowgill LW. Femoral neck-shaft angle and climate-induced body proportions. *Am J Phys Anthropol* 2017; **164**:720–735.
- Dimeglio A, Canavese F. Progression or not progression? How to deal with adolescent idiopathic scoliosis during puberty. *J Child Orthop* 2013; **7**:43–49.
- Gheno R, Nectoux E, Herbaux B, Baldisserotto M, Glock L, Cotten A, Boutry N. Three-dimensional measurements of the lower extremity in children and adolescents using a low-dose biplanar X-ray device. *Eur Radiol* 2012; **22**:765–771.
- Roszkopf AB, Ramseier LE, Sutter R, Pfirrmann CW, Buck FM. Femoral and tibial torsion measurement in children and adolescents: comparison of 3D models based on low-dose biplanar radiography and low-dose CT. *AJR Am J Roentgenol* 2014; **202**:W285–W291.
- Schlégl ÁT, Szuper K, Somoskeöy S, Than P. Three dimensional radiological imaging of normal lower-limb alignment in children. *Int Orthop* 2015; **39**:2073–2080.
- Szuper K, Schlégl ÁT, Leidecker E, Vermes C, Somoskeöy S, Than P. Three-dimensional quantitative analysis of the proximal femur and the pelvis in children and adolescents using an upright biplanar slot-scanning X-ray system. *Pediatr Radiol* 2015; **45**:411–421.
- Schlégl ÁT, O'Sullivan I, Varga P, Than P, Vermes C. Determination and correlation of lower limb anatomical parameters and bone age during skeletal growth (based on 1005 cases). *J Orthop Res* 2017; **35**:1431–1441.
- Hassel B, Farman AG. Skeletal maturation evaluation using cervical vertebrae. *Am J Orthod Dentofacial Orthop* 1995; **107**:58–66.
- Pauwels F. *Biomechanics of the normal & diseased hip*. Berlin, Heidelberg: Springer Berlin Heidelberg; 1976.
- Leet AI, Wientroub S, Kushner H, Brillante B, Kelly MH, Robey PG, Collins MT. The correlation of specific orthopaedic features of polyostotic fibrous dysplasia with functional outcome scores in children. *J Bone Joint Surg Am* 2006; **88**:818–823.
- Nelson MD. The radiological approach to precocious puberty: pictorial review. *Br J Radiol* 2000; **73**:560–567.
- Salerno M, Micillo M, Di Maio S, Capalbo D, Ferri P, Lettierio T, Tenore A. Longitudinal growth, sexual maturation and final height in patients with congenital hypothyroidism detected by neonatal screening. *Eur J Endocrinol* 2001; **145**:377–383.
- Williams GR, Bassett JHD. Thyroid diseases and bone health. *J Endocrinol Invest* 2018; **41**:99–109.
- Cantu G, Buschang PH, Gonzalez JL. Differential growth and maturation in idiopathic growth-hormone-deficient children. *Eur J Orthod* 1997; **19**:131–139.
- Vance ML, Mauras N. Growth hormone therapy in adults and children. *N Engl J Med* 1999; **341**:1206–1216.
- Nissen N, Hauge EM, Abrahamsen B, Jensen JE, Mosekilde L, Brixen K. Geometry of the proximal femur in relation to age and sex: a cross-sectional study in healthy adult Danes. *Acta Radiol* 2005; **46**:514–518.
- Azar FM, Canale ST, Beaty JH, Campbell WC. *Willis C. Campbell's Operative Orthopaedics*. 12th ed. Oxford: Mosby - Elsevier; 2013.
- Onland-Moret NC, Peeters PH, van Gils CH, Clavel-Chapelon F, Key T, Tjønneland A, et al. Age at menarche in relation to adult height: the EPIC study. *Am J Epidemiol* 2005; **162**:623–632.
- Wang Q, Chen D, Cheng SM, Nicholson P, Alen M, Cheng S. Growth and aging of proximal femoral bone: a study with women spanning three generations. *J Bone Miner Res* 2015; **30**:528–534.
- Pearce MS, Birrell FN, Francis RM, Rawlings DJ, Tuck SP, Parker L. Lifecourse study of bone health at age 49–51 years: the Newcastle thousand families cohort study. *J Epidemiol Community Health* 2005; **59**:475–480.
- Boese CK, Dargel J, Oppermann J, Eysel P, Scheyerer MJ, Bredow J, Lechler P. The femoral neck-shaft angle on plain radiographs: a systematic review. *Skeletal Radiol* 2016; **45**:19–28.
- Freedman DS, Khan LK, Serdula MK, Dietz WH, Srinivasan SR, Berenson GS. Relation of age at menarche to race, time period, and anthropometric dimensions: the Bogalusa heart study. *Pediatrics* 2002; **110**:e43.
- San Román P, Palma JC, Oteo MD, Nevado E. Skeletal maturation determined by cervical vertebrae development. *Eur J Orthod* 2002; **24**:303–311.
- Uysal T, Ramoglu SI, Basciftci FA, Sari Z. Chronologic age and skeletal maturation of the cervical vertebrae and hand-wrist: is there a relationship? *Am J Orthod Dentofacial Orthop* 2006; **130**:622–628.

AQ6

AQ7

Csontkor – a csontrendszeri érettség mérésének lehetősége EOS készülékkel

O’Sullivan Ian dr. ■ Schlégl Ádám Tibor dr. ■ Varga Péter dr.
Kerekes Kamilla dr. ■ Vermes Csaba dr. ■ Than Péter dr.

Pécsi Tudományegyetem, Általános Orvostudományi Kar, Ortopédiai Klinika, Pécs

Bevezetés: Az EOS 2D/3D rendszerrel készült felvételeken nem ábrázolódnak megfelelően a csontkor megállapítására leggyakrabban használt kéz és csukló.

Célkitűzés: Kutatásunk célja, hogy alternatív csontkormérési lehetőségeket keressünk EOS-felvételeken való alkalmazásra.

Módszer: 9 mérési módszer bevonásával pilotvizsgálatot végeztünk, amely alapján 5 módszert válogattunk be: nyaki csigolyát (Hassel–Farman), csípőlapátot (Risser ‘plus’), térdet (O’Connor), sarokcsontot (Nicholson), csípőt (Oxford) értékelve. 114 egészséges, 2–21 éves eset EOS-felvételein intra- és interobszerver megbízhatósági vizsgálatot végeztünk, valamint Spearman-korrelációval összevetettük a csont- és kronológiai kort.

Eredmények: A megbízhatósági vizsgálatok minden módszer esetében kiváló eredményt adtak (csoporton belüli korreláció $>0,9$), kivéve az O’Connor-módszert (0,865 – jó). A Nicholson- és a Hassel–Farman-módszer bizonyult a leggyorsabbnak (átlag: 17,5 mp és 33,4 mp), viszont a sarokcsontok 14%-a nem volt vizsgálható (a cervicális esetén 1%). Minden módszer szignifikáns összefüggést mutatott a korrallal (korrelációs együttható $>0,829$). Az értékelésnél nehézséget jelentettek a nem ábrázolódó (12%) vagy egymásra vetülő (23%) csontrészek.

Következtetés: Csontkor-megállapítás mind az 5 módszer alkalmazásával lehetséges, de kiemelkedett a nagy megbízhatósággal, gyorsan, közel az összes felvételen alkalmazható Hassel–Farman-módszer.

Orv Hetil. 2019; 160(16): 619–628.

Kulcsszavak: EOS 2D/3D, csontkor, biológiai kor, kronológiai kor, Risser-jel

Bone age – alternatives for skeletal maturity assessment for the EOS scanner

Introduction: Hand and wrist bone age assessment methods cannot be performed when using the recommended patient position within the EOS scanner.

Aim: We aimed to assess alternative methods for use with the EOS.

Method: After investigating 9 alternatives, five methods were selected – cervical vertebra (Hassel–Farman), iliac crest (Risser ‘plus’), hip (Oxford), knee (O’Connor), calcaneus (Nicholson) – and applied to EOS scans of 114, 2–21-year-old normal individuals. Intraclass correlation coefficient tests for reliability and Spearman correlation with calendar age were assessed.

Results: Intra- and interobserver reliabilities were all excellent, except with the knee method (0.865 – ‘good’). Calcaneal and cervical methods were the fastest to apply (mean 17.5 s, 33.4 s per evaluation), however, calcanei were unassessable in 14% of scans (*versus* 1% of cervical). All methods correlated significantly with calendar age ($r>0.829$, $p<0.05$). Difficulties were principally absent (12%) or obscured (23%) landmarks.

Conclusion: Bone age assessment is possible with all 5 methods, however, the Hassel–Farman method proved to be easily useable, fast and reliable.

Keywords: EOS 2D/3D, bone age, biological age, calendar age, Risser sign

O’Sullivan I, Schlégl ÁT, Varga P, Kerekes K, Vermes Cs, Than P. [Bone age – alternatives for skeletal maturity assessment for the EOS scanner]. Orv Hetil. 2019; 160(16): 619–628.

(Beérkezett: 2018. október 19.; elfogadva: 2018. november 24.)

Rövidítések

2D = kétdimenziós; 3D = háromdimenziós; CT = (computed tomography) számítógépes tomográfia; EOS = sztereo-röntgenfelvételi rendszer, mely álló vagy ülő helyzetben készít képet a teljes testről; ICC = (intraclass correlation) osztályon belüli korreláció; kk = korrelációs koefficiens, korrelációs együtttható; MRI = (magnetic resonance imaging) mágnesesrezonancia-vizsgálat

A csontkor a vázrendszer érettségi állapotának jó indikátora. Egy vagy több csont másodlagos csontosodási magjának elemzésével lehetőségünk nyílik megbecsülni a teljes csontváz biológiai korát. A növekedés állapotának és ütemének megállapítása fontos támpontot nyújthat endokrinológiai, fogorvostani és ortopédiai betegségek diagnosztizálásához és beavatkozások időzítéséhez [1].

Emellett fontos információkat nyújthat az igazságügyi orvoslás és az antropológia vonatkozásában.

A XIX. század vége óta számos csontkormérési módszert publikáltak – egyes módszerek már a méhen belüli fejlődést is értékelik, míg más mérőszámok nem mutatnak jelentős változásokat a késői serdülőkorig; egyesek az epiphysisporcokat elemzik, míg mások az apophysisek csontosodásának változásait; sokan csak hosszú csöves csontokat értékelnek, mások csak lapos vagy szabálytalan csontokat, míg egyesek egy érintett régió különböző típusú csontjait veszik figyelembe (1. táblázat) [2–30]. A különböző régiók vizsgálatához számos képalkotó módszert használtak, a hagyományos röntgenképtől (ez a legáltalánosabban használt) az ultrahangon és a CT-n át az MRI-ig [31].

A témakör régóta kiterjedt vizsgálata ellenére továbbra is maradtak válaszra váró kérdések, amelyek a növekedés

1. táblázat | Népszerű csontkormérési módszerek – az atlasz- és az 'egyrégió'-módszer [2–30]

	Atlaszmódszer		Egyrégió-módszer	
Kéz és csukló	Greulich–Pyle	Greulich & Pyle, 1959 [2]	Björk	Björk, 1967 [3]
			Fishman†	Fishman, 1982 [4]
			Grave & Brown	Grave & Brown, 1976 [5]
			Oxford Hand-Wrist	Acheson, 1954 [6]
			Sanders	Sanders, et al. 2008 [7]
			Singer†	Singer, 1980 [8]
			Tanner–Whitehouse	Tanner et al., 1976 [9]
Nyaki csigolya			Hassel & Farman	Hassel & Farman, 1995 [10]
			Lamparski	Lamparski, 1975 [11]
			Mito	Mito et al., 2002 [12]
			Roman	Roman, et al. 2002 [13]
Felkarcsont			Walker & Lovejoy	Walker & Lovejoy, 1985 [14]
Könyök			Sauvegrain	Sauvegrain, 1962 [15]
			Sauvegrain (módosított): csak Olecranon	Charles et al., 2007 [16]
Váll			Schaefer	Schaefer et al., 2015 [17]
Kulcsocsont			Schmeling	Schmeling et al., 2000 [18]
Első borda			Michelson	Michelson et al., 1934 [19]
Csípő, csípőlapát			Risser	Risser, 1958 [20]
			Risser 'plus'	Negrini et al., 2015 [21]
Symphysis			McKern & Stewart	McKern & Stewart, 1957 [22]
Csípő			Oxford-csípő	Acheson, 1957 [23]
			Módosított Oxford-csípő	Stasikelis et al., 1996 [24]
Femurdiaphysis			Stull	Stull et al., 2014 [25]
Szárkapocsont			Tsai	Tsai et al., 2016 [26]
Térd	Pyle & Hoerr	Pyle & Hoerr, 1969 [27]	McKern–Stewart	O'Connor et al., 2008 [28]
			Oxford-térd	Acheson, 1954 [6]
Boka	Hoerr, Pyle & Francis	Hoerr et al., 1962 [29]		
Sarokcsont			Nicholson	Nicholson et al., 2015 [30]

†Jellemzően ortodontológiában és fogorvoslásban használt módszerek.

– amely dinamikus, változó jelenség – nehéz számszerűsíthetőségéből és magas egyéni különbségeiből is adódnak: egy adott régióban tapasztalható csontkorból egyenesen következik-e a vizsgált egyén biológiai kora? Egy adott egyén növekedési üteme megbízhatóan összehasonlítható-e másokéval? Számos szerző figyelmeztet a túlzott egyszerűsítés veszélyeire, illetve az egyetlen mutató alapján történő növekedésbecslés megbízhatatlanságára. Biztosabb becslést lehet végezni a magassággörbék, a Tanner-stádiumok (a pubertás fejlődési szakaszai) és egy vagy több csontkormérési módszer kombinálásával [32].

A röntgenalapú csontkormérési módszerek két csoportba oszthatók, ezek az atlaszmódszer és az egyrégió-módszer.

– Az atlaszalapú módszerek olyan referenciaképeket használnak, amelyekhez a páciens röntgenfelvétele hasonlítható. A vizsgált csont(ok)nak a referenciaképekhez való illesztése után meghatározható a csontváz érettségi szintjének megfelelő kronológiai kor, azaz a csontkor. A fenti módszerek népszerűségét az adja, hogy könnyű őket megtanulni és használni, azonban könnyen téves eredményt adhatnak a növekedést egy-egy folyamatként kezelő megközelítések. Ezen okból az atlaszmódszerek pontossága elmarad az egyrégiós módszerekétől. Példaként említhető a Greulich–Pyle-féle kéz- és csuklóatlasz [2].

– Az egyrégiós megközelítés egy kiszemelt régió fejlődését elemzi, és fejlődési szakaszok formájában vagy százalékos formában kapunk eredményt. Az értékek csak az adott régió fejlődését írják le; a test többi részének fejlődésétől függetlenül eltérő időpontban érik el a legfejlettebb stádiumot, vagyis a 100%-ot. Ezek a módszerek általában pontosabbak, de gyakran hosszabb időt vesz igénybe a begyakorlásuk, és a kapott eredmények nem kapcsolódnak közvetlenül a kronológiai korhoz, ami az értelmezésüket megnehezíti. A kronológiai korhoz való lazább kapcsolat következtében kevésbé jellemző a túlegyszerűsítés és a teljes testre való túlzott általánosítás. Ezt a megközelítést használja a Tanner–Whitehouse-, az Oxford-csípő-, a calcaneus- és a Hassel–Farman-módszer is [6, 10, 30, 33].

A leggyakrabban használt technikák a kéz és a csukló felmérésén alapulnak, úgymint a Greulich–Pyle- vagy a Tanner–Whitehouse-módszer. Ezek során a bal oldali alkarról és csuklóról történik hagyományos anteroposterior röntgenfelvétel. A bal oldalt antropológusok egyezményesen választották ki az 1900-as években, mivel általában ez a nem domináns kéz, ezért a sérülése kevésbé valószínű [2].

Klinikánknak több mint 13 éves tapasztalata van az EOS 2D/3D rendszerrel [34–37], mely kétirányú teljes test-röntgenfelvételt lehetővé tévő képalkotó, amely utólagos 3D-rekonstrukcióra is alkalmas. A technika többek között hozzájárult az alsó végtagok biomechanikájának megértéséhez a növekedésben lévő gyermekek-

nél. A képalkotás során a páciensek a bal lábukkal 5 cm-rel előrelépve állnak, a karok pedig elől, könyökben és csuklóban hajlítva vannak. Ez a testtartás nem teszi lehetővé a csontkor-meghatározás tipikus alkar- és csuklóalapú módszereinek használatát, így szükségessé vált EOS-kompatibilis alternatív módszerek keresése.

Klinikánk korábbi vizsgálataiban igazoltuk a fogorvosok által széles körben használt nyakicsigolya-morfológián alapuló Hassel–Farman-módszer EOS-képalkotással kompatibilis magas megbízhatóságát [35].

Korábbi vizsgálatunkra alapozva a jelen tanulmány célja, hogy felmérjük az EOS 2D/3D felvételeken alkalmazható csontkormérési módszereket, elemezzük alkalmazhatóságukat, majd elvégezzük megbízhatósági vizsgálatukat.

Módszer

Klinikánkon 2007 és 2017 között a rutin ambuláns ellátás során 7127 EOS-teljestest-felvétel készült. Ebből kiválogattuk azokat az eseteket, amelyek a 2–21 éves korosztályt ábrázolták, és nem szerepelt az anamnézistükben olyan betegség vagy műtét, mely a csontváz növekedését befolyásolhatta, illetve a beteg a vizsgálat során nem mozdult meg (ami elmosódottá tette a képet), és megfelelően pozicionáltak. Az így megmaradt 1005 esetből véletlenszerűen, az életkor egyenletes eloszlását szem előtt tartva kiválasztottunk 114-et (57 férfi, 57 nő).

Az irodalom áttekintését követően kiválogattuk azokat a csontkormérési módszereket, melyek a legnagyobb eséllyel alkalmazhatók EOS-felvételeken: nyaki csigolya [10], váll [17], kulcscsont [18], első borda [19, 38], könyök [15], csípőlapát – Risser 'plus' [20], csípő (medence és proximális combcsont) [23], combcsontdiaphysis [25], térd [28] és sarokcsont [30] (*1/a-e. ábra*).

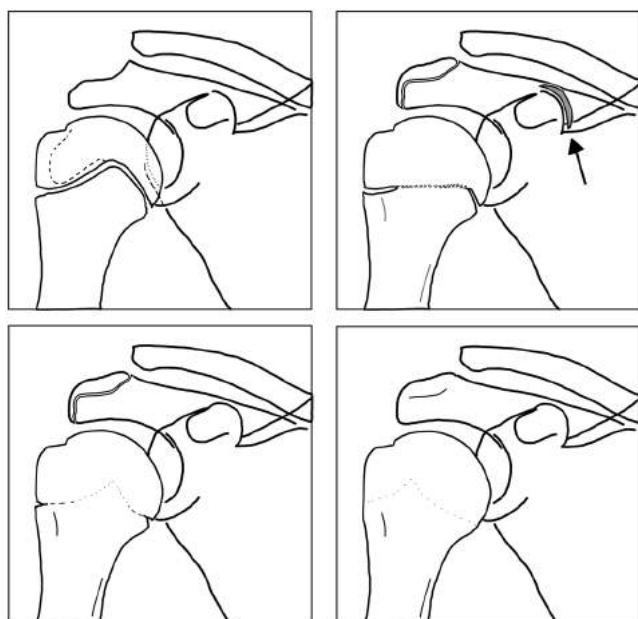
Egy pilotvizsgálat során 13 véletlenszerűen választott esetben, 3 vizsgáló bevonásával teszteltük a módszereket. A kulcscsonton, első bordán, könyökön és combcsontdiaphysisen alapuló méréseket kivitelezhetetlennek találtuk, majd a vizsgálatot követően, a vizsgálók szubjektív benyomása alapján a vállalapú módszert is kizártuk (részletek az Eredmények című fejezetben).

A pilotvizsgálat eredményei alapján mind a 114 esetben elvégeztük a mérést a nyakicsigolya-, a csípőlapát-, a csípő-, a térd- és a sarokcsontalapú módszereket alkalmazva. Ahhoz, hogy meghatározzuk, melyik módszer lenne a legmegfelelőbb, leghasznosabb a klinikai gyakorlatban EOS-képek értékelésénél, felmértük az alábbiakat:

1) A módszerek megbízhatósága

Különböző vizsgálók milyen eséllyel értékelik ugyanúgy a csontkorérési stádiumot (interobszerver), valamint a módszer milyen könnyen tanulható és reprodukálható a vizsgálók által (intraobszerver).

30 eset bevonásával is elvégeztük a vizsgálatot, melynek során 3 vizsgáló 3 különböző napon 3 alkalommal elvégezte a felvételek értékelését mind az 5 megmaradt



1/a-e ábra

A pilotvizsgálatba bevont csontkorméresi módszerek (A nyaki-csigolya-módszer leírása a Schlégl et al. 2017-ben megjelent cikkben található)

1/a ábra

Váll (Shaefer et al., 2015). A váll 3 régióját értékeli anteroposterior röntgenfelvételeken. 4 stádiumot különböztet el, igaz, nem mindegyik ábrázolódik röntgenfelvételeken. A régiók értékelésének összege adja a végző beosztást.

Proximalis humerus

1. stádium – nyitott: az epiphysis mentén folyamatos radiolucens vonal figyelhető meg. Az epiphysis éretlennek tűnik, a széli részek még nem fejlődtek ki teljesen.
2. stádium – egyesülés: elkezdődött az összezsontosodás. Az epiphysisporc centrális területén homály/elmosódottság jelenik meg. A csontosodás előrehaladtával a teljes vonal elmosódottá válhat, de még egyértelműen azonosítható.
3. stádium – széli bevágás: közel teljes összezsontosodás, csak a tuderculum majus alatt figyelhető meg.
4. stádium – teljes egyesülés: teljes összezsontosodás, nincs radiolucens terület. A fúziós vonal esetenként még felismerhető.

Acromion

0. stádium – hiányzik: nem figyelhető meg apophysis. Az acromion felülete lekerekített, esetleg hullámos.
1. stádium – megjelent: megfigyelhető apophysis, de még határozott radiolucens vonal választja el.
4. stádium – teljes egyesülés: teljes összezsontosodás, nincs radiolucens terület.

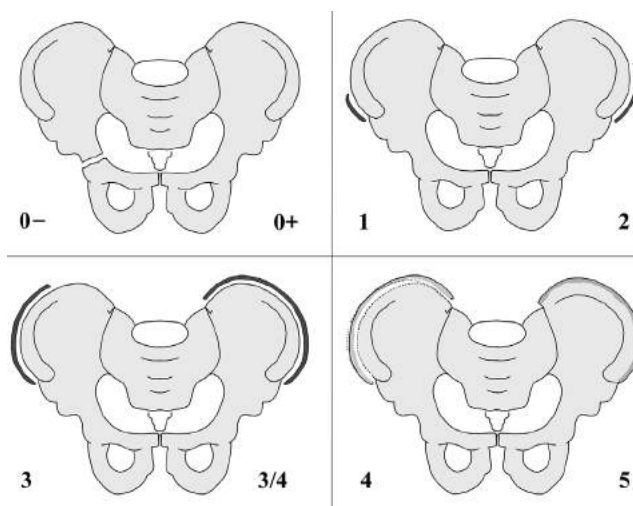
Apex

1. stádium – megjelent: megfigyelhető, az apophysis jól látható, de egyértelmű radiolucens vonal választja el

módszer alkalmazásával. A megbízhatóságot osztályon belüli korrelációs vizsgálattal elemeztük, az eredményeket a Winer-kritériumok alapján értékeltük (0–0,24: nincs vagy gyenge; 0,25–0,49: alacsony; 0,50–0,69: közepes; 0,70–0,89: jó; és 0,90–1,00: kiváló) [39]. Együttal rögzítettük a vizsgálok tapasztalatait és a mérés kivitelezhetőségét.

2) A vizsgálatok értékelhetősége

Az adott módszer milyen arányban és mennyire nehezen alkalmazható EOS-felvételeken, továbbá az esetleges problémáknak mi az oka.



1/b ábra

Risser 'plus' (Negrini et al., 2015). Az apophysis megjelenése és mérete alapján különbözteti el a stádiumokat:

0- stádium: nyitott Y-porc, apophysis nem ábrázolódik.

0+ stádium: az Y-porc elcsontosodott, apophysis nem ábrázolódik.

1. stádium: 0–25%-os fedettség.

2. stádium: 25–50%-os fedettség.

3. stádium: 50–75%-os fedettség.

3/4. stádium: 7–100%-os fedettség.

4. stádium: elkezdődött az összezsontosodás.

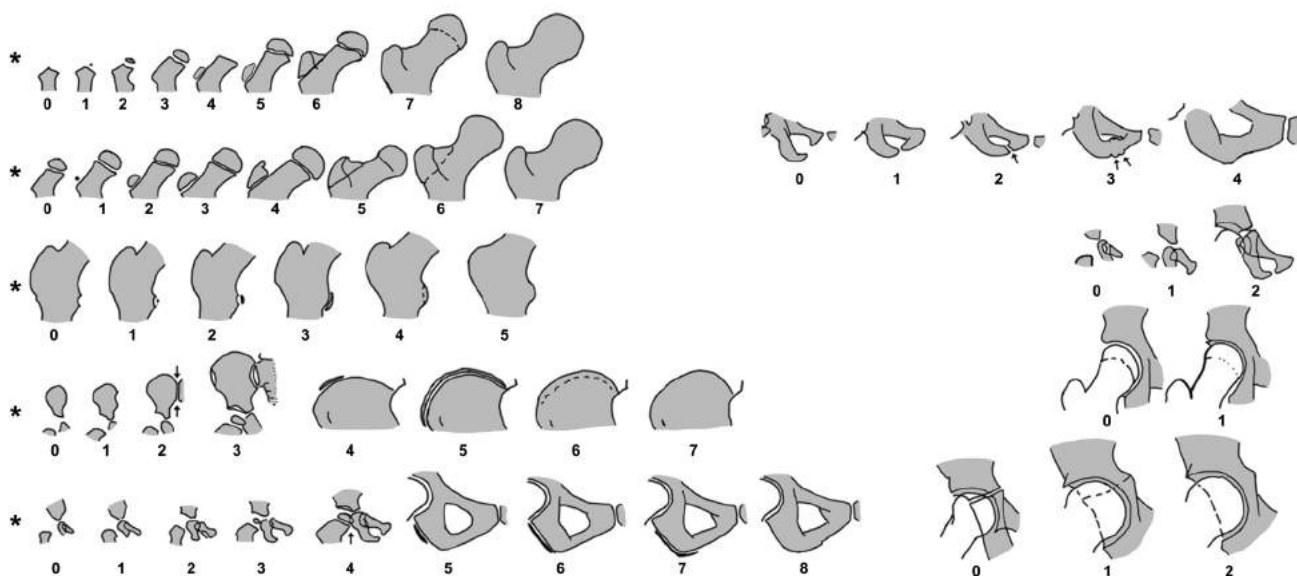
5. stádium: teljes összezsontosodás

Ehhez a vizsgálok értékelték a módszer szubjektív alkalmazhatóságát egy 4 pontos skálán: '1' – könnyű: könnyen alkalmazható; '2' – közepes: néhány kisebb nehézség, azonban a mérés határozottan kivihető; '3' – nehéz: közepes nehézségek, az értékelendő terület egy része (1/3-a vagy kevesebb) nem ábrázolódott megfelelően, a mérés nem volt teljes biztonsággal kivitelezhető; '4' – lehetetlen: az értékelendő terület nem ábrázolódott megfelelően. Azoknál a módszereknél, amelyekkel több régiót kellett értékelni, a vizsgálok külön-külön állapították meg az alkalmazhatóságot, melyet összesítettünk. Abban az esetben, ha legalább 2 régióra közepes értékelés érkezett, nehéznek minősítettük az alkalmazhatóságot, és ha legalább 2 nehéz értékelést kapott, akkor lehetetlennek.

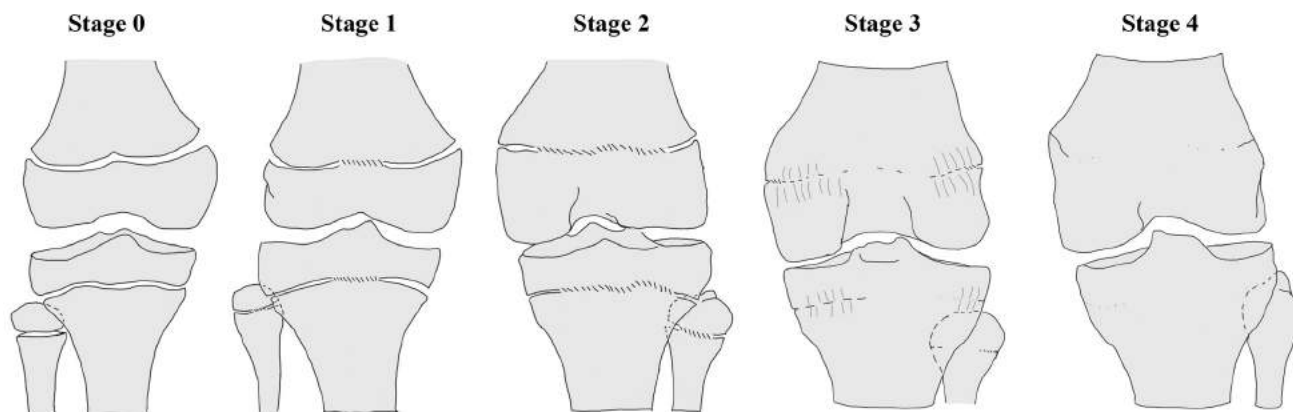
Lejegyeztük az alkalmazhatóság nehézségeinek okát, amelyeket 3 csoportra osztottunk: technikai okok (a vizsgálandó régió nem jelent meg a felvételen), felbontási problémák (például nehézséget jelentett annak megállapítása, hogy az epiphysisporc teljesen záródott-e, vagy vannak még radiolucens régiók), pozicionálási problémák (a vizsgált régió nem a megfelelő irányból ábrázolódott, vagy más csont rész belevetült).

3) A kivitelezés gyorsasága

A vizsgálat elvégzéséhez szükséges idő egyértelműen befolyásolja annak klinikai és kutatási célra történő alkalmazhatóságát.



1/c ábra | Oxford-csipő (Acheson, 1957). 9 régió értékelésével és a kapott eredmények összegzésével ad 0–45 közötti értéket. A módosított Oxford-csipő-módszer (Stasikelis et al. után) csak 5 régiót értékel (*-gal jelölve) (Az ábrát az Acheson 1957-es cikkben megjelent képek alapján készítettük)

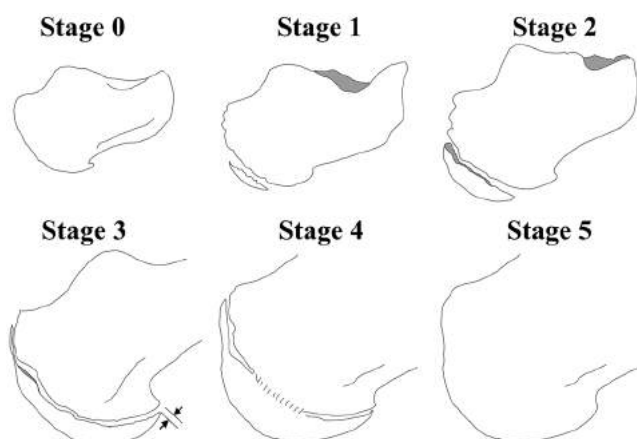


1/d ábra | Térd (O'Connor et al., 2008). Anteroposterior és oldalirányú röntgenfelvételek alapján értékeli a femur distalis, illetve a tibia és a fibula proximalis epiphysisét, majd összegzi a kapott pontszámokat.
 0. stádium – nyitott: tiszta radiolucens sáv az epi- és a metaphysis között.
 1. stádium – kezdődő egyesülés: nagyon vékony radiolucens sáv, a centrális rész elmosódott/elhomályosodott a kezdődő összecsontosodás miatt (a felületi kevesebb mint 50%-án).
 2. stádium – aktív egyesülés: 'sapkaképződés' (capping), az epiphysis túlnyúlik a metaphysisen. A csontosodási zóna meghaladja az 50%-ot, de még vannak teljesen radiolucens területek.
 3. stádium – nemrég lezajlott egyesülés: finom fúziós vonal még megfigyelhető, de az epi- és a metaphysis egyesült. A széleken még előfordulhat 2 mm-nél kisebb 'bevágás'. A trabeculavonalak nem folytonosak az epi- és a metaphysis között.
 4. stádium – teljes egyesülés: érett csont, nincsenek bevágások a széleken, folyamatosak a trabeculák. Vékony „epiphysisheg” megmaradhat az epiphysisporc vonalának megfelelően

A statisztikai analízis során Spearman-korrelációt alkalmaztunk a naptári és a csontkor összefüggésének vizsgálatára, valamint független mintás t-próbát a csoportok közti különbség megállapítására (IBM SPSS v23, IBM Corp., Armonk, NY, USA). A randomizáláshoz a Microsoft Excel v14.0.6112.5000 (Microsoft Corp., Redmond, WA, USA) VÉLETLEN.KÖZÖTT függvényét alkalmaztuk. A $p < 0,05$ -öt tekintettük szignifikánsnak.

Eredmények

A váll értékelésén alapuló módszert a pilotvizsgálat során nem találtuk az EOS-technikával kompatibilisnek, és kizártuk a vizsgálat további részéből, mivel a megfigyelők a vizsgálatok 54–72%-ában a régió értékelését ellehetetlenítő nehézségeket tapasztaltak. Az esetek 23–38%-ában három vizsgált régió közül csak egy ábrázolódott



1/e ábra

Sarokcsont (Nicholson et al., 2015). A sarokcsont oldalirányú felvétele alapján értékel.

0. stádium: nincs csontosodás az apophysis területén.

1. stádium: megjelenik csontosodás az apophysis területén, de nem haladja meg a metaphysis felületének 50%-át.

2. stádium: az apophysis területének több mint 50%-át borítja csontosodott terület, de nem ér talpi felszínét. A radiolucens terület az apophysis és a metaphysis között szélesebb a talpi és a dorsalis részen, mint a centrális területen.

2+ stádium: a távolság az apophysis talpi csúcsa és a metaphysis processus medialis/lateralis tuberis calcaneinek megfelelő szöglettérése között 2–5 mm.

3. stádium: az apophysis teljesen fedi a metaphysist (a 2+ stádiumban leírt távolság 2 mm-nél kisebb – fekete nyíl az ábrán), de határozott radiolucens terület választja el tőle. Az apophysis és a metaphysis közötti távolság egységes a teljes felszínen.

4. stádium: megjelentek az apophysis és a metaphysis összecsontosodásának jelei, de még egyértelműen elkülöníthető a két struktúra. A csontosodás a centrális régióban kezdődik, és fokozatosan halad a széli részek felé.

5. stádium: teljes összecsontosodás

megfelelően (13-ból 3–5 vizsgálatban), a processus coracoides csúcsa/szöge nem volt látható 15–38%-ban (13-ból 2–5 esetben), továbbá a megfigyelők alacsony elégedettségéről számoltak be a módszerrel kapcsolatban.

Így 5 módszer esetében végeztük el a klinikai alkalmazhatóság értékelését.

Megbízhatóság

Az intraobszerver megbízhatósági pontszámok mindegyike kiváló volt a térd vizsgálatán alapuló módszer kivételével, ahol a 2-es vizsgáló csak jó eredményt ért el (1. vizsgáló: 0,945; 2. vizsgáló: 0,841, 3. vizsgáló:

0,956). Az interobszerver megbízhatósági vizsgálat során minden módszer „kiváló” értékelést kapott, kivéve a térd- és a módosított Oxford-csípő-módszert, amelyek a „jó” kategóriába estek. Az értékek csökkenő sorrendben: nyakicsigolya- (0,976), sarokcsont- (0,945), Risser 'plus'- (0,940), Oxford-csípő- (0,902), módosított Oxford-csípő- (0,887) és térd- (0,865) módszer (lásd bővebben a 2. táblázatban). A Winer-kritériumok alapján 0,7 felett a megbízhatóság jónak mondható, ugyanakkor a vizsgálók a térdmódszer esetében alacsony elégedettségéről számoltak be, ezért úgy éreztük, a kapott megbízhatósági érték magasabb az elvártnál. Ez a magas érték adódhat ugyanakkor abból is, hogy a vizsgált populáció jelentős része a könnyen értékelhető 0. stádiumba került, mivel a térd körüli epiphysisek értékelhető változásai csak serdülőkorban kezdődnek.

A vizsgálatok értékelhetősége

A vizsgálatba bevont 114 személy esetén a legtöbb csontkorbecslési módszert a megfigyelők „egyszerűen elvégezhetőnek” minősítették a Risser 'plus'- (111/114, 97%), a térd- (110/114, 96%), a nyakicsigolya- (a vizsgálatok 98,02%-ában – a korábbi vizsgálataink alapján, részletek: [35]) és az Oxford-csípő- (102/114, 89%) módszer esetén. A sarokcsonti módszerrel 114 vizsgálatból 72 „könnyű”, 13 „közepes” minősítést kapott, ugyanakkor 29 vizsgálatot (25%) volt „nehéz” vagy „lehetetlen” értékelni. A megfigyelők értékeléseinek eredményeit a 3. táblázatban részleteztük, illetve a 4. táblázatban a vizsgálati nehézségek okait tüntettük fel.

Időfaktor

Az utolsó 30 képelemzés során mért vizsgálati idő alapján a leggyorsabban értékelhető módszernek a sarokcsont megítélése bizonyult (átlagosan 17,5 mp), míg a Risser 'plus'- (26,3 mp), a nyakicsigolya- (35,4 mp), a térd- (58,9 mp) és az Oxford-csípő- (149,0 mp) módszert lassabban elvégezhetőnek találtuk. A módosított Oxford-csípő-módszert az Oxford-csípő-értékekből számítottuk ki, így külön mérési idővel kapcsolatos adatokat nem gyűjtöttünk.

A csontkorértékelések legfontosabb eredményeit az egyének kronológiai korával összehasonlítva a 2. ábrán (a–c) mutatjuk be. A kronológiai kor és a csontkor kö-

2. táblázat | Az inter- és intraobszerver megbízhatósági vizsgálat eredményei

	Sarokcsont	Nyaki csigolya	Térd	Módosított Oxford-csípő	Oxford-csípő	Risser 'plus'
Interobszerver megbízhatóság	0,945	0,976	0,865	0,887	0,902	0,940
Intraobszerver megbízhatóság	0,953–0,999	0,949–0,959	0,841–0,956	0,975–0,993	0,949–0,993	0,982–0,969

A megbízhatóságot osztályon belüli korreláció alapján vizsgáltuk. Az osztályon belüli korrelációs koefficienseket (ICC) a Winer-kritériumok alapján értékeltük: ICC \geq 0,90 – kiváló; ICC: 0,70–0,89 – jó; ICC: 0,50–0,69 – közepes; ICC \leq 0,49.

Az intraobszerver megbízhatóságnál a három vizsgáló által elért legmagasabb és legalacsonyabb értéket adtuk meg.

3. táblázat | A vizsgálók szubjektív értékelése

	1 – könnyű	2 – közepes	3 – nehéz	4 – lehetetlen
Sarokcsont	72	13	15	14
Nyaki csigolya ¹	–	–	–	–
Térd	110	4	0	0
Módosított Oxford-csípő ²	–	–	–	–
Oxford-csípő*	102	3	9	0
Risser 'plus'	111	3	0	0

A vizsgálók értékelésének összesítése: '1' – könnyű: könnyen alkalmazható; '2' – közepes: néhány kisebb nehézség, azonban a mérés határozottan kivihető; '3' – nehéz: közepes nehézségek, az értékelendő terület egy része (1/3-a vagy kevesebb) nem ábrázolódott megfelelően, a mérés nem volt teljes biztonsággal kivitelezhető; '4' – lehetetlen: az értékelendő terület nem ábrázolódott megfelelően. Azoknál a módszereknél, amelyekkel több régiót kellett értékelni, a vizsgálók külön-külön állapították meg az alkalmazhatóságot, melyet összesítettünk. Abban az esetben, ha legalább 2 régióra közepes értékelés érkezett, nehéznek minősítettük az alkalmazhatóságot, és ha legalább 2 nehéz értékelést kapott, akkor lehetetlennek.

*17 esetben az Oxford-csípő-módszer könnyű értékelést kapott, bár a vizsgálók nehézségekről számoltak be a kistrochanter értékelésekor.

¹A nyaki csigolyára vonatkozó eredményeket korábbi vizsgálatunk tartalmazza [9].

²A módosított Oxford-csípő a hagyományos módszerből számítható, így erre vonatkozóan nem végeztünk külön értékelést.

zötti összefüggést a Spearman-korrelációval vizsgálva a következő eredményeket kaptuk: nyaki csigolya (korrelációs koefficiens [kk] = 0,829), sarokcsont (kk = 0,903), Risser 'plus' (kk = 0,882), Oxford-csípő (kk = 0,934), módosított Oxford-csípő (kk = 0,932) és térd (kk = 0,912).

A csontkor alapján felállított stádiumokat a férfi páciensek a nőkhöz képest magasabb kronológiai korban érték el (átlagosan 1,2–1,9 évvel később érték el a fiúk egy adott csontkorérettségi stádiumot, mint a lányok), azonban a különbségek többsége nem volt statisztikailag szignifikáns.

Megbeszélés

A csontérettség kronológiai kortól független első vizsgálata Londonban a Guy's Hospitalban dolgozó John Poland nevéhez fűződik az 1898-ban megjelent 'Szkiaagrafikus atlasz a kéz- és csuklócsontok fejlettségéről' kapcsán. A téma az 1930-as években kifejezetten népszerűvé vált az Egyesült Királyságban és az Amerikai Egyesült Államokban [40–42]. Miután a kronológiai kor csak az idő múlását mutatja, a kutatók régóta keresik annak lehetőségét, hogy a gyermek fejlődésének tényleges szintjét különböző vizsgálatokkal megállapítsák. Az utóbbit számtalan tényező befolyásolja, például a növekedési- és pajzsmirigyhormon-szintek, a genetikai sajátosságok, a szocioökonómiai státusz, a táplálkozás, a felzívódási zavarok, a cukorbetegség. A kronológiai kor és

4. táblázat | Nehézségek a felvételek értékelésekor.

Abszolút értékek, valamint a problémák százalékos megoszlása

(a) A nehéz vagy lehetetlen értékelések okainak megoszlása

	A 'nehéz' vagy 'lehetetlen' értékelések száma	Ok		
		Felbontás	Pozicionálás	Technikai probléma
Sarokcsont	29	–	1 (3%)	28 (97%)
Nyaki csigolya ¹	–	–	–	–
Térd	0	–	–	–
Módosított Oxford-csípő ²	–	–	–	–
Oxford-csípő	9	5 (56%)	4 (44%)	–
Risser 'plus'	0	–	–	–

(b) A közepes, nehéz vagy lehetetlen értékelések okainak megoszlása

	A 'közepes', 'nehéz' és 'lehetetlen' értékelések száma	Felbontás		
		Felbontás	Pozicionálás	Technikai probléma
Sarokcsont	42	3 (7%)	6 (14%)	33 (79%)
Nyaki csigolya ¹	–	–	–	–
Térd	4	4 (100%)	–	–
Módosított Oxford-csípő ²	3	3 (100%)	–	–
Oxford-csípő	12	5 (42%)	7 (58%)	–
Risser 'plus'	3	3 (100%)	–	–

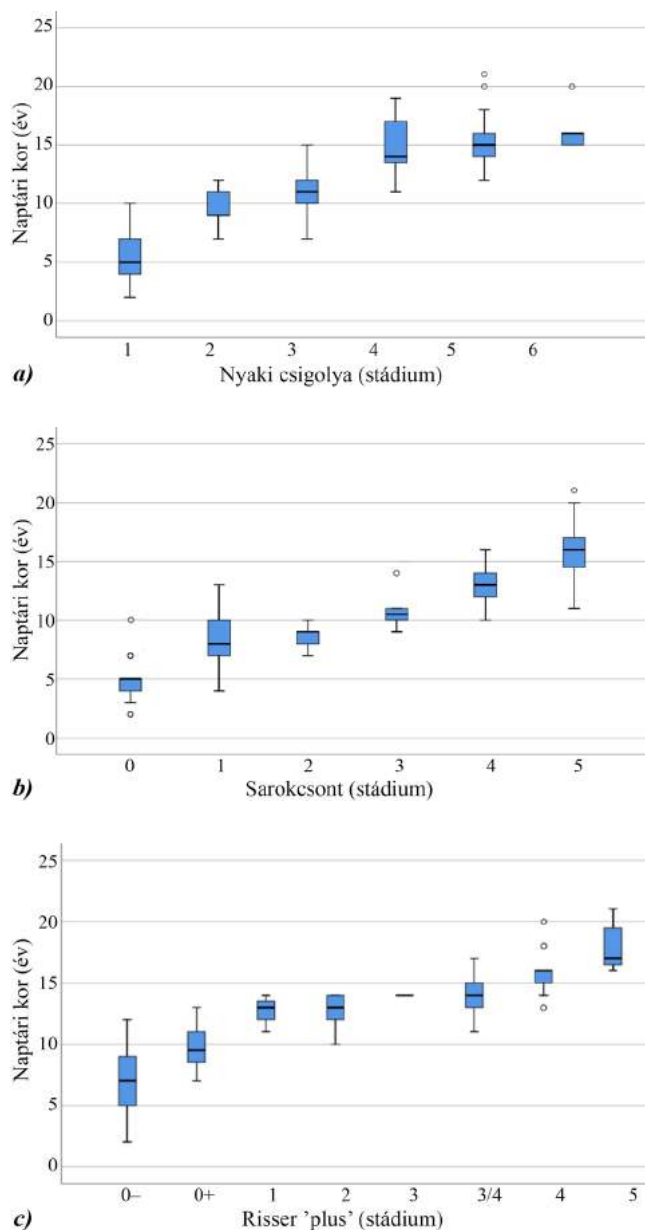
¹A nyaki csigolyára vonatkozó eredményeket korábbi vizsgálatunk tartalmazza [9].

²A módosított Oxford-csípő a hagyományos módszerből számítható, így erre vonatkozóan nem végeztünk külön értékelést.

a tényleges biológiai kor bizonyos esetekben eltérhet, ami indokolja a kronológiai kornál „természetesebb” prediktor keresését.

Vizsgálatunk célja volt azon módszerek kiválasztása és értékelése, melyek a „kéz-csukló módszeren” kívül alkalmasak lehetnek EOS 2D/3D felvételeken a csontkor megállapítására.

Az irodalom áttekintését követően 10 korábban részletesen leírt és igazolt, de ritkábban használt csontkor meghatározó módszert találtunk. Ezek közül sokat a „csukló-kéz” módszernél is nagyobb problémát jelentő technikai gondok jellemeznek, mint a pozicionálási pontatlanságok vagy más csontok képbe vetülése (első borda, kulcscsont, könyök). Egy pilotvizsgálat után a kulcscsonton, az első bordán, a könyökön és a combcsontdiaphysisen alapuló méréseket kivitelezhetetlennek találtuk, valamint a vállmódszer is túl nehezen alkalmazhatóan bizonyult, mivel az esetek 54–72%-ában komoly probléma



2. ábra A vizsgált módszerekkel mért csontkorstádiumok naptári kor szerinti megoszlása dobozábrákkal ábrázolva (Csak a legrelevánsabb módszerek eredményeit mutatjuk)

- (a) Hassel-Farman szerinti nyakicsigolya-módszer
 (b) Nicholson szerinti sarokcsontmódszer
 (c) Risser 'plus'-módszer (Negrini et al. után)

mát jelentett a vizsgált régiók megfelelő értékelése. Vizsgálatunkba végeredményben 5 módszer került be.

A „nyakicsigolya-módszer” az esetek nagyon nagy százalékában alkalmazhatónak bizonyult, a röntgenképek 98%-a volt értékelhető. Mindössze 6 stádiumot tartalmaz, így megtanulása is egyszerű, megbízhatósága magas, gyorsan alkalmazható, és stádiumai széles életkort fednek le 7-től 21 éves korig.

A csípő körül két módszert találtunk könnyen alkalmazhatónak: a vizsgálat céljától függően a Risser 'plus'- és az Oxford-módszer segítségével értékelhető a régió.

A Risser 'plus'-módszer minden röntgenen alkalmazható, gyorsan elvégezhető, megbízhatósága magas, és a Risser-stádiumok a legtöbb klinikus számára ismertek. Ráadásul az Y-porc fúziója alapján a fiatalabb korosztály is jobban kategorizálható, mint a klasszikus Risser-beosztással [43].

Az Oxford-féle csípőmódszer a maga 45 pontos skálájával a jelen vizsgálat során használt teljes életkori spektrum lefedését szolgálja, továbbá meghatározása kevés nehézséggel jár, melyek túlnyomórészt a kistemporról kapcsolatosak. Amíg az Oxford- és a módosított Oxford-módszer esetén összességében csak a képek 8%-a, illetve 3%-a esett a „nehéz” kategóriába, addig 17 esetben (15%) mutatkoztak problémák a kistemporról megítélés során. Ezek a kistemporról kapcsolatos nehézségek, melyek már más szerzők által is említésre kerültek korábban [30, 44], valószínűleg szerepet játszanak az alacsonyabb megbízhatósági értékek megjelenésében a módosított Oxford-módszernél, tekintve, hogy az 5 meghatározott anatómiai pont közül ez alkotja az egyiket. Megoldásként a kistemporról meghatározásának elhagyása [44] vagy az Acheson-féle életkortáblázat segítségével a csípő egységként történő értékelése merült fel [23]. Az ülőcsont megítélése is nehézséget jelenthet, hiszen a negyedik és a lezáró (8.) stádium röntgenmegjelenése megegyezhet. Az Acheson-féle életkortáblázatra alapozva, melyet vizsgálatunk tapasztalatai is alátámasztanak, 16 éves kor előtt nem jelenik meg a 8., lezáró stádium, így addig az apophysis hiánya a 4. stádiumra utal. A módszer másik hátránya, hogy ez a legidőigényesebb az alkalmazottak közül, mindazonáltal kutatási célra ez javasolt a leginkább, hiszen a teljes vizsgált életkort lefedi, több régiót értékel, és sok stádiumot különít el.

A Nicholson és mtsai által leírt sarokcsonti módszerrel kapcsolatosan vegyes tapasztalataink voltak [30]. A sarokcsont egyszerűen megítélhető, és a módszer gyorsan tanulható, illetve memorizálható, továbbá nagyon magas, vizsgálón belüli és vizsgálók közötti megbízhatósági értékekkel bír. Másrészt a képről lemaradó vagy egymásba vetülő anatómiai pontok miatt a 114 képpárból 15 esetben (13%) nehéznek, 14 esetben (12%) pedig lehetetlennek bizonyult a sarok értékelése, így alkalmazásának feltétele a pozicionálásra fordított kiemelt figyelem.

A térd megítélése majdnem mindenképpen lehetséges volt (114-ből 113 esetben), mégis számos probléma merült fel ezzel a módszerrel kapcsolatban. A beosztás első stádiuma viszonylag magas életkorban jelenik meg ($10,2 \pm 1,4$ év – addig 0. stádiumot nevezünk meg), tehát a módszer fiatal életkorban nem alkalmazható. A vizsgálók szubjektíve gyengébbnek ítélték a megbízhatóságát, és több kivitelezési nehézségről számoltak be. Sok időt igényelt az 1–3-as stádiumok meghatározása, mivel a relatív keskeny epiphysealis lemezek közti fúzió mértékének értékelése csak tökéletes anteroposterior és oldalirányú felvételeken kivitelezhető teljes biztonsággal. Összességében az átlagos mérési idő nem bizonyult magasnak,

mert a képalkotások több mint fele a gyorsan meghatározható 0. stádiumba esett. Amennyiben külön értékeljük az 1-es vagy az e feletti stádium értékeléséhez szükséges időt, átlagosan 78,3 másodpercet kapunk (a 0. stádium megítélése átlagosan 27,9 másodpercet vett igénybe). Amíg *O'Connor és mtsai* szerint [28] a módszer könnyen tanulható, mi mégsem tapasztaltuk olyan logikusnak és átláthatónak, mint az alkalmazott többi metódust. Összességében tehát nem tudjuk kijelenteni, hogy EOS-képalkotás mellett a térdmódszer lenne a leginkább alkalmazható eljárás.

Vizsgálatunk korlátját jelenti, hogy a relatív alacsony elemszám (114 eset) oszlik 18 korcsoportra, így kevés az egy-egy életkori csoportba kerülők száma, azonban törekedtünk arra, hogy az egyes életkorokból azonos számú esetet vonjunk be, így bízunk az eredmények reprezentativitásában. Annak megítélése, hogy egyes módszerek „jobbak” vagy „kézenfekvőbbek”, mint mások, erős szubjektív faktort is tartalmaz a vizsgálók részéről, így az ilyenfajta beosztások eredményeinek értékelésekor figyelembe kell venni a humán faktort. Az általunk alkalmazott rendszer előnyben részesítette azokat a módszereket, amelyek több anatómiai pontot értékelték, mert itt nehezebb volt „lehetetlen” kategóriába sorolódni, és könnyebb volt jobb megbízhatósági eredményt elérni. A közlemény során törekedtünk arra, hogy bemutassuk az általunk szerzett tapasztalatokat és felfedezett nehézségeket, hogy minél több, a napi gyakorlatban alkalmazható információt osszunk meg az olvasókkal.

Következtetések, javaslatok

10 csontkormérési módszer klinikai alkalmazhatóságát vizsgáltuk meg EOS-felvételeken, melyek közül 5 bizonyult kivitelezhetőnek: a nyaki csigolya, a csípőlapát, a csípő, a térd és a sarkcsont értékelésén alapuló módszerek. A módszerek megbízhatósága kiválóan bizonyult, a térdalapú módszer kivételével, mely jó eredményt ért el. A módszerek az esetek több, mint 89%-ában könnyen kivitelezhetőnek bizonyultak a sarokcsontalapú módszer kivételével, amelynek csak 63%-ban volt könnyen megítélhető a régió. A méréshez szükség idő 17,5 és 149,0 mp között mozgott, elsősorban az értékelt régiók számától függően.

Reméljük, hogy a jelen közlemény rámutat az alternatív módszerek alkalmazhatóságára a csontérettség meghatározásában, miszerint „van élet a kézen és csuklón túl”. Következtetésként javasolnánk, hogy amikor eldöntjük, milyen módszer alapján értékeljük a csontkort, több faktort is figyelembe kell venni: a vizsgált területet (alsó vagy felső végtag, ábrázolódik-e a kéz vagy a medence – hogy elkerüljük a felesleges sugárterhelést); a páciens életkorát (az Oxford-csípő-, a nyakigerinc- vagy a sarokcsonti módszer jobb a fiatalabb életkorban, ellenkéntben a térd- vagy a Risser-módszerrel, melyek csak a pubertás környékén alkalmazhatók), valamint a feldolgozásának „körülményeit” (tudományos vizsgálat esetén

érdemes több időt szánni az Oxford-módszer használatára, míg a klinikai gyakorlatban egy gyorsabban elvégezhető mérés praktikusabb lehet). A Hassel–Farman szerinti, nyakicsigolya-alapú módszer tűnik az arany középútnak, hiszen könnyen tanulható és alkalmazható, gyors, és közel az összes felvételen kivitelezhető volt.

Anyagi támogatás: A kutatás létrejöttét a GINOP-2.3.3-15-2016-00031. számú projekt támogatta.

Szerzői munkamegosztás: Minden szerző nagymértékben hozzájárult a tanulmányban bemutatott munkához. O'S. I.: A csontkor-meghatározásra alkalmas módszerek tanulmányozása, csontkor- és 3D EOS-rekonstrukciós elemzések, valamint statisztikai elemzések végzése, ábrák készítése, a kézirat összeállítása. S. Á. T.: A betegadatbázis összegyűjtése, csontkor- és 3D EOS-rekonstrukciós elemzések elvégzése, a végső kézirat áttekintése. V. P.: Csontkor- és 3D EOS-rekonstrukciós elemzések végzése, a kézirat áttekintése. K. K.: A statisztikai elemzések elvégzése és a kézirat lefordítása. V. Cs., T. P.: A tanulmány megtervezése, a csontkor és az alsó végtagi paraméterek vizsgálatának felügyelete, a betegekkel kapcsolatos adminisztratív teendők elvégzése és az intézményi követelményeknek való megfelelés biztosítása. A cikk végső változatát valamennyi szerző elolvasta és jóváhagyta.

Érdekltségek: A szerzőknek nincsenek érdekltségeik.

Irodalom

- [1] Frank D, Rill L, Kolarovszki B, et al. Classical and modern methods for the assessment of skeletal maturation and pubertal growth spurt. [Klasszikus és modern vizsgálómódszerek a csontérettségi kor és a pubertáskori növekedési csúcs meghatározására.] *Orv Hetil.* 2018; 159: 1423–1432. [Hungarian]
- [2] Greulich WW, Pyle SI. Radiographic atlas of skeletal development of the hand and wrist. Vol. 2. Stanford University Press, Stanford, CA, 1959.
- [3] Björk A, Helm S. Prediction of the age of maximum pubertal growth in body height. *Angle Orthod.* 1967; 37: 134–143.
- [4] Fishman LS. Radiographic evaluation of skeletal maturation. A clinically oriented method based on hand-wrist films. *Angle Orthod.* 1982; 52: 88–112.
- [5] Grave KC, Brown T. Skeletal ossification and the adolescent growth spurt. *Am J Orthod.* 1976; 69: 611–619.
- [6] Acheson RM. A method of assessing skeletal maturity from radiographs; a report from the Oxford Child Health Survey. *J Anat.* 1954; 88: 498–508.
- [7] Sanders JO, Khoury JG, Kishan S, et al. Predicting scoliosis progression from skeletal maturity: a simplified classification during adolescence. *J Bone Joint Surg Am.* 2008; 90: 540–553.
- [8] Singer J. Physiologic timing of orthodontic treatment. *Angle Orthod.* 1980; 50: 322–333.
- [9] Tanner JM, Whitehouse RH. Clinical longitudinal standards for height, weight, height velocity, weight velocity, and stages of puberty. *Arch Dis Child.* 1976; 51: 170–179.
- [10] Hassel B, Farman AG. Skeletal maturation evaluation using cervical vertebrae. *Am J Orthod Dentofacial Orthop.* 1995; 107: 58–66.

- [11] Lamparski DG. Skeletal age assessment utilizing cervical vertebrae. *Am J Orthod*. 1975; 67: 458–459.
- [12] Mito T, Sato K, Mitani H. Cervical vertebral bone age in girls. *Am J Orthod Dentofacial Orthop*. 2002; 122: 380–385.
- [13] San Román P, Palma JC, Oteo MD, et al. Skeletal maturation determined by cervical vertebrae development. *Eur J Orthod*. 2002; 24: 303–311.
- [14] Walker RA, Lovejoy CO. Radiographic changes in the clavicle and proximal femur and their use in the determination of skeletal age at death. *Am J Phys Anthropol*. 1985; 68: 67–78.
- [15] Sauvegrain J, Nahum H, Bronstein H. Study of bone maturation of the elbow. *Ann Radiol*. 1962; 5: 542–550.
- [16] Charles YP, Diméglio A, Canavese F, et al. Skeletal age assessment from the olecranon for idiopathic scoliosis at Risser grade 0. *J Bone Joint Surg Am*. 2007; 89: 2737–2744.
- [17] Schaefer M, Aben G, Vogelsberg C. A demonstration of appearance and union times of three shoulder ossification centers in adolescent and post-adolescent children. *J Forensic Radiol Imaging* 2015; 3: 49–56.
- [18] Schmelting A, Reisinger W, Loreck D, et al. Effects of ethnicity on skeletal maturation: consequences for forensic age estimations. *Int J Legal Med*. 2000; 113: 253–258.
- [19] Michelson N. The calcification of the first costal cartilage among whites and negroes. *Human Biol*. 1934; 6: 543–557.
- [20] Risser JC. The iliac apophysis: an invaluable sign in the management of scoliosis. *Clin Orthop*. 1958; 11: 111–119.
- [21] Negrini S, Hresko TM, O'Brien JP, et al. Recommendations for research studies on treatment of idiopathic scoliosis: consensus 2014 between SOSORT and SRS non-operative management committee. *Scoliosis* 2015; 10: 8.
- [22] McKern TW, Stewart TD. Skeletal age changes in young American males analysed from the standpoint of age identification. Quartermaster Research and Engineering Command, Natick, MA, 1957.
- [23] Acheson RM. The Oxford method of assessing skeletal maturity. *Clin Orthop*. 1957; 10: 19–39.
- [24] Stasikelis PJ, Sullivan CM, Phillips WA, et al. Slipped capital femoral epiphysis: prediction of contralateral involvement. *J Bone Joint Surg Am*. 1996; 78: 1149–1155.
- [25] Stull KE, L'Abbé EN, Ousley SD. Using multivariate adaptive regression splines to estimate subadult age from diaphyseal dimensions. *Am J Phys Anthropol*. 2014; 154: 376–386.
- [26] Tsai A, Stamoulis C, Bixby SD, et al. Infant bone age estimation based on fibular shaft length: model development and clinical validation. *Pediatr Radiol*. 2016; 46: 342–356.
- [27] Pyle SI, Hoerr NL. A radiologic standard of references for the growing knee. Charles C. Thomas Publisher, Springfield, IL, 1969.
- [28] O'Connor JE, Bogue C, Spence LD, et al. A method to establish the relationship between chronological age and stage of union from radiographic assessment of epiphyseal fusion at the knee: an Irish population study. *J Anat*. 2008; 212: 198–209.
- [29] Hoerr NL, Pyle SI, Francis CC. Radiological atlas of the foot and ankle. Charles C. Thomas Publisher, Springfield, IL, 1962.
- [30] Nicholson AD, Liu RW, Sanders JO et al. Relationship of calcaneal and iliac apophyseal ossification to peak height velocity timing in children. *J Bone Joint Surg Am*. 2015; 97: 147–154.
- [31] Breen MA, Tsai A, Stamm A, et al. Bone age assessment practices in infants and older children among Society for Pediatric Radiology members. *Pediatr Radiol*. 2016; 46: 1269–1274.
- [32] Dimeglio A. Growth in pediatric orthopaedics. *J Pediatr Orthop*. 2001; 21: 549–555.
- [33] Tanner JM, Whitehouse RH, Cameron N, et al. Assessment of skeletal maturity and prediction of adult height (TW2 method). Academic Press, London, 1975.
- [34] Schlégl ÁT, Szuper K, Somoskeöy S, et al. Three dimensional radiological imaging of normal lower-limb alignment in children. *Int Orthop*. 2015; 39: 2073–2080.
- [35] Schlégl ÁT, O'Sullivan I, Varga P, et al. Determination and correlation of lower limb anatomical parameters and bone age during skeletal growth (based on 1005 cases). *J Orthop Res*. 2017; 35: 1431–1441.
- [36] Szuper K, Schlégl ÁT, Leidecker E, et al. Three-dimensional quantitative analysis of the proximal femur and the pelvis in children and adolescents using an upright biplanar slot-scanning X-ray system. *Paediatr Radiol*. 2015; 45: 411–421.
- [37] Burkus M, Márkus I, Niklai B, et al. Assessment of sacroiliac joint mobility in patients with low back pain. [A keresztsonti ízület mobilitásának vizsgálata derékpanaszos betegcsoportban.] *Orv Hetil*. 2017; 158: 2079–2085. [Hungarian]
- [38] Garamendi PM, Landa MI, Botella MC, et al. Forensic age estimation on digital X-ray images: medial epiphyses of the clavicle and first rib ossification in relation to chronological age. *J Forensic Sci*. 2011; 56(Suppl 1): S3–S12.
- [39] Winer BJ. Statistical principles in experimental design. McGraw-Hill Book Company, New York, NY, 1962.
- [40] Todd TW. Atlas of skeletal maturation. CV Mosby Company, St. Louis, MO, 1937.
- [41] Stuart HC. Studies from the Center for Research in Child Health and Development, School of Public Health, Harvard University: I. The center, the group under observation, sources of information, and studies in progress. *Monogr Soc Res Child Dev*. 1939; 4: i-261.
- [42] Bull RK, Edwards PD, Kemp PM, et al. Bone age assessment: a large scale comparison of the Greulich and Pyle, and Tanner and Whitehouse (TW2) methods. *Arch Dis Child*. 1999; 81: 172–173.
- [43] Little DG, Sussman MD. The Risser sign: a critical analysis. *J Pediatr Orthop*. 1994; 14: 569–575.
- [44] Sanders JO. Maturity indicators in spinal deformity. *J Bone Joint Surg Am*. 2007; 89 (Suppl 1): 14–20.

(O'Sullivan Ian dr.,
Pécs, Akác u. 1., 7632
e-mail: iosullivan@gmail.com)

Determination and Correlation of Lower Limb Anatomical Parameters and Bone Age During Skeletal Growth (Based on 1005 Cases)

Ádám Tibor Schlégl, Ian O'Sullivan, Péter Varga, Péter Than, Csaba Vermes

Department of Orthopaedics, Medical School, University of Pécs, Akác str. 1. PC: 7632, Pécs, Hungary

Received 23 February 2016; accepted 5 August 2016

Published online in Wiley Online Library (wileyonlinelibrary.com). DOI 10.1002/jor.23390

ABSTRACT: The aim of this study was to evaluate bone age and its correlation with the lower limbs' developing skeletal anatomy during growth. 1005 children and young adults were evaluated for bone age and 14 different parameters measured on lower-limb reconstructions from radiological examinations carried out with an EOS 2D/3D system in the course of routine orthopedic indicated diagnostic practice. Cervical vertebral morphology evaluation for bone age using the Hassel–Farman method, which describes six stages of maturity, was selected. Intra- and inter-observer reliability tests for this method, and for the EOS 3D reconstructions were performed. Statistical analysis were performed using Spearman correlation, multiple linear regression, and *t*-test. The intra- and inter-observer reliability of the Hassel–Farman method and the EOS 3D lower-limb reconstruction were found to be excellent. Interestingly one bone age stage could include individuals across a 12.1 year range, and conversely individuals of the same calendar age could be of one of 3.2 different bone age stages. In the prepubertal age groups all six bone stages could be observed. Bone age revealed a stronger relationship, lower standard deviations with groups and proved to be a better discriminating variable than the calendar age by collodiaphyseal angle, femoral, and tibial torsion, femorotibial rotation, and mechanical tibiofemoral angle. Bone age is an indicator of skeletal maturity and may more accurately describe the growth of some lower limb parameters. As a result we suggest the consideration of bone age when evaluating lower-limb biomechanical-anatomical parameters. © 2016 Orthopaedic Research Society. Published by Wiley Periodicals, Inc. J Orthop Res

Keywords: bone age; Hassel–Farman method; lower limb; biomechanical parameters; EOS 2D/3D

The period from infancy through childhood and into early adolescence is a time of unprecedented growth. During this time height increases almost 3.5 times, weight grows almost 20 fold and the ratio between our body parts changes significantly.¹ Our bony skeleton undergoes and adapts to these changes with alterations in its' longitudinal and volumetric parameters.

The changes taking place during this growth and the transition to upright locomotion have been well-described, however, the lower limb anatomic and biomechanical parameters have not been extensively assessed in relation to the actual level of skeletal maturity, typically referred to as the bone age. Studies examining bone age have mostly focused on limb length discrepancy and the timing of surgical interventions in scoliosis, though recently it's role in Blount's disease was highlighted.^{2–6}

The bone age is typically estimated by assessing the growth cartilages of one or more regions and comparing their morphology to reference standards based on large population studies.⁷ Skeletal maturation, and hence bone age, is influenced by numerous factors including genetically determined growth rate, gender, and race and also severe illnesses, stress and nutritional, and socioeconomic status. As a result it is more unique to each individual and does not necessarily correspond with the calendar age. Many authors now

advise that the evaluation of just calendar age alone in disorders strongly influenced by skeletal maturity may not be appropriate.⁸

The most frequently applied methods are based on growth cartilage evaluation using radiographs of the skeletal anatomy of the hand and wrist, although methods specific to other regions have been described including the hip, elbow, clavicle, knee, feet, and the cervical vertebrae.⁹

Since 2007, our clinic has used the EOS 2D/3D imaging system, which can capture low distortion whole-body stereo X-ray scans of standing patients at an ultra-low radiation dose. Using such stereo images, 3D models can be generated of the spine, hip, and lower limbs.^{10–13} The reliability of this reconstruction method has been well studied, though limited reports describe its use with children.^{14–19}

We had several aims in this study. Firstly to find and examine the reliability of a method for quick, reliable assessment of bone age for our database of stored EOS 2D/3D images. Secondly to examine the correlation between this bone age and calendar age in a large pediatric population. Finally we planned to assess the relationship between the anatomical-biomechanical parameters of the lower limb in the growing child, and the bone age, calendar age, and total height of the child.

METHODS

In this Level 3 retrospective cohort study our database of 7108 full body standing stereo-radiographs was reviewed. The examinations were performed with the EOS 2D/3D system between 2007 and 2012 as part of routine diagnostic practice, with orthopedic indications. Image-pairs were captured, from two directions, in the “step forward” standing position (left foot 10 cm forward with arms held in front, with arms and

Level of Evidence: Retrospective cohort study—Level III.

Conflict of interest: None.

Grant sponsor: Fund for Clinical Research, Government of Hungary; Grant number: TÁMOP 4.1.1.C.

Correspondence to: Ádám Tibor Schlégl (T: +36-30-72-11-895; F: +36-72-536-210; E-mail: adam.schlegl@aok.pte.hu; dr.schlegl@gmail.com)

© 2016 Orthopaedic Research Society. Published by Wiley Periodicals, Inc.

Table 1. The Definitions of the Hassel–Farman Bone Age Stages, Based on Hassel, and Farman Publication²⁰

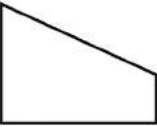





No.	Name of the Stage	Draft of the C3 Vertebra's Shape	Description of the Stage
1	Initiation		The inferior borders of C2, C3, and C4 are all flat, and upper borders taper from posterior to anterior, giving a the body a wedge shape.
2	Acceleration		C2 and C3 develop concavities in their inferior borders, while that of C4 remains flat, and bodies of C3 and C4 are almost rectangular in shape.
3	Transition		Concavities in C2 and C3 are now deeper and distinct, with C4 beginning to develop a concave inferior border too, bodies of C3 and C4 are rectangular in shape.
4	Deceleration		C2, C3, and C4 all have distinct concavities in their inferior borders, and the bodies of C3 and C4 are becoming more square in shape.
5	Maturation		Concavities of C2, C3, and C4 are more accentuated in the inferior borders, and C3, C4 bodies are almost square or square in shape.
6	Completion		Deep concavities are found in the inferior borders of C2, C3, and C4 and the bodies were square or were column like, with a vertical dimension greater than their horizontal dimension.

Table 2. The Examined Population in Age- and Gender Specific Groups, Together With the Diagnosis of the Patient

Calendar Age (Year)	Gender	<i>n</i>	Idiopathic Scoliosis (Cobb Angle <10°)	Mild Functional Kyphosis	Joint Pain With Un. Orig.	Other
2	Male	4	3	0	0	1
	Female	3	3	0	0	0
3	Male	2	2	0	0	0
	Female	3	3	0	0	0
4	Male	7	4	0	0	3
	Female	13	12	0	1	0
5	Male	14	10	0	1	3
	Female	18	16	0	1	1
6	Male	13	10	0	1	2
	Female	14	13	0	0	1
7	Male	15	10	0	1	4
	Female	18	13	0	0	5
8	Male	16	10	0	1	5
	Female	20	15	0	2	3
9	Male	18	6	1	5	6
	Female	17	11	0	3	3
10	Male	21	12	0	7	2
	Female	20	16	0	2	2
11	Male	21	11	2	6	2
	Female	23	12	1	9	1
12	Male	21	12	2	5	2
	Female	40	32	1	4	3
13	Male	24	11	1	10	2
	Female	39	30	3	5	1
14	Male	25	10	1	12	2
	Female	40	32	2	4	2
15	Male	22	12	1	6	3
	Female	51	29	3	13	6
16	Male	26	19	0	5	2
	Female	37	21	2	13	1
17	Male	25	3	1	19	2
	Female	25	3	1	20	1
18	Male	25	5	1	19	0
	Female	25	5	0	14	6
19	Male	25	4	2	17	2
	Female	25	6	1	17	1
20	Male	25	4	0	20	1
	Female	25	7	1	16	1
21	Male	25	2	2	19	2
	Female	25	3	0	20	2
22	Male	25	1	0	23	1
	Female	25	1	1	21	2
23	Male	25	2	0	21	2
	Female	25	1	0	23	1
24	Male	25	2	0	21	2
	Female	25	1	0	21	3
SUM	Male	449	165	14	219	51
	Female	556	285	16	209	46

“Other disorders” consisted of mild degenerative signs, bone cysts of various types, juvenile aseptic bone changes, like osteochondritis. Un. orig., unknown origin.

Although many subjects were included in the study that possess some milder orthopaedic disorders, to ensure the validity of data from such patients a study was conducted to assess the presence of any possible difference between the lower limb anatomy of disorder-less subjects (those who received a “diagnosis” of “joint pain of unknown origin”) and

those with such disorders. This was carried out on all bone age groups, and in all calendar age groups with a minimum of five subjects with and without diagnosed orthopaedic disorders (ages 9–24).

At the initial time of the radiological examinations, written informed consent was obtained from all individuals,

or their parent/guardian, including permission to use images for later research purposes.

3D reconstructions were made using the EOS software, and from these the following 14 parameters were measured (Fig. 1):

- Femur mechanical axis length (“femur length,” Fig. 1a);
- Tibia mechanical axis length (“tibia length,” Fig. 1a);
- Lower limb’s mechanical axis length (“limb length,” Fig. 1a);
- Femoral head diameter (Fig. 1d);
- Femoral neck length (Fig. 1e);
- Collodiaphyseal angle (“CD angle,” Fig. 1f);
- Femoral offset (Fig. 1g);
- Mechanical tibiofemoral angle (Fig. 1b);
- Femoral mechanical axis-femoral shaft angle (Fig. 1c);
- Femoral mechanical angle (Fig. 1k);
- Tibial mechanical angle (Fig. 1k);
- Femoral torsion (Fig. 1h);
- Tibial torsion (Fig. 1j);
- Femorotibial rotation (Fig. 1i).

Under the age of four the large ossification centers prevent full 3D reconstructions, so the simplified “lower limb alignment” mode of the software was applied, which only assesses six parameters:

- Femur length;
- Tibia length;

- Limb length;
- Femoral head diameter;
- Mechanical tibiofemoral angle;
- Femoral mechanical axis-femoral shaft angle.

Intraclass correlation (ICC) was used to assess the intra- and inter-observer reliability. A Spearman correlation was performed to examine the correlation between the lower limb biomechanical parameters and the bone age, calendar age, and height. The significance of any differences between groups was evaluated using independent-sample *t*-test. Multiple linear regression analysis models were created and multicollinearity examined with the Variance Inflation Factor (VIF) test. When $VIF < 1$ multicollinearity was said to be excluded, in $1 < VIF < 2$ mild multicollinearity was believed to be present, over two the multicollinearity was deemed incongruent and the model rejected. For randomized selection the RAND.BETWEEN formula of the Microsoft Excel v14.0.6112.5000 (Microsoft Corp., Redmond, WA) software was used. *p*-Value < 0.05 was accepted as significant.

RESULTS

Intraobserver reliability of the EOS system was > 0.9 , regarded as “excellent” by Winer’s criteria. The inter-observer reliability studies also achieved excellent results, except in the femoral torsion, tibial torsion, and femorotibial rotation, which achieved “good”

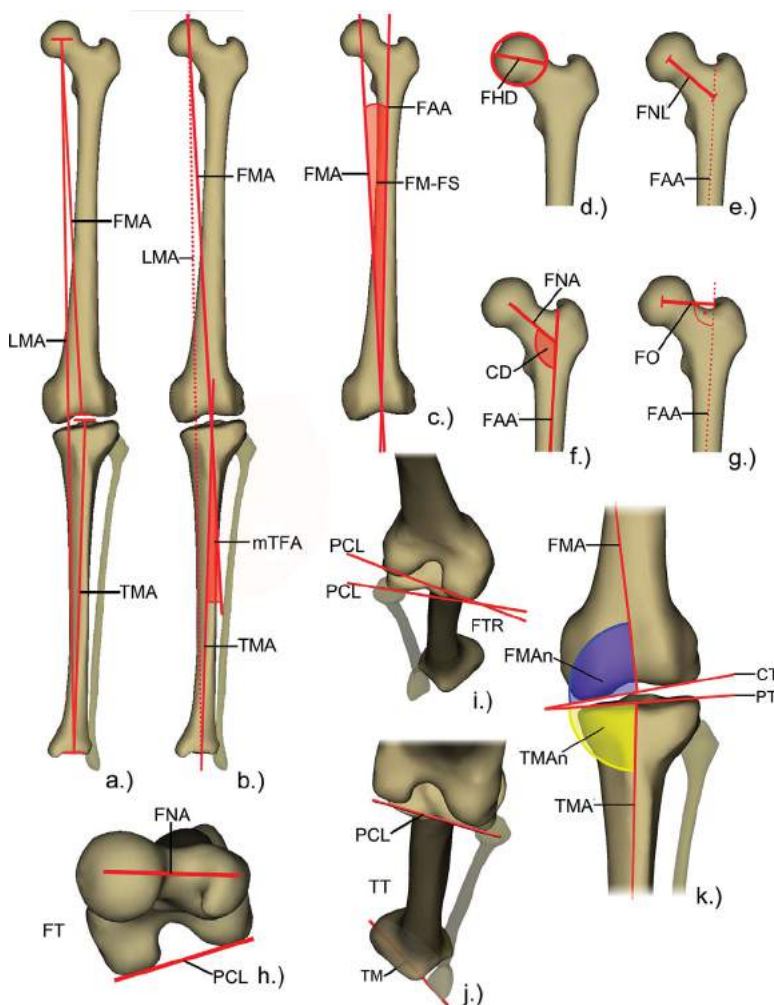


Figure 1. The measured parameters (based on our previously published figure)¹³. CD, Collodiaphyseal angle; FAA, Femur anatomical axis; FHD, Femoral head diameter; FMA, Femur mechanical axis; FMA_n, Femoral mechanical angle; FM-FS, Femoral mechanical axis-femoral shaft angle; FNA, Femoral neck axis; FNL, Femur neck length; FO, Femoral offset; FT, Femur torsion; FTR, Femorotibial rotation; LMA, Lower limb’s mechanical axis; mTFA, Mechanical tibiofemoral angle; PCL, posterior condylar line; TM, Transmalleolar line; TMA, Tibia mechanical axis; TT, Tibial torsion.

results. The Hassel–Farman method’s intra- and inter-observer reliability studies were also deemed “excellent” (Table 3).

Bone age estimation was successful in 1005 image pairs. Compared to calendar age: bone age stage 1 was found in individuals between 2 and 12 years old; stage 2 was first seen in 5-year olds, was seen predominantly in 9-year olds (48.6% of 9-year olds), and was last found in 13-year olds; stage 3 was first observed in 6-year olds, predominantly seen in 11–13-year olds (31.1–31.4%) and last seen in 16-year olds. Stage 4 started in 9-year olds, occurred most in 16-year olds (31.7% of 16-year olds), and was last seen in 23-year olds; stage 5 occurred in 11-year olds, and was the predominant stage in 14–16-year olds though it could be found in the entire examined population; stage 6 appeared in 12-year olds, and was the most frequently occurring of 17-year olds (Table 4 and Fig. 2).

On average, one bone age stage could be present in different individuals up to 12.1 years apart, and individuals in the same calendar year could have one of 3.2 bone age stages. Around 11–13, the typical time of puberty, greater differences were seen, and individuals were found in each of the six bone age stages.

No significant difference in lower limb parameters was found between those with and those without mild

orthopaedic disorders, when based on bone age group or calendar age (9–24 years old) ($p > 0.005$).

Spearman correlation tests to evaluate any correlations between the lower limb parameters and bone age, calendar age, and height showed bone age and calendar age to have strong relationships with all measured parameters, and showed similar correlation coefficients. However, the height showed either a weaker correlation with some parameters (especially the CD angle, femur mechanical angle, and FM-FS) or did not show any correlation, seen in the biomechanical parameters (mTFA, tibial mechanical angle, femoral torsion, tibial torsion, femorotibial torsion). It must be noted of course that bone age, calendar age, and height influence each other and are not truly “independent” variables (Table 5).

Next, the effect of the bone age, calendar age, and height as discriminating variables on the lower limb parameters was examined with linear regression analysis and multi-variable VIF test. The bone age was found to be a more effective discriminating variable for most biomechanical parameters, namely the CD angle, femoral, and tibial torsion and femorotibial rotation, whereas for the mTFA the calendar age performed better. With regards to femoral and tibial mechanical angles, and FM-FS, only the calendar age was found to be effective, though the difference with bone age

Table 3. Intra- and Inter-observer Reliability Tests for the Eos Reconstructions and Hassel–Farman Bone Age Estimation Method

Parameter	Intraobserver			Evaluation	Interobserver	
	ICC (Obs 1)	ICC (Obs 2)	ICC (Obs 3)		ICC (Interobs)	Evaluation
Full 3D						
Femur length	0.99	0.99	0.99	Excellent	0.99	Excellent
Tibia length	0.99	0.99	0.99	Excellent	0.99	Excellent
Limb length	0.99	0.99	0.99	Excellent	0.99	Excellent
Femoral head diameter	0.96	0.94	0.95	Excellent	0.94	Excellent
Femur neck length	0.93	0.92	0.96	Excellent	0.91	Excellent
Collodiaphyseal angle	0.94	0.93	0.91	Excellent	0.92	Excellent
Femoral offset	0.94	0.93	0.92	Excellent	0.9	Excellent
Mechanical tibifemoral angle	0.99	0.99	0.99	Excellent	0.94	Excellent
Femoral mechanical angle	0.92	0.94	0.91	Excellent	0.93	Excellent
Tibial mechanical angle	0.94	0.92	0.94	Excellent	0.95	Excellent
Femur mechanical axis—shaft angle	0.98	0.98	0.98	Excellent	0.97	Excellent
Femoral torsion	0.91	0.90	0.92	Excellent	0.85	Good
Tibial torsion	0.90	0.91	0.93	Excellent	0.81	Good
Femorotibial rotation	0.90	0.91	0.90	Excellent	0.82	Good
Lower limb alignment						
Femur length	0.99	0.99	0.99	Excellent	0.99	Excellent
Tibia length	0.99	0.99	0.99	Excellent	0.99	Excellent
Limb length	0.99	0.99	0.99	Excellent	0.99	Excellent
Femoral head diameter	0.99	0.99	0.99	Excellent	0.97	Excellent
Mechanical tibifemoral angle	0.98	0.97	0.98	Excellent	0.95	Excellent
Femur mechanical axis—shaft angle	0.97	0.96	0.94	Excellent	0.91	Excellent
Hassel–Farman method						
Bone age measurement	0.96	0.95	0.95	Excellent	0.98	Excellent

EOS system reconstructions were of the “Full 3D” mode (used in individuals 4–24 years old) or the “Lower limb alignment” mode (used in children 2–4 years old, due to alignment landmarks being obscured by the growth plates). ICC, intraclass coefficient; obs, observer.

Table 4. Distribution of the Calendar Age Within the Bone Age Stages—Absolute Values Shown on Left and the Incidence (in Percent) Within Each Age Group, on the Right

Calendar Age (Year)	Bone Age Stage							Calendar Age (Year)	Bone Age Stage							
	1	2	3	4	5	6	Sum		1 (%)	2 (%)	3 (%)	4 (%)	5 (%)	6 (%)	Sum (%)	
2	7						7	2	100							0.7
3	5						5	3	100							0.5
4	20						20	4	100							2.0
5	28	4					32	5	87.5	12.5						3.2
6	21	4	2				27	6	77.8	14.8	7.4					2.7
7	17	10	6				33	7	51.5	30.3	18.2					3.3
8	19	10	7				36	8	52.8	27.8	19.4					3.6
9	10	17	7	1			35	9	28.6	48.6	20.0	2.9				3.5
10	13	13	11	4			41	10	31.7	31.7	26.8	9.8				4.1
11	6	10	15	7	6		44	11	13.6	22.7	34.1	15.9	13.6			4.4
12	3	13	19	8	12	6	61	12	4.9	21.3	31.1	13.1	19.7	9.8		6.1
13		6	21	15	13	8	63	13		9.5	33.3	23.8	20.6	12.7		6.3
14			12	18	27	8	65	14			18.5	27.7	41.5	12.3		6.5
15			11	17	33	12	73	15			15.1	23.3	45.2	16.4		7.3
16			3	20	32	8	63	16			4.8	31.7	50.8	12.7		6.3
17				14	13	23	50	17				28.0	26.0	46.0		5.0
18				8	18	24	50	18				16.0	36.0	48.0		5.0
19				8	5	37	50	19				16.0	10.0	74.0		5.0
20				7	11	32	50	20				14.0	22.0	64.0		5.0
21				7	12	31	50	21				14.0	24.0	62.0		5.0
22				7	8	35	50	22				14.0	16.0	70.0		5.0
23				6	7	37	50	23				12.0	14.0	74.0		5.0
24					5	45	50	24					10.0	90.0		5.0
Sum	149	87	114	147	202	306	1005	Sum	15	9	11	15	20	30		

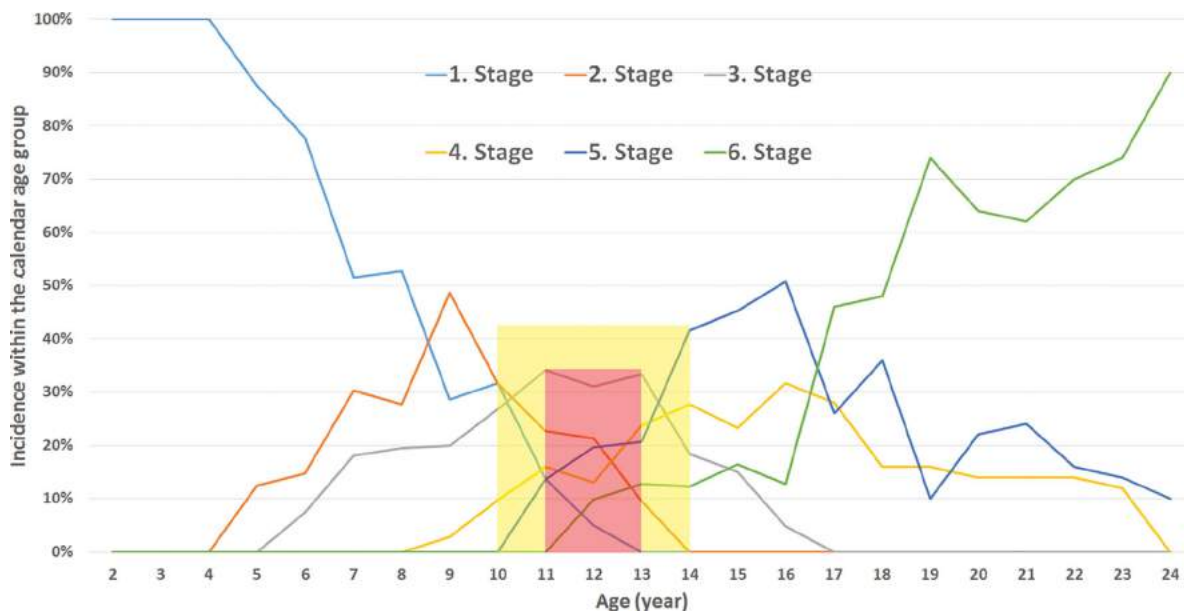


Figure 2. Incidence of the bone age stages within an age group (in percentage). Bone age stages were found to span many ages, and vice versa children of one particular calendar age may have one of many bone ages. In some cases similarly aged individuals could be in any of the six bone age stages (aged 12, shown within the red box) or one of 5 (aged 10–14, shown within the yellow box), highlighting the differences between skeletal maturation and calendar age.

Table 5. Correlations Between the Bone Age, Calendar Age, Height, and Measured Lower Limb Parameters

Parameter	Bone Age		Calendar Age		Height	
	Correlation Coefficient	<i>p</i>	Correlation Coefficient	<i>p</i>	Correlation Coefficient	<i>p</i>
Chalendar age	0.852	<0.001	—	—	—	—
Height	0.772	<0.001	0.811	<0.001	—	—
Femur length	0.747	<0.001	0.781	<0.001	0.909	<0.001
Tibia length	0.673	<0.001	0.766	<0.001	0.900	<0.001
Limb length	0.582	<0.001	0.763	<0.001	0.904	<0.001
Femoral head diameter	0.682	<0.001	0.738	<0.001	0.940	<0.001
Femoral offset	0.664	<0.001	0.743	<0.001	0.800	<0.001
Femur neck length	0.691	<0.001	0.703	<0.001	0.814	<0.001
Collodiaphyseal angle	-0.164	<0.001	-0.13	<0.001	-0.152	0.246
Mechanical tibiofemoral angle	-0.214	<0.001	-0.247	<0.001	-0.146	<0.001
Femoral mechanical angle	-0.082	0.027	-0.080	<0.001	0.016	0.583
Tibial mechanical angle	-0.117	<0.001	-0.119	<0.001	-0.134	<0.001
Femur mechanical axis—shaft angle	0.071	0.009	0.091	0.001	0.046	0.111
Femoral torsion	-0.292	<0.001	-0.153	<0.001	-0.033	<0.001
Tibial torsion	0.240	<0.001	0.146	<0.001	-0.088	<0.001
Femorotibial rotation	0.345	<0.001	0.187	0.001	0.199	<0.001

Correlation coefficients were similar between bone age and calendar age for the majority of measurements, except femoral torsion, tibial torsion, and femorotibial rotation, which showed weak correlations, but were stronger than those of calendar age.

was not large (beta-coefficients for femoral mechanical angle: -0.080 vs. -0.065 , tibial mechanical angle: -0.115 vs. -0.107 , FM-FS: 0.093 vs. 0.088) (Table 6).

Due to the scope of this paper we restrict detailed descriptions to the biomechanical metrics of the lower limb, due to their influence on function. The CD angle had a lower standard deviation (S.D.) when compared to bone age ($4,50^\circ$ vs. $5,09^\circ$), and as a discriminating variable four groups were formed with bone age (1–6), in contrast to only two large groups defined by calendar age (4–14 years old and 15–24) (Fig. 3). Femoral torsion had a S.D. 0.64° lower when compared

to bone age, and one more group was discriminated (1–6) than calendar age (Fig. 4). Tibial torsion had an average S.D. 0.29° lower, and discriminated one more group (three vs. two groups) than calendar age (Fig. 5). Femorotibial rotation was found to have only a marginally lower S.D. (5.81° vs. 5.83°) and was the only biomechanical parameter in which calendar age defined more groups, though the range of the data was also higher (rangecalendarage: -1.46 – 7.72° , rangeboneage: 2.63 – 5.65°) (Fig. 6). A single discrete group was found at 4 years old, though this may be a statistical accident. mTFA showed a lower S.D. when compared

Table 6. Calculated Linear Models Based on Stepwise Regression Analysis and Variance Inflation Factor (VIF) Test

Parameter	Calculated Linear Model	Beta-Coefficient	VIF
Femur length	Height	0.856	—
Tibia length	Height	0.811	—
Limb length	Height	0.912	—
Femoral head diameter	Height	0.912	—
Femoral offset	Height	0.834	—
Femur neck length	Height	0.857	—
Collodiaphyseal angle	Bone age—Calendar age	-0.322	0.875
Mechanical tibiofemoral angle	Calendar age—Bone age	-0.189	1.257
Femoral mechanical angle	Calendar age	-0.080	—
Tibial mechanical angle	Calendar age	-0.115	—
Femur mechanical axis—shaft angle	Calendar age	0.093	—
Femoral torsion	Bone age—Calendar age	-0.240	0.741
Tibial torsion	Bone age—Calendar age	0.335	0.984
Femorotibial rotation	Bone age—Calendar age	0.237	1.356

Beta-coefficient reflects the efficacy of the bone age, calendar age or height as a discriminating variable to separate discrete groups within the parameters.

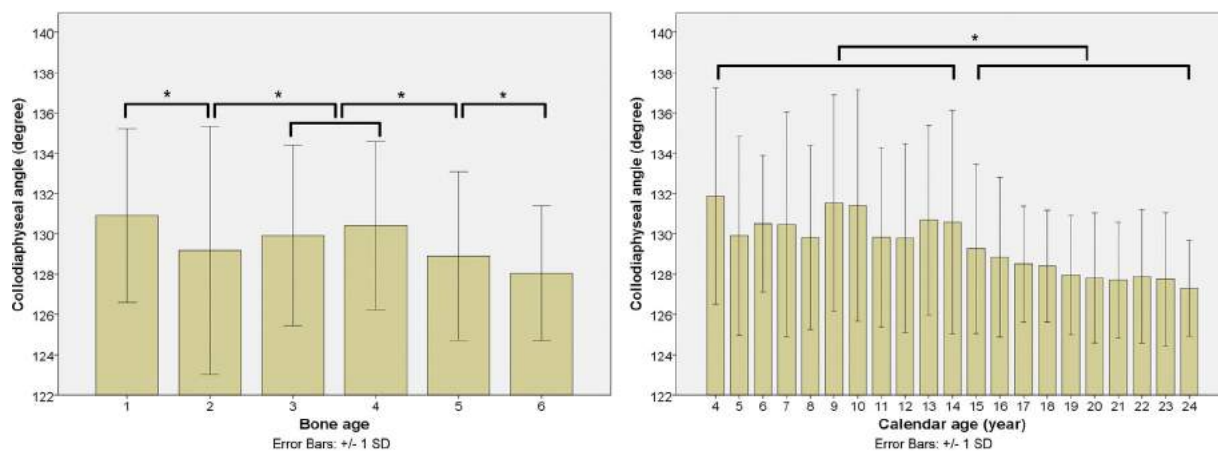


Figure 3. Colliadiaphyseal angle. Represented in mean \pm S.D. in bone age based groups (left) and calendar age based groups (right). *Significant difference between groups (based on independent-sample *t*-test, performed in ascending order).

to bone age (2.08° vs. 2.29°), and a greater number of groups were defined (two vs. three groups) (Fig. 7).

DISCUSSION

In agreement with other studies, we think this study further demonstrates the EOS 2D/3D scanners potential role as a reliable tool for measuring lower limb parameters in a pediatric population.^{13–19} While difficulties may arise due to the growth cartilages, resulting in longer processing times in those under 10 years old and may prevent full 3D reconstruction in under fours, they can be reliably carried out in the majority of children.^{13,18,19}

Although the most typical method of bone age assessment is the evaluation of the hand-wrist skeletal anatomy, the patients' position in the EOS scanner is optimized for visualizing the spine and lower limb, which obscures the distal upper limb, and required us to search for alternatives. Cervical vertebral evaluation was chosen as the spine is clearly visible and other alternatives were problematic or inappropriate.

Before committing to the Hassel–Farman method, a method reportedly both simple to use yet well-correlated

with hand-wrist methods, we carried out an intra- and inter-observer reliability test.^{8,20,22–26} Excellent results were achieved, agreeing with previous studies excepting that of Jaqueria et al. Their study, however, which found its reliability to be moderate, was based on questionnaires and a small population of only 23 X-rays.^{20,25,27} We believe our study to be the largest of its type to date.

Interestingly what arose for us as a solution to the problem of retrospectively investigating bone age in full body EOS images could be a useful technique for those routinely assessing scoliosis with the device, as no extra scans are required and indeed the accuracy of Risser staging has been questioned in recent years.^{28,29}

After assessment of scans, our results clearly showed that the lower limb parameters correlate differently to bone age and calendar age. From one point of view, bone age is the more “natural” as it influenced by gender, race, nutrition, sickness or health and socioeconomic status, rather than merely the passing of weeks, months, and years. Although like Uysal et al. we found a strong correlation between calendar age and bone age it must be noted that

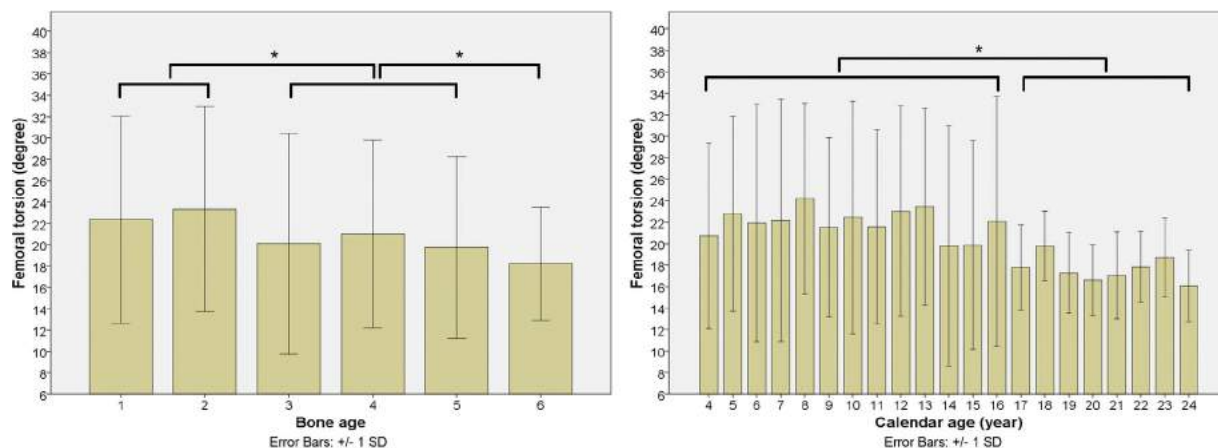


Figure 4. Femoral torsion. Represented in mean \pm S.D. in bone age based groups (left) and calendar age based groups (right). *Significant difference between groups (based on independent-sample *t*-test, performed in ascending order).

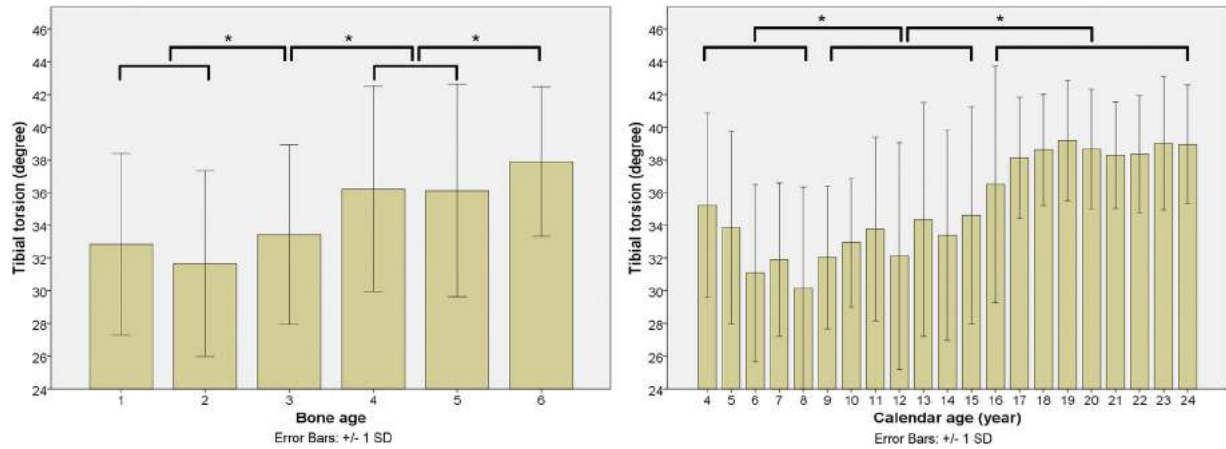


Figure 5. Tibial torsion. Represented in mean \pm S.D. in bone age based groups (left) and calendar age based groups (right). *Significant difference between groups (based on independent-sample *t*-test, performed in ascending order).

within each bone age stage great variation can be seen, with individuals in one stage differing by up to 9 years (in stage 3) or even 15 years of age (stage 4). Conversely, individuals between 11 and 13 could be of almost any bone age stage, indeed among 12-year olds all six stages were seen.^{8,25} With regards to the distribution of bone age based on calendar age our findings do not differ greatly from the studies of Uysal.²⁵

These findings suggest that bone age estimation would perhaps be a useful addition to routine lower limb assessments in children as it is influenced by some factors other than those of the calendar age.^{8,30}

The comparing of the abnormality less population and the population with mild non-lower limb connected disorder included this study has not shown any significant difference. Based on this result, we believe that the selected population is acceptable to represent the population with healthy lower limb.

The Spearman correlation test showed that like calendar age, bone age has a good correlation with each of the 14 biomechanical parameters evaluated, however, further examinations revealed some trends.

The longitudinal and volumetric parameters correlated most with height, as their values are closely related to total bone length.

Focusing on those lower limb parameters in which significant change occurs during childhood growth with clinical consequence, the femoral rotation, tibial torsion, and femorotibial rotation were all found to have a closer relationship with bone age than calendar age. This suggests the maturity of the epiphyseal plates may have a greater influence on rotational features of the long bones of the lower limb than the calendar age. mTFA, however, correlated more with calendar age, and this is likely due to an isolated valgization peak at 3 years old that was undetected with bone age analysis. The broad distribution of children (from 2 to 8 years old) in bone stage 1 averages out this peak.

These four parameters, and also the CD angle, showed lower standard deviations when correlated with bone age and served as better discriminating variables. Among them, only with femorotibial rotation could more groups be separated based on calendar age, and this may be explained by the fact that values of this

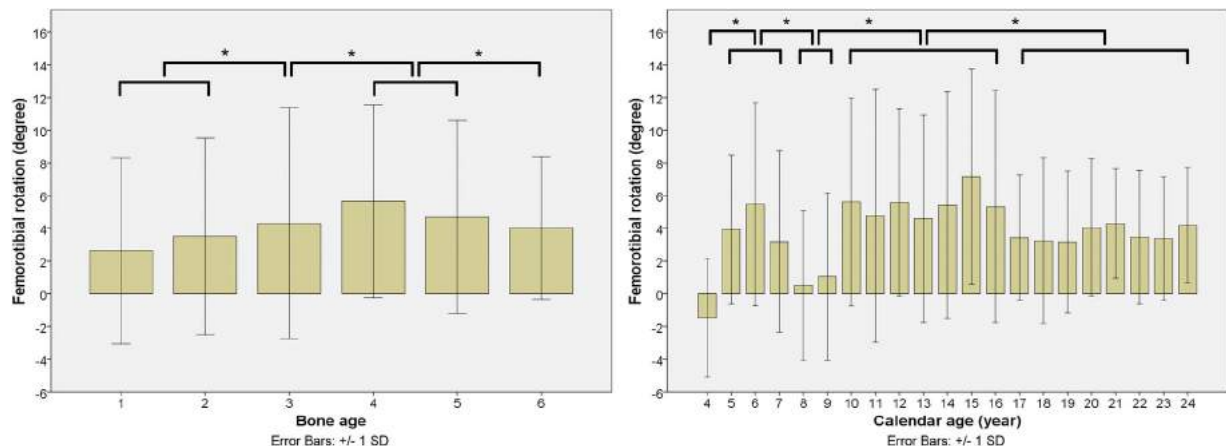


Figure 6. Femorotibial rotation. Represented in mean \pm S.D. in bone age based groups (left) and calendar age based groups (right). *Significant difference between groups (based on independent-sample *t*-test, performed in ascending order).

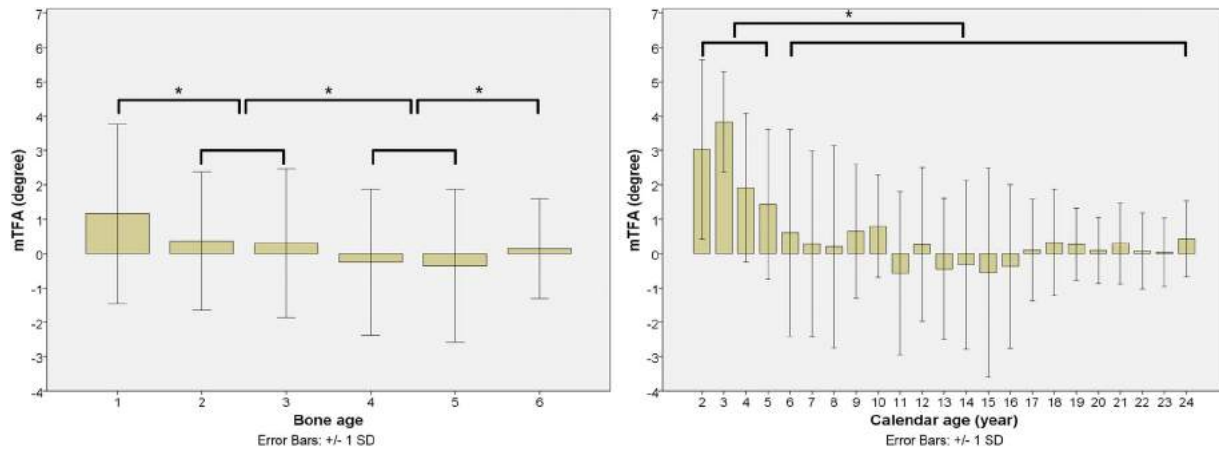


Figure 7. Mechanical tibiofemoral angle (mTFA). Represented in mean \pm S.D. in bone age based groups (left) and calendar age based groups (right). *Significant difference between groups (based on independent-sample *t*-test, performed in ascending order).

parameter fluctuate highly, such that it actually separates into three discrete statistical groups between 4 and 9 years of age (4–9). This has not been seen in other reports, however, and may be perhaps a misleading trend due to a smaller sample size at this age.

Bone age comparison can yield an alternative viewpoint for the understanding of biomechanical parameters, highlighted for example by the mTFA. Correlations based on the calendar age explicitly demonstrated an average varus position in 11-year olds, however, in the first and second bone age stages (corresponding to 1/3 of 11-year olds) a valgus position was typically seen with significantly lower standard deviation. This suggests that perhaps this more accurately reflects the reality, or allows us to subgroup and more precisely estimate a given child's stage of growth and/or growth potential.

While an optimal sample group to assess bone age and parameters of the lower limb would consist of a completely healthy population free from orthopedic symptoms, exposing such a group of children to ionizing radiation raises ethical problems. As this was a retrospective study the population was limited such that both gender and age distribution is somewhat uneven below 16 years old. The higher female prevalence is accounted for as the most common indication for our EOS examinations is scoliosis. The influence of scoliosis and functional kyphosis on the height must be noted. We feel however, that the statistical correlations found in this study were so significant that the effect of a mild scoliosis or kyphosis were unlikely to have introduced an unacceptable bias.

In conclusion, bone age as an indicator of skeletal maturation in the lower limb gives more information than calendar age alone, and provides a better means of following changes, especially with regards to rotational parameters. The bone age is influenced by gender, race, nutrition, sickness or health and socioeconomic status, and so may possess a better relationship with the physiological state of the skeleton. In

this study we also showed the Hassel–Farman method to be a reliable, practical and easily applicable measure of bone age, and is usable in conjunction with the EOS 2D/3D scanner. We would hope that this opens the door to greater use of bone age estimation by those using this technology in research and clinical practice.

AUTHORS' CONTRIBUTIONS

All authors contributed extensively to the work presented in this paper. Á.T.S.: performed the analysis of all patient related data, analyzed bone age and 3D EOS reconstructions, performed the statistical analyses, put together the final manuscript. I.O.: analyzed bone age and 3D EOS reconstructions, reviewed the manuscript. P.V.: analyzed bone age and 3D EOS reconstructions, reviewed the manuscript. P.T. and C.V.: designed the study, supervised all the analysis of bone age and lower limb parameters, managed patient-related administrative care and institutional requirements. All authors have read and approved the final submitted version.

REFERENCES

1. Dimeglio A. 2001. Growth in pediatric orthopaedics. *J Pediatr Orthop* 21:549–555.
2. Kelly PM, Diméglio A. 2008. Lower-limb growth: how predictable are predictions? *J Child Orthop* 2:407–415.
3. Sanders JO, Howell J, Qiu X. 2011. Comparison of the Paley method using chronological age with use of skeletal maturity for predicting mature limb length in children. *J Bone Joint Surg Am* 93:1051–1056.
4. Sabharwal S, Sakamoto SM, Zhao C. 2013. Advanced bone age in children with Blount disease: a case-control study. *J Pediatr Orthop* 33:551–557.
5. Paley D, Bhav A, Herzenberg JE, et al. 2000. Multiplier method for predicting limb-length discrepancy. *J Bone Joint Surg Am* 82:1432–1446.
6. Nault ML, Parent S, Phan P, et al. 2010. A modified Risser grading system predicts the curve acceleration phase of female adolescent idiopathic scoliosis. *J Bone Joint Surg Am* 92:1073–1081.
7. Cao F, Huang HK, Pietka E, et al. 2000. Digital hand atlas and web-based bone age assessment: system design and implementation. *Comput Med Imaging Graph* 24:297–307.

8. Soegiharto BM, Cunningham SJ, Moles DR. 2008. Skeletal maturation in Indonesian and white children assessed with hand-wrist and cervical vertebrae methods. *Am J Orthod Dentofacial Orthop* 134:217–226.
9. Franklin D. 2010. Forensic age estimation in human skeletal remains: current concepts and future directions. *Leg Med (Tokyo)* 12:1–7.
10. Illés T, Somoskeöy S. 2012. The EOS™ imaging system and its uses in daily orthopaedic practice. *Int Orthop* 36:1325–1331.
11. Chaibi Y, Cresson T, Aubert B, et al. 2012. Fast 3D reconstruction of the lower limb using a parametric model and statistical inferences and clinical measurements calculation from biplanar X-rays. *Comput Methods Biomech Biomed Engin* 15:457–466.
12. Journé A, Sadaka J, Bélicourt C, et al. 2012. New method for measuring acetabular component positioning with EOS imaging: feasibility study on dry bone. *Int Orthop* 36:2205–2209.
13. Schlégl AT, Szuper K, Somoskeöy S, et al. 2014. Evaluation of the usefulness of the EOS 2D/3D system for the measurement of lower limbs anatomical and biomechanical parameters in children. *Orv Hetil* 155:1701–1712.
14. Gaumétou E, Quijano S, Ilharreborde B, et al. 2014. EOS analysis of lower extremity segmental torsion in children and young adults. *Orthop Traumatol Surg Res* 100:147–151.
15. Roszkopf AB, Ramseier LE, Sutter R, et al. 2014. Femoral and tibial torsion measurement in children and adolescents: comparison of 3D models based on low-dose biplanar radiography and low-dose CT. *AJR Am J Roentgenol* 202:285–291.
16. Assi A, Chaibi Y, Presedo A, et al. 2013. Three-dimensional reconstructions for asymptomatic and cerebral palsy children's lower limbs using a biplanar X-ray system: a feasibility study. *Eur J Radiol* 82:2359–2364.
17. Gheno R, Nectoux E, Herbaux B, et al. 2012. Three-dimensional measurements of the lower extremity in children and adolescents using a low-dose biplanar X-ray device. *Eur Radiol* 22:765–771.
18. Schlégl Á, Szuper K, Somoskeöy S, et al. 2015. Three dimensional radiological imaging of normal lower-limb alignment in children. *Int Orthop* 39:2073–2080.
19. Szuper K, Schlégl Á, Leidecker E, et al. 2015. Three-dimensional quantitative analysis of the proximal femur and the pelvis in children and adolescents using an upright biplanar slot-scanning X-ray system. *Pediatr Radiol* 45:411–421.
20. Hassel B, Farman AG. 1995. Skeletal maturation evaluation using cervical vertebrae. *Am J Orthod Dentofacial Orthop* 107:58–66.
21. Winer B, Brown D, Michels K. 1991. *Statistical Principles In Experimental Design*, 3rd ed. New York: McGraw-Hill. p 283–293.
22. Cericato GO, Bittencourt MA, Paranhos LR. 2015. Validity of the assessment method of skeletal maturation by cervical vertebrae: a systematic review and meta-analysis. *Dento-maxillofac Radiol* 44:20140270.
23. Pichai S, Rajesh M, Reddy N, et al. 2014. A comparison of hand wrist bone analysis with two different cervical vertebral analysis in measuring skeletal maturation. *J Int Oral Health* 6:36–41.
24. San Román P, Palma JC, Oteo MD, et al. 2002. Skeletal maturation determined by cervical vertebrae development. *Eur J Orthod* 24:303–311.
25. Uysal T, Ramoglu SI, Basciftci FA, et al. 2006. Chronologic age and skeletal maturation of the cervical vertebrae and hand-wrist: is there a relationship? *Am J Orthod Dentofacial Orthop* 130:622–628.
26. Santiago RC, de Miranda Costa LF, Vitral RW, et al. 2012. Cervical vertebral maturation as a biologic indicator of skeletal maturity. *Angle Orthod* 82:1123–1131.
27. Jaqueira LM, Armond MC, Pereira LJ, et al. 2010. Determining skeletal maturation stage using cervical vertebrae: evaluation of three diagnostic methods. *Braz Oral Res* 24:433–437.
28. Yang J, Bhandarkar A, Suh S, et al. 2014. Evaluation of accuracy of plain radiography in determining the Risser stage and identification of common sources of errors. *J Orthop Surg Res* 9:101.
29. Reem J, Carney J, Stanley M, et al. 2009. Risser sign inter-rater and intra-rater agreement: is the Risser sign reliable? *Skeletal Radiol* 38:371–375.
30. Schmeling A, Black S. 2010. An introduction to the history of age estimation in the living. In: Black S, Aggrawal A, Payne-James J, editors. *Age Estimation in the living: the practitioner's guide*, 1th ed. Chichester: John Wiley & Sons. p 1–18.

1 **Alternative Methods for Skeletal Maturity Estimation with the EOS Scanner –** 2 **Experience from 934 Patients**

3

4 **Background:** Hand-wrist bone age assessment methods are not possible on typical EOS
5 2D/3D images without body position modifications that may affect spinal position. We aimed
6 to identify and assess lesser known bone age assessment alternatives that may be applied
7 retrospectively and without the need for extra imaging.

8 **Methods:** After review of 2857 articles, nine bone age methods were selected and applied
9 retrospectively in pilot study (thirteen individuals), followed by evaluation of EOS images of
10 934 4-24-year-olds. Difficulty of assessment and time taken were recorded, and reliability
11 calculated.

12 **Results:** Five methods proved promising after pilot study. Risser ‘plus’ could be applied with
13 no difficulty in 89.5% of scans (836/934) followed by the Oxford hip method (78.6%,
14 734/934), cervical (79.0%, 738/934), calcaneus (70.8%, 669/934) and the knee (68.2%,
15 667/934). Calcaneus and cervical methods proved to be fastest at 17.7s (95% confidence
16 interval, 16.0s to 19.38s & 26.5s (95% CI, 22.16s to 30.75s), respectively, with Oxford hip the
17 slowest at 82.0 s (95% CI, 76.12 to 87.88s). Difficulties included: regions lying outside of the
18 image - assessment was difficult or impossible in upper cervical vertebrae (46/934 images
19 4.9%) and calcaneus methods (144/934 images, 15.4%); position: lower step length was
20 associated with difficult lateral knee assessment & head/hand position with cervical evaluation;
21 and resolution: in the higher stages of the hip, calcaneal and knee methods.

22 **Conclusions:** Hip, iliac crest and cervical regions can be assessed on the majority of EOS scans
23 and may be useful for retrospective application. Calcaneus evaluation is a simple and rapidly
24 applicable method that may be appropriate if consideration is given to include full imaging of
25 the foot.

26 **Level of Evidence: Level III – Study of Non-consecutive patients (without consistently**
27 **applied reference "gold" standard)**

28

29 **Keywords:** Bone age, EOS imaging, skeletal maturity, bone growth, Risser.

30

31 Introduction:

32

33 Skeletal maturity is of interest to the paediatric orthopaedist, particularly in timing and
34 treatment of scoliosis and leg length discrepancy[1].

35

36 While the EOS scanner has recently gained popularity in the assessment of scoliosis due to its
37 low radiation dose [2,3], the position required for spinal imaging does not permit evaluation of
38 the hand or wrist (see figure 1), the region favoured by more than 97.6% of US paediatric
39 radiologists for assessing 3-18 year-olds [5]. While the Risser system can be applied, the first
40 stage typically occurs after onset of peak height velocity and as such is only useful for
41 predicting the end of the risk period for curve progression[5,6].

42

43 In the present study we aimed to identify and present promising alternative bone age methods
44 that may be of use to the clinician working with the EOS, and to evaluate their reliability and
45 usability.

46

47 Materials & Methods

48 **Literature Review**

49 A Pubmed search was conducted on March 30 2016 using terms “bone age”, “skeletal age”
50 and “skeletal maturation”, and 185 different methods were identified (see Supplementary Table
51 1 for a comprehensive list). Nine promising methods were selected:

- 52 1. Calcaneus[7];
- 53 2. Cervical vertebrae[8];
- 54 3. Clavicle[9];
- 55 4. Shoulder[10];
- 56 5. Elbow[11];
- 57 6. First rib[12];
- 58 7. Oxford Hip[13];
- 59 8. Iliac apophysis and tri-radiate cartilage: Risser 'plus' method[14];
- 60 9. Knee[15].

61

62 After discussion, clavicle, rib, and elbow methods were not included due to insufficient
63 resolution (clavicle) or severe shadowing of landmarks due to patient position in the EOS (first
64 rib, elbow).

65 **Pilot Study**

66 Three graders (one orthopaedic resident and two PhD candidate medical doctors) were given
67 text and pictorial descriptions of the remaining methods and trained with assistance of a senior
68 orthopaedic specialist and a senior radiologist. 13 normal children aged 3-16 were randomly
69 selected from our database of EOS scans taken during 2007-2016 and images evaluated by
70 each method three times by the three observers, on separate days.

71 **Method Testing**

72 After pilot study five methods (see Figure 2a-e) were assessed based on:

73 (1) Reliability: 30 images were randomly selected and assessed three times by each
74 of the three observers, on three separate days, and intraclass correlation coefficient
75 (ICC) estimated.

76 (2) Difficulty of Assessment: methods were assessed based on a four-point Likert
77 scale: '1' easy - method was easy to apply; '2' moderate - some minor exposure

78 problems or minor obstruction, but evaluation could confidently be made; '3'
79 difficult - significant obstruction, image partially cut eg. 1/3 or less of a landmark
80 obscured or not visible, such that assumption must be made; '4' impossible –
81 landmark not in image or totally obstructed. In the hip and knee methods, if the
82 sum of problematic landmarks exceeded 2 or 3, respectively, then the whole image
83 was regarded as 'difficult'.

84 (3) Speed: Two observers used digital timers to record evaluation time with each
85 method during their final 200 randomised images.

86

87 EOS images of disease-free children and adolescents were retrospectively collected from our
88 database taken during normal clinical practice from 2007-2016, a total of 7108 full body image
89 pairs. Selection criteria were: individuals aged 4-24 years old; absence of any disorder or
90 previous surgery affecting skeletal anatomy; absence of movement artefacts. Individuals from
91 age group 17-24 were limited to 50 per year (25 males and 25 females). 59 images were
92 damaged or missing from our database resulting finally in 934 disorder-free individuals.
93 Image-pairs were randomised and assigned equally to the three graders.

94

95 For randomisation and selection, Microsoft Excel v14.0.6112.5000 (Microsoft Corp.,
96 Redmond, WA) software was used. Consent at the time of imaging was attained from all
97 individuals, or their guardians. Institutional Review Board ethical permission was granted for
98 this study and all work was in accordance with the Declaration of Helsinki.

99

100 For a deeper description of methods applied, see Supplementary Figure 1.

101

102

103

104 Results

105 **Literature Review**

106 Online search yielded 4758 articles: “bone age” returned 3230 results, “skeletal age”: 808, “and
107 “skeletal maturation”: 1153. Duplicate (433) or irrelevant articles (516) and publications in
108 which the method was unlisted (555), absent from the abstract (foreign language articles) (500)
109 or the article could not be located (330) were removed, leaving 2857 articles.

110

111 **Pilot Study**

112 After pilot study, the shoulder method was no longer included as observers found serious
113 difficulties evaluating the region in 54-72% of scans. Only one of the three required landmarks
114 were found to be assessable in 23-38% of scans (3-5 of 13 scans), the apex/ angle of the
115 coracoid process was not visible in 15-38% (2-5 of 13 scans) in addition to low satisfaction
116 reported by observers using the method.

117

118 Plantar sesamoid identification is recommended to assist with the calcaneal method, however
119 sesamoids could not be clearly identified in any scans, and a ‘possible’ presence reported in
120 four of 13 scans. Identification difficulties were partly due to the absence of the dorso-volar
121 plane in EOS images but also due to deterioration of image resolution at the inferior image
122 edge. In one incidence a patient with conventional X-ray of the foot taken at the same time
123 received a negative report on the presence of sesamoids after EOS review, despite their clear
124 presence with conventional image.

125

126 All other methods could be assessed satisfactorily.

127

128 **Primary study**

129 Bone ages of individuals with each method are shown in Figure 5a-e.

130

131 1. Reliability

132 We previously reported excellent inter- and intra-observer reliability values using the cervical
133 vertebral method[16], and excellent values were also found with calcaneus, Risser ‘plus’
134 system and Oxford hip methods[17]. The knee method, although ‘good’, was not as reliable.
135 ICC values are shown in Table 1.

136

137 2. Difficulty of Assessment (see figure 3a-e, Table 2)

138 The Risser ‘plus’ system received the most favourable ratings with 89.5% of scans (836/934)
139 receiving an ‘easy’ rating and a further 9.2% of scans (82/934) rated ‘moderate’. Similarly, the
140 Oxford hip method and cervical methods saw good ratings with 78.6% & 79.0% rated ‘easy’
141 and 13.6% and 11.1% rated ‘moderate’, respectively. The calcaneus method exhibited the
142 highest number of unevaluable scans (6.2% or 58 scans) with the most common cause being
143 that the feet were not imaged (49 scans) or that feet overlapped to an extent that made them
144 unevaluable (seven scans).

145

146 The knee method received the lowest number of ‘easy’ ratings at 68.2% of scans (637/934) and
147 23.7% of scans (221/934) were reported to have moderate difficulty. Problems with the knee
148 method were distributed almost equally between regions: local problems were reported in
149 39.6% of cases to be due to the femur, 36.5% tibia, and 23.9% fibula. Reported causes behind
150 problematic scans (297) were predominantly: resolution (36.4%, 108/297), uncertainty (25.6%,
151 76/297), position (20.2%, 60/297) or other (16.8%, 50/297). Uncertainty was reported in 76
152 images (25.6% of problematic cases) as the original description was felt to be lacking in precise
153 differentiation between the stages, particularly between Stages 3 and 4.

154

155 3. Evaluation time (See Figure 4)

156 Methods with fewer stages had shorter evaluation times. The six-stage calcaneus method was
157 found to be the fastest at just 17.7 seconds, significantly quicker than the next fastest, the
158 similarly six-stage cervical method's 26.5s (independent t-test, $p < 0.05$). The Oxford hip
159 method was the slowest, sometimes taking more than four minutes due to the nine regions of
160 interest to be evaluated, and uncertainty due to problems with lesser trochanter visibility (see
161 discussion).

162

163

164 Discussion

165 Since its' introduction 12 years ago, the EOS Scanner has seen increasing popularity in clinics
166 across Europe and North America with more than 300 systems installed in 34 countries[18].
167 Our study aimed to highlight alternatives to traditionally recommended systems for bone age
168 estimation and to evaluate compatibility with the recommended patient position of the EOS
169 scanner (Table 3).

170

171 After assessment, three of the methods were more satisfactory and will be highlighted.

172

173 The Risser 'plus' system combines European and American Risser systems with tri-radiate
174 cartilage evaluation and has been included in the recommendations of the Scoliosis Research
175 Society since 2014[14]. Our raters reported the highest number of 'easy' scans with this method
176 (89.5%) and excellent reliability ICC scores. Furthermore, it was a relatively fast method (mean
177 evaluation 30.1s). The Risser system without inclusion of tri-radiate cartilage evaluation is not
178 recommended: Stage 0+ started at 6.55 years old with median 11.75, in comparison with 7.29
179 years old (or 11.53 years old when 1 outlier was excluded) at first presentation of Stage 1.
180 Resolution was a moderate issue in 59 cases, predominantly due to difficulty with identifying
181 the ending of fusion of the iliac apophysis - 40 of these images were Risser 4 or 5. The number

182 of unevaluable images was lower than that reported with Bone Xpert software, Martin et al.
183 reported seven of 1097 images (0.64%) could not be initially evaluated due to insufficient
184 image quality, contrast or size[19]. The Risser system had a rejection rate of 0.32% (3/938)
185 and similarly low were the knee 0.11% (1/938), and Oxford hip methods 0.21% (2/938). The
186 calcaneus and cervical methods had considerably higher numbers of unassessable scans (8.9%,
187 4.2%).

188

189 The calcaneus method is a new method[7] and returned mixed results. While difficulties were
190 noted in a large number of scans (29.2% or 273/934), 52% of these were due to calcanei being
191 partially or totally cut off at the time of image capture rather than due to difficulty with the
192 scan itself. Foot positioning also caused difficulty, with overlap of the feet being the cause of
193 22.7% of those with moderate difficulty. That being said, this method was found to be the
194 fastest (17.7s) and raters reported high levels of satisfaction, as it was easy to learn, use and
195 remember. In the original description inclusion of plantar sesamoid evaluation is
196 recommended, but due to the absence of the dorso-plantar plane and significant overlap
197 between feet on the lateral image it was not felt to be reliable and it was not included in our
198 assessment. The calcaneus method is based on the historical Greulich-Pyle 'Brush' population
199 and Li et al recommended mild corrections for interpretation with modern children, as they
200 found Stage 3 and 4 girls were delayed by 0.64 and 0.58 years, respectively, compared to the
201 historical population[20]. Our study showed similar delays, of 0.94 and 2.2 years in Stage 3
202 and 4 females, and even Stage 4 boys of 1.61 years, however as both these studies were
203 retrospective, this is possibly in part due to an artificial elevation of values compared to serial
204 studies in which the earliest scan at each bone age stage can be identified.

205

206 The Oxford hip method, first described in 1957[13] consists of evaluation of nine different
207 landmarks and as a result was the slowest method used with a mean 82s per evaluation. The

208 45-point scoring system however makes it a favorable instrument in a scientific setting, in
209 which precision and a finer gradation of maturity is of more importance than time taken for
210 evaluations. However, with experience the mean time taken reported by our raters was faster
211 than the two most popular hand-wrist methods: the TW2 method has been reported to take an
212 average 7.8 minute for evaluation, while the Greulich-Pyle method, is estimated to take 1.4
213 minutes per image[21,22]. In 40.9% of scans (382/946), observers reported some degree of
214 difficulty in evaluating the lesser trochanter, in comparison with the femoral head (8.7%)
215 greater trochanter (8.4%), ilium (7.4%) and tri-radiate cartilage (2.8%). A modified version
216 consisting of 5 landmarks has been described in risk assessment of slipped capital femoral
217 epiphysis[23,24] occurring in a contralateral limb. When we evaluated the method based on
218 just these 5 parameters, a greater number of scans had favorable ratings (83.9% vs. 78.6% were
219 rated 'easy', and 11.5% vs. 13.6% rated 'moderate'). The inclusion of the lesser trochanter in
220 this abbreviated method continued to cause problems, however, and so it's omission may be
221 considered, as other authors have suggested [23].

222

223 **Common problems encountered:**

224 **Step Length**

225 While lower step length was reported subjectively to cause problems in assessment of the knee
226 and calcaneus, only a mild inverse correlation was found with ratings when assessed by
227 Spearman correlation (-0.100, $p < 0.05$) in the case of the knee, and no significant correlation
228 with the calcaneus ($p = 0.202$). A significantly lower average step length however was found in
229 those where the lateral knee image was reported as unevaluable, due to the overlapping
230 contralateral knee ($58.31 \text{ cm} \pm 46.95$ vs. $78.45 \text{ cm} \pm 53.5$)

231 **Resolution**

232 While the EOS image resolution is satisfactory for most structural evaluations, some of the
233 features evaluated are very fine, and problems were specifically reported with: assessing

234 trabecular continuity in the knee, and determining whether fusion was almost complete or had
235 fully completed in calcaneus (Stage 4 vs. 5), knee (3 vs. 4) and femoral head (stage 6 vs. 7).

236 **Image size**

237 As a result of physician personal preference many of our images were not full body-length
238 images, rather they excluded part or all of the upper cervical vertebrae (partly in 20, completely
239 in 26 cases) or calcaneus (partly in 95 cases, completely in 49). Furthermore, the posterior
240 calcaneal pole of the posterior foot often lay partially outside of the image. While this problem
241 cannot be corrected retrospectively, ensuring that future scans include these areas is easily
242 achievable.

243 **Position**

244 The cervical method was affected by variations in head and hand position in 77 scans. The
245 most common causes were: lateral head tilt (37 images) leading to moderate (24), difficult (11)
246 or impossible evaluations (2); hand/fingers partially covering the upper cervical vertebrae in
247 30 images (patients with an open hand often placed their thumb posteriorly, leading to
248 shadowing over C2 and even C3 vertebrae) leading to moderate (13), difficult (11) or
249 impossible evaluations (six).

250

251 This study has a number of limitations. Ratings are subjective judgements carried out by human
252 observers in an effort to elucidate which methods are ‘better’ or ‘more suitable’ – a hard
253 concept to define. The rating system used may also have favoured methods that use more
254 landmarks, as an ‘impossible’ rating was less likely in such cases. We endeavoured however
255 to include our experiences and likely pitfalls when using each method to be more informative
256 to the reader.

257

258 Jackson et al. recently reported on altering hand position to assess bone age in EOS images,
259 however, they noted that this “may alter the spinal alignment and affect sagittal balance or

260 shoulder height”, which was neither controlled form, nor measured[25]. In our clinic, attempts
261 to alter upper limb position resulted in altered thoracic and cervical spine position and so were
262 halted (unpublished data).

263

264 Our findings supported the continued use of the Risser system but with the inclusion of tri-
265 radiate assessment as per the recommendations of the Scoliosis Research Society. The Oxford
266 hip method took the greatest time to apply, its fine scale and broad age range coverage suggests
267 its use is appropriate for a research environment, although it may be simplified by omission of
268 the lesser trochanter, as suggested by other authors[23]. While the calcaneus method was not
269 always applicable for retrospective examination of our EOS images, it may serve to be a very
270 useful and easy-to-remember alternative for maturity assessment, if efforts are made to ensure
271 to capture the foot and calcaneus during image capture.

272

273 **Conflict of Interest:** On behalf of all authors, the corresponding author states that there is no
274 conflict of interest.

275

276

277

278

279

280

281

282

283

284

285

- 286 1. Dimeglio A, Canavese F. Progression or not progression? How to deal with adolescent
287 idiopathic scoliosis during puberty. *J Child Orthop* 2013;7:43–9.
- 288 2. Schlégl ÁT, Szuper K, Somoskeöy S, Than P. Three dimensional radiological imaging of
289 normal lower-limb alignment in children. *Int Orthop* 2015;39:2073–80.
- 290 3. Gheno R, Nectoux E, Herbaux B, Baldisserotto M, Glock L, Cotten A, et al. Three-
291 dimensional measurements of the lower extremity in children and adolescents using a low-
292 dose biplanar X-ray device. *Eur Radiol* 2012;22:765–71.
- 293 4. Breen MA, Tsai A, Stamm A, Kleinman PK. Bone age assessment practices in infants and
294 older children among Society for Pediatric Radiology members. *Pediatr Radiol*
295 2016;46:1269–74.
- 296 5. Little DG, Song KM, Katz D, Herring JA. Relationship of peak height velocity to other
297 maturity indicators in idiopathic scoliosis in girls. *JBJS LWW*; 2000;82:685–93.
- 298 6. Peterson L-E, Nachemson AL. Prediction of progression of the curve in girls who have
299 adolescent idiopathic scoliosis of moderate severity. Logistic regression analysis based on
300 data from The Brace Study of the Scoliosis Research Society. *JBJS LWW*; 1995;77:823–7.
- 301 7. Nicholson AD, Liu RW, Sanders JO, Cooperman DR. Relationship of Calcaneal and Iliac
302 Apophyseal Ossification to Peak Height Velocity Timing in Children. *J Bone Jt Surg*
303 2015;97:147–54.
- 304 8. Hassel B, Farman AG. Skeletal maturation evaluation using cervical vertebrae. *Am J*
305 *Orthod Dentofacial Orthop* 1995;107:58–66.
- 306 9. Schmeling A, Reisinger W, Loreck D, Vendura K, Markus W, Geserick G. Effects of
307 ethnicity on skeletal maturation: consequences for forensic age estimations. *Int J Legal Med*
308 2000;113:253–8.
- 309 10. Schaefer M, Aben G, Vogelsberg C. A demonstration of appearance and union times of
310 three shoulder ossification centers in adolescent and post-adolescent children. *J Forensic*
311 *Radiol Imaging Elsevier*; 2015;3:49–56.

- 312 11. Sauvegrain J, Nahum H, Bronstein H. Study of bone maturation of the elbow. *Ann Radiol*
313 *(Paris)* 1962. p. 542.
- 314 12. Garamendi PM, Landa MI, Botella MC, Alemán I. Forensic age estimation on digital X-
315 ray images: medial epiphyses of the clavicle and first rib ossification in relation to
316 chronological age. *J Forensic Sci Wiley Online Library*; 2011;56:S3–12.
- 317 13. Acheson RM. The Oxford Method of Assessing Skeletal Maturity. *Clin Orthop Relat Res*
318 *LWW*; 1957;10:19–39.
- 319 14. Negrini S, Hresko TM, O’Brien JP, Price N, Bettany-Saltikov J, De Mauroy JC, et al.
320 Recommendations for research studies on treatment of idiopathic scoliosis: Consensus 2014
321 between SOSORT and SRS non-operative management committee. *Scoliosis* 2015;10:1–12.
- 322 15. O’Connor JE, Bogue C, Spence LD, Last J. A method to establish the relationship
323 between chronological age and stage of union from radiographic assessment of epiphyseal
324 fusion at the knee: an Irish population study. *J Anat Wiley-Blackwell*; 2008;212:198–209.
- 325 16. Schlégl ÁT, O’Sullivan I, Varga P, Than P, Vermes C. Determination and correlation of
326 lower limb anatomical parameters and bone age during skeletal growth (based on 1005
327 cases). *J Orthop Res* 2017;35:1431–41.
- 328 17. O’Sullivan I, Schlégl ÁT, Varga P, Kerekes K, Vermes C, Than P. Csontkor – a
329 csontrendszeri érettség mérésének lehetősége EOS készülékkel. *Orv Hetil* 2019;160:619–28.
- 330 18. EOS Imaging. EOS imaging Reports Full Year 2018 Results and First Quarter 2019
331 Revenue. 2019.
- 332 19. Martin DD, Deusch D, Schweizer R, Binder G, Thodberg HH, Ranke MB. Clinical
333 application of automated Greulich-Pyle bone age determination in children with short stature.
334 *Pediatr Radiol* 2009;39:598–607.
- 335 20. Li SQ, Nicholson AD, Cooperman DR, Liu RW. Applicability of the calcaneal apophysis
336 ossification staging system to the modern pediatric population. *J Pediatr Orthop* 2019;39:46–
337 50.

- 338 21. De Sanctis V, Maio S, Soliman A, Raiola G, Elalaily R, Millimaggi G. Hand X-ray in
339 pediatric endocrinology: Skeletal age assessment and beyond. *Indian J Endocrinol Metab*
340 2014;18:63.
- 341 22. Van Rijn RR, Thodberg HH. Bone age assessment: Automated techniques coming of
342 age? *Acta radiol* 2013;54:1024–9.
- 343 23. Stasikelis PJ, Sullivan CM, Phillips WA, Polard AJ. Slipped capital femoral epiphysis:
344 prediction of contralateral involvement. *JBJS LWW*; 1996;78:1149–55.
- 345 24. Nicholson AD, Huez CM, Sanders JO, Liu RW, Cooperman DR. Calcaneal Scoring as an
346 Adjunct to Modified Oxford Hip Scores. *J Pediatr Orthop* 2016;36:132–8.
- 347 25. Jackson TJ, Miller D, Nelson S, Cahill PJ, Flynn JM. Two for One: A Change in Hand
348 Positioning During Low-Dose Spinal Stereoradiography Allows for Concurrent, Reliable
349 Sanders Skeletal Maturity Staging. *Spine Deform Scoliosis Research Society*; 2018;6:391–6.
- 350
- 351
- 352
- 353
- 354
- 355
- 356
- 357
- 358
- 359
- 360
- 361
- 362
- 363

364 **Figure Legends**

365 **Fig. 1. Patient position inside the EOS 2D/3D scanner.** (Illustration used with permission
366 from EOS Imaging, Paris, France).

367

368 **Fig 2. (a-e). Pictorial illustration of five bone age estimation methods.** (a) Calcaneus, (b)
369 Cervical, (c) Knee, (d) Risser Plus and (e) Oxford Hip methods. See Supplementary Figure 1
370 for more in depth description of each method. (Reproduced from O’Sullivan et al.[17],
371 creative commons license <https://creativecommons.org/licenses/by/4.0/legalcode>).

372

373 **Fig 3. (a-e). Difficulties reported during image assessment with each method.** Difficulties
374 were grouped as those due to technical difficulties e.g. landmark(s) lying outside of the edge
375 of the image; resolution issues, insufficient resolution to assess image easily; positioning -
376 landmark not visible, or not clearly visible due to limb rotation or shadowing; and if rater was
377 ‘unsure’ due to problems with method description.

378

379 **Fig. 4: Timing data for each of the Bone Age Methods.**

380

381 **Fig. 5a-e: Distribution of Chronological Ages at each Bone Age Stage with each method.**
382 **Gender is shown at each stage.**

383

384 **Supplementary Fig 1: Alternative Bone Age Methods Evaluated** Summaries of the six
385 methods applied in pilot study. See original articles for full details of the individual methods.
386 (All illustrations, unless otherwise stated, are reprinted from O’Sullivan et al.[17], creative
387 commons license: <https://creativecommons.org/licenses/by/4.0/legalcode>).

388 **(a) Cervical Bone Assessment as per Hassel & Farman (1995)** (Adapted with permission
389 from Schlégl et al.[16]). *1. Initiation:* the inferior borders of C2, C3 and C4 are all flat. Upper

390 borders taper from posterior to anterior giving the body a wedge shape. 2. *Acceleration*: C2
391 and C3 develop concavities in their inferior borders, while that of C4 remains flat. Bodies of
392 C3 and C4 are almost rectangular in shape. 3. *Transition*: Concavities in C2 and C3 are now
393 deeper and distinct with C4 beginning to develop a concave inferior border too. Bodies of C3
394 and C4 are rectangular in shape. 4. *Deceleration*: C2, C3 and C4 all have distinct concavities
395 in their inferior borders, and the bodies of C3 and C4 are becoming more square in shape. 5.
396 *Maturation*: Concavities of C2, C3 and C4 are more accentuated in the inferior borders, and
397 C3, C4 bodies are almost square or square in shape. 6. *Completion*: Deep concavities are found
398 in the inferior borders of C2, C3 and C4 and the bodies are square or column-like, with a
399 vertical dimension greater than their horizontal dimension.

400

401 **b. Shoulder Assessment as per Shaefer et al. (2015)**

402 Assessment is performed on three regions of the shoulder and scores or 'phases' can be
403 compared to age values from 10-24 years old. (i) Proximal Humerus - 1. *Open union*: A
404 continuous radiolucent line at the proximal humerus epiphyseal plate is visible. 2. *Fusing*:
405 Epiphyseal fusion is imminent, indicated by central haziness, or is in process. Peripheral
406 radiolucent lines are visible; 3. *Unfused notch*: Near-complete fusion with only peripheral
407 notches visible, most commonly under the greater tubercle.; 4. *Complete union*: No
408 radiolucency remains. A radiopaque line may persist indicting the site of fusion. (ii)
409 Acromion - *Phase 0. Not present*: No apophysis is observed. The acromion is marked by a
410 rounded; *Phase 1 Present; open or fusing*: The apophysis is present and a radiolucent line is
411 clearly visible. *Phase 4 Complete union*: No line of radiolucency is evident. (iii) Angle/apex:
412 *Phase 1. Present; Phase 2. Open or fusing*: The apophysis is clearly visible sitting on top of,
413 or at the tip of, the coracoid process. A radiolucent line is clearly visible. (Note: Only the
414 proximal Humerus can be described by 4 distinct phases).

415 **(c) Risser 'Plus' Method as per Negrini et al (2015).**

416 *Risser 0-*: Open triradiate cartilage, *Risser 0+*: Fused triradiate cartilage, *Risser 1*: 10-25%
 417 coverage of iliac crest, *Risser 2*: 25-50% coverage, *Risser 3*: 50-75% coverage, *Risser 3/4*:
 418 75-100% coverage, *Risser 4*: Fusion started, *Risser 5*: Fusion completed.

419 **(d) Oxford Hip Method from Acheson (1957).**

420 Nine regions are assessed as per pictorial below and values scores summed: femoral head,
 421 greater trochanter, lesser trochanter, iliac crest, ischium, ischio-pubic junction, pubic bone,
 422 acetabulum and tri-radiate cartilage. The five regions assessed in the abbreviated or
 423 ‘modified’ version of this method are marked with an asterisk (*) (Stasikelis et al. 1996[23]).

424 **(e) Knee from O’Connor et al. (2008).**

425 *Stage 0. Non-Union*: clear radiolucent strip between both sides of epiphyseal plate, *Stage 1.*
 426 *Beginning Union*: very narrow radiolucent strip, central hazy/ blurring as fusion starts (<50%
 427 of gap); *Stage 2. Active Union*: ‘Capping’ as epiphysis overlap the metaphysis. Fusion line/
 428 area of greater density area where fusion is taking place. Some areas of radiolucency remain,
 429 but fusion area is >50% of gap. *Stage 3. Recent Union*: Fine line of fusion remains but
 430 epiphysis and metaphysis are united (so-called ‘complete capping’). May be small notches at
 431 margins of <2mm. Discontinuity of trabeculae between former epiphysis and diaphysis. *Stage*
 432 *4. Complete Union*: mature bone, with no notches at margins, and continuous trabeculae. A
 433 thin terminal line or ‘epiphyseal scar’ may remain at the site of the epiphyseal plate.

434 **(f) Calcaneus. Adapted from Nicholson et al. 2015.**

435 Stage 0: No ossification can be seen. Stage 1: The apophysis covers < 50% of the metaphysis.
 436 Stage 2: The apophysis covers \geq 50% of the metaphysis but has not reached the plantar edge.
 437 Stage 3: Apophysis is within 2 mm of the plantar edge of the calcaneal concavity, as shown
 438 by the black arrow. Stage 4: Fusion taking place, but not yet complete as areas of
 439 radiolucency visible on dorsal and plantar edges. Fusion starts in the central area of the
 440 apophysis. Stage 5: Fusion is complete.

441

Table 1. Reliability: Inter- and intra-observer reliability assessed by Intraclass Correlation Coefficient calculation. Those with ICC >0.9 were regarded as ‘excellent’ and marked with bold script (ICC = intraclass correlation coefficient). Minimum and maximum intra-observer reliability values are shown only. (Reproduced from O’Sullivan et al.²³, creative commons license <https://creativecommons.org/licenses/by/4.0/legalcode>)

	Calcaneus	Cervical	Knee	Oxford Hip	Risser Plus
Inter-observer reliability	0.945	0.976	0.865	0.902	0.94
Intra-observer reliability	0.953-0.999	0.949-0.959	0.841-0.956	0.949-0.993	0.982-0.969

Table 2. Difficulty of Evaluation with each Bone Age Method

	Easy	Moderate	Difficult	Impossible	Easy	Moderate	Difficult	Impossible
Calcaneus	661	132	83	58	70.8%	14.1%	8.9%	6.2%
Cervical	738	104	53	39	79.0%	11.1%	5.7%	4.2%
Knee	637	221	75	1	68.2%	23.7%	8.0%	0.10%
Oxford Hip	734	127	71	2	78.6%	13.6%	7.6%	0.20%
Risser Plus	836	86	9	3	89.5%	9.2%	1.0%	0.32%

Summary of observer scan ratings using 4-point Likert scale as follows: ‘Easy’: some minor exposure problems or minor obstruction, but evaluation could confidently be made; ‘Moderate’: significant obstruction, image was partially cut off eg 1/3 or less of a landmark obscured or cut, such that assumption must be made; ‘Difficult’: landmark of interest outside of image or totally obstructed.

(The knee and oxford hip methods are composed of multiple landmarks and so when the overall scan was good but individual problems with landmarks were found. they were summed such that problems with 2 landmarks=rating of ‘2’ and ≥ 3 = rating of ‘3’. Similarly if difficulties were only reported with 1 of the 3 landmarks. the scan was rated as ‘2’.)

Table 3. Advantages and disadvantages of methods assessed.

	Calcaneus	Cervical	Knee	Oxford Hip	Risser Plus
Reliability	· Excellent (0.945)	· Excellent (0.976)	· Good (0.865)	· Excellent (0.902)	· Excellent (0.940)
Readability	70.8% of scans easily assessable, 6.2% of scans unassessable · Image length affected readability: Image must cover entire length of lower limb or not possible · Resolution: can be difficult distinguishing the timing of end of fusion (stage 4 vs. 5).	70.8% of scans easily assessable · Image length affected readability: EOS image must cover entire length of cervical spine or not possible · Positioning: (i) Head tilt can lead to mild difficulties. (ii) Hand position can obscure vertebrae making evaluation difficult or position (strict EOS protocol must be applied!)	68.2% of scans easily assessable · Step length: can influence readability of lateral radiographs. · Resolution: harder to evaluate features important in more mature stages (trabecular continuity, end of fusion)	78.6% of scans easily assessable · Complicated: large no. of regions must be evaluated. · Modified Oxford: simplified 5-region method may be superior for the clinician, however, omission of lesser trochanter may be required.	· 89.5% of scans easily assessable (highest rated)
Speed	· Fastest method (17.1s)	· Fast (26.5s)	· Slower (80.9s)	· Slowest method (82s)	· Fast (30.1s)
Age Range	· Broad age range: (4.32 - 11.03y)	· Broad age range (4.73 - 13.57y)	· Broad age range (5.07 - 15.02y)	· Broadest age range (4.0 - 15.08 y)	· Stages start later than other methods (6.55 - 15.27y)
Other	· Simple & Easy to learn · High rater satisfaction	· High rater satisfaction	· Low rater satisfaction	· High rater satisfaction though time consuming.	· High rater satisfaction · Familiar to orthopaedic physicians

Reliability values listed above are intraclass coefficient estimates of inter-observer reliability, see Table 1 for intra-observer coefficient values. Age range describes the chronological of first recorded incidence of 2nd stage within each system and the first incidence of the highest stage.

Supplementary Table 1. Bone Age Methods in the Scientific Literature 1931 - 2016. Summary table of all bone age and dental age methods encountered during literature review. The website pubmed.gov was accessed on 2016.03.30 and searched using keywords "bone age", "skeletal age" and "skeletal maturation" without any restrictions on date or language. After 433 duplicates were removed, all 4758 abstracts were reviewed for bone age methods used and articles accessed if not listed in the abstract. Original articles describing each method were sought if not included in the original list. Citation number as per google scholar (scholar.google.com) were collected at the time of preparing this table (2019.10.09). '*Article not found*': In some cases the article could not be found despite attempts to locate it, '*Foreign Language [language]*': search did not exclude foreign language inclusions, as a result some lesser known methods are included, which were not described in English, and could not be located. Three methods included were described after the original search date (marked *), however due to their potential future interest to bone age investigators they have been included. One method was included that was not returned in the search (marked †), but encountered during the course of the research and was included in the interest of completeness. (AP: Anteroposterior, CT: Computed tomography, GP: Greulich-Pyle Atlas, HF: Hassel-Farman method, mo: months, MR: Magnetic resonance, y: years)

Region	Author	Year of Pub.	Type	Citations	Modality	Image type	No. of Stages	Summary of Method	Reference
Ankle & Foot	Hoerr, Pyle, Francis	1962	Atlas	5	X-ray	Lateral & AP Foot	31 ages	Atlas method of ankle and foot.	Hoerr NL, Pyle SI, Francis CC. Radiological Atlas of the Foot and Ankle. Charles C Thomas, Springfield., 1962.
Calcaneus	Nicholson	2015	Scoring	20	X-ray	Lateral foot	6 stages	Calcaneal apophysis is scored based on presence, extent and state of fusion.	Nicholson AD, Liu RW, Sanders JO, Cooperman DR. Relationship of Calcaneal and Iliac Apophyseal Ossification to Peak Height Velocity Timing in Children. J Bone Jt Surg. 2015;97(2):147-154.
	Sherif	2003	Scoring	3	Ultrasound	Ultrasound	Linear scale	Normal range of calcaneal volume values in a 0-6 year old Egyptian population have been presented, as measured by ultrasound.	Sherif H, Noureldin M, Bakr AF, Mahfouz AE. Sonographic Measurement of Calcaneal Volume for Determination of Skeletal Age in Children. J Clin Ultrasound. 2003;31(9):457-460.
Cervical	Alhadlag & Al-shayea	2013	Scoring	6	X-ray	Lateral cephalogram	5 stages	Angular based method: user traces C2-C3-C4 and calculates the angles between a line running along the base, and the highest point of the inferior concavity. 5 stages were identified correlating to Baccetti's method. Only males.	Alhadlaq AM, Al-shayea EI. New method for evaluation of cervical vertebral maturation based on angular measurements. Saudi Med J. 2013;33(4):388-394.
	Baccetti: 6-stage	2002	Scoring	655	X-ray	Lateral cephalogram	6 stages	Second to fourth cervical vertebrae are assessed by morphology: height, inferior curvature and shape. "CS" or "cervical stage" method.	Baccetti T, Franchi L, McNamara Jr JA. An improved version of the cervical vertebral maturation (CVM) method for the assessment of mandibular growth. Angle Orthod. 2002;72(4):316-323.
	Baccetti modified: Semi-automated	2012	Scoring	11	X-ray	Lateral cephalogram	6 stages	User selects 13 landmarks on C2-C4 indicating anterior inferior, posterior inferior, anterior superior (C3 & C4 only) and posterior superior points (C3 & C4 only), and the highest point of the inferior concave. Stages as per Baccetti are then applied using computer software.	Baptista RS, Quaglio CL, Mourad LMEH, et al. A semi-automated method for bone age assessment using cervical vertebral maturation. Angle Orthod. 2012;82(4):658-662.
	Baccetti modified: CT	2015	Scoring	29	CT	Cone-beam CT	6 stages	Lateral cephalogram generate from CBCT and evaluated.	Angelieri F, Franchi L, Cevidanes LHS, McNamara Jr JA. Diagnostic performance of skeletal maturity for the assessment of midpalatal suture maturation. Am J Orthod Dentofac Orthop. 2015;148(6):1010-1016.
	Baccetti modified: 5 stage	2006	Scoring	23	X-ray	Lateral cephalogram	5 stages	Sixth stage is not included.	Santos ECA, Bertoz FA, Arantes FDM, Reis PMP, Bertoz APDM. Skeletal maturation analysis by morphological evaluation of the cervical vertebrae. J Clin Pediatr Dent. 2006;30(3):265-270.
	Caldas	2007	Scoring	42	X-ray	Lateral cephalogram	Linear regression equation	Based on a formula, reader traces and then measures height, width, angle etc.	Caldas M de P, Ambrosano GMB, Haiter Neto F. New formula to objectively evaluate skeletal maturation using lateral cephalometric radiographs. Braz Oral Res. 2007;21(4):330-335.
	Caldas modified: Semi-automated	2010	Scoring	25	X-ray	Lateral cephalogram	Linear regression equation	Based on a formula, selects landmarks indicating anterior/posterior and superior/inferior poles, and software calculates bone age based on Caldas' equation.	Caldas M de P, Bovi Ambrosano GM, Neto FH. Computer-assisted analysis of cervical vertebral bone age using cephalometric radiographs in Brazilian subjects. Braz Oral Res. 2010;24(1):120-126.
	Chen	2008	Scoring	64	X-ray	Lateral cephalogram	4 stages	So-called "Quantitative cervical morphology" or QVCM. Tracings of C3, C4: ant height, posterior height, middle height and superior/midline/inferior anteroposterior length. Formula made based on these can calculate SMI (as used in Fishman maturity)	Chen L-L, Xu T-M, Jiang J-H, Zhang X-Z, Lin J-X. Quantitative cervical vertebral maturation assessment in adolescents with normal occlusion: a mixed longitudinal study. Am J Orthod Dentofac Orthop. 2008;134(6):720-e1.
	Franchi	2000	Atlas	420	X-ray	Lateral cephalogram	6 stages	Cervical vertebral morphology are assessed at C2-C6. Baccetti et al. method is based on a abbreviated system.	Franchi L, Baccetti T, McNamara JA. Mandibular growth as related to cervical vertebral maturation and body height. Am J Orthod Dentofac Orthop. 2000;118(3):335-340.

Harfin	2008	-	3	X-ray	Lateral cephalogram	-	Not found - foreign language [Polish]	Harfin, J.F., Kahn de Gruner, S.E., Porta, G. and Kaplan, A., 2008. Nowy sposób określania wieku szkieletowego oparty na wtórnych ośrodkach kostnienia kręgów szyjnych. In Forum Ortod (Vol. 4, No. 2, pp. 33-43).
Hassel-Farman	1995	Scoring	713	X-ray	Lateral cephalogram	6 stages	C2-C4 morphology based on shape, inferior curve depth, and height.	Hassel B, Farman AG. Skeletal maturation evaluation using cervical vertebrae. Am J Orthod Dentofacial Orthop. 1995;107(1):58-66.
Hassel-Farman modification: C3 only	2005	Scoring	26	X-ray	Lateral cephalogram	6 stages	HF method, only assessing C3.	Seedat AK, Forsberg CD. An evaluation of the third cervical vertebra (C3) as a growth indicator in Black subjects. SADJ. 2005 May;60(4):156,158-60
Hassel-Farman modification: Semi-automated	2015	Scoring	3	X-ray	Lateral cephalogram	6 stages	Software assisted. Physician traces the vertebrae, and it helps estimate.	Dzemidzic, V., Sokic, E., Tiro, A. and Nakas, E., 2015. Computer based assessment of cervical vertebral maturation stages using digital lateral cephalograms. Acta Informatica Medica, 23(6), p.364.
Hassel-Farman modification: 3D-CT	2016	Scoring	6	CT	Lateral image 3D CT	6 stages	HF method, using lateral aspect as generated from 3D CT images.	Bonfim MAE, Costa ALF, Fuziy A, Ximenez MEL, Cotrim-Ferreira FA, Ferreira-Santos RI. Cervical vertebrae maturation index estimates on cone beam CT: 3D reconstructions vs sagittal sections. Dentomaxillofacial Radiol. 2016;45(1):20150162.
Lamparski	1972	Scoring	17	X-ray	Lateral cephalogram	6 stages	First cervical morphology method described.	Lamparski DG. Skeletal age assessment utilizing cervical vertebrae. 1975;67(4):458-459.
Mito	2002	Scoring	180	X-ray	Lateral cephalogram	Linear regression equation	C3 & C4 tracings made and measurements of anterior height, posterior height, midpoint height and anteroposterior length. Equation made based on these.	Mito T, Sato K, Mitani H. Cervical vertebral bone age in girls. Am J Orthod Dentofac Orthop. 2002;122(4):380-385.
Rhee	2015	Scoring	2	CT	Cone-beam CT	Linear regression equation	C2-C4: 8 points per vertebra, 6 points on odontoid process. Linear regression generated equations	Rhee CH, Shin SM, Choi YS, et al. Application of statistical shape analysis for the estimation of bone and forensic age using the shapes of the 2nd, 3rd, and 4th cervical vertebrae in a young Japanese population. Forensic Sci Int. 2015;257:513.e1-513.e9.
San Roman	2002	Scoring	254	X-ray	Lateral cephalogram	Linear regression equation	C3 & C4: equation based on stages of 3 features: inferior concavity (6 stages), vertebral shape (6 stages) and height vs. width (6 stages).	Román PS, Palma JC, Oteo MD, Nevado E. Skeletal maturation determined by cervical vertebrae development. Eur J Orthod. 2002;24(3):303-311.
Santiago	2014	Scoring	5	X-ray	Lateral cephalogram	4 stages	User selects 13 landmarks on C2-C4 indicating anterior inferior, posterior inferior, anterior superior (C3 & C4 only) and posterior superior points (C3 & C4 only), and the highest point of the inferior concave. Stages as per Baccetti are then applied using computer software. Stages correlated to Fishman SMI 1:1-3, 2: 4-7, 3: 8-9, 4:10-11.	Santiago RC, Cunha AR, Júnior GC, et al. New software for cervical vertebral geometry assessment and its relationship to skeletal maturation-a pilot study. Dentomaxillofacial Radiol. 2014;43(2).
Su	2006	Scoring	0	-	-	Linear regression equation	Description in Chinese: Abstract - equation based on vertebral anterior height, height, anteroposterior length of C3 and C4.	Su L, Lü Y, Wang HM. Cervical vertebral bone age during puberty. Zhonghua kou qiang yi xue za zhi= Zhonghua kouqiang yixue zazhi= Chinese J Stomatol. 2006;41(12):728-729.
Varshosaz	2012	Scoring	9	X-ray	Lateral cephalogram	Linear regression equation	Anterior height of C4 measured and used as part of equation. 91 Iranian individuals aged 8-18 years	Varshosaz M, Ehsani S, Nouri M, Tavakoli MA. Bone age estimation by cervical vertebral dimensions in lateral cephalometry. Prog Orthod. 2012;13(2):126-131.
Yang	2014	Scoring	8	CT	Cone-beam CT	Linear regression equation	C1-C4: Axial images generated and 23 points selected across the vertebrae, (most anterior point, posterior point etc). Linear regression derived equations could then be applied to establish bone age. Equations not shown in paper, though they find several regions	Yang Y, Lee J, Kim Y, Cho B, Park S. Axial cervical vertebrae- based multivariate regression model for the estimation of skeletal-maturation status. Orthod Craniofac Res. 2014;17(3):187-196.

								alone were correlated well with maturation.	
Clavicle	Kreitner	1998	Scoring	249	CT	Multi-slice CT	3 stages	Appearance, partial fusion and complete fusion of medial epiphyseal ossification center.	Kreitner K-F, Schweden FJ, Riepert T, Nafe B, Thelen M. Bone age determination based on the study of the medial extremity of the clavicle. <i>Eur Radiol.</i> 1998;8(7):1116-1122.
	Schmeling: 5 stage	2004	Scoring	296	X-ray	Chest X-ray	5 stages	Initial 4 stages based on common schema: non-fused, fusing, almost fused, fused, in addition to a further fifth stage when no scar can be seen.	Schmeling A, Schulz R, Reisinger W, Mühler M, Wernecke K-D, Geserick G. Studies on the time frame for ossification of the medial clavicular epiphyseal cartilage in conventional radiography. <i>Int J Legal Med.</i> 2004;118(1):5-8.
	Schmeling modified: 4 stage	2015	Scoring	18	CT	Multi-slice CT	4 stages	Initial 4 stages based on common schema: non-fused, fusing, almost fused, fused (independent of presence or absence of scar) some studies such as Zhang et al. have used this 4 stage method.	Zhang K, Chen X, Zhao H, Dong X, Deng Z. Forensic Age Estimation Using Thin-Slice Multidetector CT of the Clavicular Epiphyses Among Adolescent Western Chinese. <i>J Forensic Sci.</i> 2015;60(3):675-678.
	Schmeling modified: MR	2010	Scoring	87	MR	MR	5 stages	Initial 4 stages based on common schema: non-fused, fusing, almost fused, fused, in addition to a further stage 5 when no scar can be seen.	Hillewig E, De Tobel J, Cuche O, Vandemaele P, Piette M, Verstraete K. Magnetic resonance imaging of the medial extremity of the clavicle in forensic bone age determination: A new four-minute approach. <i>Eur Radiol.</i> 2011;21(4):757-767.
	Schmeling modified: 4 stage	2010	Scoring	179	CT	Thin slice CT	9 stages	Second and third stages are expanded with 3 substages each.	Kellinghaus M, Schulz R, Vieth V, Schmidt S, Pfeiffer H, Schmeling A. Enhanced possibilities to make statements on the ossification status of the medial clavicular epiphysis using an amplified staging scheme in evaluating thin-slice CT scans. <i>Int J Legal Med.</i> 2010;124(4):321-325.
	Schmidt	2007	Scoring	133	MR	MR	4 stages	Presence of ossification at the secondary center, extent and completion are assessed at the medial clavicle.	Schmidt S, Mühler M, Schmeling A, Reisinger W, Schulz R. Magnetic resonance imaging of the clavicular ossification. <i>Int J Legal Med.</i> 2007;121(4):321-324.
	Schulz	2008	Scoring	99	Ultrasound	Ultrasound	4 stages	Appearance and fusion of medial clavicle ossification centre are assessed, in addition to epiphyseal plate shape and state of ossification.	Schulz R, Zwiesigk P, Schiborr M, Schmidt S, Schmeling A. Ultrasound studies on the time course of clavicular ossification. <i>Int J Legal Med.</i> 2008;122(2):163-167.
Cranial	Lottering	2015	Scoring	22	CT	Multi-slice Head CT	6 stages	6 stages based on Spheno-Occipital Synchronosis ossification.	Lottering N, Macgregor DM, Alston CL, Gregory LS. Ontogeny of the spheno-occipital synchronosis in a modern Queensland, Australian population using computed tomography. <i>Am J Phys Anthropol.</i> 2015;157(1):42-57.
	Lottering	2016	Scoring	9	CT	Cranial/ cervical multi-slice CT	24 stages, different region: (total 19).	6 fontanelles & osteosynchronosis regions are assessed. The time of closure of each region is described by as few as 2 or as many as 4 stages.	Lottering N, Macgregor DM, Alston CL, Watson D, Gregory LS. Introducing Computed Tomography Standards for Age Estimation of Modern Australian Subadults Using Postnatal Ossification Timings of Select Cranial and Cervical Sites. <i>J Forensic Sci.</i> 2016;61(3):39-52.
	Bassed	2010	Scoring	74	CT	Multi-slice CT	5 stages	Ossification extent from superior to inferior of the spheno-occipital chondrosis. (Staging modified from Powell and Brodie, 1963 - forensic study with X-ray).	Bassed RB, Briggs C, Drummer OH. Analysis of time of closure of the spheno-occipital synchronosis using computed tomography. <i>Forensic Sci Int.</i> 2010;200(1-3):161-164.
	Shirley & Jantz	2011	Scoring	78	CT	Cone-beam head CT	3 stages	The open/fusing/fused state is assessed at the spheno-occipital osteochondrosis.	Shirley NR, Jantz RL. Spheno-occipital synchronosis fusion in modern Americans. <i>J Forensic Sci.</i> 2011;56(3):580-585.
	Franklin & Flavel	2014	Scoring	34	CT	Multi-detector CT	4 stages	Spheno-occipital osteochondrosis is evaluated for open/fusing/fused with scar/ fused with no scar.	Franklin D, Flavel A. Brief Communication: Timing of spheno-occipital closure in modern Western Australians.

	Ertürk	1968	Scoring	5	X-ray	Lateral cephalogram	No stages	Frontal sinus maximum dimension height and width measured are measured and can be compared against standards.	Am J Phys Anthropol. 2014;153(1):132-138. Ertürk, N., 1968. Teleroentgen studies on the development of the frontal sinus. Fortschritte der Kieferorthopädie, 29(2), pp.245-248.
Dental	Cameriere	2006	Scoring	247	X-ray	Panoramic X-ray	Linear regression equation	Open root apices of the teeth are measured, and summed. Data can be entered into linear regression equation.	Cameriere R, Ferrante L, Cingolani M. Age estimation in children by measurement of open apices in teeth. Int J Legal Med. 2006;120(1):49-52.
	Demirjian	1973	Scoring	2031	X-ray	Panoramic X-ray	63 stages	Seven left mandibular permanent teeth are rated in the order of the second molar, first molar, second premolar, first premolar, canine, lateral incisors and central incisor into eight stages [A-H] of tooth mineralization, stage 0 marks absence/ non-appearance of a tooth. All ratings are compared against a table to give a maturity score per tooth, which are summed, and then overall maturity score can be compared against a developmental percentile chart for each gender.	Demirjian A, Goldstein H, Tanner JM. Demirjian, A., A New System of Dental Age Assessment, Human Biology, 45:2 (1973:May) p.211. Hum Biol. 1973;45(2):211-227.
	Demirjian modified: Chaillet	2005	Scoring	158	X-ray	Panoramic X-ray	63 stages	"Multi-ethnic weighted score" chart, that allows use independent of knowledge of ethnicity.	Chaillet N, Nyström M, Demirjian A. Comparison of Dental Maturity in Children of Different Ethnic Origins: International Maturity Curves for Clinicians. J Forensic Sci. 2005;50(5):1-11.
	Demirjian modified: Third Molar only	1993	Scoring	500	X-ray	Panoramic X-ray	8 stages	Third molar only. All 4 evaluated and averaged.	Mincer HH, Harris EF, Berryman HE. The A.B.F.O. Study of Third Molar Development and Its Use as an Estimator of Chronological Age. J Forensic Sci. 1993;38(2):13418J. doi:10.1520/jfs13418j
	Demirjian modified: Willems	2001	Scoring	417	X-ray	Panoramic X-ray	63 stages	Updated chart for Belgian children to avoid overestimation of bone age.	Willems G, Van Olmen A, Spiessens B, Carels C. Dental age estimation in Belgian children: Demirjian's technique revisited. J Forensic Sci. 2001;46(4):893-895.
	Demirjian modified: Four Tooth Modification	1989	Scoring	70	X-ray	Panoramic X-ray	36 stages	Using just 4 teeth. Based on Finnish standards.	Kataja M, Nyström M, Aine L. Dental maturity standards in southern Finland. Proc Finn Dent Soc. 1989;85(3):187-197.
	Gat	1972	Scoring	2	X-ray	Panoramic X-ray	84 stages	Fourteen permanent teeth on mandible and maxilla are scored from 1-5, excluding the third molar, and the sum of the values is the 'dental age'.	Gat H. An evaluation of dental ages of Norwegian children from the Bergen area. Univ Bergen, Bergen. 1972.
	Gleiser & Hunt	1995	Scoring	442	X-ray	Lateral mandibular	15 stages	First right mandibular permanent molar evaluated.	Gleiser I, Hunt Jr EE. The Permanent Mandibular First Molar: Its Calcification, Eruption and Decay. Am J Phys Anthropol. 1995;(13):253-283.
	Gleiser & Hunt modification: Kullman	1992	Scoring	251	X-ray	Panoramic X-ray	7 stages	Third molar root development is evaluated.	Kullman L, Johanson G, Akesson L. Root development of the lower third molar and its relation to chronological age. Swed Dent J. 1992;16(4):161-167.
	Gleiser & Hunt modification: Liversidge	2008	Scoring	157	X-ray	Panoramic X-ray/ Supplementary apical in some cases	15 stages	Third molar evaluated based on progressive stages described by changes in the crypt, cusp, crown, cleft, root and apex: applicable on from 16 years and above.	Liversidge HM. Timing of human mandibular third molar formation. Ann Hum Biol. 2008;35(3):294-321.
	Gustafson & Koch	1974	Scoring	432	X-ray	Panoramic X-ray	90 stages	Emergence and 3 maturation stages for right lower and left upper teeth are shown in their diagrams. Values are compared against a reference chart which gives weighting, and corresponding dental age.	Gustafson G, Koch G. Age estimation up to 16 years of age based on dental development. Odontol Revy. 1974;25(3):297-306.
	Haavikko	1974	Scoring	203	X-ray	Panoramic X-ray	6 stages	Upper and lower first molar, canine, 1st incisor and lower 2nd molar, 1st premolar and 2nd incisor are scored, and averaged. This can then allow division into 6 groups.	Haavikko K. Tooth formation age estimated on a few selected teeth. Proc Finn Dent Soc. 1974;70:15-19.
	Leinonen	1972	Scoring	10	X-ray	Panoramic X-ray	8 stages	Staging applied 0-7 of each mandibular tooth, the two sides were averaged.	Leinonen A, Wasz-Höckert B, Vuorinen P. Usefulness of the dental age obtained by orthopantomography as an indicator of the physical age. Proc Finn Dent Soc. 1972;68(5):235-242.

	Liljeqvist & Lundberg	1971	Scoring	172	X-ray	Full oral series	8 stages per tooth	8 weighted stages applied based on dental morphology of crown, root etc, all teeth evaluated excepting upper pre-molar and molars.	Liljeqvist B, Lundberg M. Skeletal and tooth development: a methodologic investigation. Acta Radiol Diagn. 1971;11(2):97-112.
	Moorrees	1963	Scoring	2148	X-ray	Lateral & intraoral radiographs (two population samples combined therefore differing radiograph types)	14 stages	Mandibular teeth evaluated based on progressive stages described by changes in the crypt, cusp, crown, cleft, root and apex.	Moorrees CFA, Fanning EA, Hunt EE. Age Variation of Formation Stages for Ten Permanent Teeth. J Dent Res. 1963;42(6):1490-1502.
	Moorrees modification: Anderson	1976	Scoring	332	X-ray	Panoramic Xray	14 stages	Mandibular and maxillary teeth assessed, applied to as many teeth as possible and the score averaged. They provided alternative tables that some authors prefer.	Anderson DL, Thompson GW, Popovich F. Age of attainment of mineralization stages of the permanent dentition. J Forensic Sci. 1976;21(1):191-200.
	Moorrees modification: London Atlas	2010	Atlas	577	X-ray	Panoramic X-ray	Atlas	"London Atlas" combining emergence data and the Moorrees method, applicable from the first prenatal trimester to 23 years old.	AlQatani SJ, Hector MP, Liversidge HM. Brief communication: The London atlas of human tooth development and eruption. Am J Phys Anthropol. 2010;142(3):481-490.
	Nicodemo	1974	Atlas	73	X-ray	Panoramic X-ray	Foreign Language [Chinese]	Foreign Language [Chinese]	Nicodemo RA, Moraes LC, Médiçi Filho E. Tabela cronológica da mineralização dos dentes permanentes entre brasileiros. Rev Fac Odontol São José dos Campos. 1974;3(1):55-56.
	Nolla	1960	Scoring	1129	X-ray	Full oral series	70 stages	Each permanent tooth the left mandible is rated as per calcification stage (1-10) and values summed.	Nolla CM. The development of permanent teeth. 1952.
	Schour & Massler	1941	Atlas	340	X-ray	Panoramic X-ray	21 chronologica ages	21 stages identified: 2 prenatal followed by 0 months, 6mo , 9mo, 1 year, 16mo, 2y, 3y, 4y, 5y, 6y, 7y, 8y, 9y, 10y, 11y, 12y, 15y, 21y, 35y.	Massler M, Schour I, Poncher HG. Developmental pattern of the child as reflected in the calcification pattern of the teeth. Am J Dis Child. 1941;62(1):33-67.
Elbow	Sauvegrain	1962	Scoring	53	X-ray	Elbow: AP and Lateral	27 points	Lateral condyle, trochlea, olecranon apophysis and proximal radial epiphysis evaluated.	Sauvegrain J, Nahum H, Bronstein H. Study of bone maturation of the elbow. In: Annales de Radiologie. Vol 5 ; 1962:542.
	Sauvegrain modified: Dimeglio	2005	Scoring	117	X-ray	Elbow: AP and Lateral	30 point	Intermediate scores added between 3 points, for a total of 30 points.	Accuracy of the Sauvegrain Method in Determining Skeletal Age During Puberty. 2005;1689-1696.
	Sauvegrain modified: Dimeglio (Simplified)	2001	Scoring	76	X-ray	Elbow: Lateral only	8 points	Simplified method in which only olecranon apophysis assessed.	Diméglio A. Growth in pediatrics orthopaedics. In: Lovell, Winter, eds. Vol. I chapter II, 5th ed. Lippincott; 2001 (in press).
Face	Braga	2007	Scoring	58	CT	CT	Linear Equation	8 foramina identified, computer applies a cage/ mesh made and the shape is related to maturity via linear regression equation.	Braga J, Treil J. Estimation of pediatric skeletal age using geometric morphometrics and three-dimensional cranial size changes. Int J Legal Med. 2007;121(6):439-443.
Femur	Castriota-Scanderbe & De Micheli	1995	Scoring	32	Ultrasound	Hip Ultrasound	Continuous Scale	Femoral head cartilage thickness measured, decreases with increasing age and can be compared to table.	Castriota-Scanderbeg A, De Micheli V. Ultrasound of femoral head cartilage: a new method of assessing bone age. Skeletal Radiol. 1995;24(3):197-200.
	Stull	2014	Scoring	32	X-ray	Femur: AP	Linear Equation	Based on femoral measurements, diaphyseal length can be correlated reliably with age until 6 years old, or with multivariate models entailing predominantly diaphyseal width for older individuals.	Lodox Statscan, invented in South Africa for mining industry . Similar to EOS.
Foot	Whitaker	2002	Scoring	27	X-ray	Foot AP & Lateral	10 stages	Calcaneus primary and secondary ossification centers are rated 0-4, and on their fusion state from 0-4. All three scores are summed.	Whitaker JM, Rousseau L, Williams T, Rowan RA, Hartwig WC. Scoring system for estimating age in the foot skeleton. Am J Phys Anthropol Off Publ Am Assoc Phys Anthropol. 2002;118(4):385-392.
	Whitaker	2002	Scoring	27	X-ray	Foot AP & Lateral	10 stages	All distal phalangeal and proximal phalangeal primary and secondary ossification centers are rated 1-4, and on their fusion state from 1-4. All three scores are summed and converted to a 10 point scale. Uniquely, images were marked with a special score if ossification was not visible or obscured due to image quality or obstruction.	Whitaker JM, Rousseau L, Williams T, Rowan RA, Hartwig WC. Scoring system for estimating age in the foot skeleton. Am J Phys Anthropol Off Publ Am Assoc Phys Anthropol. 2002;118(4):385-392.

Hand-wrist	Björk & Helm	1967	Scoring	563	X-ray	Right Hand	8 stages	Key events are recorded at the second finger, third finger, thumb sesamoid and radius are evaluated.	Björk A, Helm S. Prediction of the age of maximum puberal growth in body height. <i>Angle Orthod.</i> 1967;37(2):134-143.
	Cameriere	2006	Scoring	76	X-ray	Left Hand	Linear Equation	The ratio of the area occupied by the carpal bones versus the total area of the radial and ulnar epiphysis and carpals is calculated and compared against a reference line.	Cameriere R, Ferrante L, Mirtella D, Cingolani M. Carpals and epiphyses of radius and ulna as age indicators. <i>Int J Legal Med.</i> 2006;120(3):143-146.
	Cameriere modification: De Luca	2016	Scoring	4	X-ray	Left Hand	Linear Equation	Updated formula for greater accuracy.	De Luca S, Mangiulli T, Merelli V, et al. A new formula for assessing skeletal age in growing infants and children by measuring carpals and epiphyses of radio and ulna. <i>J Forensic Leg Med.</i> 2016;39(January):109-116. doi:10.1016/j.jflm.2016.01.030
	Chang et al.	1990	Scoring	4	X-ray	Hand (side not found)	9 stages	"National Taiwan University Hospital Skeletal Maturity Index". Five locations on the thumb, index finger, middle finger and radius are evaluated.	Chang HF, Wu K-M, Chen KC. A cross-sectional study on the skeletal development of the hand and wrist from preadolescence to early adulthood among Chinese in Taiwan. <i>Zhonghua ya yi xue hui za zhi.</i> 1990;9(1):1-11.
	Chinese National Sports Committee	1992	Foreign Language [Chinese]	3	X-ray	Foreign Language [Chinese]	Foreign Language [Chinese]	So-called 'Chinese Standard' method. Metacarpal, phalanges and carpal bone developmental stages are assessed.	Committee NS. Assessment of development of metacarpals, phalanges and carpals of Chinese people: national standard of People's Republic of China. <i>Beijing Natl Sport Comm.</i> 1992.
	Choi et al.	2018	Scoring	5	X-ray	Left or Right	Continuous	Area of the capitate and hamate is measured and summed. Value can be input to regression equation.	Choi JA, Kim YC, Min SJ, Khil EK. A simple method for bone age assessment: The capitohamate planimetry. <i>Eur Radiol.</i> 2018;28(6):2299-2307.
	DeRoo & Schroder	1976	Atlas	34	X-ray	Hand (side not found)	Atlas	Similarities to Greulich-Pyle atlas, though initiated in Dutch European children.	de Roo T, Schröder HJ. <i>Pocket Atlas of Skeletal Age.</i> Springer Science & Business Media; 2012.
	Luk	2014	Scoring	22	X-ray	Distal Radius-Ulna	11 & 9 stages	"DRU" (distal radius ulna) method, in which the radius epiphysis is scored from 1-11 stages and the ulna from 1-9 stages, each can be individually compared to chronological age.	Luk KDK, Saw LB, Grozman S, Cheung KMC, Samartzis D. Assessment of skeletal maturity in scoliosis patients to determine clinical management: a new classification scheme using distal radius and ulna radiographs. <i>Spine J.</i> 2014;14(2):315-325.
	Ebri	1993	Scoring	1	X-ray	Left Hand	Linear Equation	Maximum dimensions of carpal and phalangeal epiphyseal are measured and evaluated compared to a linear regression equation.	Ebri BT. New method for evaluating ossification of the carpal bone. From a study with 5225 Spanish children. <i>Pediatric.</i> 1993;48(11):813-817.
	Eklöf & Ringertz	1967	Scoring	94	X-ray	Left Hand	Linear Equation	Distances are measured that correspond to the width and length of the hand and wrist bones, in ten ossification centers.	Eklöf O, Ringertz H. A method for assessment of skeletal maturity. In: <i>Annales de Radiologie.</i> Vol 10. ; 1967:330-336.
	Eklöf & Ringertz modification: 3 bone method	2009	Scoring	1	X-ray	Left Hand	Linear Equation	Abbreviated version for only 3 ossification centers.	Olivete CJ, Rodrigues ELL. ER5 and ER3: bone age assessment by simplifications of the Eklof and Ringertz method = Maturidade óssea: estimação por simplificações do método de Eklof e Ringertz. <i>Rev Odonto Ciência.</i> 2009;24(4):361-366.
	Eklöf & Ringertz modification: 5 bone method	2009	Scoring	1	X-ray	Left Hand	Linear Equation	Abbreviated version for only 5 ossification centers.	Olivete CJ, Rodrigues ELL. ER5 and ER3: bone age assessment by simplifications of the Eklof and Ringertz method = Maturidade óssea: estimação por simplificações do método de Eklof e Ringertz. <i>Rev Odonto Ciência.</i> 2009;24(4):361-366.
	Engström	1983	Scoring	189	X-ray	Left Hand	5 stages	Only 4 key events at specific regions are noted: epiphysis of the 2nd proximal phalanx is wide as the diaphysis; the epiphysis of the 3rd middle phalanx caps its diaphysis; complete epiphyseal fusion of the distal phalanx of 3rd finger; complete union of the distal epiphysis of the radius.	Engström C, Engström H, Sagne S. Lower Third Molar Development in relation to Skeletal Maturity and Chronological Age. <i>Angle Orthod.</i> 1983;53(2):97-106.

Fishman	1982	Scoring	664	X-ray	Left Hand	11 stages	Key events are recorded at the third finger, fifth finger, radius and thumb sesamoid appearance. Fishman described these as 'skeletal maturity indicators' for correlation with mandibular and maxillary development, therefore favoured by orthodontists.	Fishman L.S. Radiographic evaluation of skeletal maturation: a clinically oriented method based on hand-wrist films. <i>Angle Orthod.</i> 1982;52(2):88-112.
Flory	1936	Atlas	155	X-ray	Right Hand	Atlas: newborn 19 years old	Phalangeal and carpal atlas.	Flory CD. Osseous development in the hand as an index of skeletal development. <i>Monogr Soc Res Child Dev.</i> 1936;1(3):i-141.
Gilsanz & Ratib	2005	Atlas	216	X-ray	Left Hand	Atlas	A digital hand atlas for assessment of phalanges, metacarpals and carpals.	Gilsanz V, Ratib O. <i>Hand Bone Age: A Digital Atlas of Skeletal Maturity.</i> Springer Science & Business Media; 2005.
Grave & Brown	1976	Scoring	382	X-ray	Hand (side not found/listed)	14 stages	Fourteen ossification events are assessed first, second and third fingers in addition to the pisiform, hamate and distal radial epiphysis. Events are also correlated with peak growth velocity.	Grave KC, Brown T. Skeletal ossification and the adolescent growth spurt. <i>Am J Orthod.</i> 1976;69(6):311-619.
Gretych	2007	Atlas	117	X-ray	Left Hand	Atlas	Second, third and fourth phalanges in addition to the carpals are evaluated with computer assistance in with reference to Caucasian, African-America, Asian and Hispanic children.	Gretych A, Zhang A, Sayre J, Pospiech-Kurkowska S, Huang HK. <i>Bone Age Assessment of Children using a Digital Hand Atlas.</i> <i>Comput Med Imaging Graph.</i> 2007;31(4-5):322-331.
Greulich & Pyle	1950/1959	Atlas	7699	X-ray	Left Hand	Atlas	The most well-known phalangeal and carpal atlas, first published in 1950, updated and expanded in 1959.	Greulich WW, Pyle SL. <i>Radiographic Atlas Of Skeletal Development Of The Hand And Wrist.</i> <i>Am J Med Sci.</i> 1959;238(3):393.
Greulich & Pyle modification: Individual Scoring	1971	Atlas	53	X-ray	Left Hand	Atlas	All bones are scored individually and then average bone age calculated.	Roche AF, Eyman SL, Davila GH. Skeletal age prediction. <i>J Pediatr.</i> 1971;78(6):997-1003. doi:10.1016/S0022-3476(71)80430-4.
Greulich & Pyle modification: Weighted Modification	1972	Atlas	23	X-ray	Right or Left Hand	Atlas	All bones are scored individually and summed by region (carpals, phalanges-metacarpals or forearm), and weighting is performed based on each region.	Kimura K. Skeletal maturation of children in Okinawa. <i>Ann Hum Biol.</i> 1976;3(2):149-155.
Greulich & Pyle modification: Weighted Modification	1986	Atlas	4	X-ray	Left Hand	Atlas	Regions are scored individually and summed according to a weighted formula.	Aicardi G, Di Battista E, Naselli A, Vignolo M, De Scrilli A. Affidabilità dei piucomuni metodi di previsione della statura adulta in un campione di adolescenti italiani. <i>Acta Med Auxol.</i> 1986;18:55-65.
Greulich & Pyle modification: Weighted Modification	1971	Atlas	10	X-ray	Left Hand	Atlas	Higher weighting to metacarpals and phalanges II to V.	Peritz E, Sproul A. Some aspects of the analysis of hand- wrist bone- age readings. <i>Am J Phys Anthropol.</i> 1971;35(3):441-447.
Greulich & Pyle modification: Line Drawings	1950	Atlas	90	X-ray	Left Hand	Atlas	Greulich-Pyle Atlas converted to line drawings for easier use.	Buckler JMH, Buckler JMH. <i>A Reference Manual of Growth and Development.</i> Blackwell Science London; 1997.
Greulich & Pyle modification: Shorthand Bone Age	2013	Atlas	30	X-ray	Left Hand	Atlas	Abbreviated version of Greulich-Pyle atlas in which 10 specific events at the first and second digit, hamate, and radial epiphysis are assessed.	Heyworth BE, Osei DA, Fabricant PD, et al. The shorthand bone age assessment: a simpler alternative to current methods. <i>J Pediatr Orthop.</i> 2013;33(5):569-574.
Greulich & Pyle modification: Ultrasound	2003	Atlas	56	Ultrasound	Left Hand	Atlas	Tracings are made from ultrasound evaluations to represent the full hand and wrist, which can then be evaluated as per the GP atlas.	Bilgili Y, Hizel S, Kara SA, Sanli C, Erdal HH, Altinok D. Accuracy of skeletal age assessment in children from birth to 6 years of age with the ultrasonographic version of the Greulich-Pyle atlas. <i>J Ultrasound Med.</i> 2003;22(7):683-690.
Greulich & Pyle modification: 'Segmented'	2001	Atlas	51	X-ray	Left Hand	Atlas	Seven regions are scored as groups - the carpals, metacarpals, proximal, medial and distal phalanges, radius, and ulna - and the sum divided by seven.	Mul D, Oostdijk W, Waelkens JJJ, Schulpen TWJ, Drop SLS. Gonadotrophin releasing hormone agonist treatment with or without recombinant human GH in adopted children with early puberty. <i>Clin Endocrinol (Oxf).</i> 2001;55(1):121-129.
Greulich & Pyle modification:	2008	Scoring	4	X-ray	Left Hand	2 stages	Binary staging of presence or absence of ulnar sesamoid of the first digit. Not recommended by the authors for use alone.	Chaumoitre K, Adalian P, Colavolpe N, et al. Value of the sesamoid bone of the thumb in the determination of

Thumb Sesamoid only Gu's method	-	-	-	-	-	-	-	Foreign Language [Chinese]	bone age. J Radiol. 2008;89(12):1921-1924. Zhang Z, Li K, Yu RJ, Zhang Q. Preliminary study on the applying value of two measurements for bone age in the cases of minors. Fa Yi Xue Za Zhi. 2004;20(4):212-214.
Haavikko	1974	-	7	-	-	-	-	Original article could not be obtained.	Haavikko K. Skeletal age estimated in a few selected ossification centres of the hand wrist. A simple method for clinical use. Proc Finn Dent Soc. 1974;70(1):7-14.
Hägg & Taranger	1980	Scoring	325	X-ray	Right Hand	10 stages	First and third finger are assessed in addition to the radial distal epiphysis. First finger ulnar sesamoid (presence/absence), 3rd finger distal phalangeal fusion/non-fusion, 3rd finger middle phalangeal fusion progression; distal radial epiphyseal fusion progression.	Hägg U, Taranger J. Skeletal stages of the hand and wrist as indicators of the pubertal growth spurt. Acta Odontol Scand. 1980;38(3):187-200.	
Hägg & Taranger modification: MP3 method	1982	Scoring	536	X-ray	Right Hand	5 stages	"MP3" Method: Third middle phalanx only evaluated, based on distal epiphyseal plate morphology.	Hägg U, Taranger J. Maturation indicators and the pubertal growth spurt. Am J Orthod. 1982;82(4):299-309.	
Hägg & Taranger modification: Modified MP3 Method	2002	Scoring	76	X-ray	Right Hand	6 stage	"Modified MP3" Method: Third middle phalanx only evaluated, with 1 additional intermediate stage.	Rajagopal R, Kansal S. A comparison of modified MP3 stages and the cervical vertebrae as growth indicators. J Clin Orthod JCO. 2002;36(7):398.	
Helm	1971	Scoring	154	X-ray	Right Hand	7 stages	Only 7 key events at specific regions are noted. Sesamoid presence in the thumb, 2nd finger proximal phalanx, and distal, middle and proximal phalanges of the third finger are evaluated.	Helm S, Siersbaek-Nielsen S, Skieller V, Björk A. Skeletal maturation of the hand in relation to maximum puberal growth in body height. Tandlaegebladet. 1971;75(12):1223-1234.	
Kopczyńska-Sikorska	1969	Atlas	22	X-ray	Left Hand	Atlas	Atlas of Polish children.	Kopczyńska-Sikorska J. Atlas Radiologiczny Rozwoju Kości Dłoni i Nadgarstka. Państwowy Zakład Wydawnictw Lekarskich; 1969.	
Li Guozhen	-	-	-	-	-	-	-	Li Guozhens' "Percent Numeration" No description found, only references in Chinese language journals.	Zhang Z, Li K, Yu RJ, Zhang Q. Preliminary study on the applying value of two measurements for bone age in the cases of minors. Fa Yi Xue Za Zhi. 2004;20(4):212-214.
Liaokawa	-	-	-	-	-	-	-	No description found, only references in abstract of Chinese language journals.	
Mackay	1952	Scoring	105	X-ray	Left & Right Hand	21 stages	Appearance of ossification centres of each carpal & phalanx in East Africans	Mackay DH, Service CM, Development C, Acts W. Skeletal maturation in the hand: a study of development in East Africa children. 1952.	
Marti-Henneberg	1974	Scoring	4	X-ray	-	-	Original article could not be obtained.	Marti-Henneberg C, Patois E, Niiranen A, Roy MP, Masse NP. Bone maturation velocity. Compte Rendu la XIIe Reun des Equipes Charg des Etudes sur la Croissance le Développement l'Enfant Norm Paris, Cent Int l'Enfance, Paris. 1974:107-112.	
Martins & Sakima	1977	Scoring	46	X-ray	Left Hand	18 stages	Carpal ossification evaluated which can be compared to pubertal growth spurt.	Martins JCR, Sakima T. Considerações sobre a previsão do surto de crescimento puberal. Ortodontia. 1977;10(3):164-170.	
Mentzel	2005	Scoring	93	Ultrasound	Right or Left Hand	Atlas-like result (score correlated to GP bone age)	BonAge' ultrasound device allows evaluation of the change in speed of waves across the distal radial and ulnar epiphyses which returns a skeletal age value correlated to the G-P atlas.	Mentzel H-J, Vilser C, Eulenstein M, et al. Assessment of skeletal age at the wrist in children with a new ultrasound device. Pediatr Radiol. 2005;35(4):429-433.	
Modi	1957/ 1969	Atlas	58	X-ray	-	-	Original article could not be obtained.	Modi JP. Modi's Textbook of Medical Jurisprudence and Toxicology. NM Tripathi; 1969.	
Rachmiel	2013	Scoring	3	Ultrasound	Ultrasound	Linear	The distance across and speed of soundwave travel across the third phalanx, carpal region and wrist are measured. A linear equation gives output correlated to the GP atlas.	Rachmiel M, Naugolani L, Mazor-Aronovitch K, Levin A, Koren-Morag N, Bistrizter T. Bone age assessment by a novel quantitative ultrasound based device (SonicBone), is comparable to the conventional Greulich and Pyle method. Horm Res Pediatr. 2013;80(Suppl 1):35.	

Roche	1988	Scoring	379	X-ray	Left Hand	Continuous Scale	Ninety-eight 'maturity indicators' across the radius, ulna, carpals, metacarpals and phalanges are recognised or measured, with different indicators assessed at different ages. Computer software returns a skeletal age with standard error and confidence limits.	Roche AF, Thissen D, Chumlea W. Assessing the Skeletal Maturity of the Hand-Wrist: Fels Method. Thomas; 1988.
Sempé & Pavia	1979	Scoring	697	X-ray	Left Hand	1000 point scale	Assessment is converted to a 'Skeletal Maturity Level' corresponding to 0 at birth to 999 at full maturity.	Sempé M, Pédrón G, Roy-Pernot M-P. Auxologie: Méthode et Séquences.; 1979.
Sempé & Pavia modification: Maturos 4.0	2001	Atlas	10	X-ray	Left Hand	Atlas	Semi-automated method in which twenty-two maturity indicators are considered and the user selects between one of 3 software-suggested ratings for each region, depending on chronological age.	Bouchard M, Sempé M. "MATUROS 4.0" CD: un nouvel outil d'évaluation de la maturation squelettique. Biométrie Hum Anthropol. 2001;19(1-2):9-12.
Sato et al.	1999	Scoring	11	X-ray	Hand (side not found/listed)	Linear	Computer aided skeletal maturity system (CASMAS). Third phalanx is extracted automatically and epiphyseal, metaphyseal widths measured, in addition to the width of the overlapping regions, and a multiple regression equation reports the bone age.	Sato K, Ashizawa K, Anzo M, et al. Setting up an automated system for evaluation of bone age. Endocr J. 1999;46(Suppl):S97-S100.
Singer	1980	Scoring	65	X-ray	Hand (side not found)	6 stages	All hand bones, with specific attention in the early stages to several events in the pisiform, hamate, ulna, second proximal phalanx, third middle and third distal phalanges.	Singer J. Physiologic Timing of Orthodontic Treatment. Angle Orthod. 1980;50(4):322-333.
Speyer	1950	Atlas	-	X-ray	Hand (side not found)	Atlas	Original article could not be obtained.	Speyer. Betekenis En Bepaling van de Skeletleeftijd. Leiden: Sijthoff; 1950.
Stuart	1962	Scoring	68	X-ray	Hand (side not found)	Ossification center appearance	Appearance and ossification of 29 centers in the hand wrist are evaluated.	Stuart HC, Pyle SI, Cornoni J, Reed RB. Onsets, completions and spans of ossification in the 29 bone-growth centers of the hand and wrist. Pediatrics. 1962;29(2):237-249.
Sugiura	1961	Scoring	5	X-ray	Hand (side not found)	-	Original article could not be obtained.	Sugiura Y, Nakazawa O, Kunishima Y, Aoki M, Ito H. A method of assessing skeletal age (2nd report). J Japanese Orthop Assoc. 1961;35:429-439.
Sugiura & Nakazawa	1968	Scoring	4	X-ray	Hand (side not found)	-	Scoring of hand and wrist centers, based on Japanese population.	Sugiura Y, Nakazawa O. Bone Age. Roentgen Diagnosis of Skeletal Development. Tokyo: Chugai-Igaku; 1968.
Tanner & Whitehouse: TW1	1959	Scoring	363	X-ray	Left Hand	Continuous Scale	Carpal, metacarpal and phalangeal assessment.	Tanner JM. A new system for estimating skeletal maturity from the hand and wrist, with standards derived from a study of 2600 healthy British children. Part II Scoring Syst. 1959.
Tanner & Whitehouse: TW1 - B5 Modification	2003	Scoring	6	X-ray	Left Hand	Continuous Scale	Radius, ulna, capitate, trapezium and the proximal epiphysis of the first phalanx of the fifth finger are evaluated individually as per TW1 and summed.	Guimarey L, Morcillo AM, Orazi V, Lemos-Marini SH V. Validity of the use of a few hand-wrist bones for assessing bone age. J Pediatr Endocrinol Metab. 2003;16(4):541-544.
Tanner & Whitehouse: TW2	1972	Scoring	2786 (1975)	X-ray	Left Hand	Continuous Scale	Carpal, metacarpal and phalangeal assessment. Alternative methods included carpals only or radius-ulna-short (RUS) bone modifications.	Tanner JM, Whitehouse RH, Healy MJR, Goldstein H. A revised system for estimating skeletal maturity from hand and wrist radiographs with separate standards for carpals and other bones (TW II system). Stand Skelet Age. 1972.
Tanner & Whitehouse: TW2 MR: RUS	2013	Scoring	47	MR	Left Hand: Open Compact MR	Continuous Scale	TW2 radius-ulna-short bones method applied to MR images from an open compact MR.	Terada Y, Kono S, Tamada D, et al. Skeletal age assessment in children using an open compact MRI system. Magn Reson Med. 2013;69(6):1697-1702.
Tanner & Whitehouse: TW2 MR: Fully automated	2014	Scoring	19	MR	Left Hand MR	Continuous Scale	Fully automated method in which 3D MR images are assessed by computer using the TW2 method.	Stern D, Ebner T, Bischof H, Grassegger S, Ehammer T, Urschler M. Fully automatic bone age estimation from left hand MR images. In: International Conference on Medical Image Computing and Computer-Assisted Intervention. Springer; 2014:220-227.
Tanner & Whitehouse:	2016	Scoring	14	MR	Left Hand MR	Continuous Scale	T1 weighted 3D VIBE sequence used and hand-wrist evaluated as per TW2 - RUS.	Urschler M, Krauskopf A, Witek T, et al. Applicability of Greulich-Pyle and Tanner-

TW2 MR:
RUS*

Whitehouse grading methods to MRI when assessing hand bone age in forensic age estimation: A pilot study. Forensic Sci Int. 2016;266:281-288.

	Tanner & Whitehouse: TW2 CASAS	1994	Scoring	69	X-ray	Left Hand MR	Continuous Scale	Computer Assisted Skeletal Assessment System (CASAS). User must position the radiograph under a camera, the computer then creates a digital representation which is scored automatically and can be output as per British or other populations. The process must be repeated individually for each bone.	Tanner JM, Gibbons RD. A computerized image analysis system for estimating Tanner-Whitehouse 2 bone age. Horm Res Paediatr. 1994;42(6):282-287.
	Tanner & Whitehouse: TW3	2001	Scoring	-	X-ray	Left Hand	Continuous Scale	Carpal, metacarpal and phalangeal assessment. Alternative methods included carpals only or radius-ulna-short bone modifications.	Tanner J, Healy M, Goldstein H, Cameron N. Assessment of Skeletal Maturity and Prediction of Adult Height (TW3 Method). 3rd ed. London: WB Saunders, Harcourt Publishers Ltd; 2001.
	Tanner & Whitehouse: Sanders modification	2008	Scoring	54	X-ray	Left Hand	8 stages	TW3 - RUS system scoring is applied to the second to fifth phalanges and metacarpals, in addition to the distal radius epiphysis. Stages were made with specific emphasis on their correlation with event in scoliosis curve progression.	Sanders JO. Maturity indicators in spinal deformity. J Bone Jt Surg - Ser A. 2008;89(SUPPL. 1):14-20.
	Thiemann & Nitz	1986	Atlas	93 (2006 edition)	X-ray	Hand (side not found)	Atlas	Atlas of German children.	Thiemann H, Nitz I. Roentgenatlas Der Normalen Hand Im Kindesalter. Leipzig: Thieme; 1986.
	Thodberg	2009	Atlas/Scoring	232	X-ray	Left Hand	Atlas/Scoring	Automated method in which fifteen bones are identified by software and each is scored individually - first to fifth metacarpals, phalanges of the first, third and fifth digits, and the distal radial and ulnar epiphyses. Bone age can then be output as per Tanner-Whitehouse or GP Atlas values.	Thodberg HH, Kreiborg S, Juul A, Pedersen KD. The BoneXpert method for automated determination of skeletal maturity. IEEE Trans Med Imaging. 2009;28(1):52-66.
	Todd	1937	Atlas	335	X-ray	Left Hand	Atlas	Atlas method.	Todd TW. Atlas of skeletal maturation. 1937.
	Tomei	2014	Scoring	10	MR	Hand MR	85 points	Radius, ulna, capitate, hamate, pisiform and first and third proximal phalanges and metacarpals are evaluated and scored.	Tomei E, Semelka RC, Nissman D. Text-Atlas of Skeletal Age Determination: MRI of the Hand and Wrist in Children. Wiley Online Library; 2014.
	Wilkins	1950	-	34	-	-	Original article could not be obtained.	Method is not separated by genders.	Wilkins L. The diagnosis and treatment of endocrine disorders in childhood and adolescence. Charles C. Thomas, Springfield. 1950;2.
Hip	Acheson	1957	Scoring	245	X-ray	Pelvic	45 stages	"Oxford method": 9 regions of the hip are evaluated - iliac, triradiate cartilage, ischiopubic junction, pubis, ischium, acetabulum, femoral head, greater trochanter and lesser trochanter.	Acheson RM. The Oxford Method of Assessing Skeletal Maturity. Clin Orthop Relat Res. 1957;10:19-39.
	Acheson modified: Modified Oxford	1996	Scoring	97	X-ray	Pelvic	30 stages	Modified Oxford: only head of femur, greater trochanter, lesser trochanter, iliac crest and triradiate cartilage are evaluated.	Stasikelis PJ, Sullivan CM, Phillips WA, Polard AJ. Slipped capital femoral epiphysis: prediction of contralateral involvement. JBJS. 1996;78(8):1149-1155.
	Triradiate cartilage	-	Scoring	-	X-ray	Pelvic	2 stages	Open or closed stages	No original publication could be found. For a useful reference however see, Dimeglio A. Growth in Pediatric Orthopaedics. 2001:549-555.
Humerus	Li*	2018	Scoring	4	X-ray	Left Shoulder	5 stages	Proximal humeral epiphyseal closure assessed from open plate until fusion. Peak height velocity correlation possible.	Li DT, Cui JJ, Devries S, et al. Humeral Head Ossification Predicts Peak Height Velocity Timing and Percentage of Growth Remaining in Children. J Pediatr Orthop. 2018;38(9):e546-e550.
	Ogden	1978	Atlas	47	X-ray	Shoulder X-Ray	Atlas	Forensic specimen derived method, the proximal humerus ossification centers appearance, fusion with each other and the developing epiphysis are assessed.	Ogden JA, Conlogue GJ, Jensen P. Radiology of Postnatal Skeletal development: The proximal humerus. Skeletal Radiol. 1978;2(3):153-160.
	Walker & Lovejoy	1985	Scoring	137	X-ray	Proximal humerus	8 stages	Proximal humerus are evaluated by relative lucency.	Walker RA, Lovejoy CO. Radiographic changes in the clavicle and proximal femur and their use in the determination of skeletal age at

Iliac	Risser	1958	Scoring	529	X-ray	Pelvic	No stages	Full excursion of the iliac crest apophysis is correlated with the ending of spinal growth (no stages described at this time).	death. Am J Phys Anthropol. 1985;68(1):67-78. Risser JC. The Iliac apophysis; an invaluable sign in the management of scoliosis. Clin Orthop. 1958; 11: 111–119.
	Risser: US system	-	Scoring	-	X-ray	Pelvic	6 stages	Presence, extent of excursion divided into quarters and initiation of fusion of the iliac crest apophysis are evaluated.	First reference could not be found, as also noted by Bitan et al. For description of this method see: Bitan FD, Veliskakis KP, Campbell BC. Differences in the Risser grading systems in the United States and France. Clin Orthop Relat Res. 2005;(436):190-195.
	Risser: EU system	-	Scoring	-	X-ray	Pelvic	6 stages	Presence, extent of excursion divided into thirds, initiation and completion of fusion of the iliac crest apophysis are evaluated.	First reference could not be found, as also noted by Bitan et al. For description of this method see: Bitan FD, Veliskakis KP, Campbell BC. Differences in the Risser grading systems in the United States and France. Clin Orthop Relat Res. 2005;(436):190-195.
	Risser: Combined	1985	Scoring	146	X-ray	Pelvic	7 stages	Combined method in which stages 2-4 are altered and one intermediate stage "3/4" is added.	Stagnara P. Les Déformations Du Rachis: Scolioses, Cyphoses, Lordoses. Masson; 1985.
	Risser modified: Triradiate evaluation	2010	Scoring	55	X-ray	Pelvic	7 stages	Triradiate cartilage evaluation is included as an additional "-1" stage.	Nault M-L, Parent S, Phan P, Roy-Beaudry M, Labelle H, Rivard M. A modified Risser grading system predicts the curve acceleration phase of female adolescent idiopathic scoliosis. JBJS. 2010;92(5):1073-1081.
Risser modified: Risser 'plus'	2015	Scoring	47	X-ray	Pelvic	8 stages	Triradiate cartilage is evaluated in addition to the iliac crest in a method combining EU and US systems. Recommended by SOSORT guidelines, 2015.	Negrini S, Hresko TM, O'Brien JP, et al. Recommendations for research studies on treatment of idiopathic scoliosis: Consensus 2014 between SOSORT and SRS non-operative management committee. Scoliosis. 2015;10(1):1-12.	
Risser modified: Ultrasound	1995	Scoring	41	Ultrasound	Ultrasound	6 stages	US Risser method applied by comparing presence of apophysis to the extent of iliac crest as palpated by clinician.	Wagner UA, Diedrich V, Schmitt O. Determination of skeletal maturity by ultrasound: a preliminary report. Skeletal Radiol. 1995;24(6):417-420.	
Risser modified: Four stage method	1985	Scoring	412	X-ray	Pelvic	4 stages	The extent of excursion is not scored, such that stages describe the absence of the apophysis, its presence, ongoing fusion, or completed fusion. First described in forensic reports.	Webb PAO, Suchey JM. Epiphyseal union of the anterior iliac crest and medial clavicle in a modern multiracial sample of American males and females. Am J Phys Anthropol. 1985;68(4):457-466.	
Schmidt	2011	Scoring	57	Ultrasound	Ultrasound Left Iliac Crest	4 stages	The absence, presence, ongoing fusion and complete fusion of the left iliac crest apophysis are evaluated.	Schmidt S, Schmeling A, Zwiesigk P, Pfeiffer H, Schulz R. Sonographic evaluation of apophyseal ossification of the iliac crest in forensic age diagnostics in living individuals. Int J Legal Med. 2011;125(2):271-276.	
Wittschieber	2012	Scoring	35	X-ray	Pelvic	8 stages	Alternative method described in forensic evaluation, evaluating iliac crest apophyseal presence/absence, extent of excursion, extent of fusion, and completion of fusion.	Wittschieber D, Vieth V, Domnick C, Pfeiffer H, Schmeling A. The iliac crest in forensic age diagnostics: Evaluation of the apophyseal ossification in conventional radiography. Int J Legal Med. 2013;127(2):473-479.	
Knee	Acheson	1954	Scoring	215	X-ray	Knee AP	12 points	Femur and tibia are scored from 0-5 based on epiphyseal morphology (though not on the presence of fusion), patella and fibular epiphyses presence is scored 0 or 1.	Acheson RM. A method of assessing skeletal maturity from radiographs; a report from the Oxford child health survey. J Anat. 1954;88(4):498-508.
	Dedouit	2012	Scoring	91	MR	Knee MR	5 stages at 2 regions	Femur and tibial epiphyses are scored separately I-V and can be compared against age charts.	Dedouit F., Auriol J., Rousseau H., Rouge D., Crubézy E. and Telmon N., 2012. Age assessment by magnetic resonance imaging of the knee: a preliminary study. Forensic science international, 217(1-3), pp.232-e1.

	Nakase	2012	Scoring	24	Ultrasound	Ultrasound Left Iliac Crest	3 stages	Developing tibial tuberosity is described by 3 events adapted from Ehrenberg's radiographic description (1962) :increased cartilage, the presence of ossifying island, or connection by bone bridge to the tibial epiphyses.	Nakase J, Aiba T, Goshima K, et al. Relationship between the skeletal maturation of the distal attachment of the patellar tendon and physical features in preadolescent male football players. <i>Knee Surgery, Sport Traumatol Arthrosc.</i> 2014;22(1):195-199.
	O'Connor	2008	Scoring	70	X-ray	Knee AP & Lateral	15 stages	Epiphyses of the long bones around the knee are scored 0-4 and summed. Modified from McKern Stewart 1957 report from a forensic sample.	O'Connor JE, Bogue C, Spence LD, Last J. A method to establish the relationship between chronological age and stage of union from radiographic assessment of epiphyseal fusion at the knee: an Irish population study. <i>J Anat.</i> 2008;212(2):198-209.
	Pennock*	2018	Atlas	7	MR	Knee MR	Atlas	Cross-sectional atlas using sagittal and coronal slices used to evaluate femur, tibia, fibula and patella based on ossification, shape and specific features of the regions such as tibial spine development and subchondral epiphyseal cartilage.	Pennock AT, Bogar JD, Manning JD, Diego S, Diego S. The creation and validation of a knee bone age atlas utilizing MRI. <i>JBJS.</i> 2018;100(4):e20.
	Pyle & Hoerr	1955	Atlas	140	X-ray	Knee AP & Lateral	Atlas	Femur, tibia, fibula and patellar are assessed by atlas method.	Pyle SI, Hoerr NL. A Radiographic Standard of Reference for the Growing Knee. CC Thomas; 1955.
	Roche-Wainer-Thissen	1975	Scoring	117	X-ray	Knee AP	34 stages	Thirty four maturity indicators at the knee are evaluated.	Roche AF, Wainer H, Thissen D. Skeletal Maturity: The Knee Joint as a Biological Indicator. Plenum Medical Book Company; 1975.
	Wang	2010	Scoring	3	X-ray	Knee AP & Lateral	-	Foreign Language [Chinese]	Wang YH, Zhu GY, Ying CL, Fan LH, Wan L. The trend of epiphyseal development of knee and ankle joints in teenagers and age estimation. <i>Fa Yi Xue Za Zhi.</i> 2010;26(2):91-96.
Lower limb	von Harnack	1974	-	-	-	-	-	Foreign Language [German]	von Harnack, G. A. "Determination of skeletal maturation in childhood (author's transl)." <i>Zeitschrift für Geburtshilfe und Perinatologie</i> 178, no. 4 (1974): 237.
Mandible	Singer	1987	Scoring	77	X-ray	Lateral cephalogram	2 stages	Antegonial notch depth is measured and rated whether "deep" (>3mm depth) or not.	Singer CP, Mamandras AH, Hunter WS. The depth of the mandibular antegonial notch as an indicator of mandibular growth potential. <i>Am J Orthod Dentofac Orthop.</i> 1987;91(2):117-124.
Metacarpal	Faruch-Bilfeld	2008	Scoring	4	X-ray	Hand X-ray	Linear	Second metacarpal is measured to establish the ratio between epiphysial diameter and metaphysial diameter. This value can be correlated to chronological age.	Faruch-Bilfeld M, Dedouit F, Soumah M, et al. Value of radiographic evaluation of the second metacarpal in the determination of bone age. <i>J Radiol.</i> 2008;89(12):1930-1934.
	Garn	1972	Scoring	227	X-ray	Left Hand	Linear	The longitudinal length of nineteen tubular bones of the hand are measured and compared against age standards. Prospective standard based on FELS population.	Garn SM, Hertzog KP, Poznanski AK, Nagy JM. Metacarpophalangeal length in the evaluation of skeletal malformation. <i>Radiology.</i> 1972;105(2):375-381.
Pubic symphysis	Omel'chenko & Sukhomlinova	1976	-	1	X-ray	Pelvic	-	Ischiopubic synchondrosis is evaluated. Foreign Language [Russian]	Omel'chenko RM, Sukhomlinova OP. Duration of synostosis of the ischiopubic synchondrosis. <i>Arkh Anat Gistol Embriol.</i> 1976;70(4):91-95.
Radius	Dvorak	2007	Scoring	137	MR	Coronal Left Hand MR	6 stages	Distal radial growth plate is evaluated and initiation, extent or completion of fusion is graded I-VI.	Dvorak J, George J, Junge A, Hodler J. Age determination by magnetic resonance imaging of the wrist in adolescent male football players. <i>Br J Sports Med.</i> 2007;41(1):45-52.
	Karami	2014	Scoring	2	Ultrasound	Ultrasound	Linear	The width of the hypoechoic growth plate is measured along the long radius' axis and compared to tables. Only cut-off points for the majority 16, 17 and 18 years old were investigated.	Karami M, Moshirfatemi A, Daneshvar P. Age determination using ultrasonography in young football players. <i>Adv Biomed Res.</i> 2014;3(1):174.
	Schmidt	2013	Scoring	38	Ultrasound	Ultrasound	4 stages	Distal radius evaluated for absence/presence of secondary center, the initiation of fusion, and the completion of fusion. (based on 4 stage ossification template as per	Schmidt S, Schiborr M, Pfeiffer H, Schmeling A, Schulz R. Age dependence of epiphyseal ossification of the distal radius in ultrasound

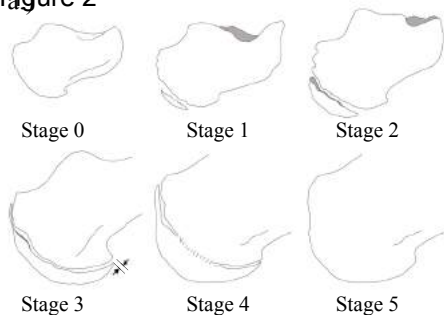
Rib	Moskovitch	2010	Scoring	25	CT	Multi-slice CT	5 stages	Schulz et al, similar to many methods) Sternal end of the right first rib is imaged and virtual reconstructions created, and assessed based on Kunos et al. macroscopic ratings, which yielded 5 stages around 15-30 years old, based on shape, surface topography and form of the margin, and on the presence of osseous bridges in the sternocostal cartilage.	diagnostics. Int J Legal Med. 2013;127(4):831-838. Moskovitch G, Dedouit F, Braga J, Rougé D, Rousseau H, Telmon N. Multislice computed tomography of the first rib: A useful technique for bone age Assessment. J Forensic Sci. 2010;55(4):865-870.
	Michelson	1934	Scoring	43	X-ray	X-ray	4 stages	Medial side of first rib is evaluated as first described in German by Ernst (1920), based on presence, extent and completion of epiphyseal ossification.	Michelson N. The calcification of the first costal cartilage among whites and negroes. Hum Biol. 1934;6(3):543.
Shoulder	Schaefer	2015	Scoring	3	X-ray	Shoulder X-Ray: AP, Axillary & Y-view.	3 scores: 4 point 3 point and 2 point	Proximal humerus , coracoid process and acromion are evaluated separately (on 4-, 3- and 2-point scales respectively).	Schaefer M, Aben G, Vogelsberg C. A demonstration of appearance and union times of three shoulder ossification centers in adolescent and post-adolescent children. J Forensic Radiol Imaging. 2015;3(1):49-56.
Sternum	Gemeler*	2019	Scoring	3	CT	Chest MDCT	5 stages	Vertical fusion between three or four ossification centers of the sternal body and manubrium are assessed, and fusions proceeds superiorly with increasing maturity. (Measured in individuals up to 30 years old)	Gumeler E, Karpinar E, Ariyurek OM. MDCT evaluation of sternal development. Surg Radiol Anat. 2019;41(3):281-286.
	Riach †	1967	Scoring	23	X-ray	Chest X-ray	Continuous	Tracings made of ossification center numbers and area calculated. Fusion is completed by 6-7 years old. (Method only described in forensic studies of excised sterna)	Riach IC. Ossification in the sternum as a means of assessing skeletal age. J Clin Pathol. 1967;20(4):589-590.
Wrist	Wang	2014	Scoring	0	X-ray	Left Hand	5 stages	Five 'developmental stages' were applied for the radius and the ulna. No more information available - foreign Language [Chinese]	Wang YH, Wang ZS, Wei H, Wan L, Ying CL, Zhu GY. Automated assessment of developmental levels of epiphysis by support vector machine. Fa Yi Xue Za Zhi. 2014;30(6):422-426.
	Kangne	1999	Scoring	12	X-ray	Hand (side not found/listed)	4 stages	Distal radius epiphyseal fusion is evaluated from no fusion, partial fusion, near total fusion leaving only a thin line to complete fusion.	Kangne RN, Sami SA, Deshpande VL. Age estimation of adolescent girls by radiography. J Forensic Med Toxicol. 1999;16(1):20-26.
	Kangne modification: Two-stage	1999	Scoring	12	X-ray	Hand (side not found/listed)	2 stages	The first and second stages are combined, as are the third and fourth, resulting in 2 stages: 'not fused' and 'fused'.	Kangne RN, Sami SA, Deshpande VL. Age estimation of adolescent girls by radiography. J Forensic Med Toxicol. 1999;16(1):20-26.
Multi-region	Francis	1940	Scoring	47	X-ray	Many	Ossification center appearance	Ossification center appearances of 17 regions from humerus to iliac crest, sesamoids etc presented from 6-15 years old	Francis CC. The appearance of centers of ossification from 6 to 15 years. Am J Phys Anthropol. 1940;27(1):127-138.
	Girdany & Golden	1952	Scoring	-	X-ray	Many	-	Based on the appearance of ossification centers, the wrist, elbow, shoulder, spine, hip, knee, ankle can be evaluated depending on age.	Girdany BR, Golden R. Centers of ossification of the skeleton. Am J Roentgenol Radium Ther Nucl Med. 1952;68(6):922-924.
	Gök	1985	Atlas	7	X-ray	Many	Atlas	Turkish atlas of boys aged 11-22 based on the epiphyses of the shoulder, elbow, hand-wrist, and pelvic bones.	Gök Ş, Erölçer N, Özen C. Age Determination in Forensic Medicine. 2nd ed. Council of Forensic Medicine Press; 1985.
	Graham	1972	-	74	-	-	-	Original article could not be obtained.	Graham CB. Assessment of bone maturation-methods and pitfalls. Radiol Clin North Am. 1972;10(2):185-202.
	Schinz	1939	-	-	X-ray	Many	-	Hand, wrist, elbow, skull, hip, iliac crest, spine and knee are assessed. No further description found. Foreign Language [German]	Schinz H., Baensch WE, Friedl E, Uehlinger E. Lehrbuch der Röntgendiagnostik. In: Stuttgart: Thieme; 1950:761–776.
	Spencer	1981	Scoring	9	Bone Scan	Full body scan with γ -camera.	Ossification center appearance	The appearance times of 71 ossification centers from 0-26 years old with ^{99m}Tc -MDP or related compound uptake bone scans are listed.	Spencer RP, Sami S, Karimeddini M, Sziklas JJ, Rosenberg R. Role of bone scans in assessment of skeletal age. Int J Nucl Med Biol. 1981;8(1):33-38.
	Zhu	2008	Scoring	2	X-ray	Many	not found foreign language	Seven regions are assessed and compared to so-called 'Grading Standards' :sternal end of clavical and left shoulder, elbow, carpal, hip, knee and ankle joints. No further description found in English (original article in Chinese).	Zhu GY, Fan LH, Zhang GZ, et al. Staging methods of skeletal growth by X-ray in teenagers. Fa Yi Xue Za Zhi. 2008;24(1):18-24.

Zhu: Knee-Ankle only	2008	Scoring	3	X-ray	Many	not found	Only knee and ankle assessed. No further description found in English (original article in Chinese).	Wang YH, Zhu GY, Ying CL, Fan LH, Wan L. The trend of epiphyseal development of knee and ankle joints in teenagers and age estimation. Fa Yi Xue Za Zhi. 2010;26(2):91-96.
Elgenmark: <5 years old	1946	Scoring	110	X-ray	Hemiskelton	24 age groups	Hand-wrist, knee, foot, prox femur, elbow, shoulder, applicable until 5 years old. In this 'numerical' method, the number of ossification centers is summed and this value is compared to chronological age.	Elgenmark O. The Normal Development of the Ossific Centres During Infancy and Childhood: A Clinical, Roentgenologic, and Statistical Study. Almqvist & Wiksell; 1946.
Ruckenstein	1931	-	47	X-ray	-	Foreign Language [German]	Does not divide based on gender.	Ruckenstein E. Die Normale Entwicklung Des Knochensystems Im Röntgenbild. Vol 15. Leipzig: Thieme; 1931.
Lurie	1943	Scoring	18	X-ray	Many	20 stages	Hand-wrist, elbow, pelvis and foot on the right side. Age at appearance and fusion times are described, with specific landmarks highlighted as indicators of age such as the greater trochanter.	Lurie LA, Levy S, Lurie ML. Determination of bone age in children. J Pediatr. 1943;23(6):131-140.
Caffey	1945	Atlas	1628	X-ray	Many	-	A method made from several regions including hand-wrist as per Vickers & Vogt, it is not usable for children older than 14 years old. Original article could not be located.	Caffey J, Silverman FN. Pediatric X-Ray Diagnosis. Chicago: Year Book Medical Publishers; 1945.
Vogt & Vickers	1938	Atlas	52	X-ray	Many	Atlas	Hand, wrist and feet from birth to 6 1/2 years old, ossification center appearance of the bones of the upper and lower extremities can be evaluated. Prospective atlas.	Vogt EC, Vickers VS. Osseous growth and development. Radiology. 1938;31(4):441-444.

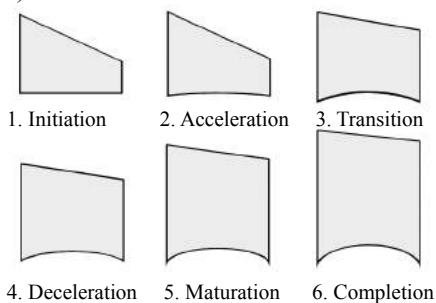
Figure 1

[Click here to access/download;Figure \(TIF or EPS only. 300 ppi Images or 1200 ppi Line-Art. Label with figure number under](#)

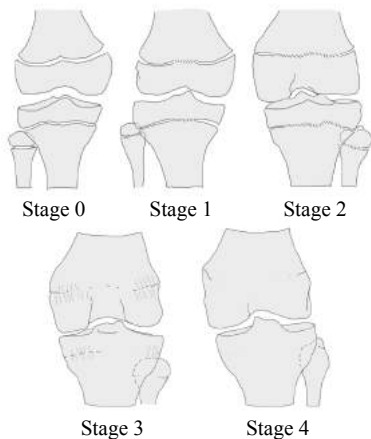


Figure 2

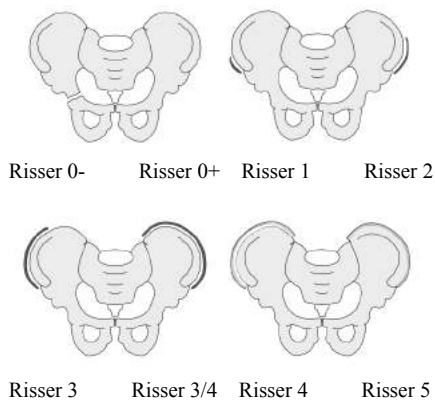
b.)



c.)



d.)



e.)

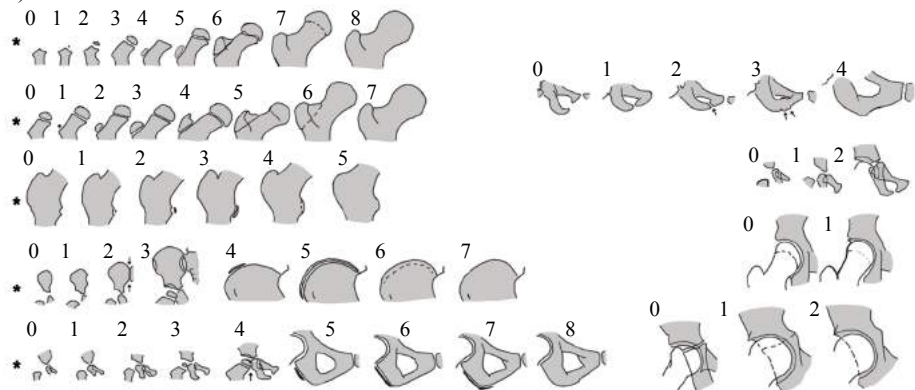
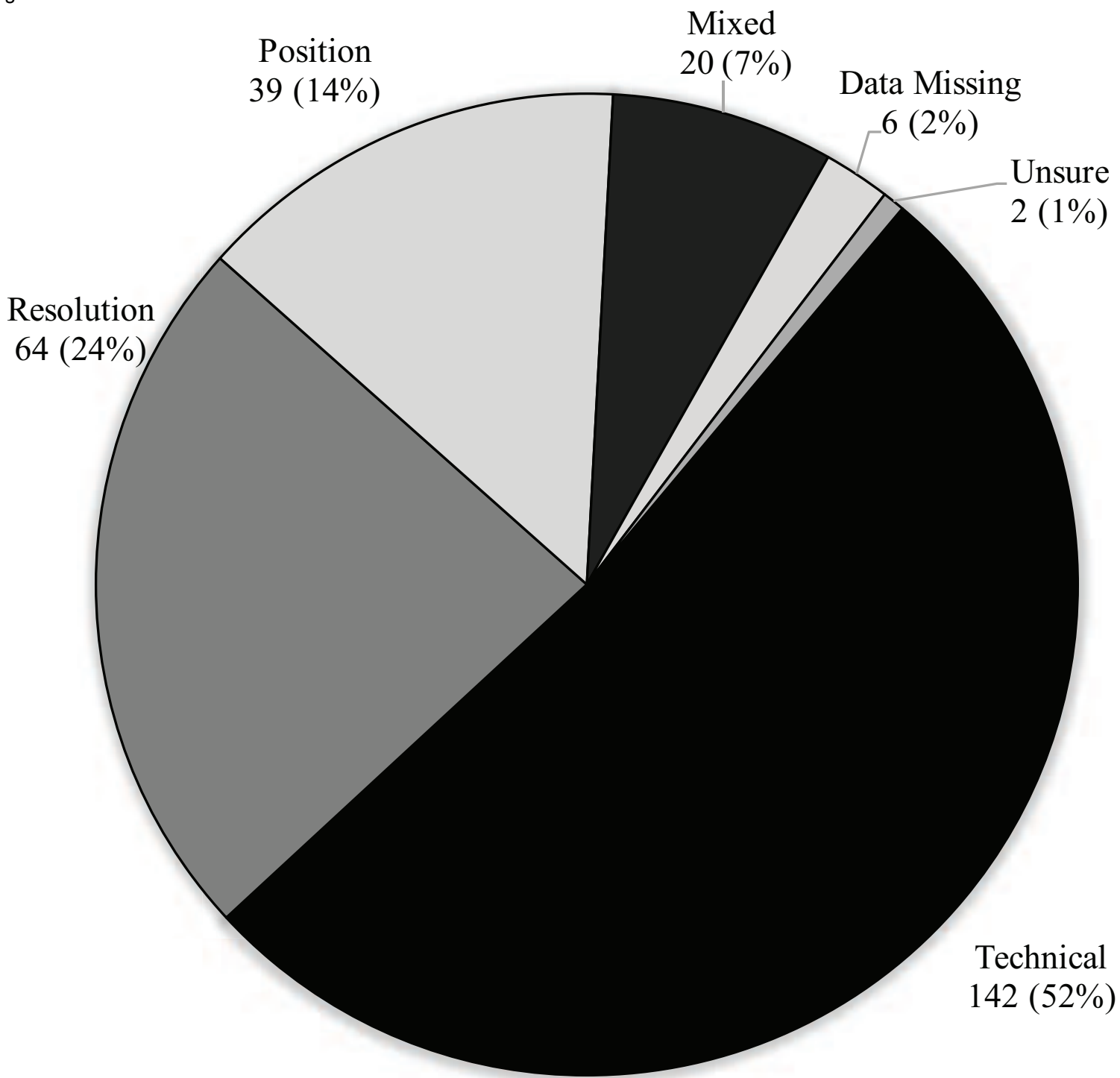
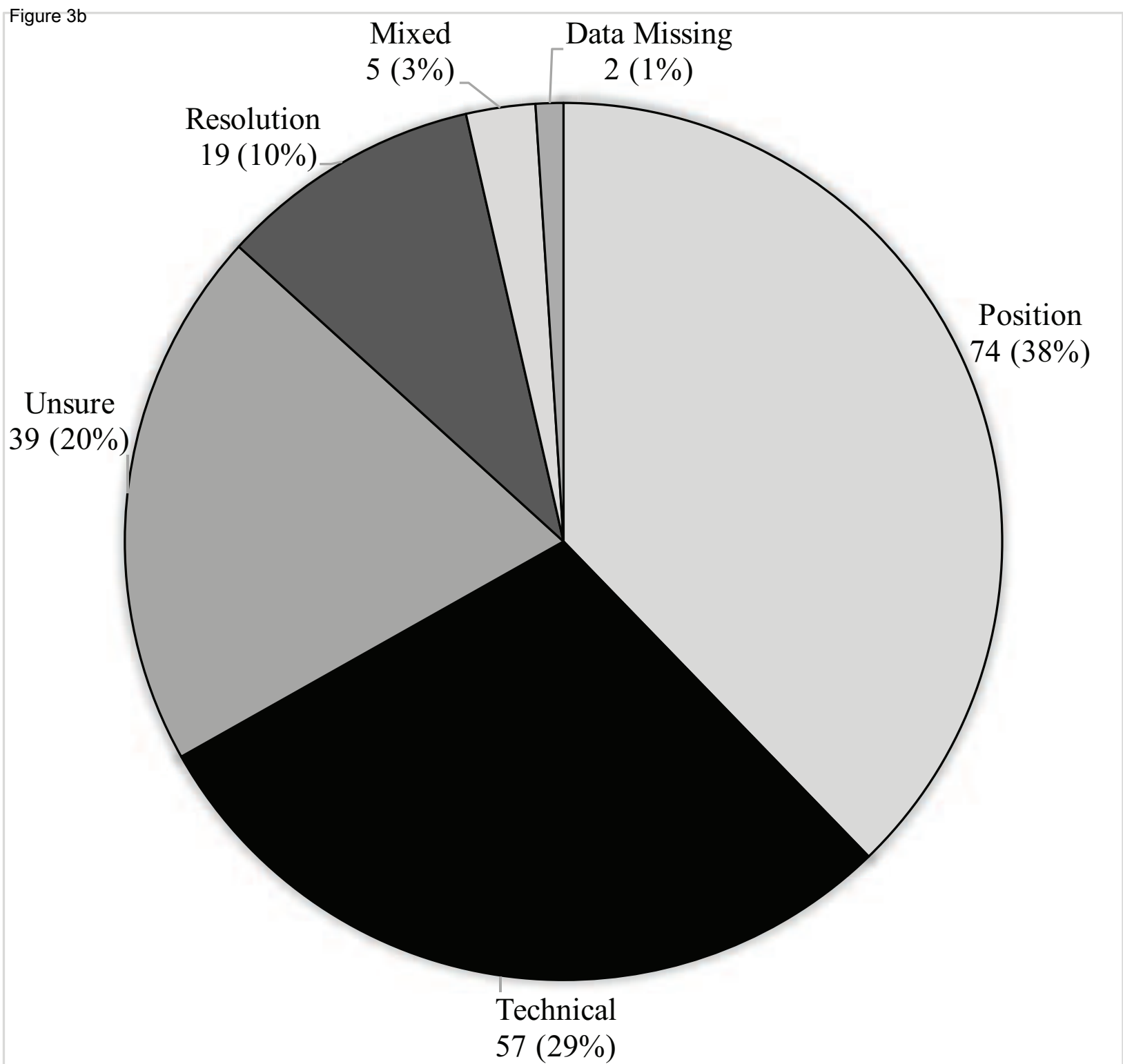


Figure 3a



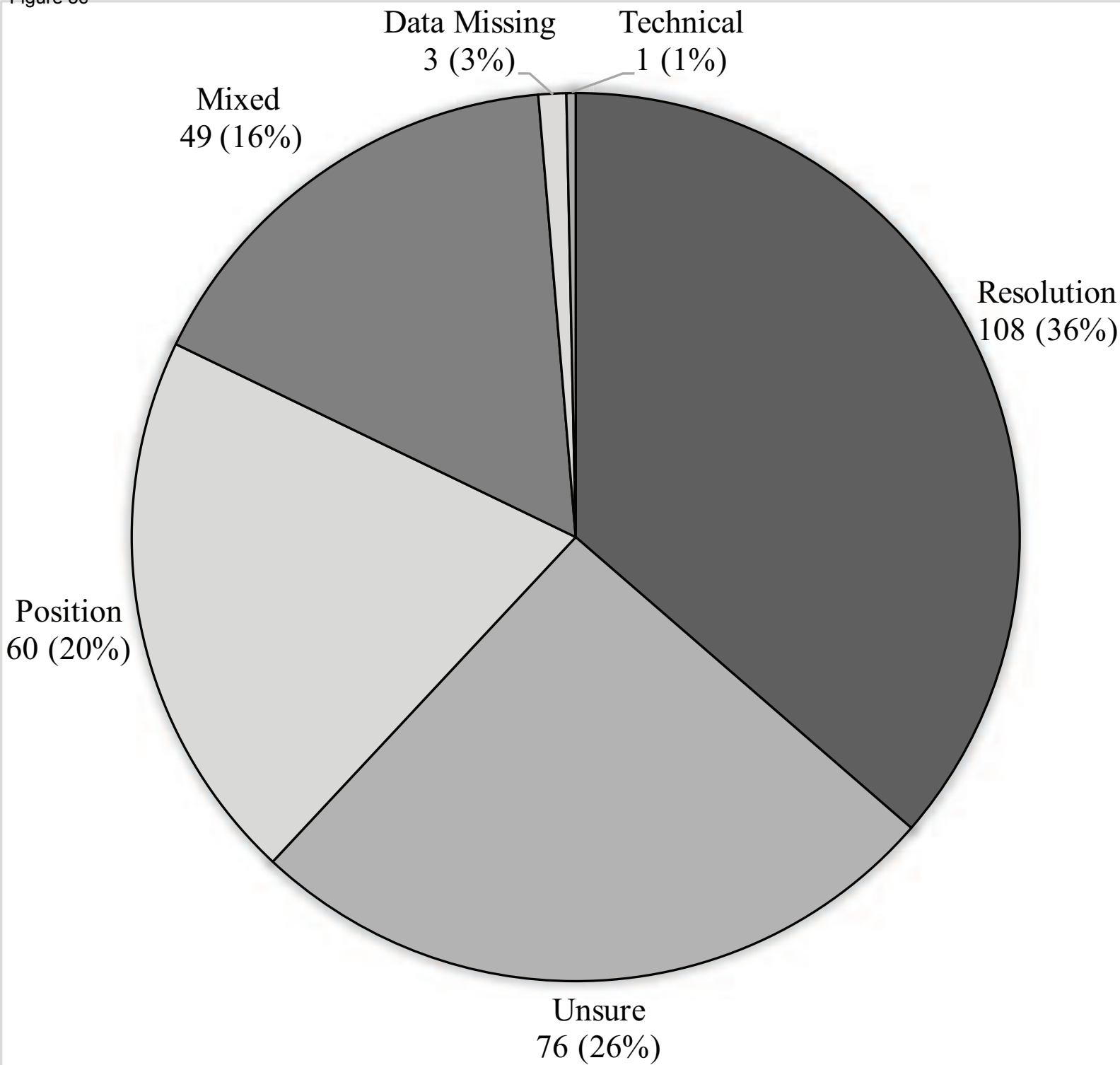
<u>Calcaneus</u>		Easy	Moderate	Difficult	Not possible	SUM
	Total	661 (70.8%)	132 (14.1%)	83 (8.9%)	58 (8.9%)	
	Technical	-	30	63	49	142
	Position	-	27	5	7	39
	Resolution	-	60	4	-	64
	Unsure	-	2	-	-	2
	Data Missing	-	5	-	1	6
	Mixed	-	8	11	1	20
	SUM					273

Figure 3b



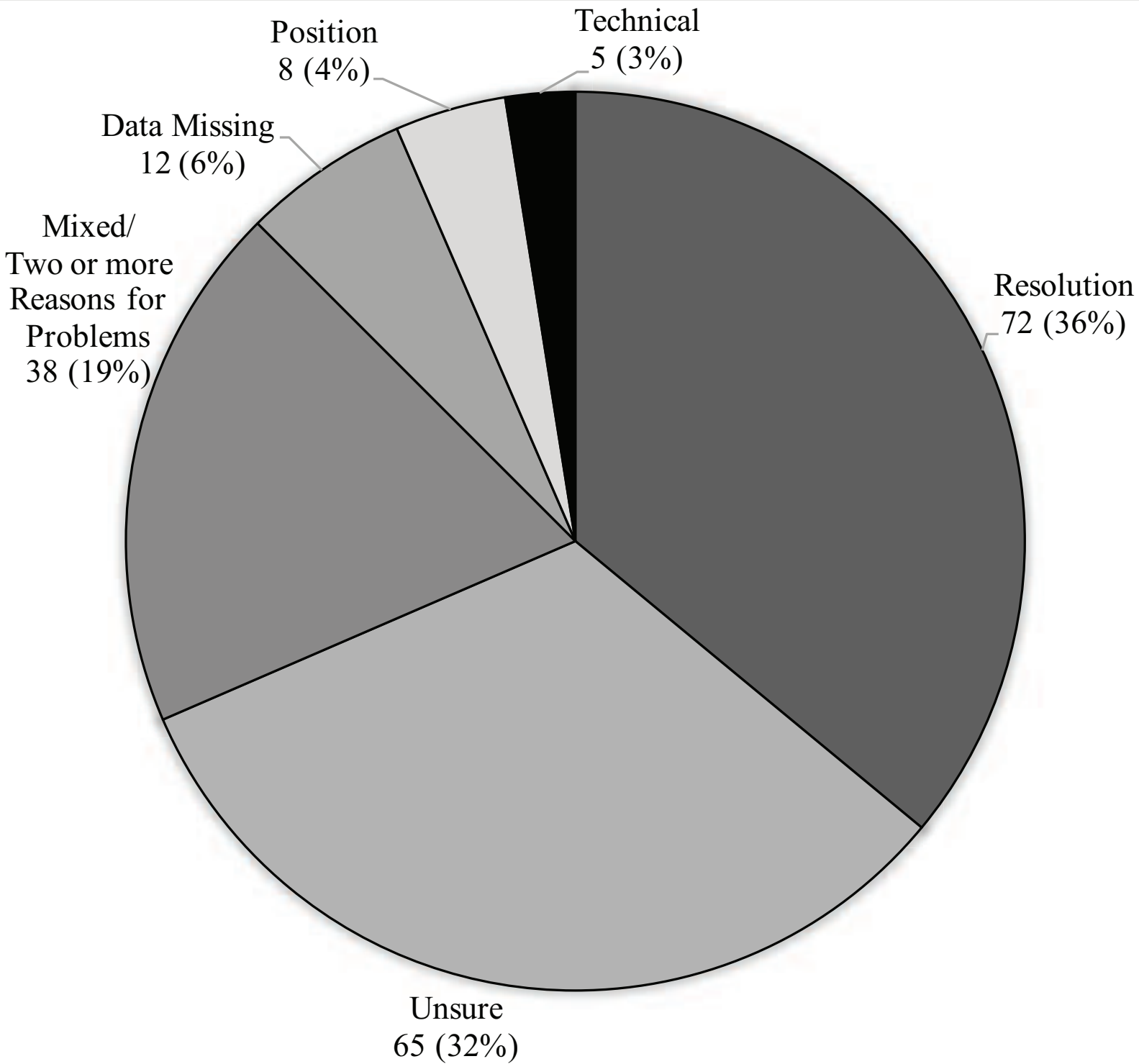
<u>Cervical</u>		Easy	Moderate	Difficult	Not possible	SUM
	Total	738 (79.0%)	104 (11.1%)	53 (5.7%)	39 (4.2%)	
	Technical	-	10	19	28	57
	Position	-	40	25	9	74
	Resolution	-	16	3	-	19
	Unsure	-	34	5	-	39
	Data Missing	-	1	-	1	2
	Mixed	-	3	1	1	5
	SUM					196

Figure 3c



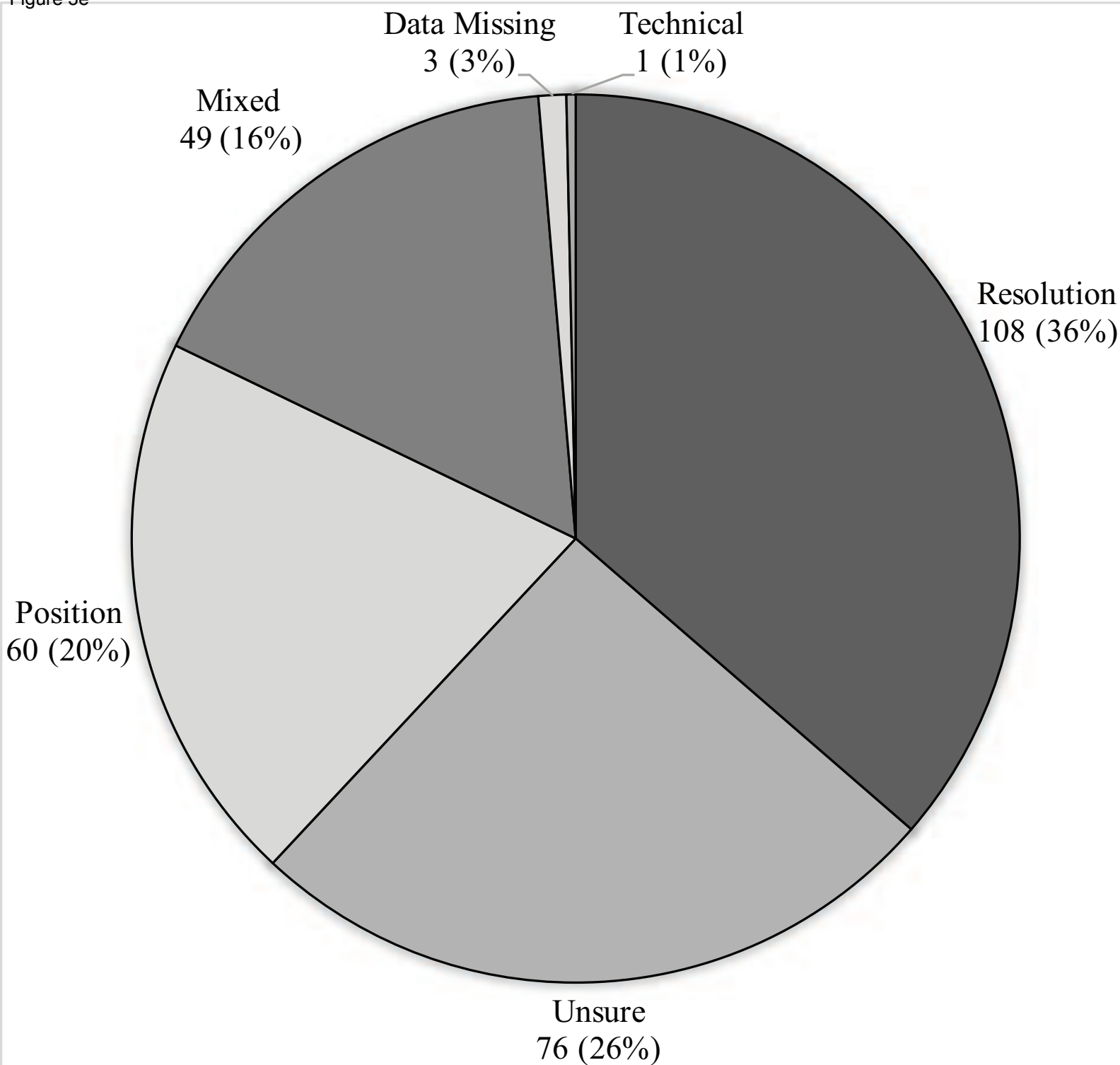
<u>Knee</u>		Easy	Moderate	Difficult	Not possible	SUM
	Total	637 (68.2%)	221 (23.7%)	75 (8.0%)	1 (0.1%)	
	Technical	-	-	-	1	1
	Position	-	52	8	-	60
	Resolution	-	73	35	-	108
	Unsure	-	65	11	-	76
	Data Missing	-	3	-	-	3
	Mixed	-	21	28	-	49
	SUM					297

Figure 3d



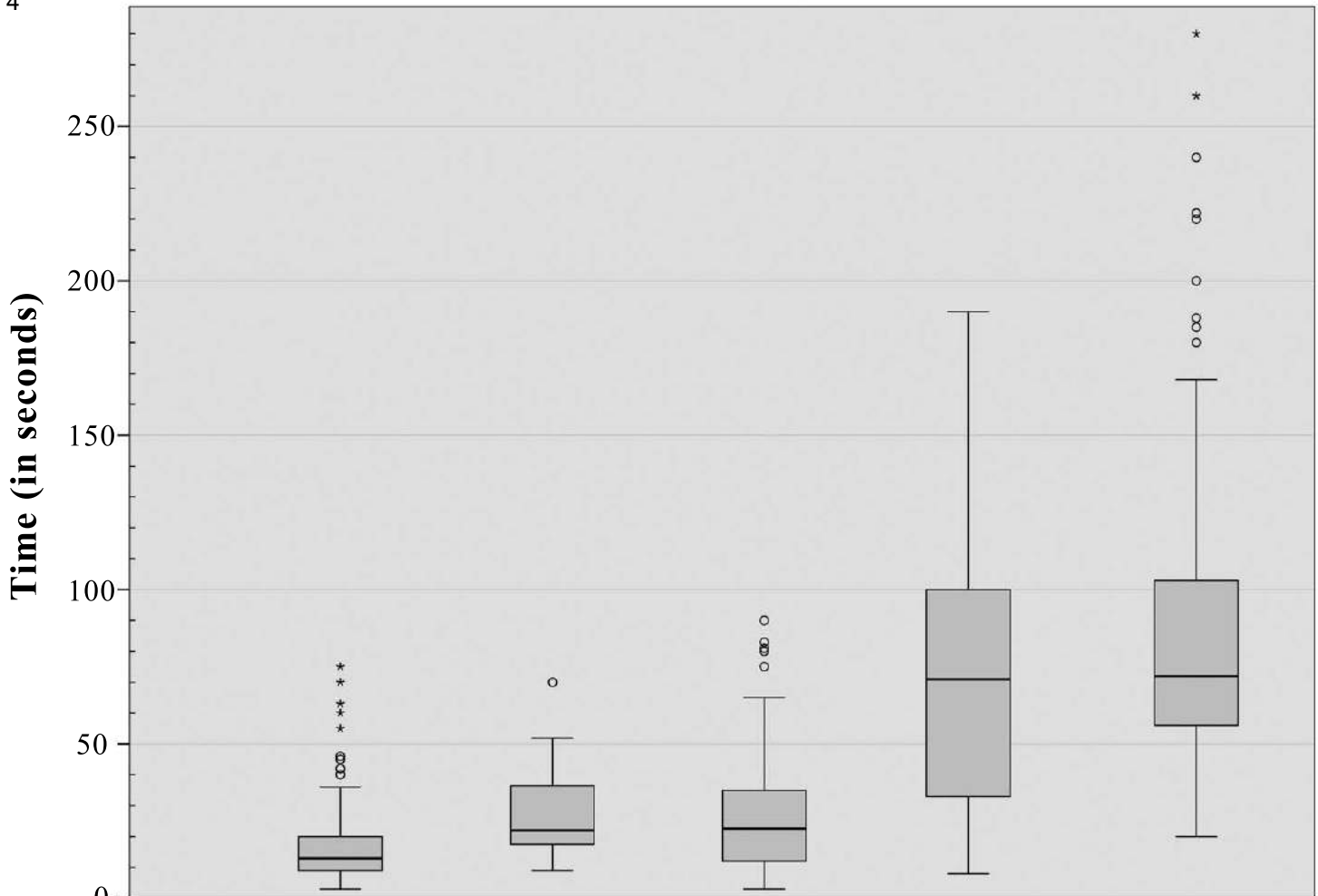
<u>Oxford Hip</u>		Easy	Moderate	Difficult	Not possible	SUM
	Total	734 (78.6%)	127 (13.6%)	71 (7.6%)	127 (13.6%)	
	Technical	-	3	2	-	5
	Position	-	5	3	-	8
	Resolution	-	30	42	-	72
	Unsure	-	57	8	-	65
	Data Missing	-	10	-	2	12
	Mixed	-	22	16	-	38
	SUM					200

Figure 3e



<u>Knee</u>		Easy	Moderate	Difficult	Not possible	SUM
	Total	637 (68.2%)	221 (23.7%)	75 (8.0%)	1 (0.1%)	
	Technical	-	-	-	1	1
	Position	-	52	8	-	60
	Resolution	-	73	35	-	108
	Unsure	-	65	11	-	76
	Data Missing	-	3	-	-	3
	Mixed	-	21	28	-	49
	SUM					297

Figure 4



	Calcaneus	Cervical	Risser Plus	Knee	Oxford Hip
Mean	17.7s	26.5s	30.1s	80.9s	82.0s
Range	3-75s	9 - 70s	8 - 90s	17 - 190s	20 - 280s
95%CI	16.0-19.38	22.16-30.75	27.49-32.71	76.09- 85.66	76.12- 87.88
N	192	200	203	225	200

Figure 5a

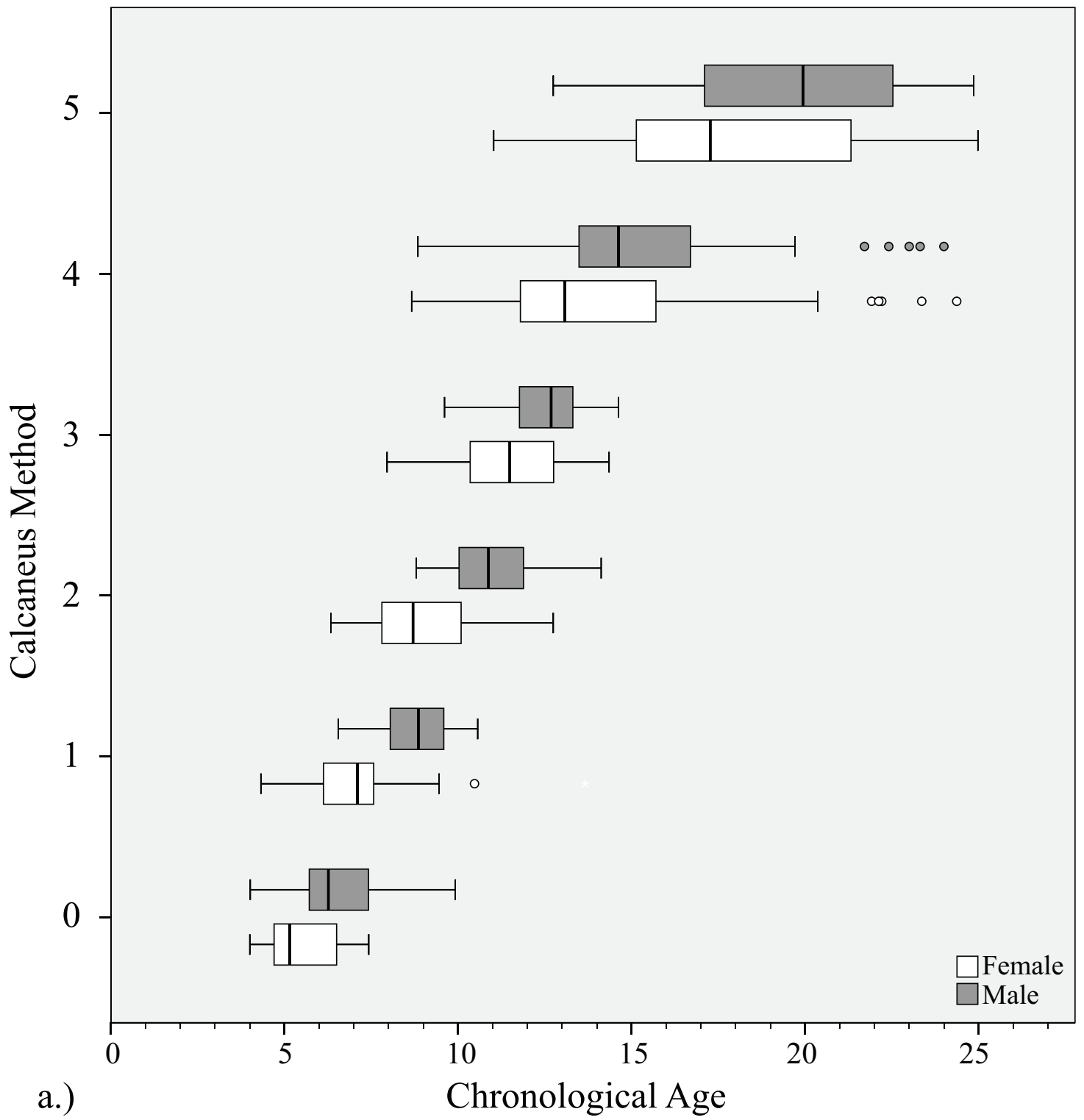
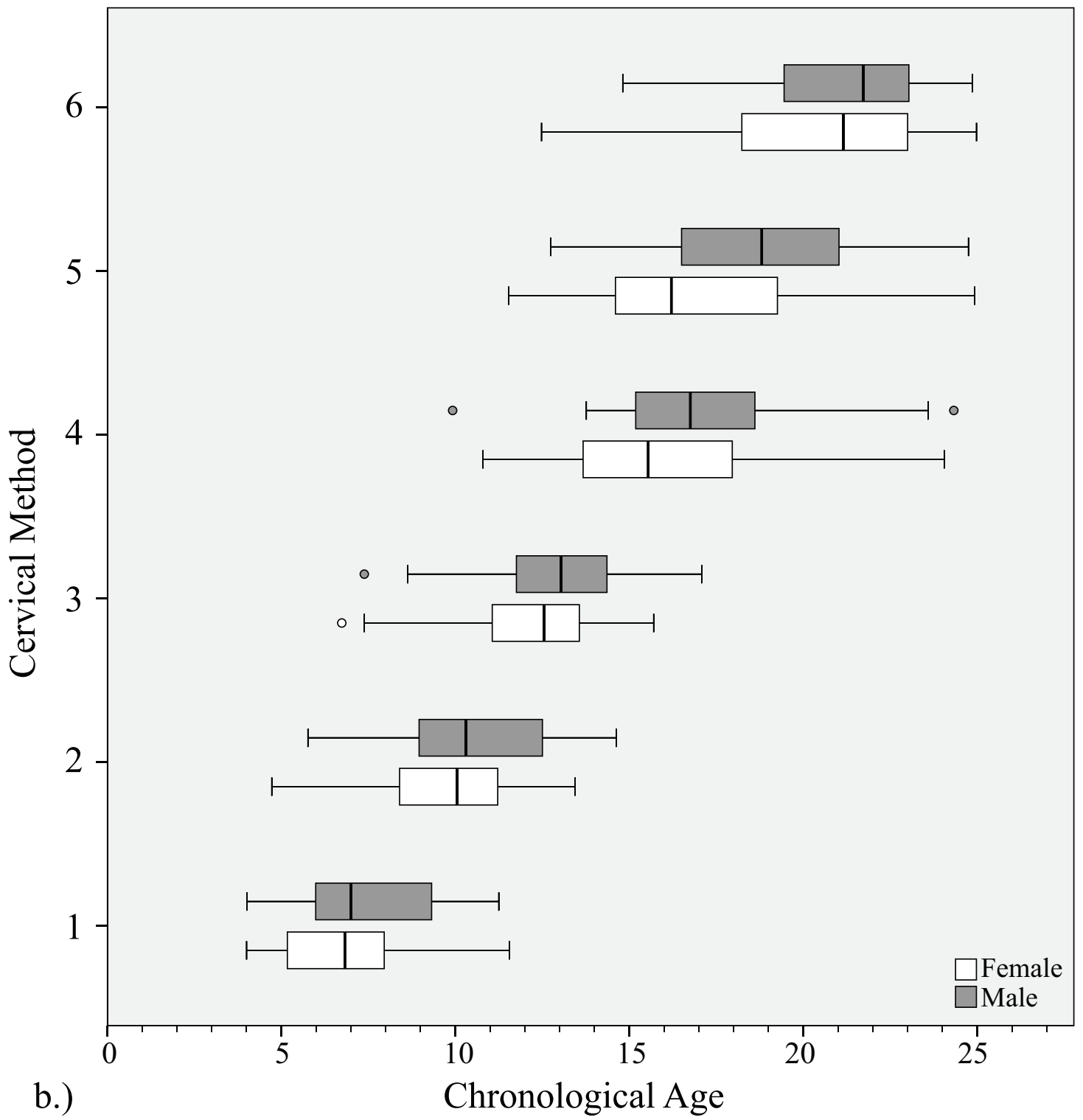
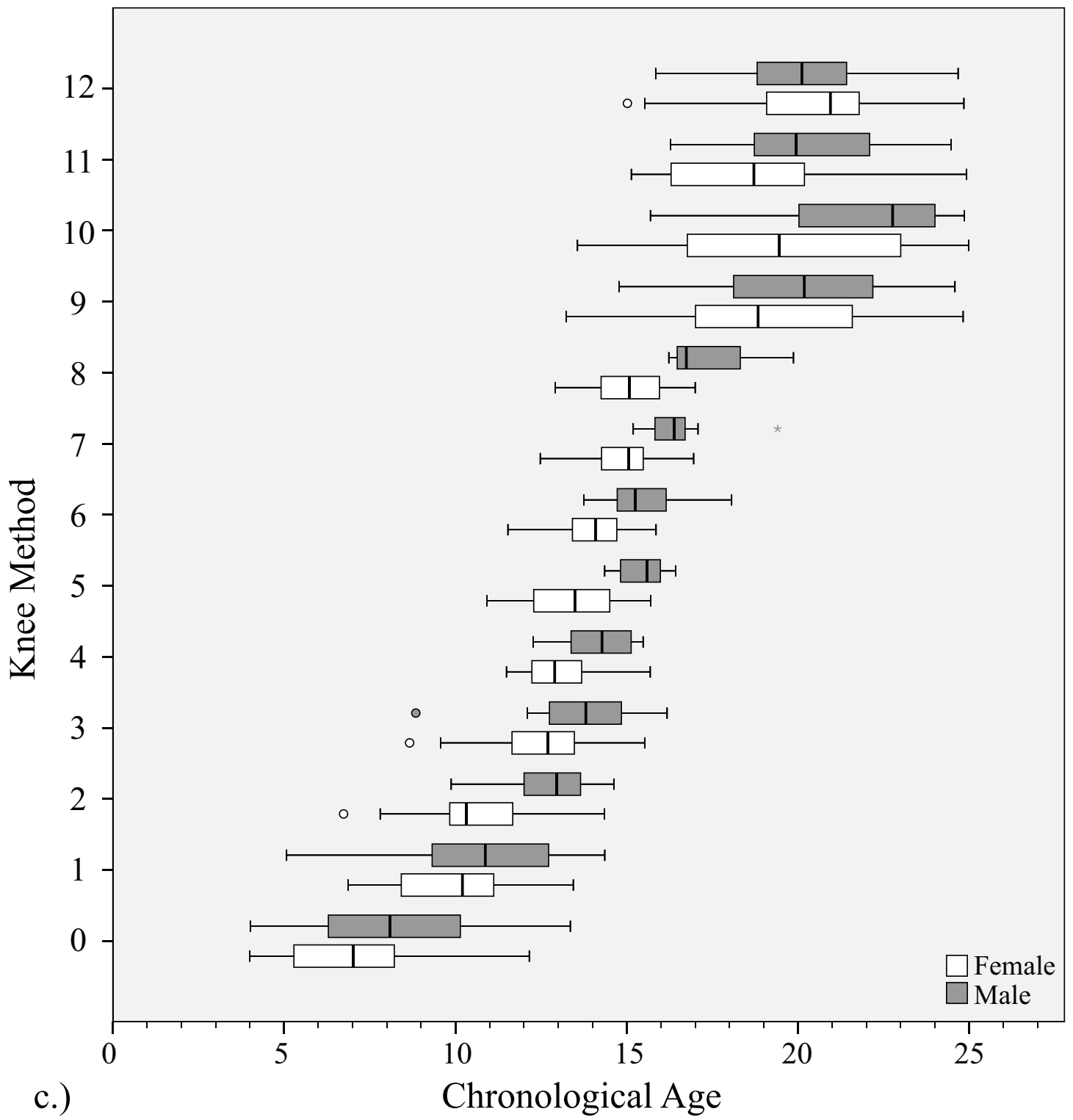


Figure 5b



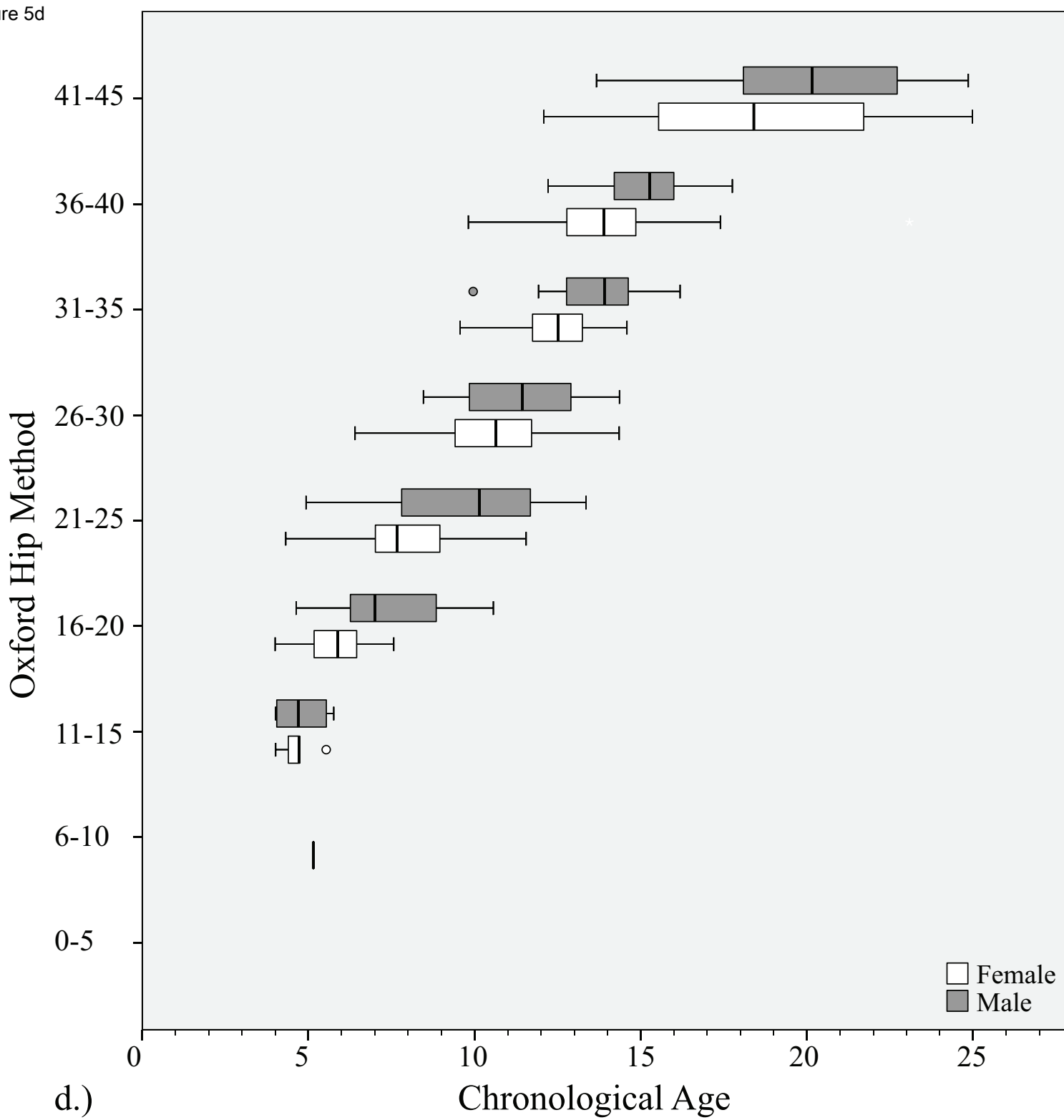
b.)

Figure 5c



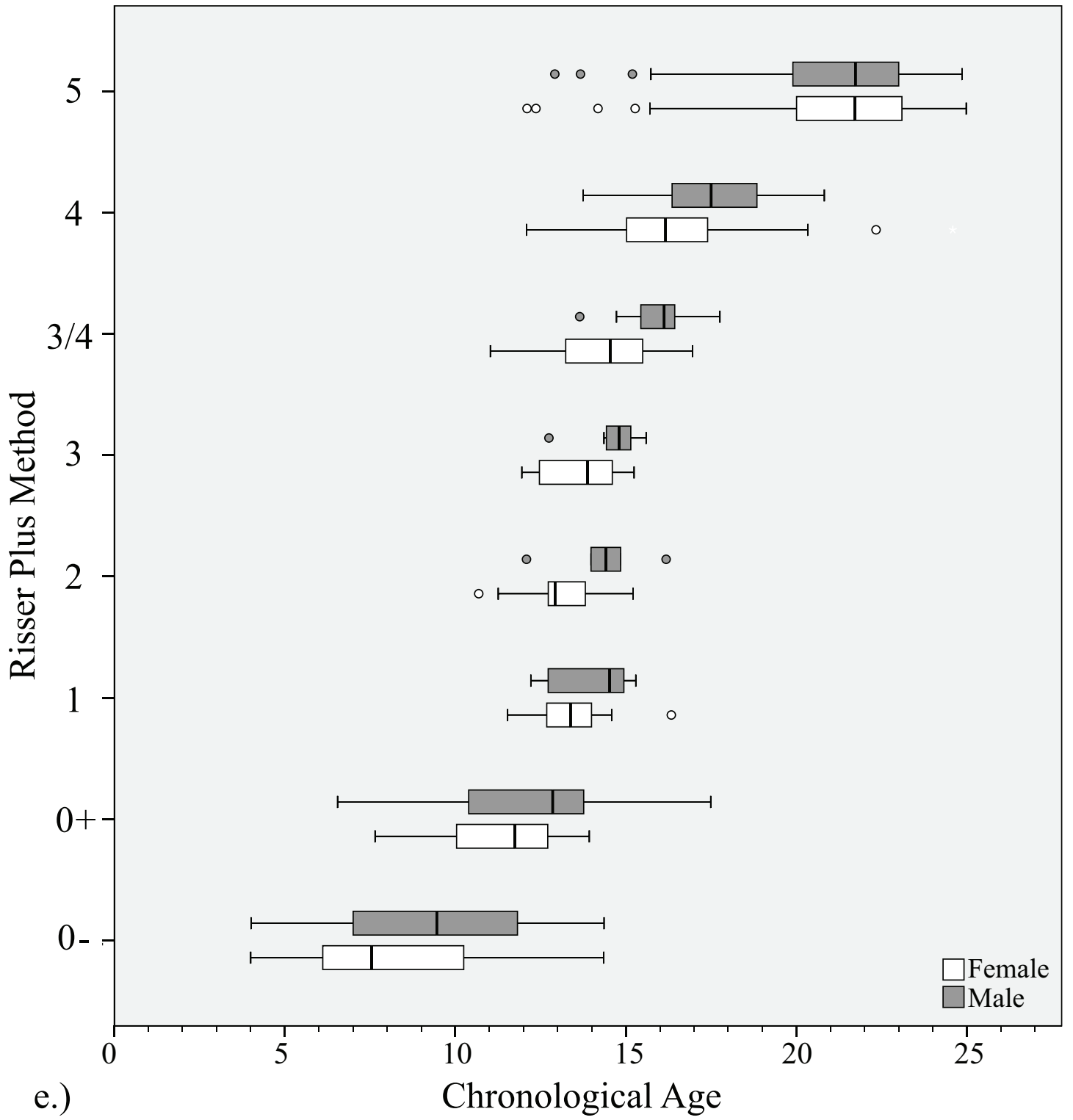
c.)

Figure 5d

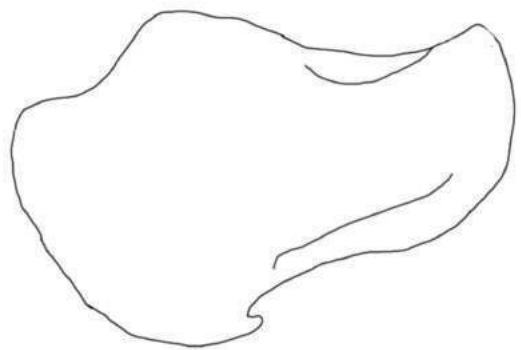


d.)

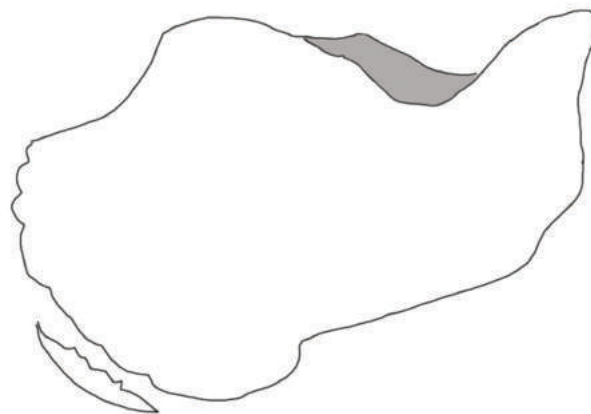
Figure 5e



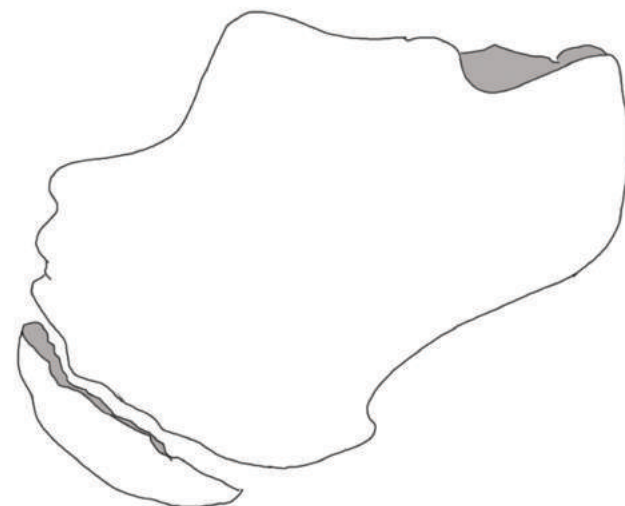
e.)



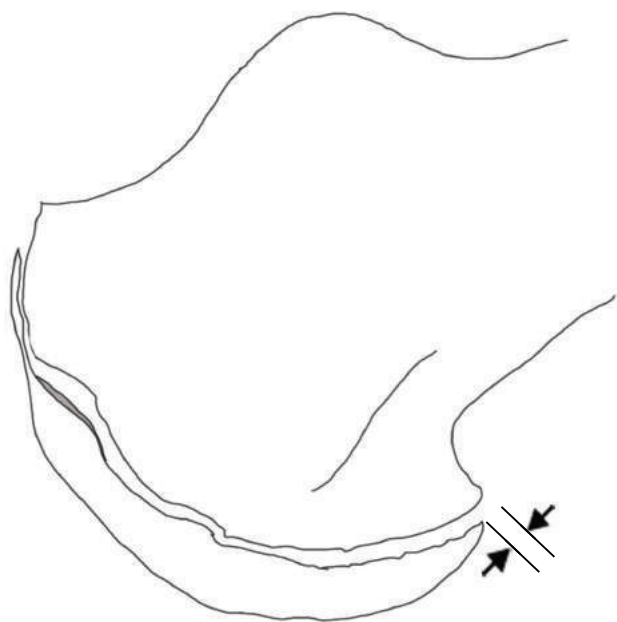
Stage 0



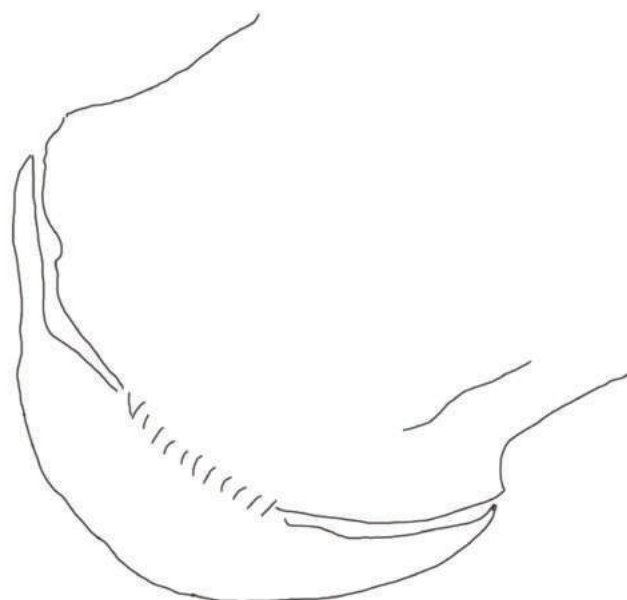
Stage 1



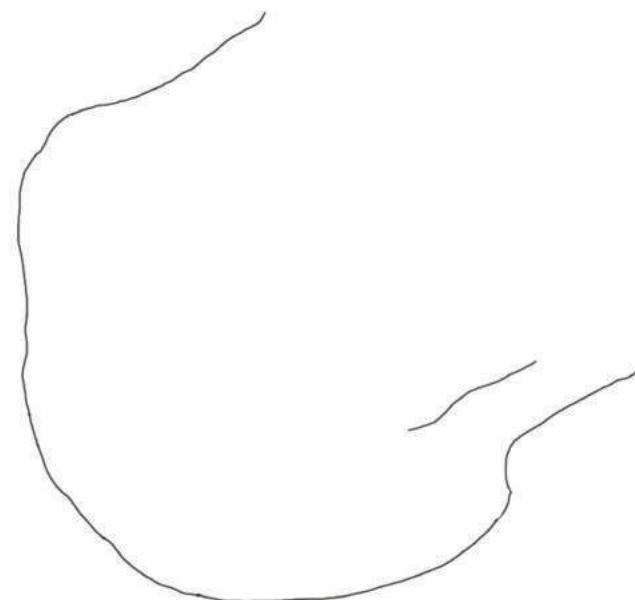
Stage 2



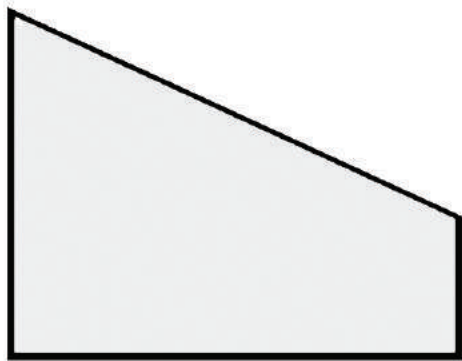
Stage 3



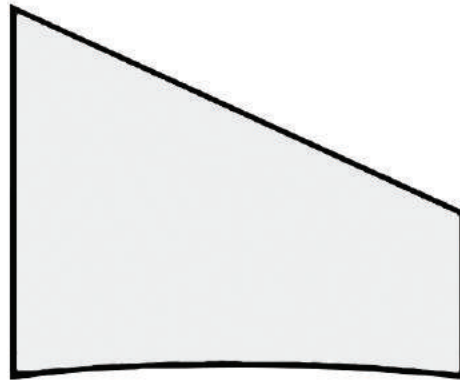
Stage 4



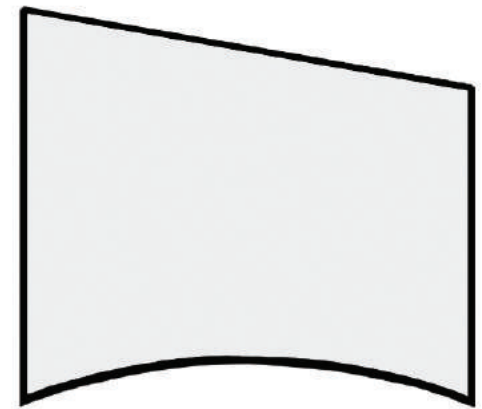
Stage 5



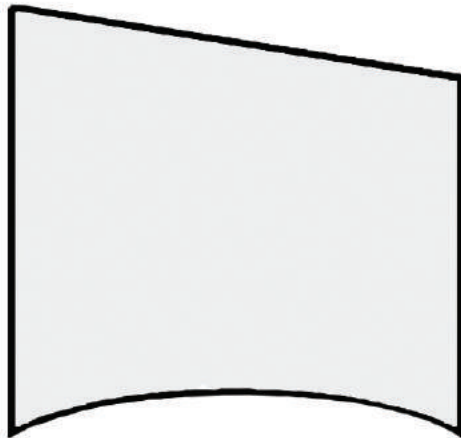
1. Initiation



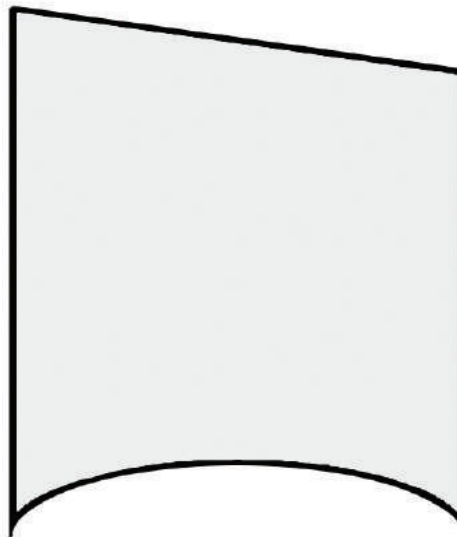
2. Acceleration



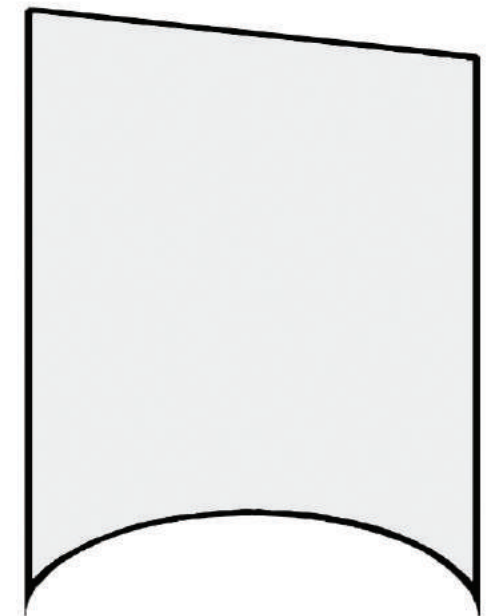
3. Transition



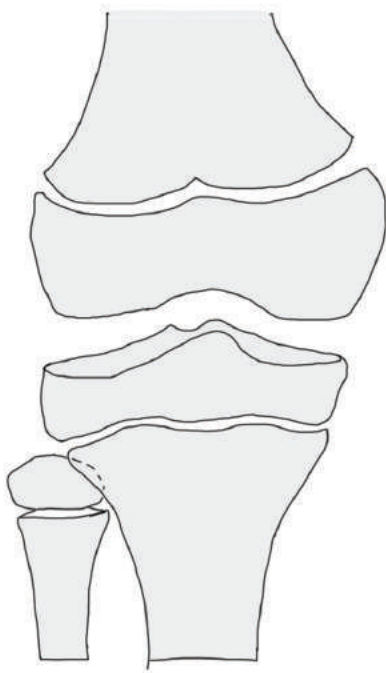
4. Deceleration



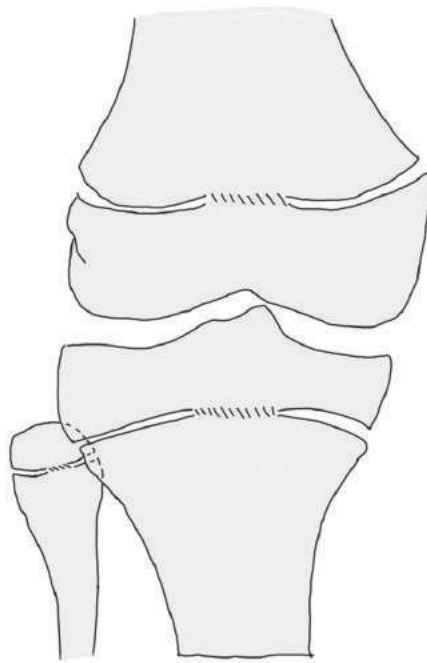
5. Maturation



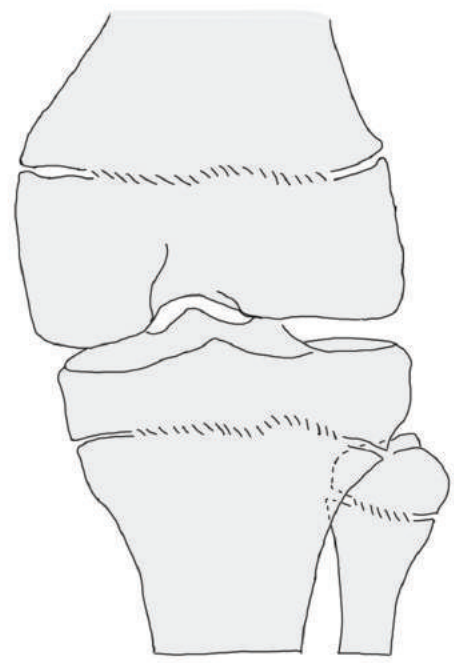
6. Completion



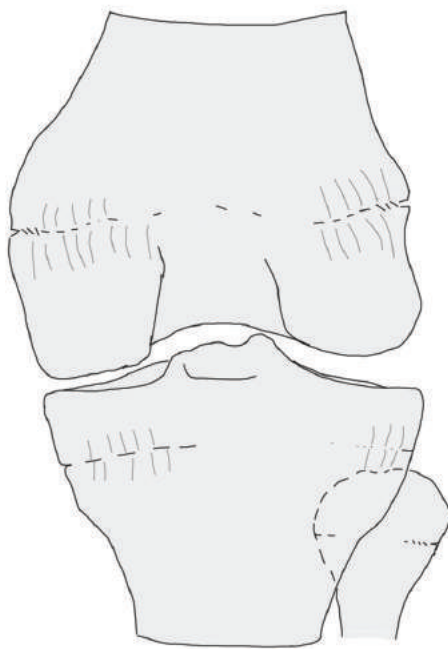
Stage 0



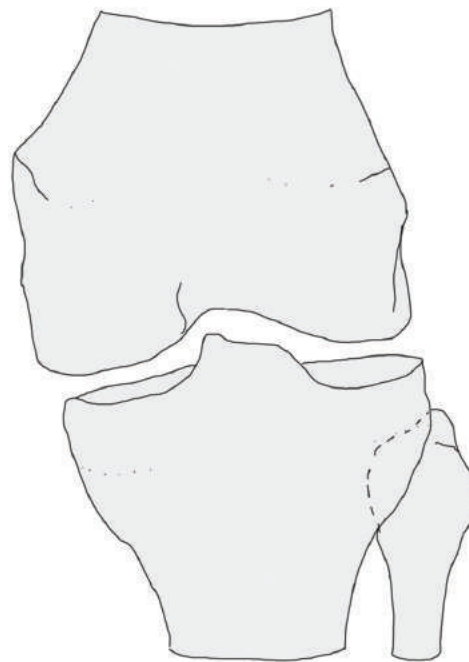
Stage 1



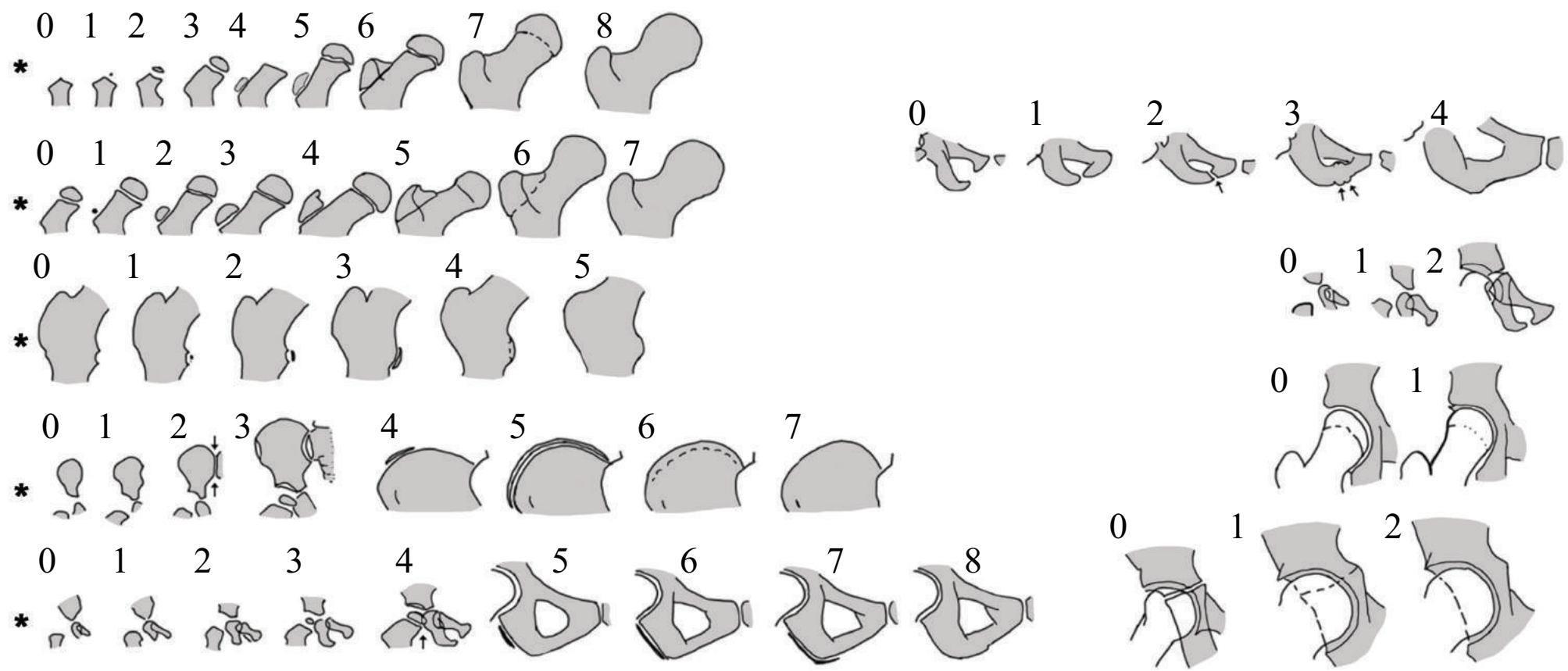
Stage 2



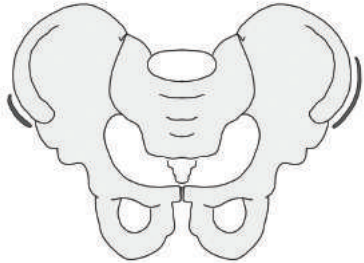
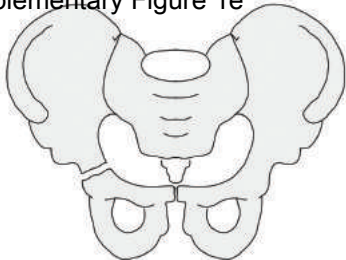
Stage 3



Stage 4



Supplementary Figure 1e

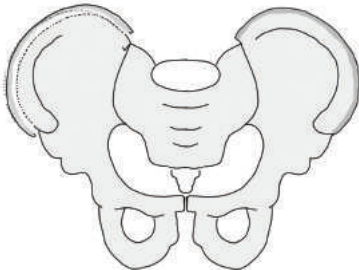
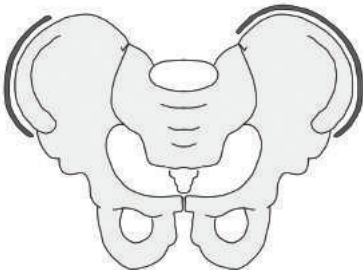


Risser 0-

Risser 0+

Risser 1

Risser 2



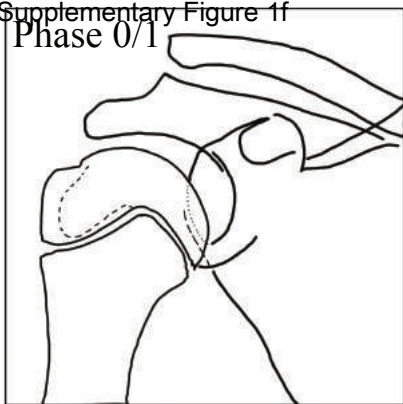
Risser 3

Risser 3/4

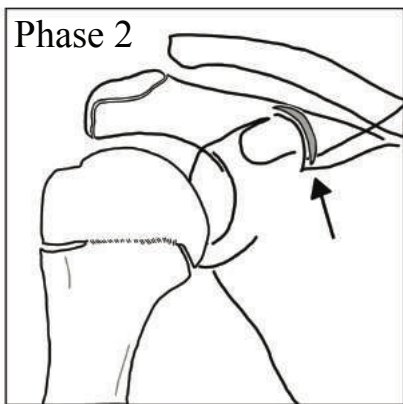
Risser 4

Risser 5

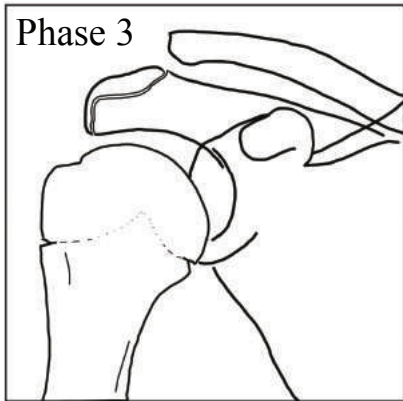
Phase 0/1



Phase 2



Phase 3



Phase 4

